

A MATHEMATICAL MODELLING APPROACH
FOR THE ELIMINATION OF MALARIA IN
MPUMALANGA, SOUTH AFRICA



Sheetal Prakash Silal

Thesis presented for the degree of
DOCTOR OF PHILOSOPHY

in the Department of Statistical Sciences
University of Cape Town

August 2014

Supervisors: A/Prof Francesca Little, Prof Karen Barnes & Dr Lisa White



The copyright of this thesis vests in the author. No quotation from it or information derived from it is to be published without full acknowledgement of the source. The thesis is to be used for private study or non-commercial research purposes only.

Published by the University of Cape Town (UCT) in terms of the non-exclusive license granted to UCT by the author.

List of Publications

1. Exploring the seasonality of reported treated malaria cases in Mpumalanga, South Africa

Journal: PLoS ONE

Authors: Sheetal Prakash Silal¹, Karen I Barnes², Gerdalize Kok³, Aaron Mabuza³, and Francesca Little¹

Author contributions:

SPS, KIB and FL conceived and designed the experiments. SPS analysed the data. GK and AM provided the data. SPS wrote the paper and KIB, FL, GK and AM reviewed manuscript and provided extensive comments.

Status: Published on 29 August 2013

2. Sensitivity to model structure: A comparison of compartment models in epidemiology

Journal: Operations Research for Health Care

Authors: Sheetal Prakash Silal¹, Francesca Little¹, Karen I Barnes², Lisa J White^{4,5}

Status: Under review

3. Towards malaria elimination in Mpumalanga, South Africa: a population-level mathematical modelling approach

Journal: Malaria Journal

Authors: Sheetal Prakash Silal¹, Francesca Little¹, Karen I Barnes², and Lisa J White^{4,5}

Status: Published on 3 August 2014

4. Hitting a moving target: a model for malaria elimination in the presence of population movement

Journal: Science

Authors: Sheetal Prakash Silal¹, Francesca Little¹, Karen I Barnes², and Lisa J White^{4,5}

Status: Under review

5. Predicting the impact of border control on malaria transmission: A Simulated Focal Screen and Treat campaign

Journal: Malaria Journal

Authors: Sheetal Prakash Silal¹, Francesca Little¹, Karen I Barnes², and Lisa J White^{4,5}

Status: Under review

Author contributions for papers 2 to 5:

SPS wrote the paper and performed the mathematical model development and analysis. SPS and LJW conceptualised the mathematical model and analysis. FL, KIB and LJW reviewed the manuscript extensively.

Signed by candidate	Signed by candidate	Signed by candidate	Signed by candidate	Signed by candidate
_____	_____	_____	_____	_____
G Kok	A Mabuza	KI Barnes	LJ White	F Little

¹ Department of Statistical Sciences, University of Cape Town, Cape Town, South Africa

² Division of Clinical Pharmacology, Department of Medicine, University of Cape Town, Cape Town, South Africa

³ Malaria Elimination Programme, Mpumalanga Department of Health, Nelspruit, South Africa

⁴ Mahidol-Oxford Tropical Medicine Research Unit, Mahidol University, Bangkok, Thailand

⁵ Centre for Tropical Medicine, Nuffield Department of Clinical Medicine, Churchill Hospital, University of Oxford, Oxford, UK

Plagiarism Declaration

I know the meaning of plagiarism and declare that all of the work in the dissertation, save for that which is properly acknowledged, is my own.

Signature: _____

Note from the National Research Foundation

This material is based upon work supported financially by the National Research Foundation in South Africa. Any opinion, findings and conclusions or recommendations expressed in this material are those of the authors and therefore the NRF does not accept any liability in regard thereto.

A mathematical modelling approach for the elimination of malaria in Mpumalanga, South Africa

Sheetal Prakash Silal

11 August 2014

Mpumalanga in South Africa is committed to eliminating malaria by 2018 and efforts are increasing beyond that necessary for malaria control. The eastern border of Mpumalanga is most affected by malaria with imported cases in Mpumalanga overtaking local cases in recent years. Mathematical modelling may be used to study the incidence and spread of disease with an important benefit being the ability to enact exogenous change on the system to predict impact without committing any real resources. Three models are developed to simulate malaria transmission: (1) a deterministic non-linear ordinary differential equation model, (2) a stochastic non-linear metapopulation differential equation model and (3) a stochastic hybrid metapopulation differential equation, individual-based model. These models are fitted to weekly case data from Mpumalanga from 2002 to 2008, and validated with data from 2009 to 2012. Interventions such as scaling-up vector control, mass drug administration, focal screen and treat campaign at the Mpumalanga-Maputo border-control point and source reduction are applied to the model to assess their potential impact on transmission and whether they may be used alone or in combination to achieve malaria elimination. The models predicted that scaling up vector control results in substantial decreases in local infections, though with little impact on imported infections. Mass drug administration is a high impacting but short-lived intervention with transmission reverting to pre-intervention levels within three years. Focal screen and treat campaigns are predicted to result in substantial decreases in local infections, though success of the campaign is dependent on the ability to detect low parasitemic infections. Large decreases in local infections are also predicted to be achieved through foreign source reduction. The impact of imported infections is such that malaria elimination is only predicted if all imported infections are treated before entry into Mpumalanga, or are themselves eliminated at their source. Thus a regionally-focused strategy may stand a better chance at achieving elimination in Mpumalanga and South Africa compared to a nationally-focused one. In this manner, mathematical models may form an integral part of the research, planning and evaluation of elimination-focused strategies so that malaria elimination is possible in the foreseeable future.

Acknowledgements

I am eternally grateful to my Guru Sri Swami Sivananda, beloved Pujye Swami Sahajananda, Saraswati Ma, Ganga Ma and my beloved Manmohana for always doing what is best for me.

I would like to thank A/Prof Francesca Little, Dr Lisa White and Prof Karen Barnes for their excellent supervision, guidance and support. I am grateful to the Malaria Elimination Programme of the Department of Health in South Africa, the Mozambique National Ministry of Health and the South African Weather service for the provision of data. Particularly, thanks are extended to Aaron Mabuza and Gerdalize Kok from the Mpumalanga Malaria Elimination Programme and John Freaan and Jaishree Raman from the National Institute for Communicable Diseases. I am grateful to the University of Cape Town's University Research Council and the Emerging Researcher Programme (Gaelle Ramon in particular) for their support and the National Research Foundation of South Africa for funding this PhD through the Thuthuka grant programme.

Lastly, I would like to thank my friend and colleague, Miguel Lacerda for being a willing sounding board and my husband Amrish and all my furry and feathered children for their endless love, support and warmth.

how do you write jay shree krishna in hindi - Google Search

2014/08/07 5:47 PM

About 766,000 results (0.63 seconds)

English - detected	Hindi
jay shree krishna	जय श्री कृष्णा Jaya śrī kṛṣṇā iii

[Open in Google Translate](#)

I am tryin to write jay shree krishna in Hindi any now how t...

<https://answers.yahoo.com/question/?qid=20090426211223AAhuoGh>

Apr 27, 2009 - जय श्री कृष्ण. Chris's answer has the first word spelt wrong.

पुष्टिमार्ग | हे कृष्ण, मैं आपका दास हूँ

pushtimarg.wordpress.com/

If you wish to add any Kirtan/Paath/Literature, Please **type** in Hindi/English and Jai

Contents

1	Introduction	1
2	Literature Review	5
2.1	Malaria	5
2.1.1	Biology	5
2.1.2	Diagnosis	6
2.1.3	Tools against Malaria	7
2.1.4	Elimination	7
2.2	Malaria Incidence and Control in Mpumalanga	9
2.2.1	History	9
2.2.2	Imported Infections	10
2.3	Mathematical Modelling in Epidemiology	11
2.3.1	Mathematical Modelling of Malaria	12
2.3.2	Mathematical Modelling of Malaria in South Africa	15
3	Data	17
3.1	Abstract	19
3.2	Introduction	20
3.3	Methods	22
3.3.1	Ethics statement	22
3.3.2	Data	22
3.3.3	Data Analysis	23
3.4	Results	24
3.4.1	Case Data	24
3.4.2	Cases and Rainfall	25
3.4.3	Cases and Source of Infection	26
3.4.4	Cases and Physical Geography	27
3.5	Discussion	28
3.6	Conclusion	32

4	Model structure	35
4.1	Abstract	37
4.2	Introduction	38
4.3	Compartment Models in Epidemiology	38
4.4	Model Development	40
4.5	Results	44
4.5.1	No treatment	44
4.5.2	With treatment	44
4.5.3	Treatment coverage and the probability of treatment	45
4.5.4	Data Fitting	50
4.5.5	Impact of other interventions	50
4.6	Discussion	54
4.7	Conclusion	56
4.8	Model Equations	57
4.9	Additional Output	59
5	Model 1 - Population model of malaria transmission	61
5.1	Abstract	63
5.2	Background	64
5.3	Methods	66
5.3.1	Transmission Model	66
5.3.2	Data fitting	67
5.3.3	Assessing elimination	69
5.4	Results	70
5.4.1	Model fitting and validation	70
5.4.2	Interventions	70
5.5	Discussion	75
5.6	Conclusions	78
5.7	Additional File 1: Mathematical Model Description	81
5.7.1	Base Model of Transmission	81
5.7.2	Transmission model with interventions	82
5.7.3	Vector Control	87
5.7.4	Asymptomatic Infections	87
5.7.5	Data Fitting Method	87
6	Model 2 - Metapopulation model of malaria transmission	93
6.1	Abstract	95
6.2	Introduction	96
6.3	Methods	98
6.3.1	Transmission Model	98

6.3.2	Data Fitting	98
6.4	Results	100
6.4.1	Estimation of Parameters through data-fitting	100
6.4.2	Interventions	103
6.5	Discussion	106
6.6	Conclusion	109
6.7	Additional File 2: Mathematical Model Description	111
6.7.1	Summary Equations: Metapopulation Model of Transmission	111
6.7.2	Summary Equations: Metapopulation Transmission model with interventions	118
6.7.3	Vector Control	126
6.7.4	Data Fitting Method	126
7	Model 3 - A Hybrid Metapopulation DE-IBM model of malaria transmission	131
7.1	Abstract	134
7.2	Background	135
7.3	Methods	137
7.3.1	Transmission Model	137
7.3.2	FSAT model	140
7.3.3	Hybrid metapopulation DE-IBM model	142
7.3.4	Data Fitting	143
7.4	Results	143
7.4.1	Estimation of Parameters through data-fitting	143
7.4.2	Simulated FSAT	144
7.5	Discussion	148
7.6	Conclusion	150
7.7	Additional File 3: Mathematical Model Description	151
7.7.1	Summary Equations: Metapopulation Model of Transmission	151
7.7.2	Hybrid metapopulation DE-IBM model	160
7.7.3	Data Fitting Method	160
8	Discussion and Conclusions	163
8.1	Mathematical models of malaria	163
8.2	Malaria elimination in Mpumalanga	166
8.3	Conclusion	170
	Bibliography	173
A	Model Code	191
A.1	Model 1 - Population model of malaria transmission	191
A.2	Model 2 - Metapopulation model of malaria transmission	201

CONTENTS

A.3 Model 3 - Hybrid Metapopulation DE-IBM model of malaria transmission	214
B Ethical Clearance	229

List of Figures

2.1	Malaria Life Cycle (credit: NIAID[79])	6
2.2	Epidemiological milestones from control to elimination. SPR: slide or rapid diagnostic test positivity rate. These milestones are indicative only: in practice, the transitions will depend on the malaria burden that a programme can realistically handle (including case notification, case investigation, etc.) Source: [80]	8
2.3	Mpumalanga Province (white) with the five municipalities of Ehlanzeni District (credit: Mpumalanga Malaria Elimination Programme (unpublished))	10
2.4	Evolution and grouping of different types of SEIR malaria models. Subscripts 'h' and 'm' stands for human and mosquito. Double-folded boxes are for both human & mosquito population, and single fold boxes are only for human. First time addition of a new compartment is shown in red. The subscript 'j' (= 1, 2, 3) indicates further subdivision of the corresponding compartment. Three models inside the big grey box are considered as the Basic malaria models. Dotted arrows show the incorporation of complex factors in different models or specific compartment (red circle). Total population size is constant for all models, except the ones inside the dashed box. Sourced from [82].	13
3.1	The number of reported treated cases for all the municipalities in Mpumalanga Province for 2002 and 2012.	21
3.2	The weekly and annual reported treated malaria cases in Mpumalanga Province between 2002 and 2012.	24
3.3	STL decomposition on reported treated malaria cases in Mpumalanga Province between 2002 and 2012.	26
3.4	Two year seasonal trend of reported treated malaria cases in Mpumalanga Province between 2002 and 2012.	27
3.5	Weekly malaria cases and monthly average rainfall (mm) in Mpumalanga Province between 2002 and 2012.	28
3.6	Seasonal trend of weekly malaria cases and monthly average rainfall in Mpumalanga Province between 2002 and 2012.	29

3.7	Seasonality and trend components of an STL decomposition of locally and foreign-sourced malaria cases in Mpumalanga Province between 2002 and 2012.	30
3.8	Percentage plot of locally and foreign-sourced malaria cases in Mpumalanga Province between 2002 and 2012.	31
3.9	Weekly malaria cases in Nkomazi, Mbombela and Bushbuckridge Municipalities (blue) between 2002 and 2012 are shown against the backdrop of the total cases in Mpumalanga province (orange).	32
3.10	Seasonal trend of weekly malaria cases in Nkomazi, Mbombela and Bushbuckridge Municipalities between 2002 and 2012.	33
3.11	Monthly malaria cases in Mpumalanga and Maputo, Mozambique between 2002 and 2012.	34
3.12	Seasonal trend of monthly malaria cases in Mpumalanga and Maputo, Mozambique between 2002 and 2012.	34
4.1	Model Flowcharts	42
4.1	Model Flowcharts	43
4.2	No Treatment: Incidence and Prevalence for Model 1(red), Model 2 (blue) and Model 3(green)	45
4.3	10% Treatment Probability: Incidence (a), Prevalence (b), Treated Cases (c) and Treatment Coverage (d) for Model 1 (red), Model 2 (blue), Model 3 (green), Model 4 (orange), Model 5 (black) and Model 6 (purple)	46
4.4	Mass Drug Administration (8 weeks, 75% probability of treatment): Incidence (a & b), Prevalence (c & d), Treated Cases (e & f) and Treatment Coverage (g & h) for Model 1(red), Model 2 (blue), Model 3 (green), Model 4 (orange), Model 5 (black) and Model 6 (purple)	52
4.5	Vector Control (50% Coverage, 50% Efficacy): Incidence (a & b), Prevalence (c & d), Treated Cases (e & f) and Treatment Coverage (g & h) for Model 1(red), Model 2 (blue), Model 3 (green), Model 4 (orange), Model 5 (black) and Model 6 (purple)	53
4.6	50% Treatment Probability: Incidence (a), Prevalence (b), Treated Cases (c) and Treatment Coverage (d) for Model 1 (red), Model 2 (blue), Model 3 (green), Model 4 (orange), Model 5 (black) and Model 6 (purple)	59
4.7	100% Treatment Probability: Incidence (a), Prevalence (b), Treated Cases (c) and Treatment Coverage (d) for Model 1 (red), Model 2 (blue), Model 3 (green), Model 4 (orange), Model 5 (black) and Model 6 (purple)	60
5.1	A map of Mpumalanga Province in relation to Mozambique and Swaziland (Source: Mpumalanga Malaria Elimination Programme (unpublished))	65
5.2	Annual incidence of locally sourced (blue) and imported (green) malaria cases that have been reported and treated at health facilities in Mpumalanga province. . .	66

5.3	Flowchart underlying the population level ordinary non-linear differential equation model of malaria transmission. (l - locally sourced infections, f - imported infections, u - untreated infections, tr- treated infections)	67
5.4	(a) Model fitting results for data (black) to model output: locally sourced (blue) and imported (green) reported treated malaria cases and (b) Model validation results of model output: locally sourced (blue) and imported (green) reported treated malaria cases against data (black) from 2009 to 2013.	71
5.5	Predicted impact of a scale up of vector control (from 2013) that reduces the number of infections by a further 10% (red) and 20% (blue).	72
5.6	Predicted impact on the number of infections of annual rounds of MDA performed (from 2013) at the peak (red) and trough (blue) of the season on local and imported infections	74
5.7	Predicted impact on the number of infections of (a) six consecutive 2-monthly rounds of MDA on local and imported infections and (b) six months of FSAT of new imported infections at 70% coverage (border screen and treat)	75
5.8	Predicted impact on local infections of combination of interventions on local infections: Black: No additional interventions, Red: 70% coverage of FSAT on local population with new imported infections following six consecutive two-monthly rounds of MDA at 80% coverage, Blue: same as red (MDA+FSAT) with increased vector control to decrease transmission by a further 20%, Green: six consecutive two-monthly rounds of MDA with increased vector control, and 70% decrease in the foreign force of infection, Purple: six consecutive two-monthly rounds of MDA with zero imported infections	76
5.9	Model flow: Base Model (black) with interventions: FSAT(red), MDA(blue). The assimilation of the population having been subjected to MDA, but infected during the MDA cycle though after the prophylactic protection period of the drug, is represented in green. This is necessary as the duration of the MDA cycle is 8 weeks where as the prophylactic period of the drug is only 4 weeks, so it is possible to get infected again within the 8 week period after being subjected to MDA. If these infections were accounted for in the base model compartments, it would be possible to receive MDA again, which is not usually the case.	88
5.10	Number of structures sprayed in Mpumalanga between 2002 and 2012	89

5.11	50% probability of treatment: Predicted impact on local infections of combination of interventions on local infections: Black: No additional interventions, Red: 70% coverage of FSAT on local population with new imported infections following six consecutive two-monthly rounds of MDA at 80% coverage, Blue: same as red (MDA+FSAT) with increased vector control to decrease transmission by a further 20%, Green: six consecutive two-monthly rounds of MDA with increased vector control, and 70% decrease in the foreign force of infection, Purple: six consecutive two-monthly rounds of MDA with zero imported infections	90
6.1	A map of Mpumalanga Province in relation to Mozambique and Swaziland (Source: Mpumalanga Malaria Elimination Programme (unpublished))	97
6.2	Metapopulation Model flow (a) Compartment transmission model for each sub-patch j (1-3) in patch i (1-6) at time step t with compartments S -Susceptible, BT - Blood stage and treated, BU - Blood stage and untreated, IT - Infectious and treated, and IU - Infectious, asymptomatic and untreated. (b) Metapopulation structure highlighting human movement between each local patch $i \in \{1, 2, 3, 4, 5\}$ and foreign patch 6. Movement between the five local patches is not shown. Other parameters are described in Table 6.1 and Additional file 2.	99
6.3	Predicted average weekly treated cases (blue: 2002 - 2008; red: 2009-2012) fitted to and validated with data (black). The 95% uncertainty range for weekly case predictions is shown.	100
6.4	Predicted impact of interventions on the number of local infections in the Ehlanzeni district (summation of the five local patches). (a) shows the <u>number of cases averted</u> due to the interventions between 2013 and 2018 as a percentage of total local infections in the absence of interventions and (b) shows the impact of the interventions on local infections in Ehlanzeni district through time compared to the base case of no interventions (black). (1) Local Scale-up: Increase in local vector control so as to reduce the mosquito-human contact rate by a further 10% (red)& three consecutive two-monthly rounds of MDA in Mbombela, Nkomazi and Bushbuckridge Municipalities (green). (2) FSAT at the border: at 70% coverage for 26 weeks (red), 39 weeks (green), 52 weeks (blue) and 52 weeks at 100% coverage (purple). (3) Reducing Vector Control: FSAT at the border at 70% coverage administered all year round while simultaneously reducing vector control by 10% (red), 20% (green) and stopping vector control altogether (blue). (4) Source Reduction: 10% scale up of vector control in Maputo (red), three consecutive two-monthly rounds of MDA in Maputo (green) and eliminating malaria in Maputo (blue).	104
6.5	Transmission model with interventions for a single patch. Migration flows between patches are not shown. Note that the full model may be depicted as this single patch model, replicated 18 times, with migration flows between the 18 patches as described in the paper.	119

6.6	Number of structures sprayed in Mpumalanga between 2002 and 2012	126
6.7	Model fit and validation with 95% uncertainty range for individual predictions	129
7.1	A map of Mpumalanga Province in relation to Mozambique and Swaziland (Source: Mpumalanga Malaria Elimination Programme (unpublished))	136
7.2	Hybrid Metapopulation DE-IBM Model flow (a) Compartment transmission model for each patch i (1-6) with sub-patch j (1-3) at time step t with compartments S -Susceptible, I - Infectious and treated (tr), C - Infectious, symptomatic and untreated (u), A - Infectious, asymptomatic and untreated, M - Infectious, sub-patent and untreated and P - Susceptible with prior asymptomatic infection. (b) Metapopulation structure highlighting human movement between each local patch $i \in \{1, 2, 3, 4, 5\}$ and foreign patch 6. Other parameters are described in Table 7.1 and Additional file 3.	138
7.3	FSAT IBM algorithm	141
7.4	Predicted weekly treated cases (blue: 2002 - 2008; red: 2009-2012) fitted to and validated with data (black). The 95% uncertainty range for weekly case predictions is shown.	144
7.5	Predicted impact due to FSAT between 2014 and 2018 using the following diagnostic tools: microscopy (red), qPCR (orange), LAMP (green), RDT (blue) and a hypothetical RDT (purple). (a) shows the percentage decrease in local infections due to the FSAT and (b) shows the impact of FSAT on local infections in Ehlanzeni district through time compared to the base case of no interventions (black).	146
7.6	Predicted impact due to FSAT between 2014 and 2018. (a) shows the percentage decrease in local infections due to the FSAT and (b) shows the impact of FSAT on local infections in Ehlanzeni district through time compared to the base case of no interventions (black). The impact of FSAT is predicted for different (1) coverage proportions, (2) thresholds of detections for the diagnostic tool used (parasites / μ L), (3) take-up proportions, (4) coverage proportions for Mass Drug Administration and (5) weekly targets (capacity) keeping all other variables constant. 95% Confidence Intervals are depicted for the average percentage decrease.	147
7.7	Model fit and validation with 95% uncertainty range	162
8.1	Mathematical models of transmission	164

List of Tables

3.1	Malaria Incidence Rates and the change in cases in Mpumalanga Province and the municipalities in Ehlanzeni District.	21
4.1	Model Parameters: Description and value	44
4.2	Time to elimination (weeks) for vector control and scale-up of drug therapy . . .	54
5.1	Providing the values, descriptions and sources of the parameters driving the mathematical model of transmission.	68
5.2	Model 1: Compartment Descriptions table	84
5.3	Model 1: Full Parameter table	85
6.1	Values, descriptions and sources of the parameters driving the base metapopulation model of transmission. ($i = \{TC; MB; UJ; NK; BB; MP\}$)	101
6.2	Model 2: Compartment Descriptions	116
6.3	Model 2: Full Parameter table	116
7.1	Model 3: Full Parameter table	138
7.2	Values, descriptions and sources of the parameters driving the FSAT Individual Based Model.	142
7.3	Descriptions of diagnostic tools used in FSAT model	145
7.4	Compartment Descriptions	157
7.5	Values, descriptions and sources of the parameters driving the base metapopulation model of transmission. ($i = \{TC; MB; UJ; NK; BB; MP\}$)	157

Chapter 1

Introduction

Malaria is a vector borne disease that is both preventable and treatable. Despite this, malaria was responsible for more than 627 000 deaths in 2012; the majority of which occurred among children in Africa [144]. Since the call in October 2007 for renewed efforts towards achieving global malaria eradication, more than 25 previously endemic countries are in the pre-elimination/elimination phase of the eradication effort [51, 108]. South Africa, having already experienced a sharp decline in malaria cases since the last epidemic in 2000, also meets the pre-elimination phase criteria set out by the World Health Organisation (WHO) (< 5 cases per 1000 population at risk) and has been ear-marked to achieve elimination by 2018 [93].

Mpumalanga is one of three provinces in South Africa where malaria control activities still take place. Within Mpumalanga, malaria is distributed mainly in the low-lying areas bordering Swaziland and Maputo Province in Mozambique. Between 2002 and 2012, there were 40 650 cases reported and treated in Mpumalanga, with the proportion of imported cases increasing from 39% in 2002 to 87% in 2012. In a low transmission area such as Mpumalanga, imported infections may affect malaria transmission in two key ways. Firstly, people from the low transmission area move to areas of high transmission and having little or no immunity to malaria, become infected and transmit infections upon return to the low transmission area. Secondly, people from areas of high transmission may harbour parasites and transmit these when they move to areas of low transmission. Having partial or full immunity, they may not exhibit clinical symptoms and therefore act as hidden reservoirs of infection [136]. To achieve malaria elimination by 2018, Mpumalanga along with the other malaria-endemic South African provinces are increasing efforts beyond that necessary for malaria control. In shifting focus from control to elimination, it has been acknowledged that a "more of the same" approach will not work [89]. For example, while a control strategy focuses on treating clinical malaria and the prevention of onward transmission through vector control, an elimination strategy would focus its activities towards the foci of infections (both clinical and asymptomatic) that sustain transmission. Hence it may be the case

that new tools or strategies tailored to malaria elimination, will be employed in the future.

Mathematical models have in the past provided a valuable framework for analysing the dynamics of malaria transmission with an important benefit being the ability to enact exogenous change on the modelled system to predict the impact of interventions without committing any real resources; a key benefit in a scarce resources setting. While mathematical models have been useful in malaria control efforts, they become even more important when malaria elimination is in the foreseeable future. Malaria control efforts are often assessed through the use of cross-sectional prevalence surveys and new drugs/therapies are tested through clinical trials. This data is then analysed statistically and conclusions can be drawn on the impact of past efforts and the efficacy of new drugs. These surveys and clinical trials can be performed because infected individuals are easily sourced due to high transmission rates. As malaria elimination gets closer to reality, it is not going to be as easy to source infected individuals for clinical trials. Previously, for every 1000 people, one has been able to source tens to hundreds of infected individuals, but as elimination draws closer, one may only be able to source one or two infected people per 1000. The validity of sample data analysis relies heavily on there being sufficient data to analyse, yet it thus becomes so costly to source sufficient individuals for studies to inform elimination efforts that such studies are not feasible. This is where mathematical models can help statistical analysis.

This study aims to use mathematical models to simulate malaria transmission in Mpumalanga in order to test a variety of elimination-focused tools and assess their impact on local malaria prevalence and whether these tools may be used to achieve and maintain malaria elimination. Particular attention will be paid to the impact of imported cases on the malaria elimination effort. Thus the research questions (and underlying theme of analysis) for this study are:

1. What is the temporal pattern of malaria transmission in Mpumalanga and what are the drivers of this pattern?
2. How long will it take to eliminate malaria with a strategy of maintaining current interventions at current levels?
3. How long will it take to eliminate malaria with a strategy of scaling up current interventions?
4. What alternative/additional interventions should be considered to make the elimination efforts more effective?

To answer these research questions, three mathematical models of malaria transmission are presented, each with a different focus. All three models are informed by a statistical analysis of malaria case data that identifies an atypical triple-peaked pattern of malaria cases as well as the importance of imported cases as a major driver of this pattern. The first model is a population level deterministic non-linear ordinary differential equation model developed for Mpumalanga province to provide broad-stroke, average estimates of the impact of the suite of interventions

assessed. This model is improved on by the second model which disaggregates the population of interest into five administrative areas in the district most affected by malaria using a metapopulation stochastic non-linear ordinary differential equation approach. Malaria transmission in neighbouring Maputo Province is also included in this model. This model improves on the first model by incorporating heterogenous levels of malaria transmission in Mpumalanga and movement between Mpumalanga and Maputo Province is modelled to facilitate imported infections. This allows for more accurate modelling of certain antimalarial interventions. The third model is developed to explore the impact on local infections that a Focal Screen and Treat campaign would have, if implemented at the border control point between Mpumalanga and Maputo Province.

Chapter 2 presents an extensive literature review on the malaria biology, control and elimination as well as a history of malaria in South Africa with a focus on Mpumalanga. Applications of mathematical modelling in malaria both globally and in Mpumalanga are discussed. Chapter 3 is a description of the case notification data for Mpumalanga and Maputo Province between 2002 and 2012. This is the secondary dataset that is used throughout the study to inform the mathematical models. Chapter 4 is an extensive discussion of ordinary differential equation modelling (the main methodology employed in the mathematical models) and the sensitivity of results to model structure in epidemiological modelling. Chapters 5, 6 and 7 describe and discuss the development and analysis of the three mathematical models concluding with a chapter for discussion and study conclusions.

This dissertation includes five papers (two published and three in submission to international peer-reviewed journals at the time of submission for examination). Each paper is contained in a chapter that is prefaced with a synopsis and where relevant, supplementary material (also submitted to the journals) detailing the extent of work for each paper at the end of each chapter. The results of each chapter are therefore presented and discussed within the chapter. As each manuscript contains a short introduction and literature review, some material from the initial literature review is repeated in order for each paper to stand on its own. The candidate is the first author on all papers. Supervisors appear as co-authors and the contribution of all authors has been clearly outlined for each paper. In general, the candidate has developed all models, performed all model analysis and written all the papers. Supervisors have contributed to conceiving the study and reviewing the manuscripts.

In order to present the thesis in a single format, the references have been listed alphabetically, at the end of the document. Thus, the reference numbers in the thesis are different to those in the published papers available online.

Chapter 2

Literature Review

2.1 Malaria

Despite being a treatable and preventable mosquito-borne disease, malaria is still an immense global health, economic and social burden. Latest estimates suggest 207 million cases in 2012 with an uncertainty range of (135 million, 287 million) cases globally [144]. There were 627 000 deaths due to malaria; with the majority of deaths occurring among children in Africa. Malaria has been recognised as a disease of poverty with vulnerable groups facing several barriers to access antimalarial interventions [111, 146].

2.1.1 Biology

Malaria is a vector-borne parasitic disease involving two kind of hosts: female *Anopheles* mosquitos and humans (Figure 2.1) [79]. A malaria infected mosquito, when taking a blood meal, injects sporozoites into the human. These sporozoites infect the liver cells where they multiply asexually without causing any symptoms over the next seven to ten days [69]. The parasites are released from the liver and infect the blood cells in the form of merozoites where they multiply again bringing the onset of symptoms (fever, headaches, vomiting and chills) between ten and fifteen days after the initial mosquito bite [145]. Some merozoites mature into male and female gametocytes. A mosquito taking a blood meal from an infected human at this stage ingests the gametocytes to begin the sporogonic cycle in the mosquito where the gamete cells multiply and develop into sporozoites over a period of eight to 15 days [81].

Four species of parasites infect humans: *Plasmodium falciparum*, *Plasmodium vivax*, *Plasmodium malariae* and *Plasmodium ovale* with a few cases of *Plasmodium knowlesi* in humans in recent years [145]. *Plasmodium falciparum* is one of the most common and deadly species and

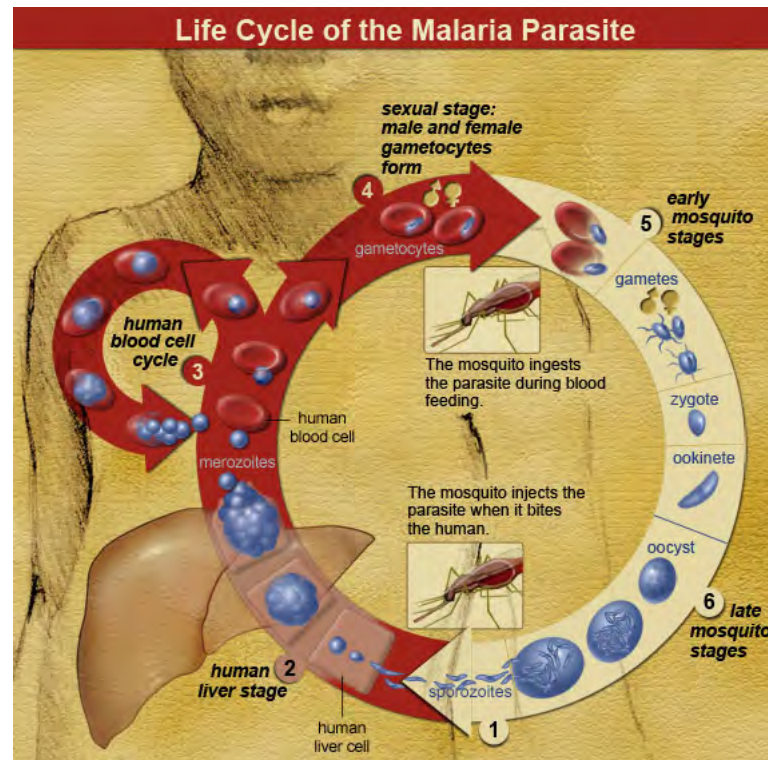


Figure 2.1: Malaria Life Cycle (credit: NIAID[79])

the prominent species in South Africa. There are different kinds of naturally acquired immunity which may develop in the human host against malaria. Anti-disease immunity provides protection against clinical disease reducing the risks and level of morbidity for a given parasite density. Anti-parasite immunity, provides protection against the degree of parasitemia while premunition provides protection against new infections by maintaining low-grade, usually asymptomatic parasitemia [30]. Malaria is treatable, with the best currently available treatment for *Plasmodium falciparum* malaria being artemisinin-based combination therapy (ACT). Drug resistance is an important factor in malaria with widespread resistance of *Plasmodium falciparum* to drugs like chloroquine and sulfadoxine-pyrimethamine (SP) in the 1970s and 1980s. Resistance to artemisinin-based drugs has in recent times emerged in the Greater Mekong subregion with the World Health Organisation (WHO) supporting countries in their efforts to monitor the situation.

2.1.2 Diagnosis

It is during the blood stage of malaria parasite cycle that diagnosis may occur. Microscopy of blood smears is considered the "gold standard" of diagnostic tools and with experienced technicians, may exhibit a sensitivity of 20 to 50 parasites/ μL but is more likely to achieve

a sensitivity of 100 parasites/ μL [47, 48]. The use of microscopy requires training and quality control of microscopists and adequate equipment. Polymerase chain reaction (PCR) and real-time quantitative polymerase chain reaction (qPCR) are highly sensitive diagnostic tools (0.05-10 parasites/ μL) needing sophisticated equipment at a laboratory at a substantial cost to achieve a processing time of three hours. Rapid Diagnostic Tests (RDTs) are low cost tools with varying sensitivity and specificity depending on the manufacturer. Sensitivity of RDTs is typically 200 parasites/ μL or lower resulting in infections with low parasitemia often testing negative for malaria. Loop-mediated isothermal DNA Amplification (LAMP) has exhibited a sensitivity of 5 parasites/ μL in trials conducted with a theoretical processing time of one hour [47, 59, 104]. The choice of diagnostic tool is a critical one as many countries may not have the expertise nor be able to afford expensive equipment required for highly sensitive techniques. On the other hand, the use of simpler, less sensitive tools like RDTs may result in a number of asymptomatic and sub-patent infections remaining undetected to contribute further to the infectious reservoir.

2.1.3 Tools against Malaria

Vector Control through Insecticide Treated bedNets (ITN), Indoor Residual Spraying (IRS) and larviciding are methods of combatting malaria transmission by acting on the mosquito vector. ITNs prevent mosquito bites on those sleeping beneath them while IRS of building structures aims to prevent vectors from entering the structure. Larviciding of identified breeding sites aims to decrease the mosquito-human ratio as an additional measure of decreasing the force of infection (Entomological Inoculation Rate (EIR)). Other interventions include Mass Drug Administration (MDA), the treatment of an entire population of interest with an antimalarial drug regardless of disease status or the presence of symptoms. This strategy may be targeted at smaller geographical locations through targeted MDA (tMDA) and at targeted populations (Infants, Pregnant women etc) through Intermittent Preventative Treatment (IPT). Mass Screen and Treat (MSAT) involves screening populations first to determine the presence of infection before administering a drug and when aimed at smaller geographical units, is known as Focal Screen and Treat (FSAT). Mass Fever Treatment (MFT) is another mass action tool aimed at treating members of a population who are febrile [137].

2.1.4 Elimination

Since the call in October 2007 for renewed efforts towards achieving global malaria eradication, more than 25 previously endemic countries are in the pre-elimination/elimination phase of the eradication effort [51, 108]. Since 2007 the United Arab Emirates, Morocco, Turkmenistan and Armenia have been certified as having eliminated malaria [145]. Malaria elimination has been officially defined "as reducing to zero the incidence of locally acquired malaria infection in a specific geographic area through deliberate efforts" [31, 37]. The milestones and progress from

control to elimination are depicted in Figure 2.2. A country enters the pre-elimination phase when the slide positivity rate is less than 5% in fever cases or incidence is less than 5 cases per 1000 population at risk per year. Once in this pre-elimination phase, the country attempts to decrease incidence to less than 1 case per 1000 population at risk per year to enter the elimination phase. Having successfully achieved zero *locally* sourced cases in three years, a country may apply for certification from WHO [80].

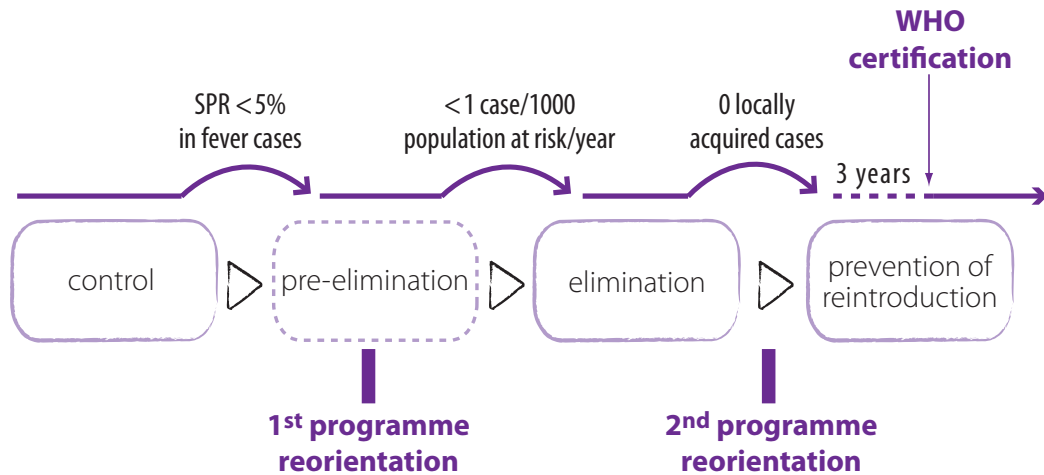


Figure 2.2: Epidemiological milestones from control to elimination. SPR: slide or rapid diagnostic test positivity rate. These milestones are indicative only: in practice, the transitions will depend on the malaria burden that a programme can realistically handle (including case notification, case investigation, etc.) Source: [80]

With vector-borne diseases like malaria, strategies to eliminate may be unsuccessful if they focus only on the biology of vector and parasite, and ignore the mobility patterns of humans [3]. This is particularly true in countries where the majority of infections are imported. A malaria elimination strategy should aim to interrupt the transmission cycle and prevent it from being re-established. An elimination strategy that employs ‘more of the same’ approach may decrease malaria incidence, but will be insufficient to eliminate it as the focus needs to shift from better overall control to the identification of residual transmission foci leading to the last few infections. The interruption of the transmission cycle and prevention of its re-establishment theoretically requires three elements: (1) the elimination of the mosquito vector to prevent onward transmission, (2) blockading the inflow of imported infections and (3) reduction of infections at their source [89]. The first element is realistically and operationally infeasible and has not been recommended [80]. The second element could be achieved if borders were closed, or more realistically if imported infections were identified and treated at border entry points before they can contribute to the local infectious reservoir. The third element would require regional collaboration with

these sources of imported infections to reduce transmission in the region [89].

Since the call for renewed efforts towards global malaria eradication in 2007, it has been acknowledged that new tools will be required to achieve this ambitious goal. [129–133]. Drugs will need to be developed for a variety of purposes including use in elimination-focused strategies like Mass Drug Administration and Mass Screen and Treat campaigns, prophylactic use and transmission prevention [131]. New insecticides and formulations will need to be developed incorporating varied vector biology and habits[133]. Importantly, diagnostic tools that are easily implemented with increased sensitivity and a decreased processing time will be necessary to quickly and successfully diagnose both patent and sub-patent infections[130].

2.2 Malaria Incidence and Control in Mpumalanga

2.2.1 History

South Africa, having experienced a sharp decline in malaria cases since the last epidemic in 2000, already meets the pre-elimination phase criteria set out by the World Health Organisation (WHO) (< 5 cases per 1000 population at risk) and has been ear-marked to achieve elimination by 2018 [93]. Mpumalanga is one of three provinces in South Africa where malaria transmission still occurs and malaria is actively controlled (Figure 2.3). Malaria in Mpumalanga is seasonal, starting with the first rains in October, peaking in January and remaining high till May; yet transmission is still unstable and prone to sporadic outbreaks. Malaria control in South Africa and Mpumalanga is well documented [11, 42, 88, 95, 113–115]. Malaria is distributed mainly in the low-lying areas bordering Swaziland and Mozambique, with a favourable climate for malaria transmission. Nkomazi, Bushbuckridge, Mbombela, Umjindi and Thaba Chewu local municipalities (part of the Ehlanzeni district) are the areas mostly affected by malaria. Transmission is most intense in the municipalities bordering Mozambique.

As malaria is a notifiable disease in South Africa, malaria information systems have been developed to record all malaria cases that are *Plasmodium* positive through a rapid diagnostic test or by slide microscopy [49]. The rapid diagnostic test currently in use at South African public health facilities has a theoretical detection threshold of 200 parasites/ μ L and a maximum processing time of 20 minutes. Active case detection, a strategy of following up notified cases to verify the source of infection that then allows for further screening and treating of symptomatic people, is also employed in the province. Owing to an increase in gametocyte carriage following sulphadoxine-pyremethamine (SP) treatment in 2002, the province made a switch to SP-artesunate in 2003, followed by artemether-lumefantrine (AL) in 2006 [9, 49, 73]. Vector control in the province includes indoor residual spraying using primarily dichlorodiphenyl-trichloroethane (DDT) and larviciding at identified breeding sites [95]. There were also two collaborative cross-border initiatives aimed at reducing incidence in participating countries. The

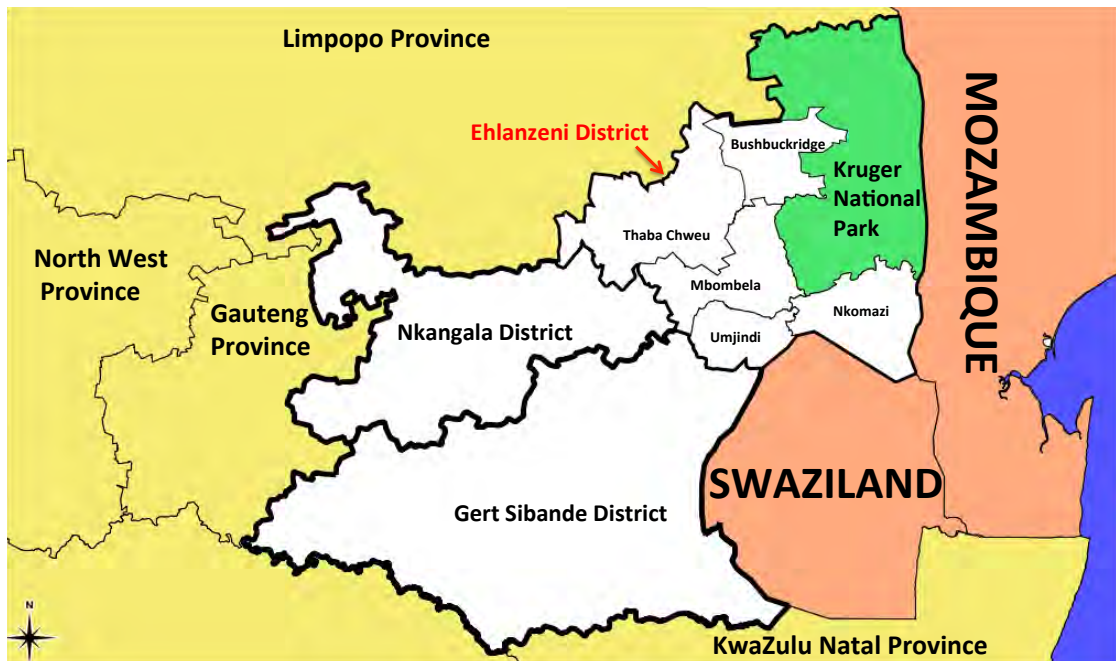


Figure 2.3: Mpumalanga Province (white) with the five municipalities of Ehlanzeni District (credit: Mpumalanga Malaria Elimination Programme (unpublished))

Trans-Limpopo Malaria Initiative targeted the Matabeleland South province of Zimbabwe and Limpopo province in South Africa, and the Lubombo Spatial Development Initiative (LSDI) targeted eastern Swaziland, Maputo and Gaza provinces in Mozambique and Kwazulu-Natal province in South Africa [74, 114]. The LSDI malaria programme focused its activities in Mozambique where malaria is regarded as the most important public health problem and is responsible for 29% of all deaths[105]. Antimalarial intervention took place primarily in Maputo province and was later extended to Gaza Province in Mozambique resulting in substantial decreases in prevalence[70]. The programme was however terminated early in September 2010 and the reduced IRS in Maputo thereafter correlated with increased malaria incidence observed from 2011[105].

2.2.2 Imported Infections

Migration and its impact on malaria transmission are affected by both the primary physical location where the infection resides as well as the source of the infection. Migrant human populations may affect transmission in two key ways. Firstly, people from areas of low malaria transmission move to areas of high transmission and having little or no immunity become infected. In the second case, people from areas of high transmission may harbour parasites and transmit

these when they move to areas of low transmission. Having partial or full immunity, they may not exhibit clinical symptoms and hence become hidden reservoirs of infection [136]. In Mpumalanga, the number of imported cases is large, exceeding the number of locally sourced cases in 2005. Between 2002 and 2012, 41% of treated cases were sourced in South Africa and 54% sourced from Mozambique (the remaining 5% being sourced from other African and Asian countries). The proportion of annual imported cases has increased from 39% in 2002 to 87% in 2012 [116].

The Mozambican civil war in the 1980's resulted in an influx of refugees into the Transvaal (now Limpopo and Mpumalanga provinces) and between 1990 and 2004, Mozambicans more than any other foreign national group were deported [63]. It is likely that illegal migrants entering South Africa work for short periods on farms in Mpumalanga as a form of "involuntary repayment" for assistance in crossing the border unlawfully [78]. The high concentration of Mozambican workers on the South African side of the border is partly explained by the relative ease with which illegal immigrants can cross the border [12]. In April 2005 the South African and Mozambican governments waived the visa requirements between these two countries and this subsequently led to increased movement between the two countries [97].

2.3 Mathematical Modelling in Epidemiology

The first known contribution of mathematical modelling in epidemiology is Daniel Bernoulli's work on the inoculation against smallpox in 1760 [14]. Ross, Halmer, Soper, Kermack and McKendrick all contributed to the application of compartment models to epidemiology between 1900 and 1935 [2]. The model proposed by Kermack and McKendrick in 1927 has come to be known as the Susceptible-Infective-Recovered (SIR) model with underlying equations:

$$\frac{dS}{dt} = -\beta SI \quad (2.1)$$

$$\frac{dI}{dt} = \beta SI - \frac{1}{\alpha} I \quad (2.2)$$

$$\frac{dR}{dt} = \frac{1}{\alpha} I \quad (2.3)$$

where t is time, S is the susceptible population (at risk of infection), I is the infectious population (capable of transmitting infection) and R is the recovered population (removed and playing no further role in the epidemic). β is the number of contacts per unit time and $1/\alpha$ is the rate of recovery.

This model results in a fixed population N ($S+I+R$) where members of the population mix homogeneously (interact with one another to the same degree). There is no entry into or departure from the population as the dynamics of the disease are much faster than the time scale of birth

and death processes; and hence the impact of these processes on the population can be ignored. Any inherent age, demographic and spatial structure is also ignored. There is no initial immunity as all ‘members’ of the susceptible population are equally likely to get infected. The model infers permanent immunity; once recovered, a second infection is impossible. The incubation period of the infectious agent is instantaneous and the duration of infectivity is the same as the duration of the disease (one is infectious as long as one has the disease). Discrete individuals do not exist in the model and it is assumed that individuals who reside in the compartments are identical and as such variation among individuals is unimportant. Thus compartment models are described as population-level models. It is fractions of the population that flow between compartments and these movements are continuous. The rate of recovery $1/\alpha$ is constant for each ‘member’ of the population and hence the average duration of infectiousness (and in this case disease) is α .

There are several extensions of the SIR model, including the Susceptible-Infectious (SI) model where immunity is ignored (by excluding the Recovered compartment), the Susceptible-Exposed-Infectious-Recovered (SEIR) model that allows for a period of latency/exposure before becoming infectious, the Susceptible-Infectious-Recovered-Susceptible (SIRS) model that allows for temporary immunity and other similar models [60]. As diseases have different characteristics, these models may be extended to include biology (stages of immunity, vector/pathogen dynamics, super-infection), demography (birth and death processes, age, gender), interventions (drug therapy, vaccines, vector control) and geography (spatial structure, migration). Even the same disease may be modelled with very different structures.

2.3.1 Mathematical Modelling of Malaria

Groups such as the MalERA Consultative Group on modelling, have recognised the contribution mathematical modelling can make to the elimination of malaria globally and have highlighted priority areas that modelling can inform, such as optimal resource allocation, strategies to minimise the evolution of drug and pesticide resistance, assessment of new tools to interrupt malaria transmission, assessment of combinations of such tools, the coverage targets and expected timelines needed to achieve elimination goals and the assessment of operational feasibility with respect to costs and human resource capacities [132].

With malaria, a single infection does not confer lifelong immunity resulting in a need for an additional flow from the Recovered to the Susceptible state in an SIR model i.e. an SIRS model. There have been several such models applied to different aspects of malaria (Figure 2.4) [82]. For example, Koella and Antia published SIRS models incorporating resistance to drug therapy and super-infection, Yang incorporated socio-economic and environmental factors into SEIR models for hosts and vectors (incorporating dynamics in an SEI model for mosquitoes), Torres-Sorando and Rodriguez included migration and visitation in an SIS model and Auger *et al* extended the Ross-Macdonald model to several patches in a meta-population compartment

model [7, 66, 82, 110, 135, 147, 148].

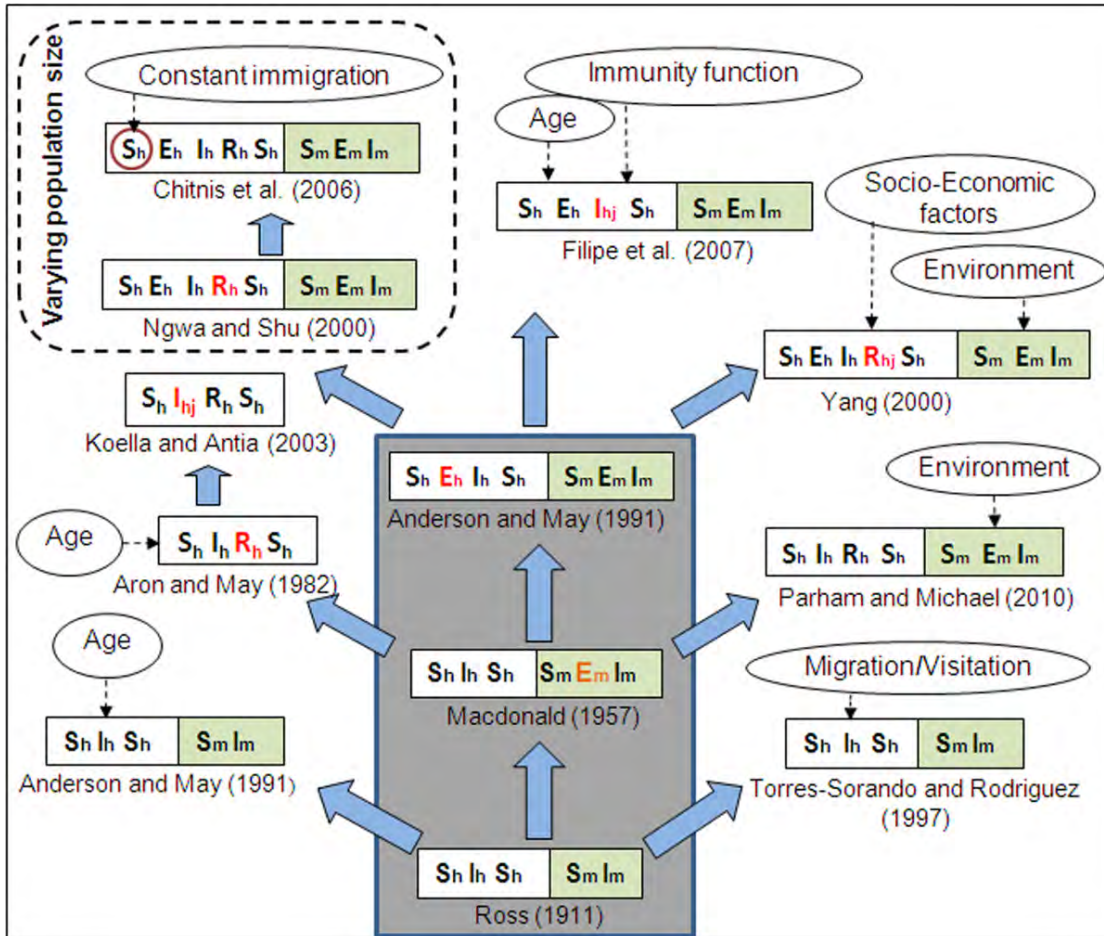


Figure 2.4: Evolution and grouping of different types of SEIR malaria models. Subscripts 'h' and 'm' stands for human and mosquito. Double-folded boxes are for both human & mosquito population, and single fold boxes are only for human. First time addition of a new compartment is shown in red. The subscript 'j' (= 1, 2, 3) indicates further subdivision of the corresponding compartment. Three models inside the big grey box are considered as the Basic malaria models. Dotted arrows show the incorporation of complex factors in different models or specific compartment (red circle). Total population size is constant for all models, except the ones inside the dashed box. Sourced from [82].

There have been several mathematical models developed to inform policy by predicting the impact of interventions such as IPT, Vaccine usage, Vector Control, MDA and MSAT. O'Meara *et al.* and Alexander *et al.* modelled the potential impact of IPT on the spread of drug-resistant malaria, Gosling *et al.* and Cairns *et al.* investigated the impact of IPT on infants, and Carneiro *et al.* developed a decision support tool for sub-Saharan Africa to model IPT in infants [1, 16, 17, 39, 40, 101]. Halloran *et al.*, Struchiner *et al.*, and Smith *et al.* modelled the impact

of malaria vaccines [53, 120, 121, 126]. Applications of mathematical modelling to vector control include Chitnis *et al.*, who used mathematical modelling to compare the effectiveness of vector control interventions and Killeen *et al.* who considered the implications of mosquito dispersal for control interventions [20, 65]. The global focus on malaria elimination has sparked renewed interest in the potential of mass treatment to decrease malaria incidence. Okell *et al.*, Maude *et al.*, Gosling *et al.*, Slater *et al.*, Crowell *et al.* and White *et al.* all considered the impact of mass treatments as a potential intervention [27, 41, 84, 85, 99, 118, 141].

The complexity of the mathematical models developed is often determined by a series of factors: how the population is described (individual membership or proportions of a population), the incorporation of randomness in the model, how progress in time is measured (discretely versus continuously), the inclusion of time-dependent rates and the degree of mixing in the model [112]. In compartment models, members of a population are described by the characteristics of the state to which they belong. It is these characteristics that define their behaviour and their potential to transmit infection. Population-level models assume that populations are large enough to average out any deviations caused by the heterogeneity in individual behaviour. This assumption is not always suitable, particularly if a rare disease is being modelled or in the case of malaria, elimination of the last-remaining infections is being explored. Unlike population models, Individual Based Modelling (IBM) models the behaviour of individuals, thereby allowing the heterogeneous behaviour of individuals to be captured by the model. In this manner, each individual is tracked and both population and individual characteristics are taken into account to determine transmission potential. Executing an individual based model requires developing an algorithm that subjects individuals to a set of user-defined rules to stochastically govern individual behaviour. The focus on the individual in IBMs allows such models to include more detailed and realistic descriptions of a disease process and with greater ease than population level models. [112]. There have been several applications of IBMs in malaria. Maire *et al.* used IBMs in a model for natural immunity to blood stage malaria infections in endemic areas, Smith *et al.* and Griffin *et al.* developed simulation models to predict the impact of interventions on infection, for Africa in particular, in the case of Griffin *et al.* and Okell *et al.* assessed the contribution of mass interventions to malaria control [46, 76, 99, 122].

Calibrating IBMs to data requires a comprehensive dataset with individual level data on the characteristics modelled. As such data is not always available, other population-based methods exist to incorporate heterogeneity in models such as metapopulation or patch modelling. Metapopulation modelling, an extension of population level modelling, involves disaggregating a population into several groups of interest that results in homogeneity in one or more aspects in each group [112]. This allows the groups to be modelled with parameters suitable to each group rather than using one set of parameters to describe the entire population. Dependencies between the groups may also be included in the models where for example, the number of infections in one group is dependent on the number of infections in other groups. This is one method which may be used to describe movement between geographical areas where each geographical area is

modelled as separate group. There have been several applications of metapopulation modelling in malaria and other infectious diseases. Ariey *et al.* used the metapopulation concept to examine the spread of chloroquine resistance, while Oluwagbemi *et al.*, Le Menach *et al.* and Smith *et al.* modelled malaria transmission assuming the migration of the mosquitoes only and Arino *et al.*, Zorom *et al.*, Auger *et al.* and Rodriguez and Torres-Sorando accounted for human migration [4, 5, 7, 67, 100, 109, 119, 152].

2.3.2 Mathematical Modelling of Malaria in South Africa

Applications of mathematical modelling in Mpumalanga include a climate-based fuzzy distribution model of malaria transmission in sub-Saharan Africa (including a region containing Mpumalanga) [26]. Coleman *et al.* used the SaTScan methodology in Mpumalanga to detect local malaria clusters to guide the provincial control programme, and Montosi *et al.* considered soil-water content as a driver of malaria incidence; applying both an eco-hydrological model and a transfer function model to incidence data in three South African provinces (including Mpumalanga) [24, 87].

The mathematical models developed in this dissertation constitute the first study designed for the purpose of predicting the impact of elimination-focused interventions in Mpumalanga and the first to do so since the call for malaria elimination in South Africa.

Chapter 3

Data

Describing malaria transmission requires data on both treated and untreated cases to capture the populations that are unable to access treatment, as well as the asymptomatic population. It is rarely the case that such data is available as the asymptomatic population would not usually present for treatment at a health facility. The only data available in Mpumalanga are case notification data, i.e. those cases that presented for treatment at a public health facility, and actively detected cases where index cases are followed up in home and malaria diagnostic tests are performed on members of nearby households. This data is sourced from the provincial Integrated Malaria Information System (IMIS) under the management of the Malaria Elimination Programme of the Mpumalanga Department of Health. Ethical approval for the use of this secondary notification data was obtained from the University of Cape Town Human Research Ethics Committee and the Mpumalanga Department of Health.

The data includes the the following information: date of diagnosis, age, gender, mortality indicator, drug, facility name, administrative municipality, source of infection (country, province, locality) and place of residence (country, province, locality). Source of infection has been determined for all cases in the province, whereby a case is classified as imported if the patient travelled to a malaria-endemic area in the past month or if there is no evidence of local transmission (vectors or cases within 500 m radius of the place of residence)[74]. Monthly case data from the province of Maputo in Mozambique was obtained for the study period from the Mozambique National Ministry of Health.

Understanding malaria transmission in Mpumalanga requires the exploration of the number of cases per year (to measure annual incidence) and the temporal and spatial patterns in which those cases occur. This paper "Exploring the Seasonality of reported treated malaria cases in Mpumalanga, South Africa" is an exploration of the IMIS dataset to describe the temporal and spatial patterns that underpin the malaria season in Mpumalanga. This paper is an es-

sential component of this dissertation as it is necessary to understand malaria transmission in Mpumalanga first before attempting to replicate it through mathematical modelling.

SPS, KIB and FL conceived and designed the experiments. SPS analysed the data. GK and AM provided the data. SPS wrote the paper and KIB, FL, GK and AM reviewed manuscript and provided extensive comments.

We are grateful to the National Research Foundation in South Africa for funding provided to support this research. We are also grateful to the Malaria Elimination Programme of the Department of Health in South Africa, the Mozambique National Ministry of Health and the South African Weather service for the provision of data.

Exploring the seasonality of reported treated malaria cases in Mpumalanga, South Africa

Sheetal Prakash Silal^{1,*}, Karen I Barnes², Gerdalize Kok³, Aaron Mabuza³, Francesca Little¹

1 Department of Statistical Sciences, University of Cape Town, Cape Town, South Africa

2 Division of Clinical Pharmacology, Department of Medicine, University of Cape Town, Cape Town, South Africa

3 Malaria Elimination Programme, Mpumalanga Department of Health, Nelspruit, South Africa

3.1 Abstract

South Africa, having met the World Health Organisation's pre-elimination criteria, has set a goal to achieve malaria elimination by 2018. Mpumalanga, one of three provinces where malaria transmission still occurs, has a malaria season subject to unstable transmission that is prone to sporadic outbreaks. As South Africa prepares to intensify efforts towards malaria elimination, there is a need to understand patterns in malaria transmission so that efforts may be targeted appropriately. This paper describes the seasonality of transmission by exploring the relationship between malaria cases and three potential drivers: rainfall, geography (physical location) and the source of infection (local/imported). Seasonal decomposition of the time series by locally estimated scatterplot smoothing is applied to the case data for the geographical and source of infection sub-groups. The relationship between cases and rainfall is assessed using a cross-correlation analysis. The malaria season was found to have a short period of no/low level of reported cases and a triple peak in reported cases between September and May; the three peaks occurring in October, January and May. The seasonal pattern of locally-sourced infection mimics the triple-peak characteristic of the total series while imported infections contribute mostly to the second and third peak of the season (Christmas and Easter respectively). Geographically, Bushbuckridge municipality, which exhibits a different pattern of cases, contributed mostly to the first and second peaks in cases while Maputo province (Mozambique) experienced a similar pattern in transmission to the imported cases. Though rainfall lagged at 4 weeks was significantly correlated with malaria cases, this effect was dampened due to the growing proportion of imported cases since 2006. These findings may be useful as they enhance the understanding of the current incidence pattern and may inform mathematical models that enable one to predict the impact changes in these drivers will have on malaria transmission.

Published in PLoS ONE on 29 October 2013

3.2 Introduction

Despite being a treatable and preventable mosquito-borne disease, malaria is still an immense global health, economic and social burden. In 2010, latest estimates suggest 219 million cases with an uncertainty range of (154 million, 289 million) cases globally. There were 660 000 deaths due to malaria; with 90% of deaths occurring in Africa and most cases and deaths occurring in sub-Saharan Africa [143]. Malaria has been recognized as a disease of poverty with vulnerable groups facing several barriers to access for antimalarial interventions [111, 146]. South Africa, having experienced a sharp decline in malaria cases since the last epidemic in 2000, already meets the pre-elimination phase criteria set out by the World Health Organisation (WHO) (< 5 cases per 1000 population at risk) and has been ear-marked to achieve elimination by 2018 [93]. Mpumalanga is one of three provinces in South Africa where malaria transmission still occurs. Malaria in Mpumalanga is seasonal, starting with the first rains in October, peaking in January and remaining high till May; yet transmission is still unstable and prone to sporadic outbreaks. As government begins to intensify efforts and commit scarce resources towards malaria elimination, there is a need to understand patterns in transmission so that efforts may be targeted appropriately. Mathematical modelling is increasingly being used to test policy interventions so as to determine their impact on simulated transmission before implementing the intervention in the field. Understanding the nature of the seasonality of transmission will enable better mathematical modelling and this may lead to better allocation of scarce resources and ultimately a greater impact on malaria. This paper aims to explore the seasonality of malaria cases in the Mpumalanga province as part of a larger project in mathematical modelling of malaria transmission and the impact of antimalarial interventions. We analyse data on reported treated malaria cases from 2002 to 2012. In particular, this paper explores the temporal and geographic behavior patterns as well as potential drivers behind these patterns.

Malaria control in South Africa and Mpumalanga is well documented [11, 42, 88, 95, 113–115]. Malaria is distributed mainly in the low-lying areas bordering Swaziland and Mozambique, with a favourable climate for malaria transmission. Nkomazi, Bushbuckridge, Mbombela, Umjindi and Thaba Chewu local municipalities (part of the Ehlanzeni district) are the areas mostly affected by malaria (Figure 3.1). Kruger National Park and surrounding lodges have been incorporated into the Bushbuckridge and Mbombela municipalities and comprise 1.7% of all cases in the study period. Transmission is most intense in the municipalities bordering Mozambique. Table 3.1 shows the incidence rates for all cases treated in the province by local municipality using population estimates from Statistics South Africa [125]. While there is a sharp decrease in incidence in the province between 2002 and 2012, this decrease is not consistent over the local municipalities. *Plasmodium falciparum* is the predominant parasite that is transmitted primarily by the *Anopheles arabiensis* vector [43].

As malaria is a notifiable disease in South Africa, malaria information systems have been devel-

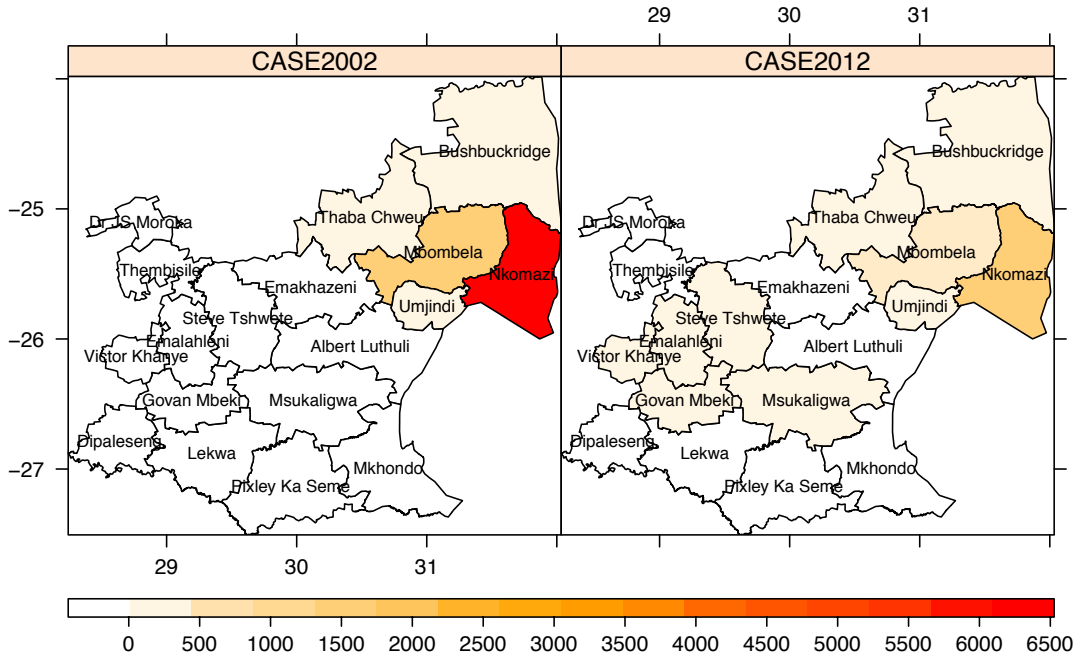


Figure 3.1: The number of reported treated cases for all the municipalities in Mpumalanga Province for 2002 and 2012.

Table 3.1: Malaria Incidence Rates and the change in cases in Mpumalanga Province and the municipalities in Ehlanzeni District.

Area	2002 Cases	2002 Incidence per 1000 people	2012 Cases	2012 Incidence per 1000 people	% Change in Cases
Mpumalanga	7933	238	2745	68	-65%
Nkomazi Municipality	6100	1793	1540	394	-75%
Mbombela Municipality	1316	270	637	108	-52%
Bushbuckridge Municipality	282	56	312	58	11%
Umjindi Municipality	177	320	120	172	-32%
Thaba Chewu Municipality	34	41	23	23	-32%

oped to record all malaria cases that are *Plasmodium* positive through a rapid diagnostic test or by slide microscopy [49]. Active case detection, a strategy of following up notified cases to verify the source of infection thereby allowing further screening and treating of symptomatic people, is also employed in the province. Owing to an increase in gametocyte carriage following sulphadoxine-pyremethamine (SP) treatment in 2002, the province made a switch to SP-artesunate in 2003, followed by artemether-lumefantrine (AL) in 2006 [9, 49, 73]. Vector control in the province includes indoor residual spraying (IRS) using primarily dichorodiphenyl-

trichloroethane (DDT) and larviciding at identified breeding sites [95]. There were also two collaborative cross-border initiatives aimed at reducing incidence in participating countries. The Trans-Limpopo Malaria Initiative targeted the Matabeleland South province of Zimbabwe and Limpopo province in South Africa, and the Lubombo Spatial Development Initiative targeted eastern Swaziland, Maputo and Gaza provinces in Mozambique and Kwazulu-Natal province in South Africa [74, 114].

This paper will examine the seasonal pattern of malaria cases using time series methods and explore the relationship between cases and three potential drivers: rainfall, geography and source of infection. The relationship between malaria transmission and climate has been examined extensively [26, 36, 56, 83, 127] and Ngomane and de Jager [95] showed that rainfall was the only significant climatic factor in this Mpumalanga dataset examined between 2001 and 2009. Migration and its impact on malaria transmission are affected by both the primary physical location where the infection resides as well as the source of the infection. Migrant human populations may affect transmission in two key ways. Firstly, people from areas of low malaria transmission move to areas of high transmission and having little or no immunity become infected. In the second case, people from areas of high transmission may harbour parasites and transmit these when they move to areas of low transmission. Having partial or full immunity, they may not exhibit clinical symptoms and hence become hidden reservoirs of infection [136]. As Mpumalanga shares a border with Mozambique (which has a higher malaria prevalence) and Swaziland, it is of interest to assess both the geography and source of infection as potential drivers of the seasonality of cases in Mpumalanga.

3.3 Methods

3.3.1 Ethics statement

This study is an analysis of secondary data. Ethical approval for use of the notification data was obtained from the University of Cape Town Human Research Ethics Committee and the Mpumalanga Department of Health. Written consent was given by the patients for their information to be stored in the hospital database and used for research.

3.3.2 Data

To explore malaria cases, one would require data on both the treated and untreated cases to capture the populations that are unable to access treatment, as well as the asymptomatic population. As asymptomatic people would not usually present for treatment at a facility, it is rarely the case that such data is available. The only data available in Mpumalanga are those cases that presented for treatment at a public health facility and actively detected cases where index

cases are followed up in home and malaria diagnostic tests are performed on nearby households. This data is sourced from provincial Integrated Malaria Information System (IMIS) under the management of the Malaria Elimination Programme of the Department of Health. The data also included the following information: date of diagnosis, age, gender, mortality indicator, drug, facility name, administrative municipality, source of infection (country, province, locality) and place of residence (country, province, locality). Source of infection has been determined for all cases in the province, whereby a case is classified as imported if the patient travelled to a malaria-endemic area in the past month or if there is no evidence of local transmission (vectors or cases within 500m radius of the place of residence) [74]. Provincial border changes in the study period required the addition of malaria cases from Bushbuckridge pre-2006 (then part of Limpopo province) and the exclusion of cases from Limpopo post-2006. Source of infection data was not always available for this additional data, which comprises only 3.4% of all cases. Monthly case data from the province of Maputo in Mozambique was obtained for the study period from the Mozambique National Ministry of Health. The analysis of the relationship between rainfall and cases required obtaining monthly rain data for the Ehlanzeni district from the South African Weather Services for the study period.

3.3.3 Data Analysis

Case data was compiled in a weekly format in Stata 11 and analysed using time series methods [124]. As case data usually exhibits noise, it is often difficult to draw conclusions on seasonal patterns based on the case data itself and hence there is a need to extract the seasonal pattern from the data. In particular, Seasonal decomposition of Time series by LOESS (STL) method of extracting components was used to assess the seasonal pattern of the data. Decomposition methods generally separate a time series into a trend (moving average) component, a seasonal (systematic temporal variation) component, a cyclical (repeated non-periodic fluctuations) component and a residual (remainder; irregular random) component [15]. STL is one such decomposition method where LOESS (LOcally Estimated Scatterplot Smoothing) is applied iteratively to the observations in moving time windows to filter the time series in a way that results in estimates of trend and seasonality that are robust to aberrant behaviour in the time series (Cleveland, 1990). As STL decomposition is used for descriptive purposes only, it is not necessary for the residual series to be normally distributed.

The relationship between weekly rainfall and weekly reported treated cases is assessed through a cross-correlation analysis of the pre-whitened series (removing all autoregressive, moving average, integrated components and seasonal dynamics to achieve a series that has a zero mean, constant variance and no correlation between observations at different points in time) to determine if any lagged values of rainfall are significantly correlated with reported treated cases. The series are pre-whitened using Seasonal AutoRegressive Iterated Moving Average (SARIMA) methods.

Data analysis is performed in R v3.0.1 [106].

3.4 Results

The analysis for the case data is presented first followed by an assessment of the relationship between cases and rainfall, cases and physical geography and thirdly, cases and source of infection.

3.4.1 Case Data

Figure 3.2 shows the annual and weekly counts of reported treated cases over the period 2002 to 2012. In this period, there were 40 650 reported malaria cases (imported and local) and 256 deaths due to malaria in the province. Efforts to scale-up IRS in the province and the switch to artemisinin-based combination therapy have contributed to the 65% decrease in reported cases since 2002. Annual reported figures for malaria remained consistently low after the surge of cases in 2006, but the 2011 and 2012 counts are considerably higher than preceding years. The total time series of reported treated cases is decomposed into trend, seasonal and random components using the STL decomposition.

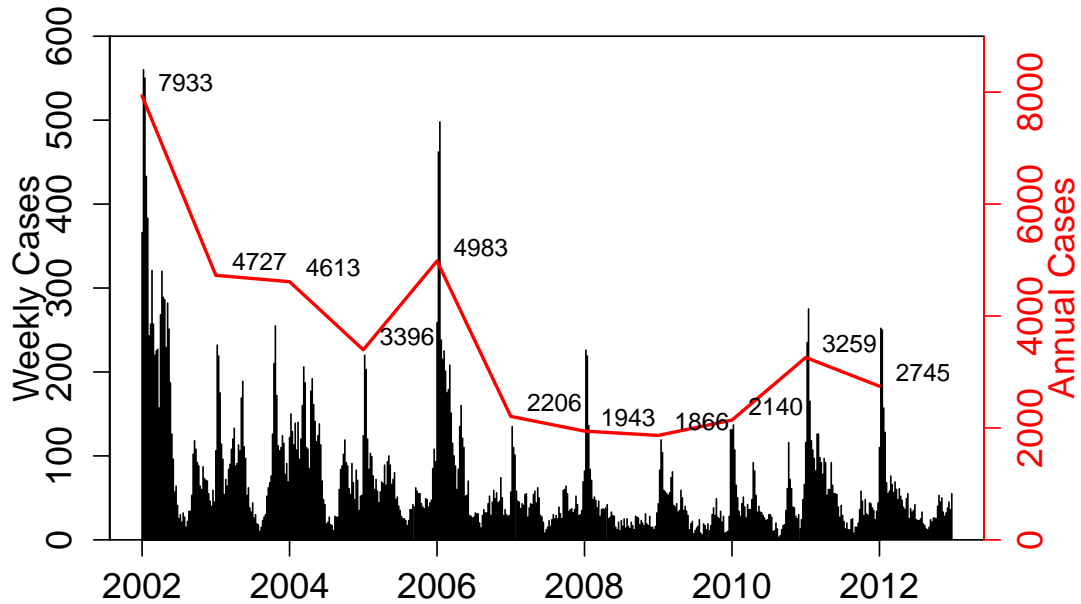


Figure 3.2: The weekly and annual reported treated malaria cases in Mpumalanga Province between 2002 and 2012.

The crude data series in Figure 3.3 (top panel) appears at face value to have pronounced seasonal pattern from 2002 to 2006, but this becomes less distinct post-2006. The STL decomposition however extracts the general seasonal pattern that is unlike standard single-peaked sinusoidal annual seasonal patterns. The seasons are characterized by very short periods of no/low level of reported cases and a triple peak in reported cases between September and May. The trend component shows the steady decrease in reported cases since 2002, with a sharp increase in 2006 and a more moderate increase recently in 2011. The span in lags of the loess window used for the seasonal, trend and low pass filter extraction are 53, 79 and 53 respectively. Other smoothing parameters may be used to perform the extraction of the trend. While fine or coarse smoothing parameters may lead to a more aggregated trend or a less smooth trend respectively, the general decline in cases is still very evident. The remainder component is the component of the time series that remains after the trend and seasonal components have been removed from the series. It can be used to detect anomalies in the data; points in the data set where the reported cases series has deviated from the trend and seasonal patterns. For example, the seasonal component suggests that the second peak is usually higher than the first peak; yet in 2004 the upward spike in the remainder component highlights that the first peak of the season was higher than the second peak. The remainder component also depicts the sharp increase in the series in 2006.

Figure 3.4 focuses on 2 years so as to highlight the timing of the season. It can be seen that the first peak in reported cases occurs approximately between weeks 38 and 44 (mid-September to end-October), the second peak occurs between weeks 52 and 4 (end-December to end-January) and the third peak occurs between weeks 14 and 22 (start-April to end-May).

3.4.2 Cases and Rainfall

Ngomane and de Jager [95] assessed the relationship between malaria incidence and rainfall, relative humidity and minimum and maximum temperature in an ARIMA framework and found rainfall to be the only significant climatic factor. The seasonal pattern of monthly rainfall coincides with the height of the malaria season early on in the time series but appears to lag the season post 2006 (Figure 3.5). Further the period of higher rainfall pre-2006 appears to correspond with the higher number of cases reported (and treated) in 2006, but this does not appear to be the case for the higher number of cases in 2011 and 2012.

The STL seasonal decomposition of rainfall reveals a single peak that coincides generally with the main peak of the case data (Figure 3.6). This analysis is pursued as epidemiologically, rainfall has a delayed impact on malaria incidence due to the incubation and latent phases of the parasite in the vector and the host. Of interest is thus to analyse the correlation between lagged rainfall values and malaria incidence. A cross correlation analysis is performed between lagged rainfall and the case data. The case and rain series are pre-whitened to avoid spurious correlations. The series are square-rooted first to stabilise the variance and then the Box-Jenkins

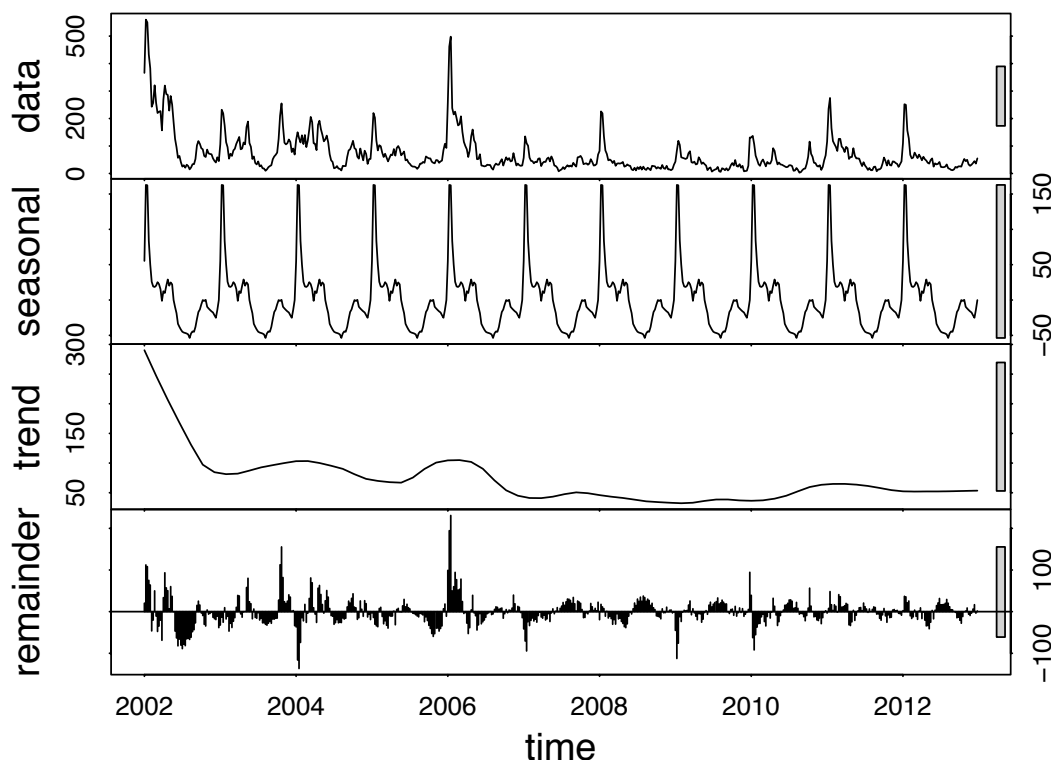


Figure 3.3: STL decomposition on reported treated malaria cases in Mpumalanga Province between 2002 and 2012.

modelling algorithm is used to select the resultant SARIMA(1, 1, 1)(0, 1, 1)₁₂ model [102]. This model was selected as it had the lowest Akaike Information Criterion value among all models and made epidemiological sense. There is no autocorrelation or partial autocorrelation present in the residual series. It was found that there is a significant positive correlation of 0.21 between values of monthly rain at lag 1 (4 weeks) and monthly cases (assessing negative lags, as lagged cases cannot be used to predict rainfall).

3.4.3 Cases and Source of Infection

To further explore the drivers behind the three-peaked seasonal pattern of the case data, foreign and locally sourced case counts are assessed. Each reported case is assessed to determine if the infection is obtained from a local source (within South Africa) or from a foreign source (outside South Africa). Figure 3.7 compares the trend and seasonal components for locally and foreign-sourced infections for all reported treated cases. Locally sourced infections have been on a steady decrease since 2002, remaining at very low levels while foreign-sourced infections show

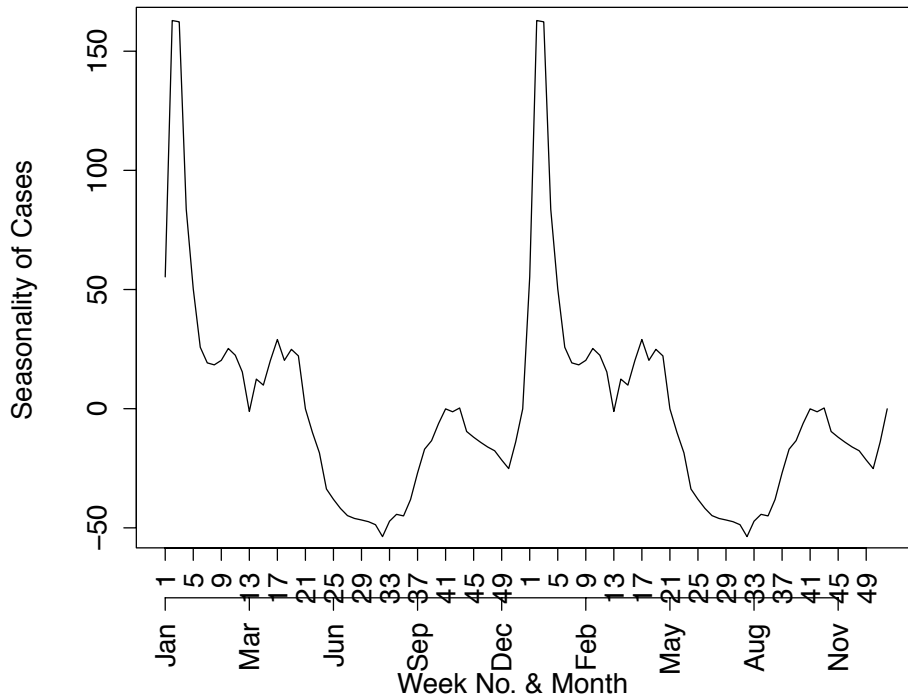


Figure 3.4: Two year seasonal trend of reported treated malaria cases in Mpumalanga Province between 2002 and 2012.

an increase in 2006, with a further increase in 2010 and has remained at this level since.

The seasonal pattern of the locally-sourced infection mimics the triple-peak characteristic of the total series while foreign-sourced infections appear to contribute mostly to the second and third peak of the malaria season, and not the first peak of the total series (Figure 3.3: 2nd panel). The annual distribution of foreign and locally sourced infections has changed considerably during the study period (Figure 3.8). Foreign-sourced infections have dominated locally sourced infections since 2005, and this proportion has been increasing since. At the end of 2012, 87% of all reported treated cases had a foreign-source.

3.4.4 Cases and Physical Geography

Physical geography is assessed with regards to location within Mpumalanga (local municipalities) and the pattern of cases in the contiguous Maputo province in Mozambique.

Nkomazi, Mbombela and Bushbuckridge have consistently been the municipalities with the highest number of reported treated cases. Figure 3.9 shows the weekly counts of reported treated cases for each of the municipalities against the backdrop of the time series for all municipalities. Nkomazi is clearly home to most of the reported malaria compared to Mbombela, and

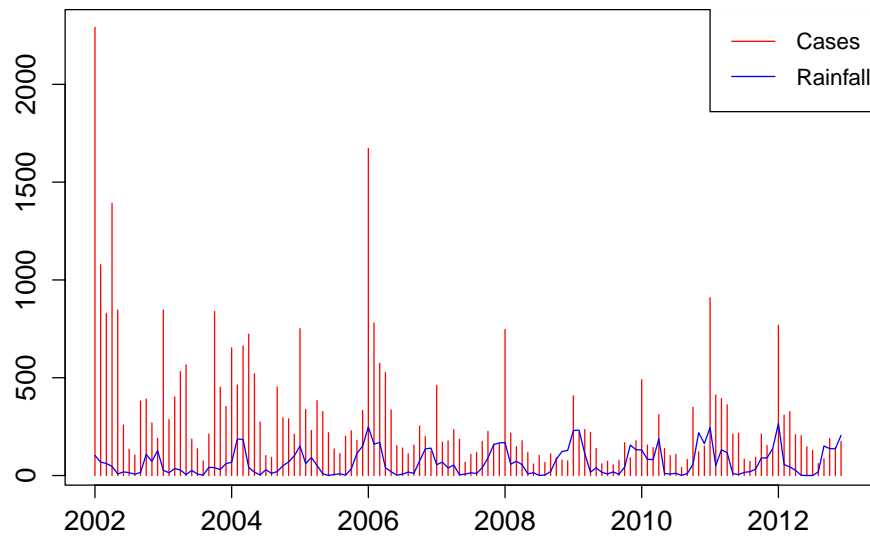


Figure 3.5: Weekly malaria cases and monthly average rainfall (mm) in Mpumalanga Province between 2002 and 2012.

while Bushbuckridge on its own, does not contribute greatly to total malaria, its contribution is sporadic with unusually large number of cases in 2004, 2006 and 2010 - 2012.

Looking at the seasonal components extracted from these municipalities, one can see that both Nkomazi and Mbombela municipalities exhibit the triple-peak pattern as seen for the total series. Reported treated cases in Bushbuckridge municipality also exhibit a triple-peak but the first and second peaks are approximately the same size unlike in the other municipalities (Figure 3.10).

Of the 40 650 cases analysed, 41% of cases were sourced in South Africa and 54% sourced from Mozambique (the remaining 5% being sourced from other African and Asian countries). Figure 3.11 depicts the monthly case profile for Maputo province and Figure 3.12 shows the seasonal profile for the two provinces where the peak of the malaria season in Maputo corresponds to the second and third peaks of the Mpumalanga season. This is consistent with the seasonal pattern of foreign-sourced infections presented earlier.

3.5 Discussion

Malaria transmission in Mpumalanga is characterized by a triple-peak in the season where the first peak occurs in September/October, the second (and also main) peak occurs in January and the third peak occurs in April/May. Assessing the STL seasonal components of the source and geographical location of infection shows that the first peak is driven by mainly locally-sourced infections and the second and third peaks are driven mainly by foreign-sourced infections. This

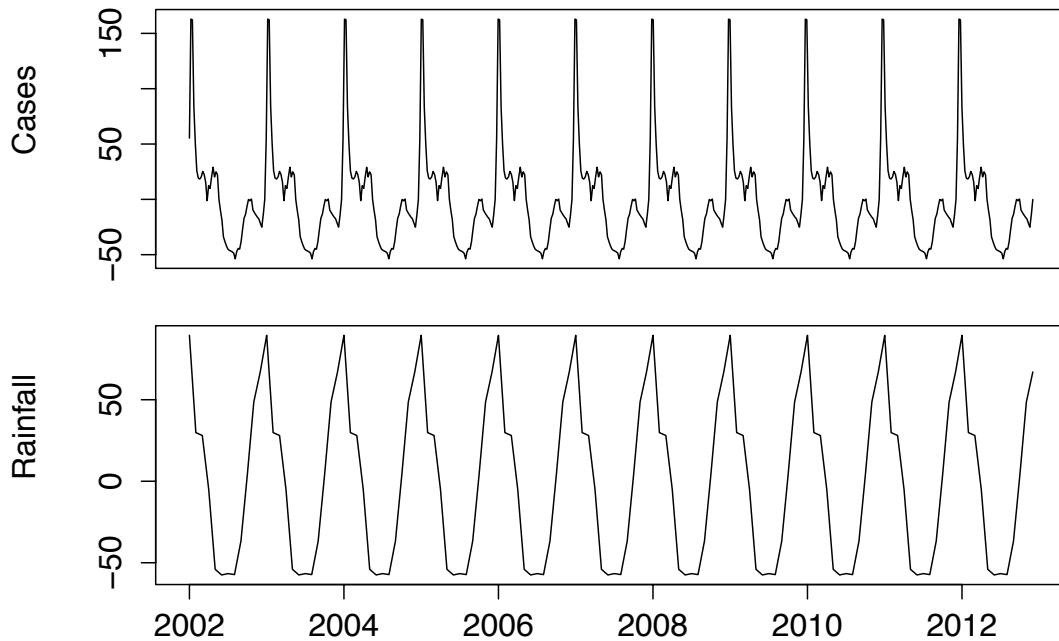


Figure 3.6: Seasonal trend of weekly malaria cases and monthly average rainfall in Mpumalanga Province between 2002 and 2012.

is supported by the Maputo data where the peak of the season in Maputo corresponds to the second and third peak of the Mpumalanga season. Geographically, Bushbuckridge, the northern most municipality, contributes specifically to the first and second peaks, while the other two municipalities studied contribute equally to all three peaks.

Monthly rainfall lagged at 1 month was found to be significantly associated with monthly cases, yet the seasonal pattern of rainfall does not appear to characterize the triple peak pattern of the case data. The decline of local cases in Mpumalanga may be a reason for this, where cases from a foreign source are more likely to be affected by rainfall in the source area (e.g. Mozambique) than local rainfall. If the increase in the proportion of foreign-sourced cases persists, rainfall may become even less of a driver for malaria.

Having reduced its malaria burden significantly since 2002, South Africa has embraced a malaria elimination target of 2018 [93]. To achieve this, suites of malaria control interventions will be deployed in Mpumalanga and other provinces affected by malaria. The likely impact of these interventions may be measured through mathematical modelling. The MalERA Consultative Group on Modelling has recognized the contribution mathematical modelling can make to the elimination of malaria globally and has developed a framework of priority areas for modelling to

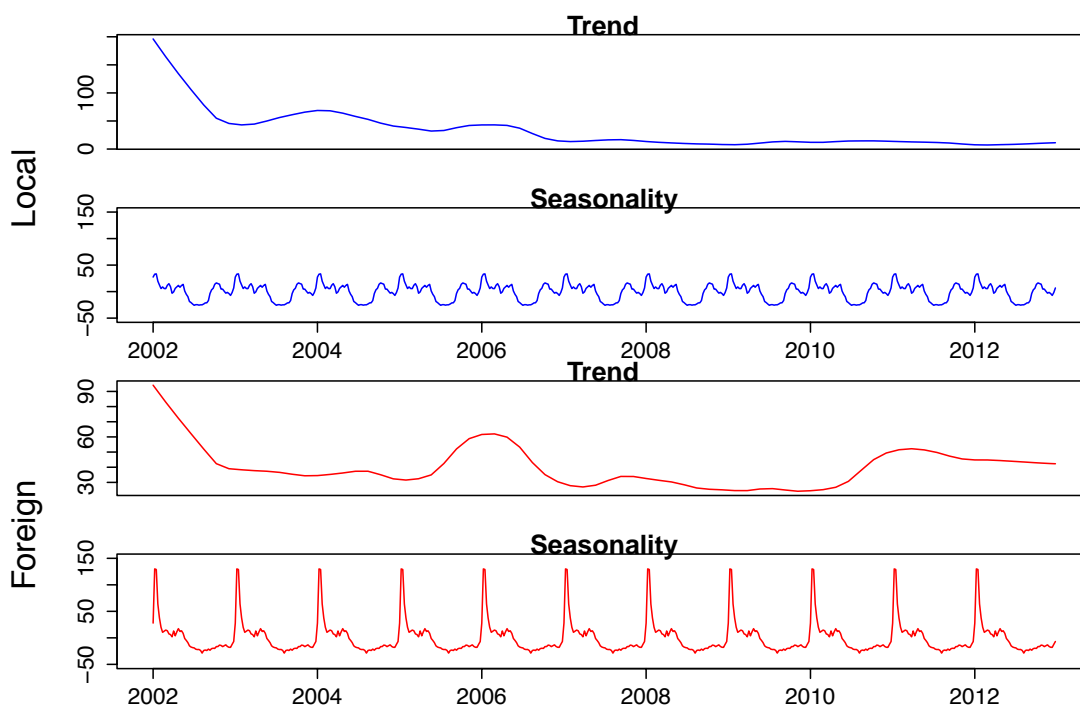


Figure 3.7: Seasonality and trend components of an STL decomposition of locally and foreign-sourced malaria cases in Mpumalanga Province between 2002 and 2012.

assess and inform: optimal resource allocation, strategies to minimize the evolution of drug and pesticide resistance, new tools to interrupt malaria transmission, combinations of tools, coverage targets and expected timelines to achieve goals as well as to assess operational feasibility with respect to costs and human resource capacities [132]. Using mathematical modelling to adequately represent malaria transmission requires knowledge on the drivers of the geographic and temporal trends in malaria transmission and this in turn may lead to finding malaria control strategies that target these drivers directly rather than strategies that may generally control transmission but not interrupt it. The primary interest of mathematical modelling in this setting is to provide practical guidance to malaria programme managers on how to conduct more efficient and effective control and elimination activities. This paper assesses the seasonal trend of cases for different sub-groups of the population, based on the source of infection and geography. If an elimination activity such as the scale-up of larviciding is under consideration, knowing the seasonal pattern of locally sourced cases (larviciding impacts locally sourced cases directly) allows managers to optimally time the larviciding activities with the breeding patterns of the mosquitoes. While malaria elimination requires the reduction to zero of locally sourced cases only, interventions aimed at reducing foreign sourced cases can reduce onward transmission. Knowing the seasonal

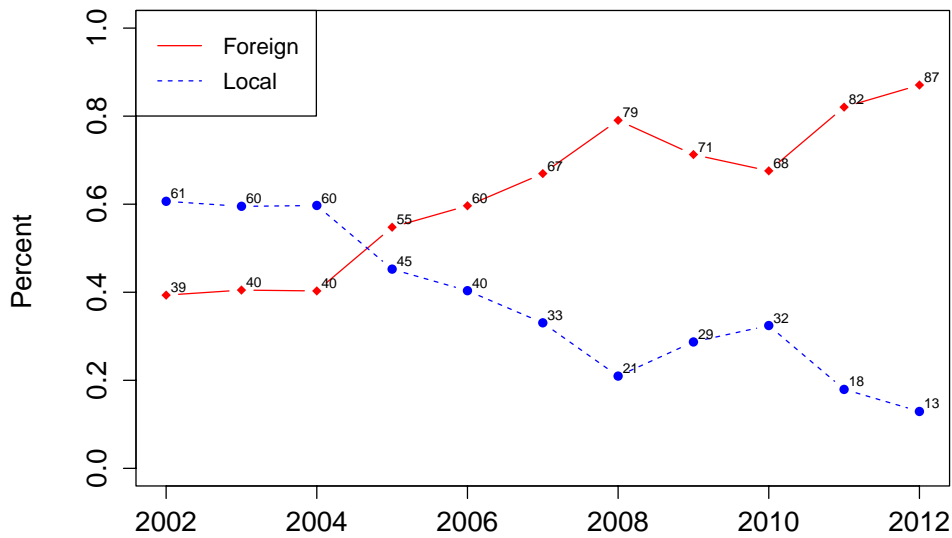


Figure 3.8: Percentage plot of locally and foreign-sourced malaria cases in Mpumalanga Province between 2002 and 2012.

pattern of foreign sourced cases allows programme managers to optimally time interventions such as mass screen and treat campaigns at border posts with travel/migration patterns. Understanding the seasonal differences between managerial districts like municipalities can also assist with optimal allocation of drugs and staff. These are some of the many practical uses of mathematical modelling in health management.

The rising percentage of imported or foreign-sourced cases suggests the need for intensive monitoring. The second and third peaks of the season (which comprise mainly foreign-sourced cases) correspond to holiday seasons (Christmas and Easter). As the majority of cases are sourced from Mozambique, there is a need to intensify cross-border collaborations now and even more so after elimination has been achieved in South Africa. This increase in foreign-sourced cases also highlights the importance of including migration in mathematical models of malaria transmission to obtain realistic estimates of the impact of malaria control and malaria elimination focused strategies.

There are two main limitations of this study. Firstly, the case data available is for those who were treated at public health facilities and some private practices and no malaria case information is known for others treated in the private sector and the untreated population. The untreated population may represent vulnerable groups such as the very poor who are often unable to access treatment and illegal immigrants who may avoid the health system. If the latter group has developed immunity to malaria and is therefore asymptomatic, they could be responsible for

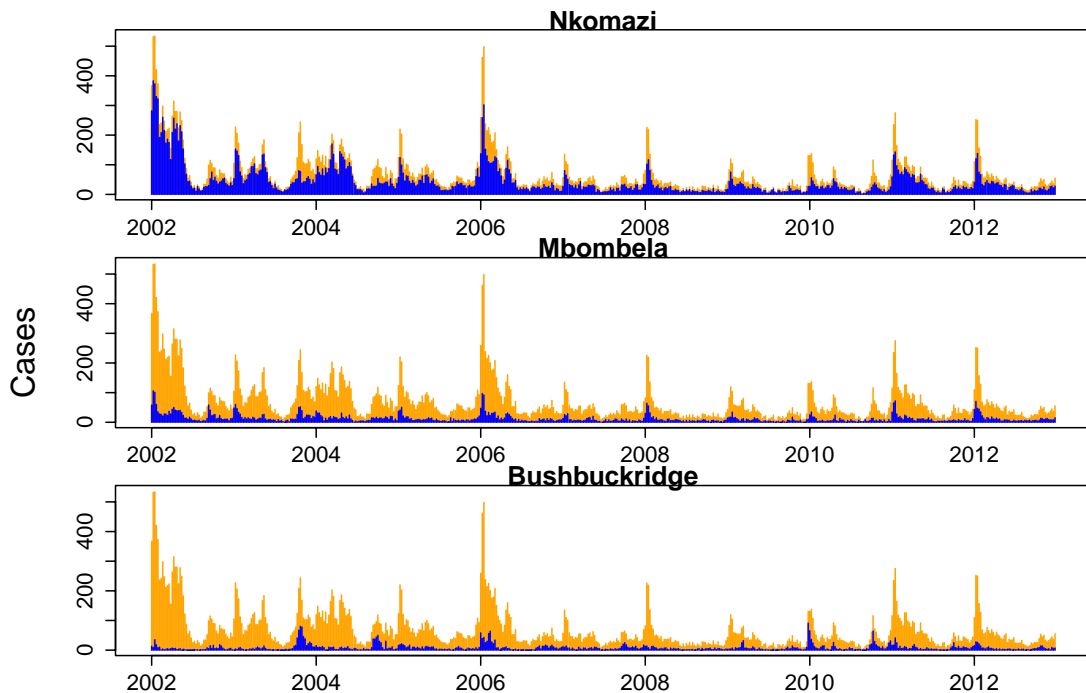


Figure 3.9: Weekly malaria cases in Nkomazi, Mbombela and Bushbuckridge Municipalities (blue) between 2002 and 2012 are shown against the backdrop of the total cases in Mpumalanga province (orange).

unknowingly transmitting the disease. Secondly, routine surveillance data are also subject to errors in reporting that may bias the analysis. The collection of notification data is still recommended by WHO with active/passive case detection assisting in the identification of additional asymptomatic cases. A provincial census or a mass screen and treat campaign could provide cross-sectional data on the untreated population, but this is both costly and non-informative temporally.

3.6 Conclusion

Mpumalanga province in South Africa has experienced a 65% decrease in reported treated cases since 2002. In this time, the percentage imported cases of this total has increased from 39% to 87%. Using weekly reported treated cases, the geographic and temporal trends in malaria transmission was explored to reveal an atypical triple-peak pattern in cases with a short period of a small number of cases. This seasonality was explored in relation to rainfall, source of infection and geographic location. A cross correlation analysis revealed that one month lagged rainfall was

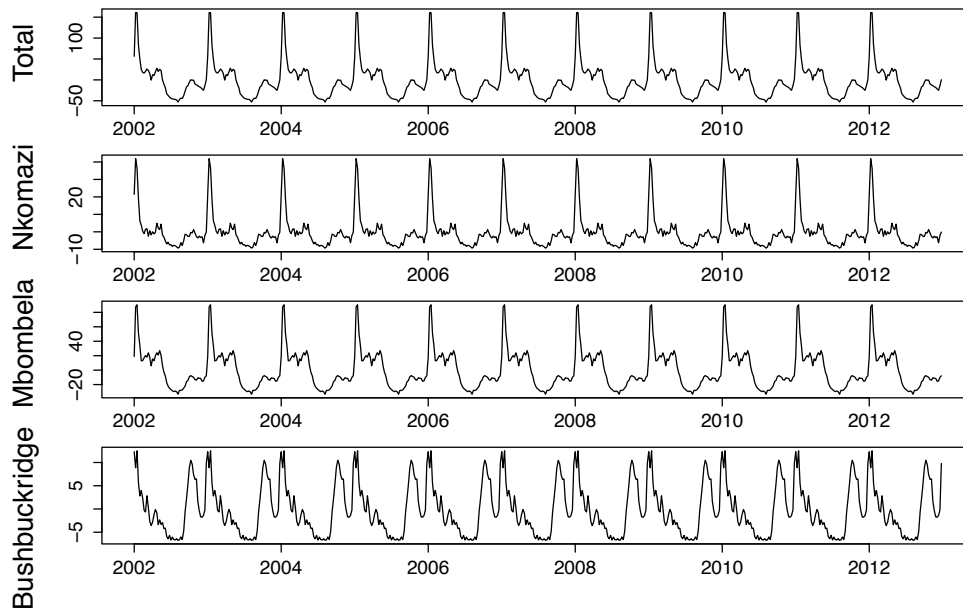


Figure 3.10: Seasonal trend of weekly malaria cases in Nkomazi, Mbombela and Bushbuckridge Municipalities between 2002 and 2012.

significantly associated with reported treated cases, but the seasonality of rain did not appear to explain the unusual pattern of malaria cases. Analysis of the source of infection revealed that local cases contribute to all three peaks but foreign cases contribute primarily to the Christmas and Easter peaks. Geographically, Bushbuckridge municipality (northern most municipality) had a greater relative contribution of cases in the first (September/October) peak. Malaria transmission in Mpumalanga may be low, but it is also unstable and a change in climate and the source of infection may lead to a spike in infection and generally a modification of the incidence pattern. These findings may be useful as they enhance the understanding of the current incidence pattern and can be incorporated in mathematical models that enable one to predict the impact changes in these drivers will have on malaria transmission. Further, as mathematical modelling is being used to assess timeframes for malaria elimination and the potential impact of elimination-focused interventions, understanding the seasonal trends of malaria is key to designing a targeted temporal and spatial approach that can be applied in resource-scarce settings.

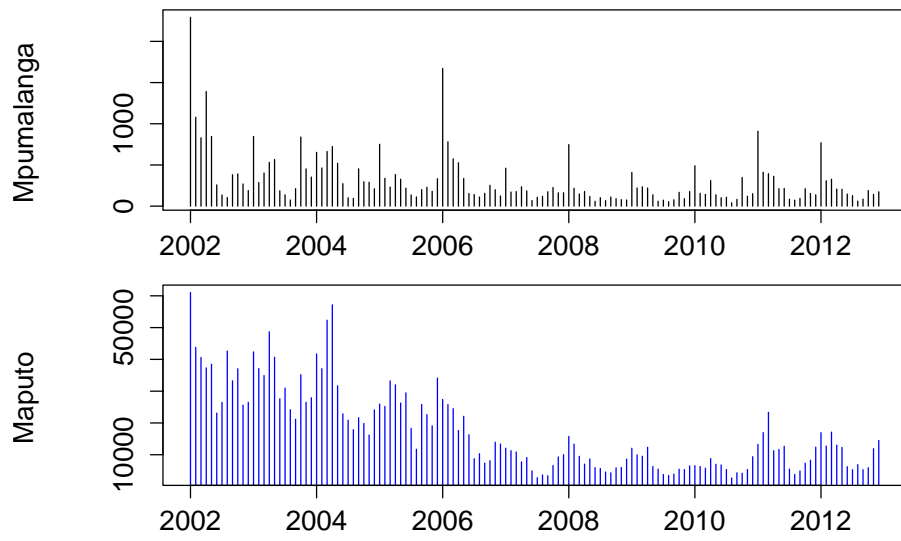


Figure 3.11: Monthly malaria cases in Mpumalanga and Maputo, Mozambique between 2002 and 2012.

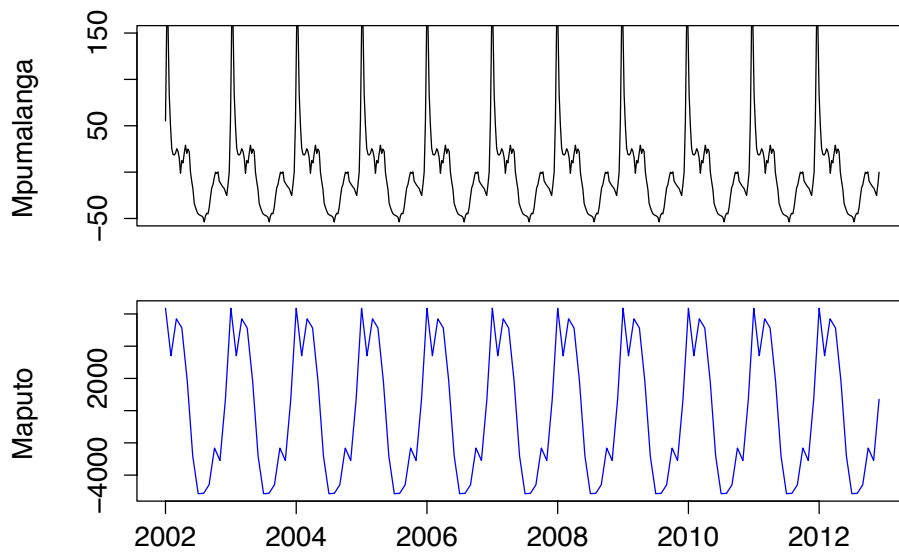


Figure 3.12: Seasonal trend of monthly malaria cases in Mpumalanga and Maputo, Mozambique between 2002 and 2012.

Chapter 4

Model structure

The very first step in choosing to replicate a transmission pattern using a mathematical model is to decide on the class of model and structure for that model. In choosing to model malaria transmission for the population of Mpumalanga, it is more efficient to use a population level compartment model structure rather than an IBM structure as modelling individual characteristics for a large population is very computationally intensive and individual heterogeneity in results is likely to even out in a large population. More importantly, there is no data for Mpumalanga that may be used to calibrate such a model. As outlined in Chapter 2, a variety of compartment model structures have been used to simulate disease transmission. Even for a specific disease, different model structures have been used depending on the use to which the model was put.

Compartment models have been used to provide a framework for understanding disease transmission dynamics in the human population for over 100 years. The predictions from these models are often policy-relevant and as such need to be robust to model assumptions, parameter values and model structure. While sensitivity to model assumptions and parameter values is routinely assessed, model structure is often chosen in advance and not subject to sensitivity testing. Hence it is necessary to first explore the sensitivity of compartment models to model structure before selecting a structure to model malaria transmission in Mpumalanga.

The following paper entitled "Sensitivity to model structure: A comparison of compartment models in epidemiology" assesses sensitivity to model structure by comparing a selection of epidemiologically relevant compartment models in a number of ways: differences in model predictions in the implementation of routine drug therapy, general vector control, mass drug administration and whether these predictions differ between models if the models have been fitted to data or not. The paper finds that compartment models produce wide-ranging estimates of treatment coverage, incidence and prevalence of disease but when the models are fitted to data, the estimates obtained are robust to model structure. This suggests that there may be an argument for

selecting simple models over complex ones, but the complexity of the model should be determined by the purpose of the model and the use to which it will be put. It is necessary to include this paper in this dissertation as it provides an introduction to compartment modelling and provides the foundation and reason for the model structures employed to simulate malaria transmission in Mpumalanga.

This paper has been submitted to a special edition of the Operations Research for Health Care journal. SPS wrote the paper and performed the mathematical model development and analysis. SPS and LJW conceptualised the mathematical models and analysis. FL, KIB and LJW reviewed the manuscript extensively. All authors have read and approved the manuscript.

Sensitivity to model structure: A comparison of compartment models in epidemiology

Sheetal Prakash Silal^{1,*}, Francesca Little¹, Karen I Barnes², Lisa J White^{3,4},

1 Department of Statistical Sciences, University of Cape Town, Cape Town, South Africa

2 Division of Clinical Pharmacology, Department of Medicine, University of Cape Town, Cape Town, South Africa

3 Mahidol-Oxford Tropical Medicine Research Unit, Mahidol University, Bangkok, Thailand 4 Centre for Tropical Medicine, Nuffield Department of Clinical Medicine, Churchill Hospital, University of Oxford, Oxford, UK

4.1 Abstract

Mathematical models, and in particular compartment models, have been used to provide a framework for understanding disease transmission dynamics in human population for over 100 years. The predictions from these models are often policy-relevant and as such need to be robust to model assumptions, parameter values and model structure. While sensitivity to model assumptions and parameter values is routinely assessed, model structure is often chosen in advance and not subject to sensitivity testing. In this paper, various compartment models with the same parameter values but different model structures (ranging from simple structures to complex ones) were compared in the absence and presence of drug therapy. Models were fitted to data to assess if this might reduce sensitivity to model structure. Several policy interventions were tested on both the data-dependent and data-independent sets of models. The compartment models produced wide-ranging estimates of treatment coverage, incidence and prevalence of disease but when the models were fitted to data, the estimates obtained were robust to model structure. When scaling-up drug therapy in an attempt to eliminate the disease, models were found to produce wide ranging estimates of the time to elimination regardless of being fitted to data. Given that differences in model predictions between compartment models can at times be reduced by data fitting, there may be an argument for selecting simple models over complex ones, but the complexity of the model should be determined by the purpose of the model and the use to which it will be put.

Under review at *Operations Research for Health Care*

4.2 Introduction

Advances in computational power have led to mathematical modelling being used increasingly to solve real-world problems in all fields and levels of decision-making. In epidemiology, mathematical models and in particular compartment models, have been used to explore (among other things) the emergence and spread of disease, and the impact and efficacy of interventions such as drug treatment, vaccine introduction and parasite control [92]. There is no single compartmental model structure that fits all diseases and there are many different structures that may be used to model the same disease. The results of these models are often policy-relevant and in many cases used by policy makers to estimate populations at risk, design and implement strategies to combat disease and monitor and evaluate on-going interventions. In this regard, models are and should be subjected to rigorous sensitivity testing [21]. This testing process involves identifying parameters that strongly influence model outcomes and testing assumptions that when relaxed, strongly influence model results. These model assumptions can pertain to population size and initial conditions among other things. While sensitivity is assessed in the case of model assumptions and parameter values, sensitivity to model structure is not often explored, as the particular model structure is chosen in advance from a suite of models. Studies exploring sensitivity to model structure include Rahmandad and Sterman, who compared compartment models with agent-based models to assess heterogeneity and network structure and Ferrer *et al.* who evaluated the impact of anti-malarial interventions on compartment and agent-based models [34, 107]. Yet there may still be differences in model predictions between compartment models of the same disease with equivalent parameters but different model structure. In this regard, this paper explores the sensitivity of a selection of epidemiologically relevant compartment models that differ only in model structure. While this may seem limited, it serves to show that differences due to model structure may not only occur between classes of models but within them as well. In this paper this sensitivity to model structure is assessed in a number of ways: differences in model predictions in the implementation of routine drug therapy, general vector control, mass drug administration and whether these predictions differ between models if the models have been fitted to data or not. Section 4.3 provides an introduction to compartment models in epidemiology. The models are developed in Section 4.4 and the results (Section 4.5) and discussion (Section 4.6) follow.

4.3 Compartment Models in Epidemiology

The first known contribution of mathematical modelling in epidemiology is Daniel Bernoulli's work on the inoculation against smallpox in 1760 [14]. Ross, Halmer, Soper, Kermack and McKendrick all contributed to the application of compartment models to epidemiology between 1900 and 1935 [2]. The model proposed by Kermack and McKendrick in 1927 has come to

be known as the Susceptible-Infective-Recovered (SIR) model with underlying equations and parameters defined as durations:

$$\frac{dS}{dt} = -\beta SI \quad (4.1)$$

$$\frac{dI}{dt} = \beta SI - \frac{1}{\alpha} I \quad (4.2)$$

$$\frac{dR}{dt} = \frac{1}{\alpha} I \quad (4.3)$$

where t is time, S is the susceptible population (at risk of infection), I is the infectious population (capable of transmitting infection) and R is the recovered population (removed and playing no further role in the epidemic). β is the number of contacts per unit time and $1/\alpha$ is the rate of recovery.

This model results in a fixed population N ($S+I+R$) where members of the population mix homogeneously (interact with one another to the same degree). There is no entry into or departure from the population as the dynamics of the disease are much faster than the time scale of birth and death processes; and hence the impact of these processes on the population can be ignored. Any inherent age, demographic and spatial structure is also ignored. There is no initial immunity as all ‘members’ of the susceptible population are equally likely to get infected. The model infers permanent immunity; once recovered, a second infection is impossible. The incubation period of the infectious agent is instantaneous and the duration of infectivity is the same as the duration of the disease (one is infectious as long as one has the disease). Discrete individuals do not exist in the model and it is assumed that individuals who reside in the compartments are identical and as such variation among individuals is unimportant. Thus compartment models are described as population-level models. It is fractions of the population that flow between compartments and these movements are continuous. The rate of recovery $1/\alpha$ is constant for each ‘member’ of the population and hence the average duration of infectiousness (and in this case disease) is α .

There are several extensions of the SIR model, including the Susceptible-Infectious (SI) model where immunity is ignored (by excluding the Recovered compartment), the Susceptible-Exposed-Infectious-Recovered (SEIR) model that allows for a period of latency/exposure before becoming infectious, the Susceptible-Infectious-Recovered-Susceptible (SIRS) model that allows for temporary immunity and other similar models [60]. As diseases have different characteristics, these models may be extended to include biology (stages of immunity, vector/pathogen dynamics, super-infection), demography (birth and death processes, age, gender), interventions (drug therapy, vaccines, vector control) and geography (spatial structure, migration). Even the same disease may be modelled with very different structures. In the case of malaria, Koella and Antia published SIRS models incorporating resistance to drug therapy and super-infection, Yang incorporated socio-economic and environmental factors into SEIR models for hosts and vectors

(incorporating dynamics in an SEI model for mosquitoes), Torres-Sorando and Rodriguez included migration and visitation in an SIS model and Auger *et al.* extended the Ross-Macdonald model to several patches in a meta-population compartment model [7, 66, 82, 110, 135, 147, 148].

In using several different structures to model the same disease, it is of interest to assess if there are large differences in model predictions due to model structure alone. This paper compares a selection of model structures and the predicted impact of policy interventions. This paper also explores whether fitting the models to data to determine parameter values empirically, reduces sensitivity to model structure.

4.4 Model Development

Different model structures are compared for a disease that has a latent period (L), a period where clinical symptoms have manifested but the host is not yet infectious (B), and an infectious period (I) that does not grant immunity i.e. a person may be re-infected once susceptible (S) again. For example, with the malaria disease, B would represent the state of being febrile and parasitaemic but not yet gametocyaemic, while I represents the gametocyaemic state. These models are compared in the absence and presence of drug therapy. Once infected and clinically ill, a patient has the potential to receive drug therapy and those who do not receive drug therapy recover naturally i.e. they do not die from the disease but recover through the body's natural defences at a period longer than the drug recovery period. Patients may seek drug therapy when symptoms have manifested (they feel ill) as well as at the infectious stage. The natural recovery period is assumed to be longer than the drug recovery period and the time to infectiousness, hence natural recovery is only possible once the disease is at the infectious stage and not any earlier. Birth and death, super-infection and the development of immunity through repeated infections are ignored. Such a disease with a latent period and no immunity would need to be modelled using variants of an SEIS general model structure.

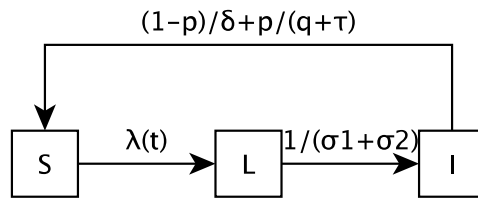
Three models are compared in the absence of drug therapy (SLI, SBI, SLBI) and five models are compared in the presence of drug therapy (SLI, SBI, SLBI, stratified SBI, and stratified SLBI) (Figure 4.1). These models are compared to an alternate version of the SLBI model where the probability of receiving treatment is applied *at the time of acquiring infection* rather than during the infection, as an alternative way of capturing the proportion of infections that are treated (Model 6 in Figure 4.1). This alternate SLBI model assumes a per-infection probability of treatment whereas the other models assume a per unit-time probability of treatment. Differences between models are estimated by measuring incidence and prevalence of the disease and the treatment coverage. This alternate SLBI model is used to simulate data for data-fitting purposes so as to assess if validating models with data through empirical estimation of parameter values reduces the sensitivity of the models to differences in model structure. Finally policy interventions

(vector control and mass drug administration) are also modelled to assess differences in model predictions due to model structure.

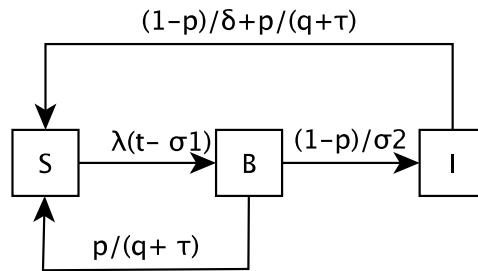
The model parameters driving these models and their assumed values are in Table 4.1. All models are from the Susceptible-Exposed-Infectious-Susceptible (SEIS) class of models where L is used to characterize the latent phase of the disease. In Model 1 (SLI), the latent (L) and symptomatic (B) stages of the disease have been combined; hence the rate of flow between Latent compartment and the Infectious compartment is $1/(\sigma_1 + \sigma_2)$. When incorporating drug therapy into the models, one has to consider at what stage of the disease the population has access to drug therapy. As the disease has a latent stage, it is only in the infectious compartment that the population may seek drug therapy and this occurs at the rate $p/(q + \tau)$ (incorporating the treatment probability (p), the time to seek treatment (τ) and the drug recovery period). This rate naturally comprises two steps: treatment seeking and recovery through drug therapy. As there is no treated compartment in this model to explicitly allow for this, the total time to move from being infectious to becoming susceptible again is $q + \tau$ and hence the population who receive drug therapy (with probability p) do so at a rate of $p \times 1/(q + \tau)$. The population that is infectious but remains untreated recover naturally at the natural recovery rate $((1 - p)/\delta)$.

Models 2 (SBI) and 4 (Stratified SBI) do not have a latent compartment, only compartments reflecting the symptomatic (B) and infectious (I) stages of the disease, where the subscripts u and t in Model 4 represent untreated and treated infections respectively. These models account for the latent period by including a time delay in the force of infection (λ) of size σ_1 . As symptoms have manifested (population feels ill) in the symptomatic compartment (B), the population may receive drug therapy from both this and the infectious compartments. At the symptomatic stage, $p\%$ of the population will seek and receive drug therapy (Model 2) or seek treatment (Model 4) while $(1 - p)\%$ of the population will remain untreated and become infectious. In Model 2, the time to seek treatment is incorporated in the same manner as for Model 1. In Model 4, owing to the inclusion of Symptomatic and Infectious compartments for the *treated* population, the time to seek treatment is incorporated explicitly. The latent and symptomatic stages of the disease are captured separately in Models 3 (SLBI) and 5 (Stratified SLBI) and treatment is incorporated in the same way as Models 2 and 4 respectively. Model 6 stratifies the population into the ‘never treated’ and those ‘destined to be treated’ by multiplying the force of infection λ by the treatment probability (p). Treatment can take place at both the symptomatic and infectious compartments and occurs at the rate $1/(q + \tau)$ (incorporating the time to seek treatment and time to drug recovery) while the untreated recover naturally at the natural recovery rate $(1/\delta)$. The equations underlying all these models are in Section 4.8 at the end of the chapter.

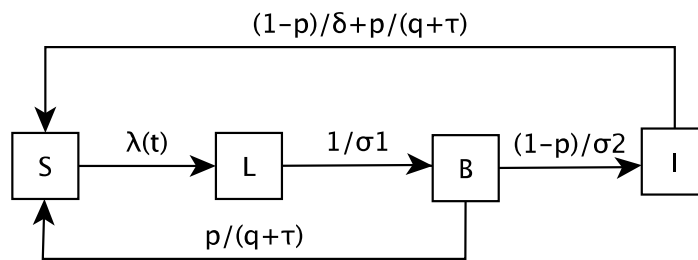
Models are compared using steady state measures of incidence, prevalence and treatment coverage. Incidence is measured as the number of new cases at each time step, prevalence is measured as the population infected with the disease (L, B or I) at each time step and treatment coverage is estimated by cumulative treated cases as a proportion of cumulative cases.



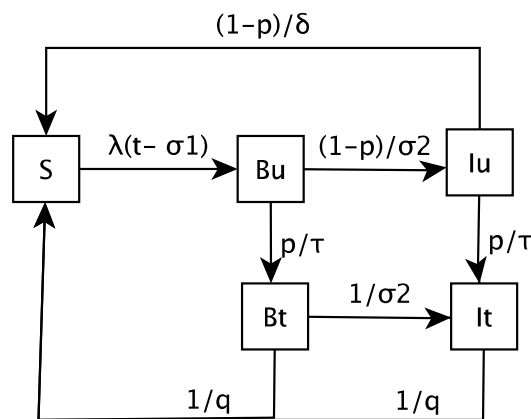
(a) Model 1: SLI (With treatment)



(b) Model 2: SBI (With treatment)

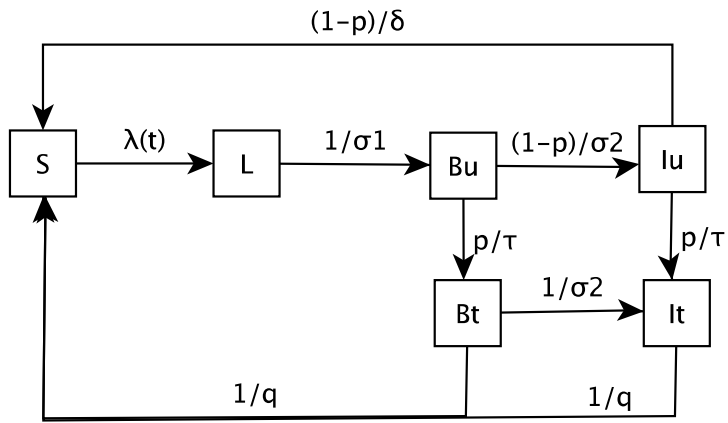


(c) Model 3: SLBI (With treatment)

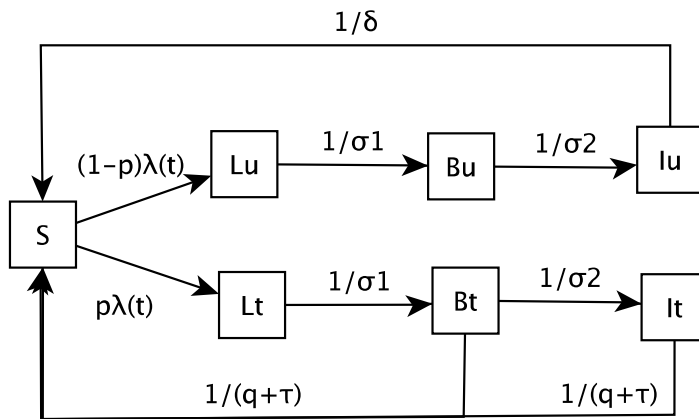


(d) Model 4: Stratified SBI (With treatment)

Figure 4.1: Model Flowcharts



(e) Model 5: Stratified SLBI (With treatment)



(f) Model 6: Alternate Stratified SLBI (With treatment)

Figure 4.1: Model Flowcharts

Table 4.1: Model Parameters: Description and value

Parameter	Description	Value	Rate of flow
σ_1	Period of latency	1 week	$1/\sigma_1$
σ_2	Time to infectiousness	1 week	$1/\sigma_2$
τ	Time to seek treatment	0.5 week	$1/\tau$
q	Drug recovery period	1 week	$1/q$
δ	Natural recovery period	12 weeks	$1/\delta$
p	Probability of treatment	0, 0.1, 0.5, 1	
N	Population Size	1000 people	
β	Contact Rate	10 per annum	β
λ	Force of Infection	$\beta \times I/N$ (Models 1, 2&3) $\beta \times (I_u + I_t)/N$ (Models 4, 5&6)	

4.5 Results

Models were fitted to data using least squares approach [54] and differential equations were solved using the linearised analytic method for ordinary differential equations. All models were programmed in R v3.02 [106]. Model results are presented under the conditions of no treatment, treatment at different levels, and where external anti-disease interventions are imposed on the models. These results are contrasted between models that have been fitted to data and models that have not.

4.5.1 No treatment

Of the six models, only models 1, 2 and 3 are tested under the condition of no drug treatment. This is because when the probability of treatment (p) is 0, model 4 collapses to model 2 and models 5 and 6 collapse to model 3. Under the condition of no treatment, prevalence in the three models is equivalent while incidence differs slightly among model structures (Figure 4.2). Incidence in model 2 is higher than models 1 and 3 because the force of infection λ is a function of the Infectious compartment and the rate of flow between the Symptomatic and Infectious compartments is faster than that between the Latent and Infectious compartments in model 1. Similarly, incidence in model 3 is lower than in models 1 and 2 as the infectious reservoir is comparatively smaller in model 3.

4.5.2 With treatment

Figure 4.3 shows that when imposing a 10% treatment probability on the infected population, models 1-5 predict a higher number of treated cases than model 6 and the treatment coverage, as measured by cumulative treated cases as a proportion of cumulative incidence, is estimated

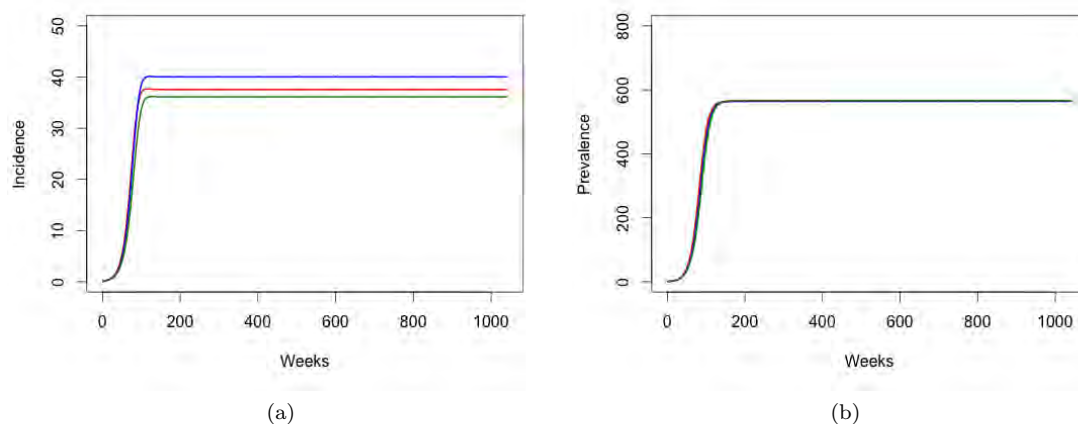
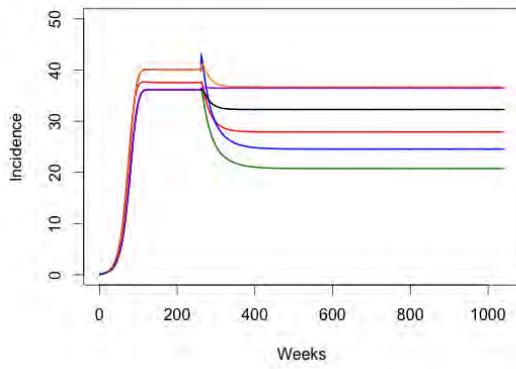


Figure 4.2: No Treatment: Incidence and Prevalence for Model 1 (red), Model 2 (blue) and Model 3 (green)

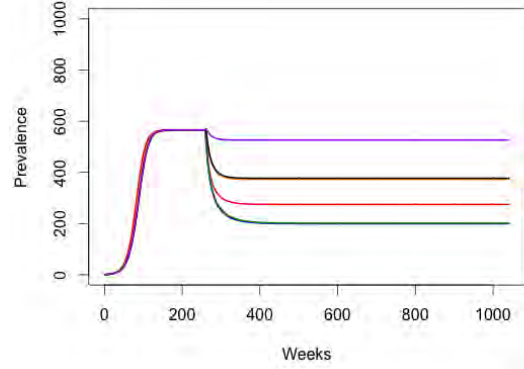
correctly by model 6 (10%) but overestimated by the other 5 models. A 10% probability of treatment implies a treatment coverage between 34% and 39% in models 1-5. The two stratified models (4 and 5) behave similarly in that they have the same prevalence and treatment coverage. Likewise models 2 and 3 behave similarly. The treatment coverage is higher in all models compared to the model 6 because these models predict a higher number of treated cases and lower incidence. At a 50% treatment probability models 1-5 predict a lower number of treated cases than model 6 and the treatment coverage is estimated correctly by model 6 (50%) but underestimated by the other five models (10.6%-17.2%). This is because Models 1-5 also predict that incidence and prevalence will decrease to zero, albeit at different rates, while model 6 maintains stable non-zero prevalence and incidence levels. At a 100% treatment probability, all models predict a decrease in incidence and prevalence to zero, again at varying rates, with model 6 decreasing to zero at the slowest rate compared to the other models. These results are shown in Section 4.9.

4.5.3 Treatment coverage and the probability of treatment

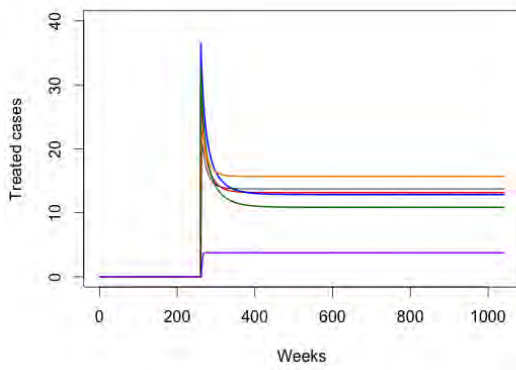
The results in Section 4.5.2 show large differences in treatment coverage in all six models. It is only in model 6 that the treatment coverage reflects the treatment probability. Exploring why this may be so requires understanding of how treatment coverage is estimated mathematically. Generally values of the parameters that drive compartment models may be sourced from literature, take on assumed values or may be estimated from data. In modelling the impact of drug therapy, the proportion of infections that are treated (treatment coverage in this paper)



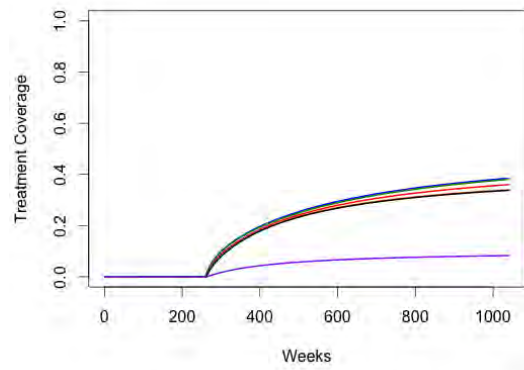
(a)



(b)



(c)



(d)

Figure 4.3: 10% Treatment Probability: Incidence (a), Prevalence (b), Treated Cases (c) and Treatment Coverage (d) for Model 1 (red), Model 2 (blue), Model 3 (green), Model 4 (orange), Model 5 (black) and Model 6 (purple)

is sometimes the best source of data available to mathematical modellers to use to estimate the treatment probability (the chance of receiving drug therapy) in their models. As shown in the results, depending on the structure of the compartment model, these two values (treatment coverage and the treatment probability) will not always be equal. Treatment probability p is *used in the models* to determine the proportion of the infected and infectious populations that get treated and treatment coverage is *estimated from the models* to determine cumulatively, the proportion of cases that actually get treated.

In order to assess the relationship between treatment probability (p) and treatment coverage (denoted as π), consider a simple SIS model ($S+I=1$) for a cohort of infected individuals governed by the equation:

$$\frac{dI}{dt} = \beta IS - \left(\frac{p}{q} + \frac{1-p}{\delta}\right)I \quad (4.4)$$

where β is the number of contacts per unit time, p is the probability of treatment, $1/q$ is the drug recovery rate and $1/\delta$ is natural recovery rate. For ease of computation let $a = p/q + (1-p)/\delta$ and assume initial conditions of $S(0) = 0$ and $I(0) = 1$.

Using the result that in an SIS model, $S = 1 - I$,

$$\frac{dI}{dt} = \beta I(1 - I) - aI. \quad (4.5)$$

Solving this differential equation amounts to solving,

$$\int_{I(0)}^{I(t)} \frac{dI}{\beta I(1 - I) - aI} = \int_0^t ds. \quad (4.6)$$

Using the initial condition $I(0) = 1$, this integrates to

$$- \left(\frac{\ln(I) - \ln(a + \beta I - \beta)}{a - \beta} - \frac{\ln(a)}{a - \beta} \right) = t \quad (4.7)$$

and hence

$$I = \frac{(a - \beta)e^{(\beta-a)t}}{a - \beta e^{(\beta-a)t}}. \quad (4.8)$$

The treatment coverage (π) is a function of the cumulative treated cases (pI/q) and the cumulative cases (βIS).

In particular,

$$\pi = \lim_{t \rightarrow \infty} \frac{\int_0^t \frac{pI}{q} dt}{\int_0^t \beta I(1 - I) dt} \quad (4.9)$$

$$\approx \lim_{t \rightarrow \infty} \frac{\int_0^t \frac{pI}{q} dt}{\int_0^t \left(\frac{p}{q} + \frac{1-p}{\delta}\right)I dt} \quad (4.10)$$

$$(4.11)$$

because in the absence of a warm-up period, the cumulative number of people who enter I will equate to the cumulative number of people who exit stage I . Therefore,

$$\pi = \lim_{t \rightarrow \infty} \frac{\int_0^t \frac{p}{q} \left(\frac{(a-\beta)e^{(\beta-a)t}}{a-\beta e^{(\beta-a)t}} \right) dt}{\int_0^t \beta \left(\frac{(a-\beta)e^{(\beta-a)t}}{a-\beta e^{(\beta-a)t}} \right) \left(1 - \frac{(a-\beta)e^{(\beta-a)t}}{a-\beta e^{(\beta-a)t}} \right) dt} \quad (4.12)$$

$$= \lim_{t \rightarrow \infty} \frac{\frac{p}{q\beta} \left(\ln(\beta e^{\beta t} - a e^{at}) - at - \ln(\beta - a) \right)}{\frac{-a(a-\beta)}{\beta} \left(\frac{\beta e^{\beta t}}{a(\beta e^{\beta t} - a e^{at})} + \frac{at}{a-\beta} + \frac{\ln(\beta e^{\beta t} - a e^{at})}{\beta - a} - \frac{\beta}{a(\beta - a)} - \frac{\ln(\beta - a)}{\beta - a} \right)}. \quad (4.13)$$

Using L'Hospital's rule to simplify the limit equation [68]:

$$\pi = \lim_{t \rightarrow \infty} \frac{\frac{p}{q\beta} \left(\frac{\beta(a-\beta)e^{\beta t}}{a e^{at} - \beta e^{\beta t}} \right)}{\frac{-a(a-\beta)}{\beta} \left(\frac{\beta^2 e^{\beta t} (e^{\beta t} - e^{at})}{(a e^{at} - \beta e^{\beta t})^2} \right)} \quad (4.14)$$

$$= \lim_{t \rightarrow \infty} \frac{p}{-qa(a-\beta)} \times \frac{a-\beta}{\beta} \left(\frac{a e^{at} - \beta e^{\beta t}}{e^{\beta t} - e^{at}} \right). \quad (4.15)$$

Equation 4.15 will tend to a finite limit depending on the relation between a (the average recovery rate) and β (the transmission coefficient). To establish this relation, one can look at the dynamics of the disease when the SIS model has reached a steady state. At equilibrium, the sum of the inflows to a compartment is equal to the sum of its outflows. Thus for the infectious compartment (I) in an SIS model,

$$\beta IS = \left(\frac{p}{q} + \frac{1-p}{\delta} \right) I \quad (4.16)$$

Substituting $a = p/q + (1-p)/\delta$ and $S = 1 - I$ into Equation 4.16 leads to

$$\beta I(1 - I) = aI \quad (4.17)$$

This simplifies to

$$I = \frac{\beta - a}{\beta}. \quad (4.18)$$

This system has two equilibria:

1. The trivial (infection-free) equilibrium
2. The non-trivial equilibrium where infection is present

Both equilibria exist depending on the relationship between β and a . If $\beta < a$, the trivial equilibrium is stable but if $\beta > a$ then the non-trivial equilibrium, the equilibrium where infection

is present is non-negative and stable.

Including $\beta > a$ and multiplying through by $e^{-\beta t}/e^{-\beta t}$ leads to

$$\pi = \lim_{t \rightarrow \infty} \frac{p}{-qa(a-\beta)} \times \frac{a-\beta}{\beta} \left(\frac{ae^{(a-\beta)t} - \beta}{1 - e^{(a-\beta)t}} \right) \quad (4.19)$$

$$= \frac{p}{-qa(a-\beta)} \times \frac{a-\beta}{\beta} \times (-\beta) \quad (4.20)$$

$$= \frac{p}{qa} \quad (4.21)$$

$$= \frac{\frac{p}{q}}{\left(\frac{p}{q} + \frac{1-p}{\delta}\right)}. \quad (4.22)$$

Thus for an SIS model, treatment coverage (π) is not equal to the treatment probability (p), but rather a function of the p , δ and q .

This result holds for Model 1 but will change for models with different structures (Models 2-5). The results in Section 4.5.2 showed that treatment coverage in Model 6 correctly represented the 10% treatment probability. This is because at equilibrium in Model 6,

$$p\lambda S = \frac{1}{\sigma_1} L \quad (4.23)$$

$$\frac{1}{\sigma_1} L = \left(\frac{1}{\sigma_2} + \frac{1}{q+\tau} \right) B \quad (4.24)$$

$$\frac{1}{\sigma_2} B = \frac{1}{q+\tau} I. \quad (4.25)$$

$$(4.26)$$

Therefore,

$$p\lambda S = \frac{1}{q+\tau} (B + I) \quad (4.27)$$

and,

$$p = \frac{\frac{1}{q+\tau} (B + I)}{\lambda S}. \quad (4.28)$$

Treatment coverage (π) at equilibrium is treated cases $((B + I)/(q + \tau))$ as a proportion of incidence (λS) and hence for Model 6, $\pi = p$. Thus while treatment coverage data is often used by modellers as the best estimate of treatment probability, depending on the model structure, the treatment coverage predicted by the model may be very different from the treatment probability.

4.5.4 Data Fitting

Showing that for different model structures, treatment coverage is not always equal to treatment probability, demonstrates that even for routine anti-disease interventions like drug therapy, model structure has a large impact on model results. This section explores if fitting models to data reduces this sensitivity to model structure i.e. if models are fitted to data, does model structure matter less or at all? Model 6 is used to simulate the number of treated cases for data fitting purposes as this was the only one of the six models where $p = \pi$. Many national health systems collect routine data on cases that are treated so this would be typical of data available to mathematical modellers. It is not usually the case that true incidence data would be available as the untreated infected population is generally hidden from the health system. The treated cases from all five models are fitted to the model 6 data estimating the value of p (0.1 in the model 6). All other parameter values are held constant at their assumed values in Table 4.1. Parameter estimation is achieved using the Least Squares algorithm for data fitting. All five models fit the data well with the estimated value of p , the probability of being treated, being in the range of 0.0063 and 0.0097. At these values of p , the six models make identical predictions for prevalence, treated cases and treatment coverage with only small differences observed in the prediction of incidence, thereby showing the decrease in sensitivity to model structure that can be achieved by fitting models to data.

4.5.5 Impact of other interventions

Compartment and other models of disease transmission may be used to assess the impact of policy interventions on transmission. Two interventions are applied to the six models to assess sensitivity due to model structure; mass drug administration and vector control. These interventions are then scaled up, aimed at eliminating the disease.

Mass Drug Administration

Mass drug administration involves administering drug therapy to the population at risk regardless of disease status [44]. An example of this intervention is reflected in the models by an increase in the treatment probability p . Mass drug administration is implemented over 8 weeks at 75% probability in all models. The graphs on the left in Figure 4.4 show the impact of this intervention on models that have not been fitted to data while the graphs on the right show the impact this intervention has on the models once they were fitted to the data from model 6. The results show that when mass drug administration is applied to the fitted models, all models reach the same equilibrium before the intervention and show an increase in the number treated at the time of the intervention but revert to the previous equilibrium eventually, whereas models that were not fitted to data reached different points of equilibrium. Even though the fitted models achieve the

same pre and post-intervention equilibrium, the immediate impact (decrease in incidence and prevalence) of the intervention varies between model structures.

Vector Control

In some diseases like malaria and dengue, vectors are an active part of disease transmission. Vector control (VC) as an intervention, requires acting on the vector population in a way that interrupts transmission. This may for example be achieved through larviciding, the use of insecticide treated bednets and household spraying with pesticides [138]. In models 1-6, this intervention is captured as having a decreasing effect on β ; the number of contacts with vectors. The coverage of the control as well as the efficacy of process are taken into account in decreasing β where $\beta_{VC} = (1 - \text{coverage} * \text{efficacy}) * \beta$. In these models an example of vector control is introduced into the models with 50% coverage and 50% efficacy. Figure 4.5 (left) shows that the different model structures (not fitted to data) measure the impact of vector control very differently; some showing a much greater impact on prevalence and incidence than others. Once the models have been fitted to data however, these differences are minimal (Figure 4.5 (right)).

Modelling to Disease Elimination

When interventions are used to eliminate a disease rather than attempt to control it, mathematical models will aim to produce estimates of the length of time to eliminate the disease, the intensity of each of intervention as well as the combinations of interventions that may be used to eliminate a disease. Elimination of infection is defined as the reduction to zero of locally acquired incidence in a geographical area as the result of deliberate efforts [31]. Two very resource-intensive interventions aimed at eliminating a disease are tested on the six models: vector control with a 90% coverage and at a 90% efficacy and a scaling up of drug therapy from a 10% treatment probability to a 90% treatment probability. As the compartments and hence the flows between compartments will never actually reach zero to achieve elimination as outlined above, the disease is assumed to be eliminated when prevalence decreases below 10^{-6} . The impact of these interventions is estimated as the time to elimination (in weeks) from the start of the interventions. These interventions are tested on the six models that have not been fitted to data and on the models once they have been fitted to data.

Table 4.2 shows that by scaling up vector control, the models that are not fitted to data predict widely varying time to elimination values ranging from 193 weeks (< 4 years) to 458 weeks (< 9 years). When fitted to data the predictions fall in a narrower range between 416 and 458 weeks. The results are quite different for a drug scale up intervention. When fitting the models to data, p , the probability of treatment, is the estimated parameter from the data-fitting process. Thus when uniformly increasing the p to 0.9 at the start of the intervention, the previously fitted value falls away and hence the time to elimination estimates are the same regardless of whether the

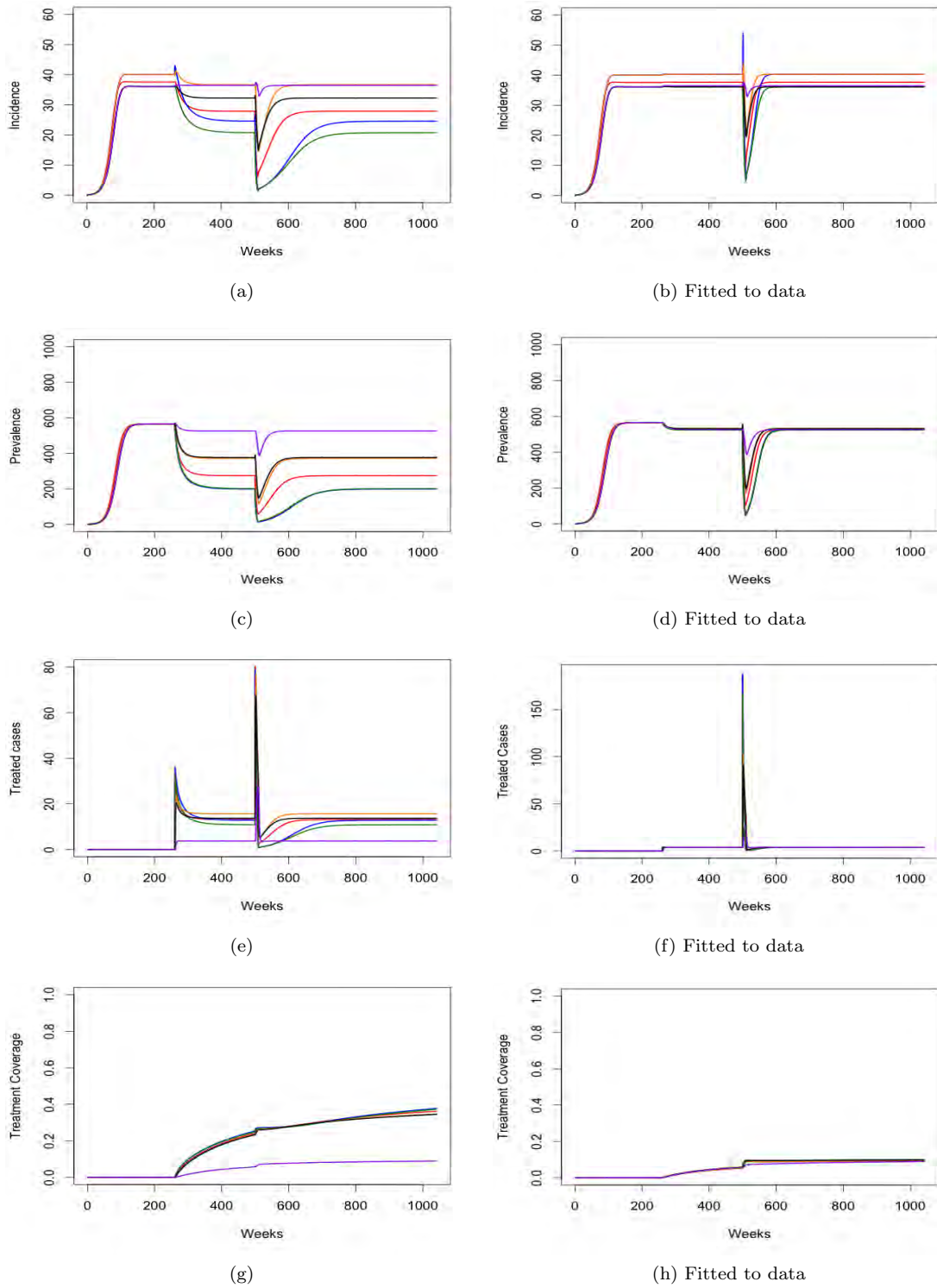
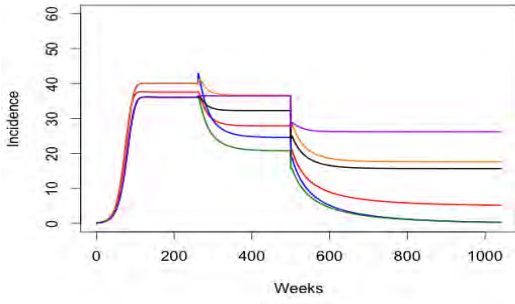
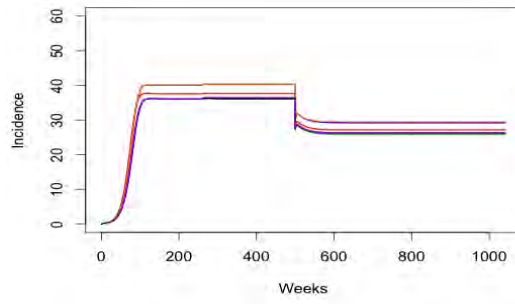


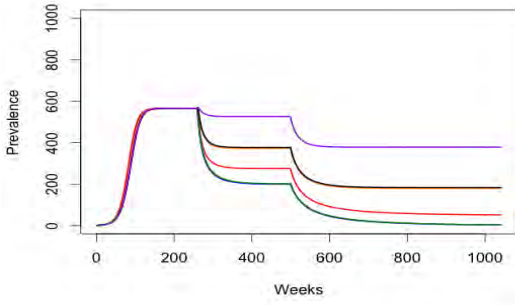
Figure 4.4: Mass Drug Administration (8 weeks, 75% probability of treatment): Incidence (a & b), Prevalence (c & d), Treated Cases (e & f) and Treatment Coverage (g & h) for Model 1 (red), Model 2 (blue), Model 3 (green), Model 4 (orange), Model 5 (black) and Model 6 (purple)



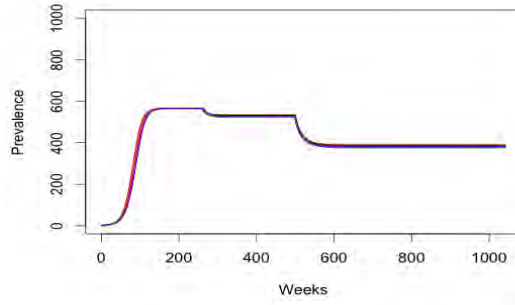
(a)



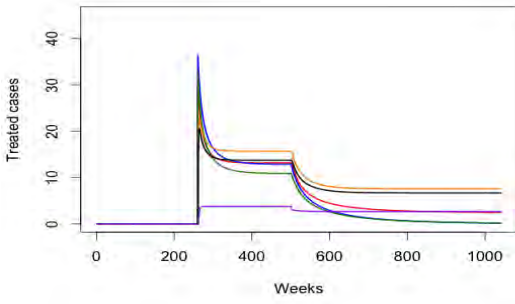
(b) Fitted to data



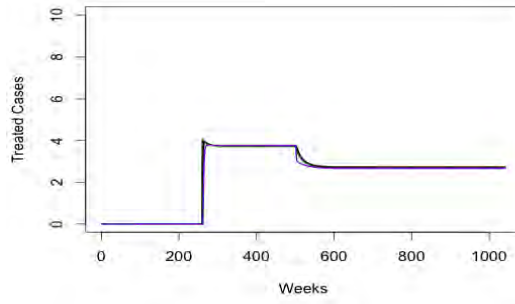
(c)



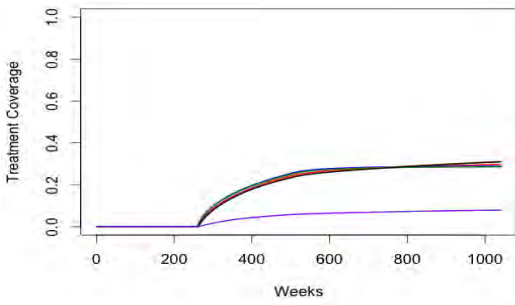
(d) Fitted to data



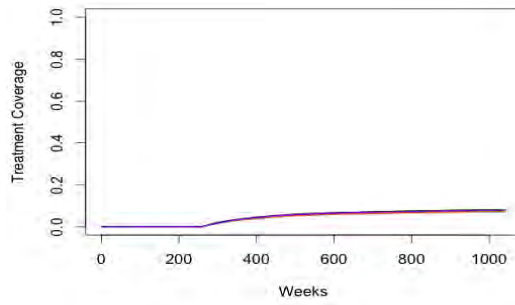
(e)



(f) Fitted to data



(g)



(h) Fitted to data

Figure 4.5: Vector Control (50% Coverage, 50% Efficacy): Incidence (a & b), Prevalence (c & d), Treated Cases (e & f) and Treatment Coverage (g & h) for Model 1(red), Model 2 (blue), Model 3 (green), Model 4 (orange), Model 5 (black) and Model 6 (purple)

Table 4.2: Time to elimination (weeks) for vector control and scale-up of drug therapy

Time to Elimination (weeks)	Vector Control		Drug Scale-up	
	Not Fitted	Fitted	Not Fitted	Fitted
Model 1	206	416	120	120
Model 2	193	424	50	50
Model 3	197	426	54	54
Model 4	260	432	121	121
Model 5	266	434	241	241
Model 6	458	458	399	399

models are fitted or not. These estimates range widely from 50 weeks (<1 year) to 399 weeks (< 8 years) depending on the model structure. These estimates are not robust and clearly sensitive to model structure.

4.6 Discussion

As mathematical modelling is increasingly used to aid decision making in the public health sector, models need to be rigorously tested for sensitivity to parameter values and model assumptions so that model predictions are robust [21]. Incorporating the standard intervention of drug therapy produced very different results for all models tested in terms of prevalence, incidence and the treatment coverage. With only a 10% treatment probability, the decrease in prevalence of the disease ranges between 3% and 49%. At higher treatment rates (> 50%), the disease was even eliminated in some models. These differences occurred for models with the same parameter values and model assumptions but different model structures. The practical significance of these differences is great in that reducing a disease marginally (3%) or reducing a disease by half have very different impacts on a public health sector with minimal scarce resources and high opportunity cost on these resources. This is reiterated by groups such as the MalERA Consultative Group on Modelling, who recognized the contribution modelling can make to the elimination of malaria globally and developed a framework of priority areas for modelling to inform: optimal resource allocation, strategies to minimize the evolution of drug and pesticide resistance, assess new tools to interrupt malaria transmission, assess combinations of tools, coverage targets and expected timelines to achieve goals and to assess operational feasibility with respect to costs and human resource capacities [132]. The impact of interventions tested on the models in this paper (mass drug administration and vector control) yield a wide range for the impact these interventions could have on the disease, both in terms of magnitude of the effect and the time taken to re-establish the post-intervention equilibrium. When attempting to eliminate the disease with vector control, all six models produced estimates for the time to elimination ranging from 193 weeks to 458 weeks depending on the model structure. Model results need to be robust to model

structure if they are to play a role in informing strategy and policy design, where scarce resources will be committed on the basis of the models' predictions.

Fitting the five models to data simulated from model 6 (to empirically estimate the treatment probability), shows that the sensitivity due to model structure can be reduced. As countries become better at collecting routine data and performing clinical trials, opportunities exist for modellers to validate their models with real data. Data quality issues aside, modellers may still be able to use their models to reproduce the data, as well as validate model predictions with a testing dataset. As models are extended to incorporate specific disease dynamics such as immunity [6, 120, 148], vector populations [29, 71] and geography [13, 62, 136], different model structures may well produce very different results and predictions. Fitting models to data where possible can reduce the sensitivity of the model results to model structure. This is not to say that sensitivity testing of parameter values and model assumptions should not take place.

In attempting to eliminate the disease using vector control, it was found that fitting the models to data decreased the sensitivity to model structure, but this was not the case for drug scale-up. The varying predictions on time to eliminate the disease can be partly explained by the treatment seeking behaviour defined in each model. In model 1, the population only has one chance at receiving drug therapy (Infectious compartment), whereas in models 2 and 3, the population has two chances to receive drug therapy (Symptomatic and Infectious compartments) and hence it is harder to eliminate the disease in model 1 than in models 2 and 3. The longest time to elimination estimate is from model 6 (the alternate stratified SLBI). In this model, a segment of the population has no chance to receive drug therapy in the course of the infection and will have to wait until the next round of infections to stand a chance of receiving drug therapy. In this case, it is much harder to eliminate the disease. Modellers should be aware of the treatment-seeking behaviour of the populations they model, but where this information is not available, there is an argument for modelling different treatment-seeking behaviours so that this heterogeneity may be better understood and prudent and conservative estimates may be produced. O'Connell *et al.* found in their study of malaria in Cambodia that treatment-seeking behaviour is complex; often driven by cultural norms and other practicalities [96].

Some of the models in this paper have a simple structure while others have more complex structures. The results have shown that models seeking to measure the same phenomenon (e.g. estimating the impact of drug therapy) that differ in structure only, can produce very similar results *if they are fitted to the same set of data*. Does the argument exist for choosing simple models over complex ones? The answer is yes, but the converse is also true. On one extreme one could have a model that is too simple to be biologically plausible and on the other extreme, the most biologically plausible model may be too complex to be of any practical use. There needs to be a balance between model simplicity and biological plausibility for models to be of practical relevance. White *et al.* compared the results of a simple deterministic compartmental model with other agent-based stochastic complex models in a malaria elimination context [141].

They concluded that in situations where data is sparse, yet urgency exists to provide input into strategy design, simple model structures are suitable but complex models can provide more information (on the context being modelled), especially in the long term. It is important that the focus of the model is decided before the model structure is chosen so that the appropriate level of complexity may be included. If the focus of the model is to assess the effect of drug therapy, the results have shown that it may not be necessary to have separate compartments for the clinical stage (B) and infectious stage (I) of the disease; yet if the focus is to test the effect of a transmission blocking vaccine, then the separation of these stages may be crucial.

Section 4.5.3 has shown that even in the simplest SIS model, the treatment coverage (proportion of cases treated) is different from the probability of treatment. Modellers may be tempted to use known estimates of treatment coverage as the value for treatment probability in their models, but that may be incorrect in the case of compartment models. The treatment probability may be truly known if all cases were detected and tracked to know how many were treated. This is a resource-intensive exercise and is almost impossible to achieve as many infections that go untreated arise in populations that are hidden from the health system (that collects the data). These populations can include illegal immigrants, the very poor and socially-marginalised groups. Hence as a reliable estimate of treatment probability is not always achievable, one can fit the model to routine data and estimate the treatment probability parameter in the process. Various options exist for parameter estimation including Markov Chain Monte Carlo methods, least squares and maximum likelihood optimization [10, 54].

This paper sought to compare results between deterministic compartment models only and did not extend to include other model structures such as agent-based models and time series models. While this is a limitation of the paper, it also serves to show that differences in results due to model structure arise not only among different classes of models but among models in the *same* class also. Several aspects have been ignored such as immunity, super infection, chemoprophylaxis, drug resistance, heterogeneity of the population and vector population dynamics. Stochasticity was also ignored. It was not in the scope of the paper to include all aspects of disease, but rather to show that even in the most basic disease context, differences still exist due to model structure. These are all areas where further work can be undertaken.

4.7 Conclusion

This paper has assessed differences in predictions from deterministic compartment models of disease with different model structures. These model structures ranged from simple structures to complex ones. Differences were observed in model predictions of the number of cases treated, incidence and prevalence of disease and the treatment coverage. Further differences were observed when interventions such as mass drug administration and vector control were introduced into the models. These differences were at times found to be reduced when models were fitted to the same

dataset leading to the conclusion that fitting a model to data can reduce a model's sensitivity to model structure. While this is an argument for selecting simple models over complex ones, model structure (and its complexity) needs to be chosen carefully depending on the focus of the model and ultimately the use to which it will be put.

4.8 Model Equations

Model 1 (SLI)

$$\begin{aligned}\frac{dS}{dt} &= -\lambda_t S + \frac{1-p}{\delta} I + \frac{p}{q+\tau} I \\ \frac{dL}{dt} &= \lambda_t S - \frac{1}{\sigma_1 + \sigma_2} L \\ \frac{dI}{dt} &= \frac{1}{\sigma_1 + \sigma_2} L - \frac{1-p}{\delta} I - \frac{p}{q+\tau} I\end{aligned}$$

Model 2 (SBI)

$$\begin{aligned}\frac{dS}{dt} &= -\lambda_{(t-\sigma_1)} S + \frac{1-p}{\delta} I + \frac{p}{q+\tau} (B+I) \\ \frac{dB}{dt} &= \lambda_{(t-\sigma_1)} S - \frac{1-p}{\sigma_2} B - \frac{p}{q+\tau} B \\ \frac{dI}{dt} &= \frac{1-p}{\sigma_2} B - \frac{1-p}{\delta} I - \frac{p}{q+\tau} I\end{aligned}$$

Model 3 (SLBI)

$$\begin{aligned}\frac{dS}{dt} &= -\lambda_t S + \frac{1-p}{\delta} I + \frac{p}{q+\tau} (B+I) \\ \frac{dL}{dt} &= \lambda_t S - \frac{1}{\sigma_1} L \\ \frac{dB}{dt} &= \frac{1}{\sigma_1} L - \frac{1-p}{\sigma_2} B - \frac{p}{q+\tau} B \\ \frac{dI}{dt} &= \frac{1-p}{\sigma_2} B - \frac{1-p}{\delta} I - \frac{p}{q+\tau} I\end{aligned}$$

Model 4 (Stratified SBI)

$$\begin{aligned}\frac{dS}{dt} &= -\lambda_{(t-\sigma_1)}S + \frac{1-p}{\delta}I_U + \frac{1}{q}(B_T + I_T) \\ \frac{dB_U}{dt} &= \lambda_{(t-\sigma_1)}S - \frac{1-p}{\sigma_2}B_U - \frac{p}{\tau}B_U \\ \frac{dI_U}{dt} &= \frac{1-p}{\sigma_2}B_U - \frac{1-p}{\delta}I_U - \frac{p}{\tau}I_U \\ \frac{dB_T}{dt} &= \frac{p}{\tau}B_U - \frac{1}{\sigma_2}B_T - \frac{1}{q}B_T \\ \frac{dI_T}{dt} &= \frac{p}{\tau}I_U + \frac{1}{\sigma_2}B_T - \frac{1}{q}I_T\end{aligned}$$

Model 5 (Stratified SLBI)

$$\begin{aligned}\frac{dS}{dt} &= -\lambda_t S + \frac{1-p}{\delta}I_U + \frac{1}{q}(B_T + I_T) \\ \frac{dL}{dt} &= \lambda_t S - \frac{1}{\sigma_1}L \\ \frac{dB_U}{dt} &= \frac{1}{\sigma_1}L - \frac{1-p}{\sigma_2}B_U - \frac{p}{\tau}B_U \\ \frac{dI_U}{dt} &= \frac{1-p}{\sigma_2}B_U - \frac{1-p}{\delta}I_U - \frac{p}{\tau}I_U \\ \frac{dB_T}{dt} &= \frac{p}{\tau}B_U - \frac{1}{\sigma_2}B_T - \frac{1}{q}B_T \\ \frac{dI_T}{dt} &= \frac{p}{\tau}I_U + \frac{1}{\sigma_2}B_T - \frac{1}{q}I_T\end{aligned}$$

Model 6 (Alternate Stratified SLBI)

$$\begin{aligned}\frac{dS}{dt} &= -\lambda_t S + \frac{1}{\delta}I_U + \frac{1}{q+\tau}(B_T + I_T) \\ \frac{dL_U}{dt} &= (1-p)\lambda_t S - \frac{1}{\sigma_1}L_U \\ \frac{dB_U}{dt} &= \frac{1}{\sigma_1}L_U - \frac{1}{\sigma_2}B_U \\ \frac{dI_U}{dt} &= \frac{1}{\sigma_2}B_U - \frac{1}{\delta}I_U \\ \frac{dL_T}{dt} &= p\lambda_t S - \frac{1}{\sigma_1}L_T\end{aligned}$$

$$\frac{dB_T}{dt} = \frac{1}{\sigma_1} L_T - \frac{1}{\sigma_2} B_T - \frac{1}{q + \tau} B_T$$

$$\frac{dI_T}{dt} = \frac{1}{\sigma_2} B_T - \frac{1}{q + \tau} I_T$$

4.9 Additional Output

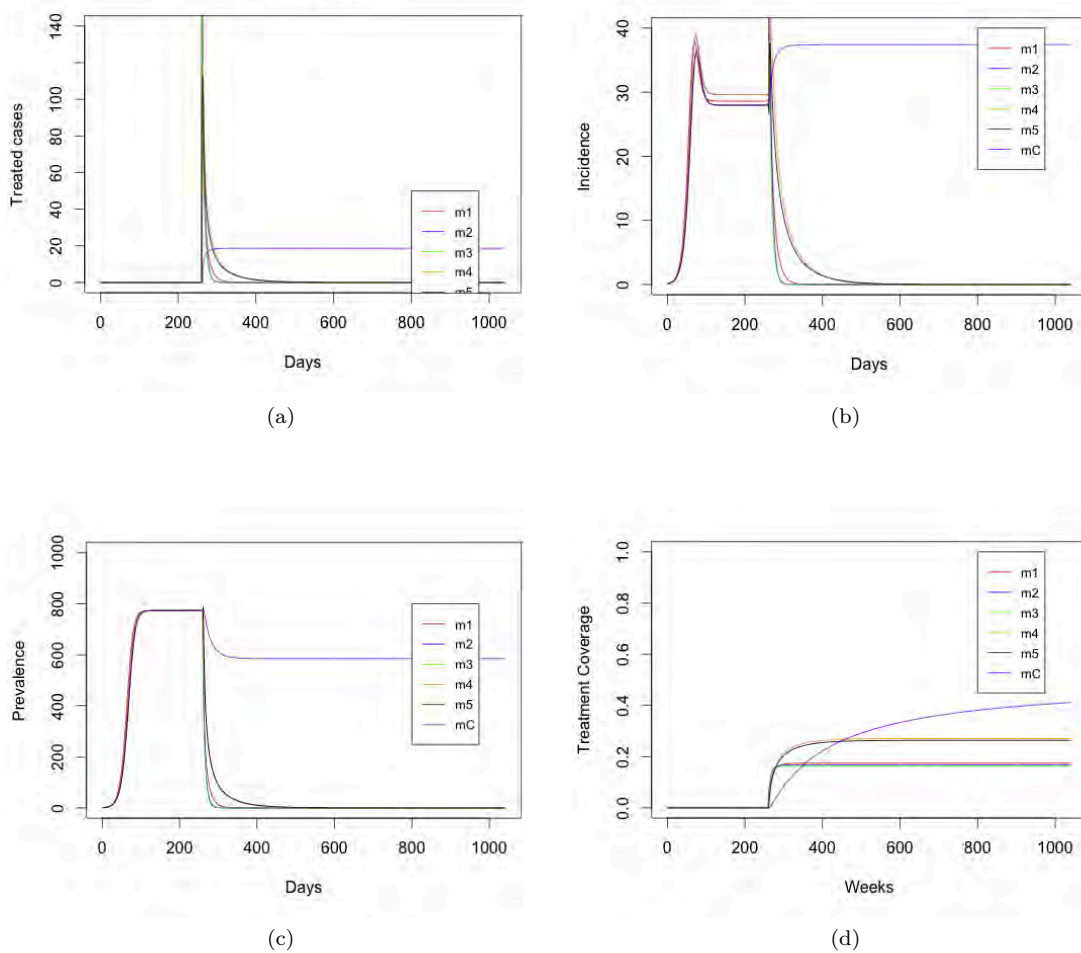


Figure 4.6: 50% Treatment Probability: Incidence (a), Prevalence (b), Treated Cases (c) and Treatment Coverage (d) for Model 1 (red), Model 2 (blue), Model 3 (green), Model 4 (orange), Model 5 (black) and Model 6 (purple)

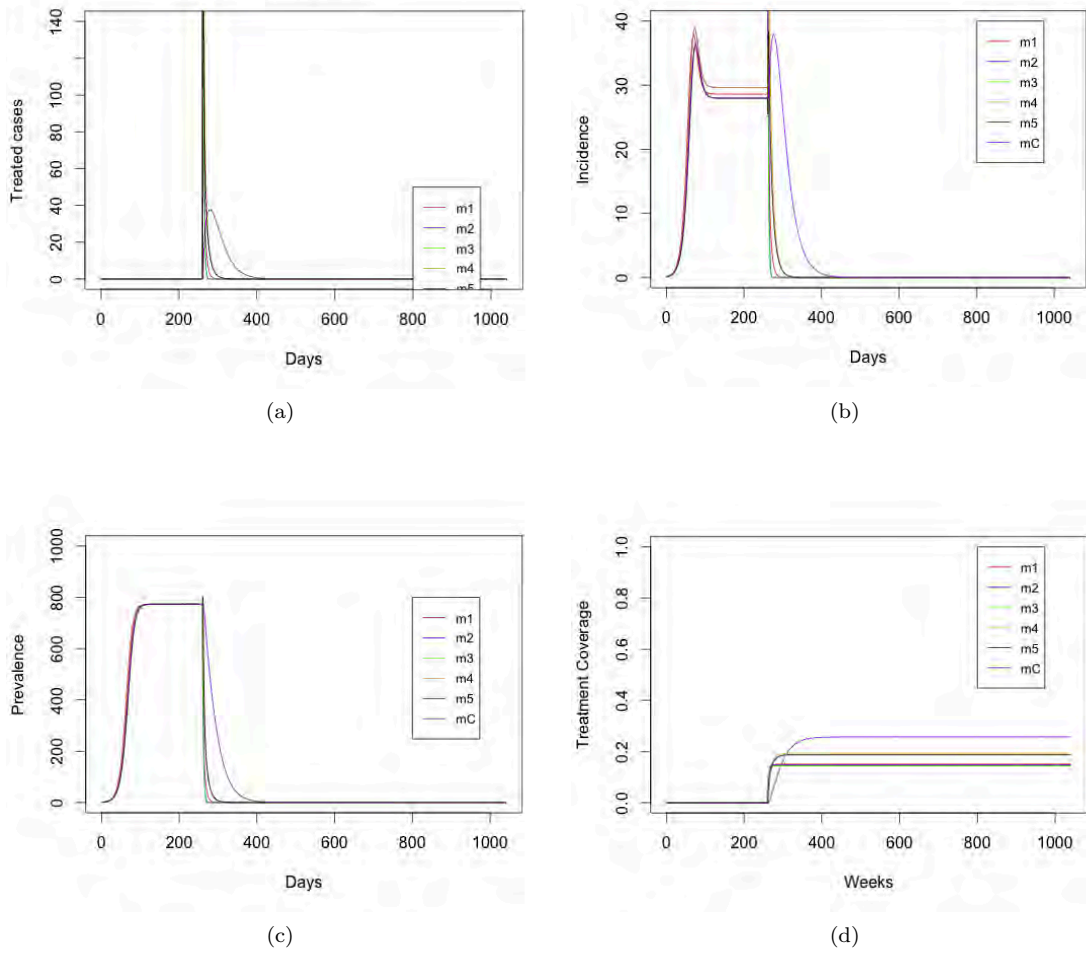


Figure 4.7: 100% Treatment Probability: Incidence (a), Prevalence (b), Treated Cases (c) and Treatment Coverage (d) for Model 1 (red), Model 2 (blue), Model 3 (green), Model 4 (orange), Model 5 (black) and Model 6 (purple)

Chapter 5

Model 1 - Population model of malaria transmission

Chapter 4 on the sensitivity to model structure concludes that differences in model predictions among deterministic compartment models with different structures may be reduced if models are fitted to data, leading to the conclusion that fitting a model to data can reduce a model's sensitivity to model structure. The first model of malaria transmission in Mpumalanga, presented in this chapter, will be fitted to the routinely collected case data described in Chapter 3 to decrease the model's sensitivity to model structure. A further conclusion from Chapter 4 is that though there may be an argument for selecting simple models over complex ones, model structure (and its complexity) needs to be chosen carefully depending on the focus of the model and the use to which it will be put. The model structure selected for this population model of malaria transmission is an SBI model that has been stratified according to treatment and source of infection. In its most basic form, it is closest in structure to Model 6, with the exception that the Liver stage of the disease is incorporated as a delay in the flow between the Susceptible and Blood stages.

Infections are stratified by treatment. That is, the model is replicated to account for both the untreated population and the population destined to be treated, to adequately capture the treatment proportion as demonstrated in Chapter 4. The high proportion of imported infections in Mpumalanga and the varying seasonal patterns of imported and local infections described in Chapter 3 justify a further stratification by source of infection. It is also necessary to classify infections by their source so that elimination-focused interventions targeting either local or imported infections only, may be adequately modelled.

The model presented in this chapter is used to assess the impact of proposed policy interventions in Mpumalanga. This is the first study designed for this purpose in Mpumalanga and the first

to do so in South Africa since the call for malaria elimination. A deterministic population-based non-linear ordinary differential equation model fitted to the Mpumalanga malaria data, is used to predict the impact of the following interventions (alone and in combination): scale-up of Vector Control, Mass Drug Administration (MDA), a Focal Screen and Treat campaign (FSAT) and foreign source reduction. The model is fitted to weekly treated case data from 2002 to 2008, and then validated with data from 2009 to 2012. The model predicts that while all strategies (in isolation or combined) contributed to decreasing local infections, none was able to decrease local infections to zero due mainly to the continuous stream of imported infections, thus highlighting the importance of cross-border collaborative initiatives. An additional file which contains detailed descriptions of the model fitting process and model equations is presented at the end of this chapter.

SPS wrote the paper and performed the mathematical model development and analysis. SPS and LJW conceptualised the mathematical model and analysis. FL, KIB and LJW reviewed the manuscript extensively. All authors have read and approved the manuscript.

We are grateful to the Malaria Elimination Programme of the Department of Health in Mpumalanga, South Africa for the provision of data and are particularly grateful to Aaron Mabuza and Gerdalize Kok from the Malaria Elimination Programme for their support. This material is based upon work supported financially by the National Research Foundation in South Africa. We are grateful to the National Research Foundation in South Africa for financial support. Any opinion, findings and conclusions or recommendations expressed in this material are those of the authors and therefore the NRF does not accept any liability in regard thereto. Mahidol-Oxford Tropical Medicine Research Unit is funded by the Wellcome Trust.

Towards malaria elimination in Mpumalanga, South Africa: a population-level mathematical modelling approach

Sheetal Prakash Silal^{1,*}, Francesca Little¹, Karen I Barnes², Lisa J White^{3,4},

1 Department of Statistical Sciences, University of Cape Town, Cape Town, South Africa

2 Division of Clinical Pharmacology, Department of Medicine, University of Cape Town, Cape Town, South Africa

3 Mahidol-Oxford Tropical Medicine Research Unit, Mahidol University, Bangkok, Thailand

4 Centre for Tropical Medicine, Nuffield Department of Clinical Medicine, Churchill Hospital, University of Oxford, Oxford, UK

5.1 Abstract

Background: Mpumalanga in South Africa is committed to eliminating malaria by 2018 and efforts are increasing beyond that necessary for malaria control. Differential Equation models may be used to study the incidence and spread of disease with an important benefit being the ability to enact exogenous change on the system to predict impact without committing any real resources. The model is a deterministic non-linear ordinary differential equation representation of the dynamics of the human population. The model is fitted to weekly treated cases data from 2002 to 2008, and then validated with data from 2009 to 2012. Elimination-focused interventions such as the scale-up of vector control, mass drug administration, a focal screen and treat campaign and foreign source reduction are applied to the model to assess their potential impact on transmission.

Results: Scaling up vector control by 10% and 20% resulted in substantial predicted decreases in local infections with little impact on imported infections. Mass drug administration is a high impact but short-lived intervention with predicted decreases in local infections of less than one infection per year. However, transmission reverted to pre-intervention levels within three years. Focal screen and treat campaigns at border-entry points are predicted to result in a knock-on decrease in local infections through a reduction in the infectious reservoir. This knock-on decrease in local infections is also predicted to be achieved through foreign source reduction. Elimination is only predicted to be possible under the scenario of zero imported infections in Mpumalanga.

Conclusions: A constant influx of imported infections show that vector control alone will not be able to eliminate local malaria as it is insufficient to interrupt transmission. Both mass interventions have a large and immediate impact. Yet in countries with a large migrant population, these interventions may fail due to the reintroduction of parasites and their impact may be short-lived. While all strategies (in isolation or combined) contributed to decreasing local infections, none was predicted to decrease local infections to zero. The number of imported infections highlights the importance of reducing imported infections at source, and a regional approach to malaria elimination.

Published in Malaria Journal on 3 August 2014

5.2 Background

Mpumalanga is one of three malaria-endemic provinces in South Africa. As South Africa is committed to eliminating malaria by 2018, efforts are increasing in each of these three provinces beyond that which was necessary for malaria control [93]. In shifting focus from control to elimination, additional activities need to be incorporated into the operational strategy as elimination may not be achieved through a "more of the same" approach [89]. Groups such as the MalERA Consultative Group on modelling, have recognized the contribution mathematical modelling can make to the elimination of malaria globally and have highlighted priority areas that modelling can inform, such as optimal resource allocation, strategies to minimize the evolution of drug and pesticide resistance, assessment of new tools to interrupt malaria transmission, assessment of combinations of such tools, the coverage targets and expected timelines needed to achieve elimination goals and the assessment of operational feasibility with respect to costs and human resource capacities [132]. While such models may be used to understand/explore the underlying system, an important benefit of modelling is the ability to enact exogenous change on the system to predict impact without committing any real resources. This is particularly important in environments with scarce competing resources. In this paper, a population-based non-linear ordinary differential equation model is used to simulate malaria transmission in Mpumalanga province to assess the potential impact of various policy interventions that may be used to achieve malaria elimination.

Malaria in Mpumalanga has been documented extensively[11, 42, 88, 95, 113–115]. Sharing borders with both Mozambique and Swaziland (Figure 5.1), Mpumalanga experiences seasonal unstable transmission that is prone to sporadic outbreaks from the first rains in October to late May.

The Ehlanzeni District on the eastern border of Mpumalanga is most affected by malaria with the number of imported cases in Mpumalanga overtaking locally sourced cases in recent years (Figure 5.2). Between 2002 and 2012, 41% of cases were sourced in South Africa and 54% sourced from Mozambique (the remaining 5% being sourced from other African and Asian countries). Source of infection has been determined for all cases in the province, whereby a case is classified as imported if the patient travelled to a malaria-endemic area in the past month or if there is no evidence of local transmission(vectors or cases within 500 m radius of the place of residence) [74]. The proportion of imported cases has increased from 39% in 2002 to 87% in 2012 [116]. Extensive vector control through indoor residual spraying, the implementation of an artemisinin-based combination therapy policy of artesunate plus sulphadoxine-pyremethamine in 2003, followed by artemether-lumefantrine (AL) in 2006 and the Lubombo Spatial Development Initiative (LSDI) are considered responsible for the decline in malaria cases and malaria deaths in the province [88]. The LSDI malaria programme was a collaborative project conceived by the Medical Research Councils of South Africa, Swaziland and Mozambique to decrease malaria in



Figure 5.1: A map of Mpumalanga Province in relation to Mozambique and Swaziland (Source: Mpumalanga Malaria Elimination Programme (unpublished))

the areas surrounding the Lubombo Mountains [70]. With well-functioning programmes in place in both South Africa and Swaziland, intervention took place primarily in Maputo province and Gaza Provinces in Mozambique. The programme was terminated early in September 2010 and the resultant reduced IRS in Maputo thereafter coincides with the increase observed in malaria incidence in Maputo from 2011.

Differential Equation or compartment models, have been used in the past to study the incidence and spread of disease, and the impact of interventions such as drug treatment and parasite control [92]. Compartment models and their applications in malaria in particular, have a history that spans more than 100 years [82]. Applications of mathematical modelling in Mpumalanga include a climate-based fuzzy distribution model of malaria transmission in sub-Saharan Africa (including a region containing Mpumalanga) [26]. Coleman *et al.* used the SaTScan methodology in Mpumalanga to detect local malaria clusters to guide the provincial control programme, and Montosi *et al.* considered soil-water content as a driver of malaria incidence; applying both an ecohydrological model and a transfer function model to incidence data in three South African provinces (including Mpumalanga) [24, 87]. The model presented in this paper is used to assess the impact of proposed policy interventions in Mpumalanga. This is the first study designed for this purpose in Mpumalanga and the first to do so since the call for malaria elimination in South

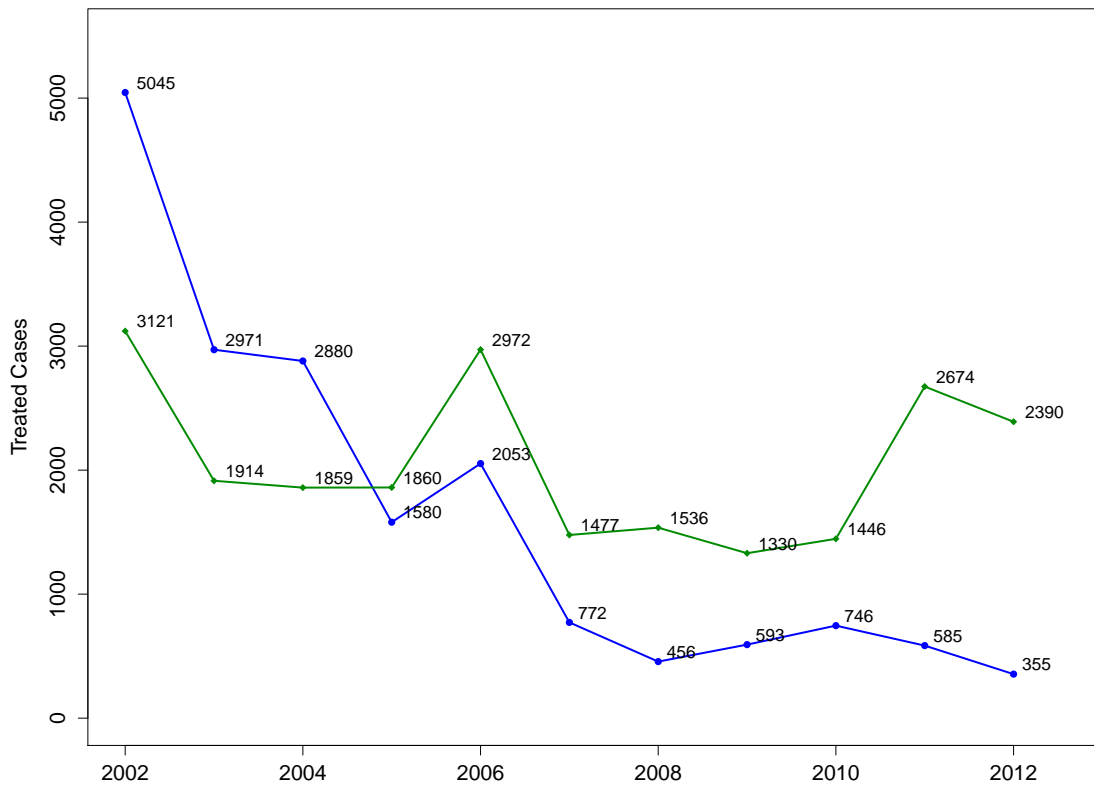


Figure 5.2: Annual incidence of locally sourced (blue) and imported (green) malaria cases that have been reported and treated at health facilities in Mpumalanga province.

Africa. A deterministic population-based non-linear ordinary differential equation model fitted to the Mpumalanga malaria data, is used to predict the impact of the following interventions (alone and in combination): scale-up of vector control, mass drug administration (MDA), a focal screen and treat campaign (FSAT) and foreign source reduction.

5.3 Methods

5.3.1 Transmission Model

The model is a deterministic ordinary non-linear differential equation representation of the dynamics of the human population. In the model, the population is divided into nine compartments: the susceptible population (S), the asexual blood stage only (B_l and B_f) for locally and imported infections respectively and the infectious gametocyte stage (I_l and I_f) for locally and imported infections respectively (Figure 5.3 with parameter descriptions in Table 5.1). The blood stage and infectious stage compartments are further stratified according to whether the infection is

treated or not. The liver stage of the infection is incorporated as a delay in the flow between the susceptible and blood stage compartments. As this is a low transmission environment, immunity and super-infection are rare and are excluded from this model. While the seasonal nature of transmission is incorporated in the model, the mosquito population is not modelled directly as it is assumed that the mosquito dynamics operate on a faster time-scale than the human dynamics and as such the mosquito population can be considered to be at equilibrium with respect to changes in the human population [66]. A full description of the model is presented in Additional File 1 at the end of the chapter.

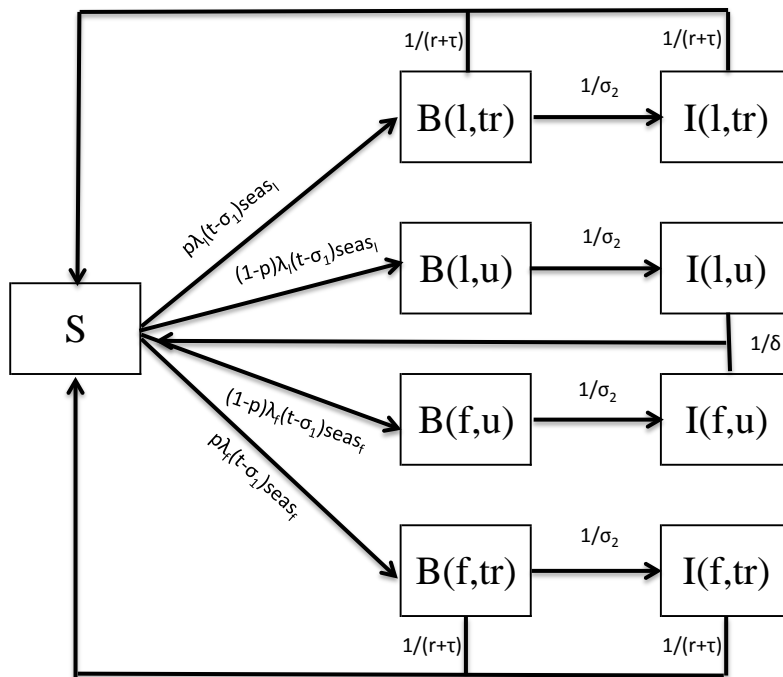


Figure 5.3: Flowchart underlying the population level ordinary non-linear differential equation model of malaria transmission. (l - locally sourced infections, f - imported infections, u - untreated infections, tr- treated infections)

5.3.2 Data fitting

The model is fitted to weekly treated case data from 2002 to 2008, and then validated with data from 2009 to 2012. Ethical approval for use of the data was obtained from the University of Cape Town Human Research Ethics Committee and the Mpumalanga Department of Health. The seasonal forcing functions (functions that determine the seasonal behaviour of transmission in the area) for local and imported cases are derived from the data. Silal *et al.* describes in detail the characteristic triple peaked pattern in the incidence data with peaks in the malaria season

Table 5.1: Providing the values, descriptions and sources of the parameters driving the mathematical model of transmission.

Parameter	Description	Value	Source
N	Population size	4×10^6	[125]
μ	Mortality Rate	$\frac{105}{10000}$	[90]
δ	Natural recovery period	26 weeks	[61, 86, 141]
σ_1	Period between liver stage and blood stage	7 days (5-10)	[19, 25, 33]
σ_2	Period between blood stage and onset of gametocytemia	1 week	[61, 134]
r	AL elimination half-life	6 days	[77]
τ	Time to seek treatment	1/2 week	Expert opinion
p	Proportion that receive treatment	0.95	[18, 58]
$seas_l$	Seasonal forcing function for locally sourced cases	Derived from data	[116]
$seas_f$	Seasonal forcing function for imported cases	Derived from data	[116]
β_l	Annual number of mosquito bites per person x proportion of bites testing positive for sporozoites	39.170 (38.894, 39.448)	Estimated from model fitting process
λ_f	Force of imported infections	0.002163 (0.002124, 0.002202)	Estimated from model fitting process
λ_l	Force of locally sourced infections	$(1 - vc[t])\beta_l \times \frac{I_{l,u} + I_{l,tr} + I_{f,u} + I_{f,tr}}{N}$	
$vc[t]$	$vccov \times vceff$		
$vccov$	Vector Control Coverage	0.22-0.90	Derived from data
$vceff$	Effectiveness of vector control	0.9060 (0.8884, 0.9212)	Estimated from model-fitting process

occurring in September/October, December/January and April/May. While locally sourced infections exhibit this triple-peaked pattern, imported infections occur mainly in the second two peaks of the malaria season [116]. The two seasonal forcing functions used to model seasonality were derived using the "Seasonal decomposition of Time series by LOESS" (STL) methods for extracting time series components [22]. In order for the data-fitting process to be plausible, interventions that were implemented between 2002 and 2008 were included in the model, namely, ACT drug therapy and Indoor Residual Spraying (IRS). Ngomane and de Jager outline in detail the IRS procedure and physical structures sprayed in the province between 2001 and 2009 [95].

The model is run from 1990 to reach a steady state before being fitted to data from 2002. The model output (local and imported treated cases) are fitted to the data from 2002 to 2008 using the maximum likelihood approach by treating the model output as the rate λ of the Poisson distribution. The parameters β_l , $veff$ and λ_f are estimated through the data fitting process with initial values sampled from a Latin hypercube framework. The model with the estimated parameter values is then run for a further three years to be further validated by comparison to data between 2009 and 2012. The impact of routine drug therapy and IRS implemented between 2009 and 2012 is also included in the model. A full description of IRS and the data-fitting method are presented in Additional file 1.

5.3.3 Assessing elimination

Elimination of a disease is a term that has had several definitions over time [23]. Currently, the World Health Organization (WHO) defines elimination generally to be "interrupting local mosquito-borne malaria transmission in a defined geographical area, i.e. zero incidence of locally contracted cases, although imported cases will continue to occur. Continued intervention measures are required" [38]. The framework of deterministic differential equation models are such that compartments may approach zero but will never actually decrease to zero; hence it is technically impossible for the model to predict zero incidence of locally contracted cases. It is then necessary to set a threshold below which the number of locally contracted cases is deemed equivalent to zero. This approach has been used in several papers. For example, White *et al.* defined elimination as having been achieved when parasite prevalence is reduced to 0.0001% and the rate of change in parasite prevalence thereafter is negative [141]. Maude *et al.* defined elimination to be achieved when there is fewer than one malaria parasitaemic individual in the population [85]. The threshold for elimination that is adopted in this paper is less than one locally sourced malaria infection per year in the population and the rate of change of locally sourced infections is negative thereafter. When the model predicts that the number of locally contracted cases is below this threshold and the rate of change of locally sourced infections is negative thereafter, then elimination is predicted to occur.

5.4 Results

The results of the model fitting and validation are presented first before evaluating the predicted impact of the elimination-focused interventions.

5.4.1 Model fitting and validation

The parameters driving the model and their 95% confidence intervals estimated through data-fitting procedures are presented in Table 5.1. A parameter that is usually unknown and estimated from the data is the proportion of cases treated (p). Case data usually includes cases that have been treated, comprising patients presenting themselves at a health facility (passive case detection), or those cases that have been detected actively. There is often no indication of the number of infections that have remained untreated, and hence there is no/little data from which to derive p . Castillo-Riquelme *et al.* conducted household surveys in Mozambique and South Africa between 2001 and 2002 to evaluate treatment-seeking behaviour for malaria-related events [18]. It was found that in the Tonga sub-district of Mpumalanga, all of the 457 people with recent cases of malaria (previous month) sought treatment, with 98.5% of cases being treated at a public health facility. More recently, Hlongwana *et al.* conducted a study on the knowledge and practices towards malaria in Bushbuckridge Municipality in Mpumalanga in 2008 after South Africa was declared ready for malaria elimination [58]. The study revealed that 99% of respondents would seek malaria treatment (95% Confidence interval: (97.5, 99.5)%) with 82% doing so within 24 hours of the onset of symptoms. Based on these two studies, a probability of treatment of 95% is assumed in the model for the entire modelling period as it is informed by studies conducted in 2002 and 2008.

Model fitting was performed using different starting values of the parameters with the optimisation routine reaching the global minimum in almost all fits. The narrow confidence intervals of the parameter estimates are indicative of the stability of the estimates. Figure 5.4(a) shows the fit of the model to the data for the local and imported treated cases while Figure 5.4(b) shows the application of the model to the treated case data from 2009 to 2012. The model captures the timing of the season well. As seen in Figure 5.4(b), there is a sudden unanticipated rise in the number of imported cases in 2011 and 2012 coinciding with the end of the Lubombo Spatial Development Initiative and the model does not capture this.

5.4.2 Interventions

The model is used to predict the impact of the following interventions (alone and in combination): scale-up of vector control, mass drug administration, a focal screen and treat campaign and foreign source reduction.

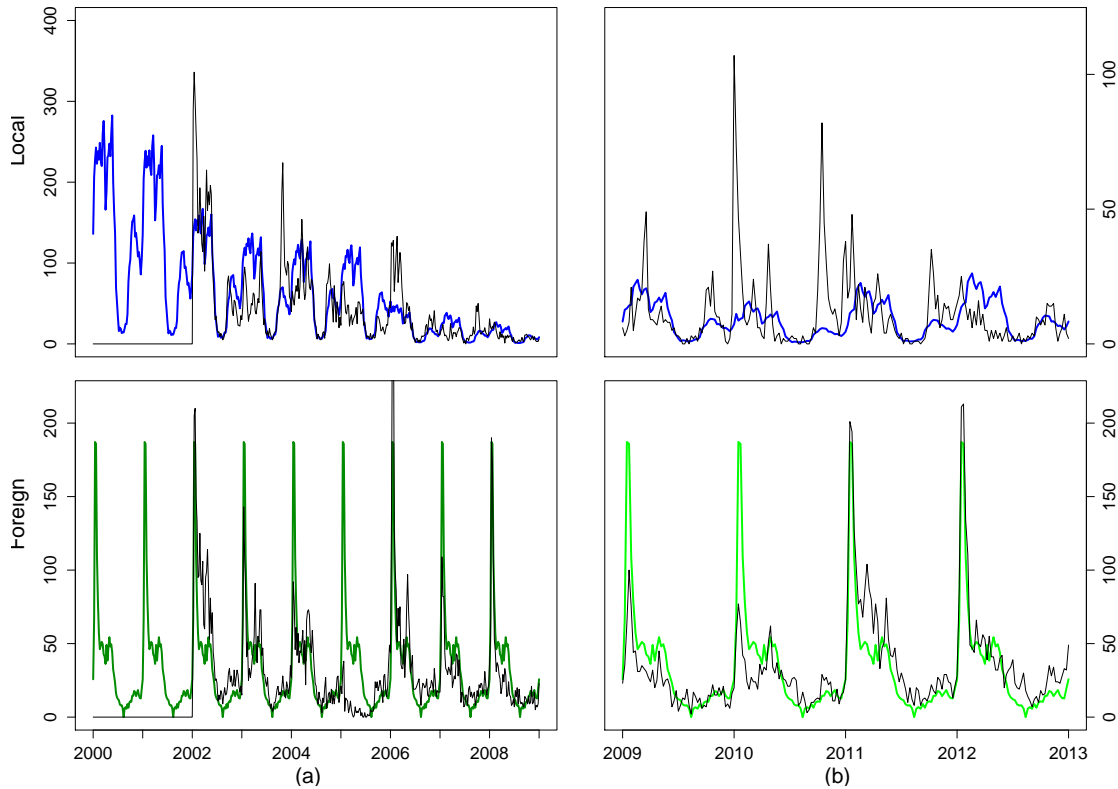


Figure 5.4: (a) Model fitting results for data (black) to model output: locally sourced (blue) and imported (green) reported treated malaria cases and (b) Model validation results of model output: locally sourced (blue) and imported (green) reported treated malaria cases against data (black) from 2009 to 2013.

Scaling up vector control

The primary exogenous vector control intervention in use currently is IRS with larviciding at specified sites. As these interventions act directly on local vectors and hence local transmission, their impact is included in the model as a percentage decrease in β_l , the number of local human contacts with infectious mosquitoes. By 2012, the vector control activities decreased β_l to 30% of its initial value (Figure 5.5, black). Scaling up vector control (through increased IRS or larviciding for example) so as to decrease β_l by a further 10% (Figure 5.5, red) and 20% (Figure 5.5, blue) results in local infections decreasing substantially without any sizeable decrease in total infections. This is to be expected as the majority of infections are imported, and as such vector control may assist with onward local transmission of these imported infections but not change the number of imported infections itself. IRS already takes place on a large scale in the Ehlanzeni district [95]. Scaling up vector control by these amounts will require other vector control activities to be implemented such as larviciding. To achieve such reductions will require large-scale identification

and coverage of breeding sites and even still the model does not predict the reduction to zero of local cases. Local infections will still occur because of onward transmission from imported infections.

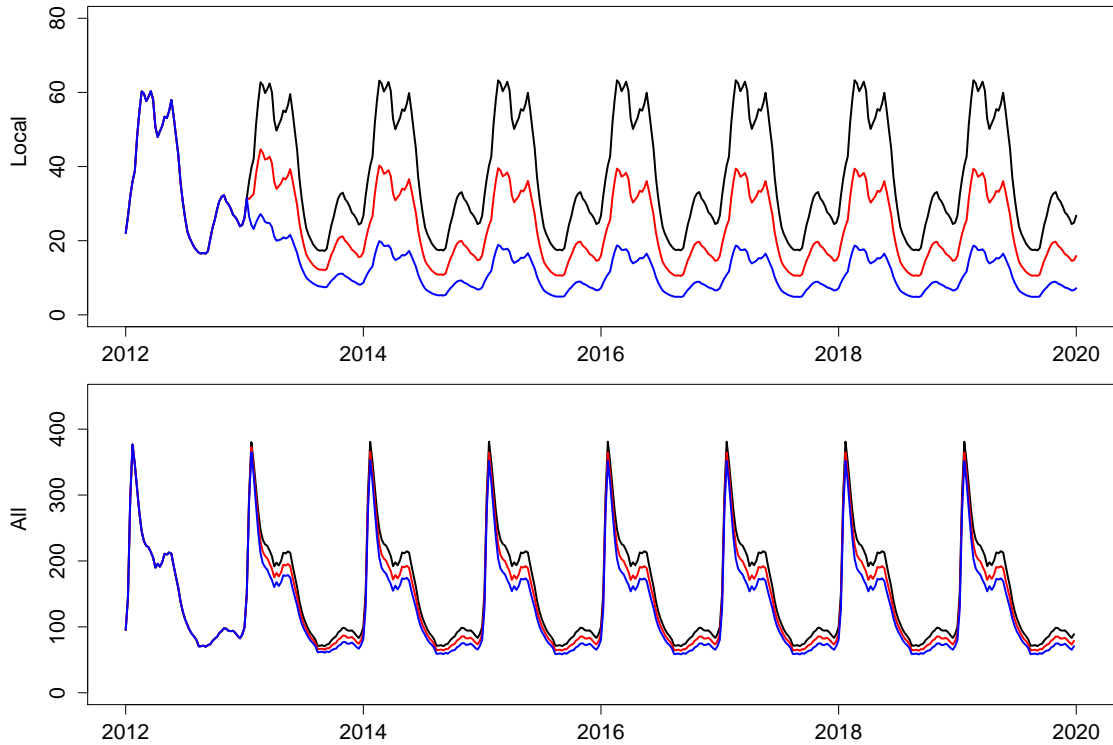


Figure 5.5: Predicted impact of a scale up of vector control (from 2013) that reduces the number of infections by a further 10% (red) and 20% (blue).

Mass interventions

One intervention that simultaneously impacts both local and imported infections is mass drug administration. Mass drug administration involves treating all individuals without prior screening to assess disease status. While MDA is aimed at the entire population of interest, it is rarely the case that every single individual will be treated and hence MDA should be modelled with a less-than 100% coverage. The choice of drug is key to the intervention as drugs that infer a long period of chemoprophylaxis may result in fewer infections after the intervention, but also expose parasites to sub-therapeutic levels of drugs which may in turn lead to the development of resistance. The most likely choices for drugs in Mpumalanga are the first-line of treatment, artemether-lumefantrine, and dihydroartemisinin plus piperaquine with Primaquine, inferring a protective period of approximately one month [103]. The timing of the MDA is also vital to its

effectiveness. It may be the case that performing MDA at the trough of the season will result in fewer malaria infections and a decrease in the infectious reservoir, leading to fewer infections at the peak of the season. Figure 5.6 shows the predicted impact of MDA applied over a two month period annually to the whole population with 80% coverage. The timing of MDA was investigated at both the peak (Figure 5.6, red) and trough of the season (Figure 5.6, blue). It is predicted that applying MDA leads to a substantial decrease in local infections regardless of the timing of application. However, the predictions show that applying annual rounds of MDA at the peak of the season leads to substantial decreases in both local and imported infections unlike MDA at the trough of the season. A possible reason for this difference in impact is the large proportion of imported infections. Applying MDA at the season's trough decreases imported infections then but there is no further decrease during the peak of the season as imported infections are sourced outside South Africa and so, are not impacted by the decrease in onward transmission brought about by MDA. What is also evident from Figure 5.6 is that annual rounds of MDA are predicted to be insufficient to bring about malaria elimination. A single round of MDA is predicted to cause an immediate decrease in infections but future transmission recovers quickly. Figure 5.7(a) shows the application of six consecutive two-monthly rounds of MDA to the malaria transmission model. In this scenario, local infections are predicted to decrease substantially during the MDA, reaching less than one local case per year ($1/52$ cases per week) 29 weeks after the start of the intervention and take approximately two years to recover to pre-MDA levels once the MDA has stopped. Imported infections are predicted to decrease substantially during MDA acting as a form of intermittent preventative treatment and recover immediately after the MDA cycle.

MDA is a resource-intensive process attempting to access an entire population of interest while administering a drug regardless of whether individuals have the disease or not. Mass and focal screen and treat campaigns on the other hand treat only those that have tested positive for the disease. Figure 5.7(b) shows the predicted impact of administering FSAT at the border to residents of Mpumalanga who have imported infections i.e. before entering Mpumalanga. The rationale behind this intervention is that it is less resource-intensive than MDA and specifically targets imported infections before they enter the province and impact local transmission. In Figure 5.7b, FSAT is applied continuously in the model to new imported infections before entering Mpumalanga for six months from November to April with a coverage below 100% as many imported infections may be missed for reasons such as illegal immigration and sensitivity of the screening tools. Figure 5.7b also shows the substantial predicted decrease in locally sourced infections that can be achieved by treating local people who have *imported infections only* through FSAT with 70% coverage. Once again however, as soon as the intervention stops, imported infections are predicted to revert immediately to previous levels while local infections take approximately two years to reach previous levels. Lower coverage rates ($< 70\%$) have also been explored, with the result of even smaller decreases in locally sourced infections.

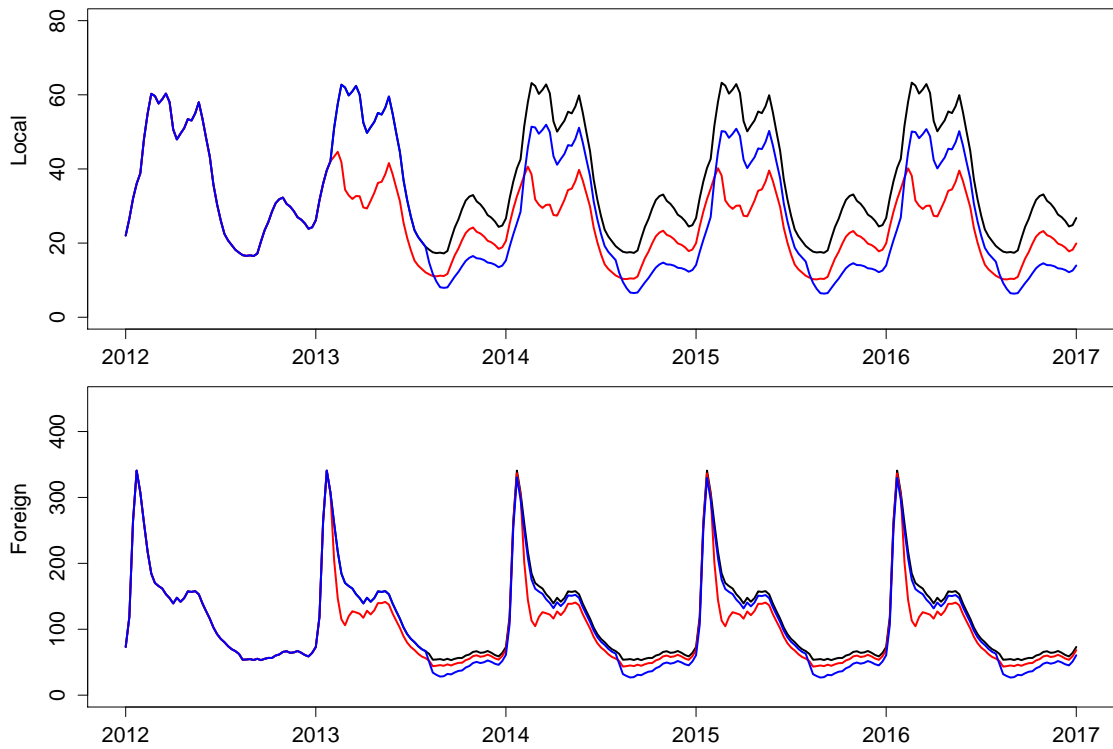


Figure 5.6: Predicted impact on the number of infections of annual rounds of MDA performed (from 2013) at the peak (red) and trough (blue) of the season on local and imported infections

Combining interventions

Figure 5.8 shows the predicted impact of a number of different combinations of interventions on locally sourced infections. The red line depicts the predicted impact of six consecutive two-monthly rounds of MDA followed immediately by FSAT (at the border on local people with new imported infections) enacted annually for six months from November to April at a 70% coverage rate. While these two mass interventions are not enough to eliminate local infections, a new substantially lower stable cycle is reached for local infections. If these interventions are supplemented with increased vector control (so as to decrease transmission by a further 20%), local infections reach very low levels with a maximum of 16 local infections per week at the peak of the season (blue). However, this resource-intensive combination of interventions is also predicted to be insufficient to achieve elimination of local malaria infections. The modelling of FSAT shows that acting on the imported infections of local people traveling back into Mpumalanga alone decreases the number of locally sourced cases. It is expected that the impact would be greater if the source of imported infections were targeted. Thus the green line is the model prediction based on foreign source reduction i.e. if the force of imported infection λ_f were decreased by

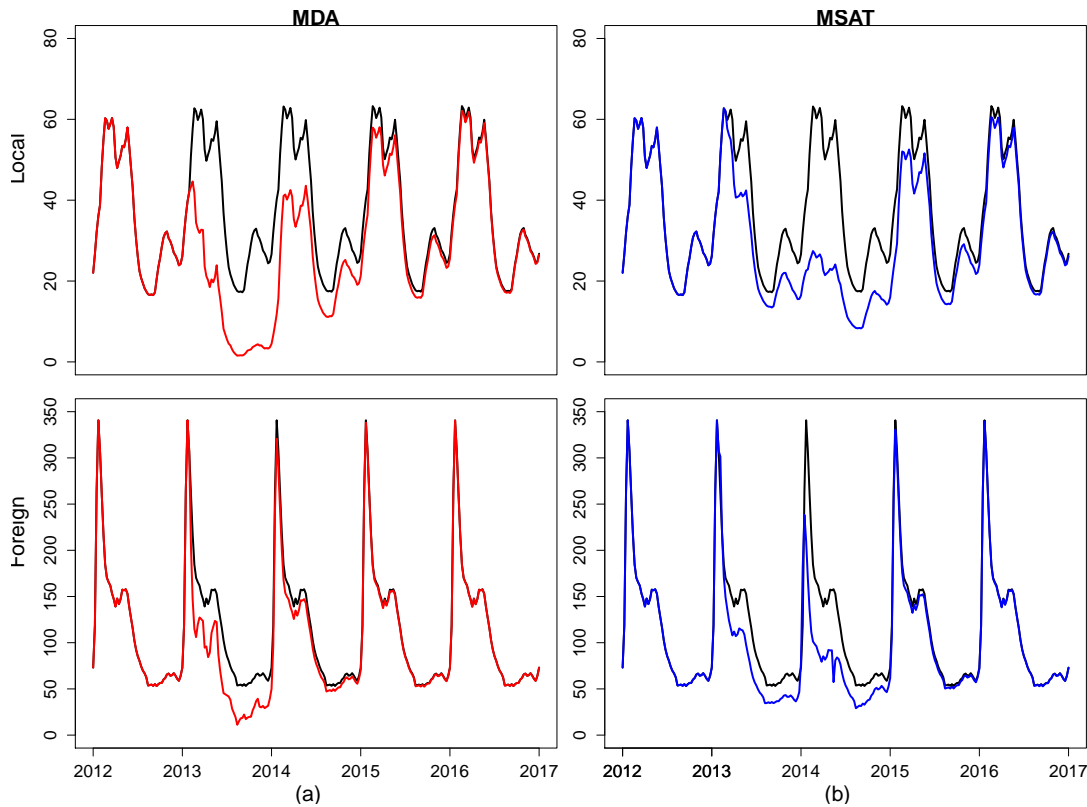


Figure 5.7: Predicted impact on the number of infections of (a) six consecutive 2-monthly rounds of MDA on local and imported infections and (b) six months of FSAT of new imported infections at 70% coverage (border screen and treat)

70% and locally six consecutive two-monthly rounds of MDA were applied and vector control was increased. Additionally, the purple line shows the predicted impact on local infections if there were no imported infections at all. In this scenario, the only other intervention that was applied was six rounds of MDA. This combination is sufficient to eliminate local malaria in Mpumalanga. It is predicted to take only 28 weeks on average from the end of the MDA cycle to reach below one local infection per year.

5.5 Discussion

South Africa has been employing vector control to control malaria since 1931 [72]. Reliance on vector control has been such that insecticide resistance to pyrethroids in 2000 resulted in a surge in malaria cases that could not be controlled through drug therapy alone. Consistent and large-scale IRS is considered one of the key reasons why malaria has been so well controlled in the country and in Mpumalanga. Scaling up IRS even further through targeted larviciding of

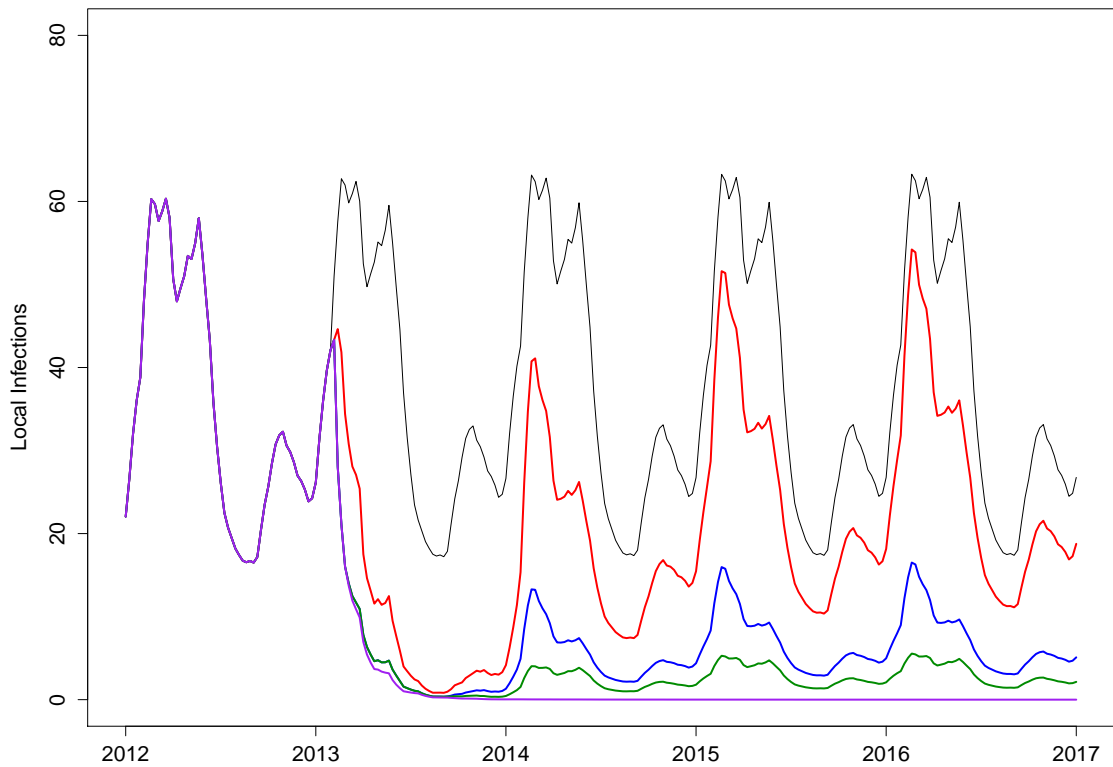


Figure 5.8: Predicted impact on local infections of combination of interventions on local infections: Black: No additional interventions, Red: 70% coverage of FSAT on local population with new imported infections following six consecutive two-monthly rounds of MDA at 80% coverage, Blue: same as red (MDA+FSAT) with increased vector control to decrease transmission by a further 20%, Green: six consecutive two-monthly rounds of MDA with increased vector control, and 70% decrease in the foreign force of infection, Purple: six consecutive two-monthly rounds of MDA with zero imported infections

vector breeding sites may be contemplated as a strategy to achieve malaria elimination. Scaling up vector control in the mathematical model for Mpumalanga, allowed local infections to decrease to a new equilibrium but did not eliminate local infections or decrease total infections substantially. It is expected that total infections will not decrease substantially as the majority of infections in Mpumalanga are imported and local vector control will not impact the number of imported infections in the province but will work towards decreasing onward transmission of these infections. It is because of this constant influx of imported infections that vector control alone will not be able to eliminate local malaria. A "more of the same" approach does not appear to work as it is insufficient to interrupt the transmission stable cycle.

Mass drug administration is a resource intensive intervention that needs to be acted out quickly, systematically and efficiently. It is a strategy that has not found favour in recent years; one

reason being that drug resistance is a feared consequence of MDA [142]. In a global environment seeking to protect the artemisinins (and their partner drugs) from drug resistance, the choice of drug for mass interventions has both global and economic importance. Economically, the drug needs to be affordable to be deployed on a large scale and globally, if resistance spreads to a point where the drug is no longer useful, the drug should be one that can be sacrificed. While the emergence of drug resistance has not been directly linked with MDA, it is possible that MDA will increase the selection pressure on the parasite population, with the possibility of losing the drug eventually [41]. In contrast, in fitting a mathematical model to trial results from Western Cambodia to assess the effects of elimination strategies and their interactions with artemisinin resistance, Maude *et al.* found that the proportion of artemisinin resistant infections increased quickly when ACT was introduced for treatment (in an area where treatment comprised non-artemisinin anti-malarial drugs and a low level of artemisinin monotherapy) and only slightly more when MDA with an ACT was implemented [85].

Both MDA and FSAT are interventions that have an immediate and large impact. Yet in countries with a large migrant population or populations with sub-optimal coverage, these interventions can fail because of the reintroduction of parasites and their impact may be short-lived [41]. Given the large proportion of imported cases in Mpumalanga, the model predicts that when a mass intervention targeting imported infections is stopped, both local and imported infection levels revert back to pre-intervention levels with a few years. This is because forces within Mpumalanga do not determine the level of imported infections; it is determined by the prevalence of malaria in the source country itself. Hence as the results of applications of MDA and FSAT in the model have shown, the large predicted impact can only be sustained if the mass interventions are applied often, and this is a resource-intensive strategy. Applying FSAT to local residents with imported infections in the model has predicted a substantial "knock-on" decrease in local infections. This is expected as decreasing imported infections decreases the infectious reservoir in the province, which in turn decreases local malaria transmission. The model also predicted the substantial impact, decreases in the foreign force of infection (foreign source reduction) have on local transmission. The scenario of zero imported infections was the only situation in which the model predicted that elimination of malaria could be achieved. This highlights the importance of source-reduction, monitoring imported infections and the receptivity of key areas within Mpumalanga. If the malaria vectors are present and ecological and climatic factors favour transmission in these areas, then onward transmission is probable even in the presence of good malaria control [50]. One strategy to decrease malaria transmission to zero would be to eliminate the mosquito vector population. This is highly unlikely to be feasible. As a result, even if low levels of malaria prevalence have been achieved, imported infections will augment the infectious reservoir, and since the vector remains, imported infections may lead to onward transmission to the local population and a resurgence of malaria generally [89].

In this deterministic model, a threshold was defined to determine elimination as it is mathematically impossible to achieve zero cases in a differential equation framework. As is the case with

selecting any threshold, more severe thresholds could always be selected. It is of interest in this manuscript that malaria elimination could not even be predicted with the current threshold, let alone more severe thresholds. In a review on the historical and current definitions of malaria, Cohen *et al.* defines three states of malaria transmission to be controlled low-endemic malaria, elimination and controlled non-endemic malaria. This third state describes the situation where the interruption of endemic transmission has occurred but there is still malaria resulting from onward transmission from imported infections and this onward transmission is sufficiently high that elimination has not yet been achieved [23]. This implies that if all onward infection from imported infections could be prevented, elimination of malaria would follow naturally. The results of this modelling exercise suggest that Mpumalanga is in this third state of transmission as elimination of malaria is only predicted to be possible with unrealistic, resource-intensive interventions that result in a drastic reduction in imported infections. In realising that the key to decreasing local infections further is to prevent imported infections, new approaches must be explored both nationally and regionally.

The transmission model presented in this paper is a deterministic population-level one considering only the population of Mpumalanga. While population-level models are useful to assess aggregate effects, the entire population is treated as homogeneously affected by malaria transmission. Thus there is no scope to include spatial variation or heterogeneous behaviour in the transmission model or in the interventions themselves. Imported infections play an important role in transmission dynamics in Mpumalanga and human migration is modelled indirectly. Current work includes disaggregating the population into smaller groups such as administrative districts, and using a stochastic, meta-population model of transmission to model these districts while explicitly incorporating human migration between Mozambique (the main source of imported infections) and Mpumalanga. This will allow one to assess the impact of deploying interventions sequentially in the administrative districts as well as in Mozambique itself. For example, Silal *et al.* found that infections in Bushbuckridge municipality occur at higher levels at the start of the season compared to other municipalities in Mpumalanga [116]. It may be of interest then to assess if intervening in this municipality at the start of the season has a knock-on effect on malaria in the rest of the province. Spatial heterogeneity will also allow for improved modelling of interventions that target imported infections such as border control through FSAT, and source reduction in Mozambique. Future work also includes incorporating vector population dynamics in the model so that vector control activities such as indoor residual spraying and larviciding may be modelled explicitly.

5.6 Conclusions

South Africa aims to achieve malaria elimination by 2018. This requires synchronized action in the three provinces in which malaria occurs in order to decrease local infections to zero. In the case

of Mpumalanga, given the large proportion of imported cases, interventions also need to target imported infections to decrease the infectious reservoir impacting local transmission. In isolated countries, a nationally focused elimination programme may stand a better chance of success than countries with high levels of visitation from higher transmission regions [128]. This paper has used population level mathematical modelling to model transmission in Mpumalanga and test out strategies (FSAT, MDA, increased vector control and foreign source reduction) that may be used to achieve malaria elimination. While all strategies (in isolation or combined) contributed to decreasing local infections, none was able to decrease local infections to zero due mainly to the continuous stream of imported infections highlighting the importance of source reduction and a regional approach to malaria control and elimination. Disaggregating the model into smaller groups will allow for the spatial heterogeneity required to optimize elimination strategy that may lead to different results. Mathematical modelling has the potential to inform government policy to achieve malaria elimination and with effective and efficient interventions, adequate sustainable finance, local and international political commitment and an epidemiological understanding of malaria elimination, malaria elimination in Mpumalanga may be possible in the foreseeable future.

5.7 Additional File 1: Mathematical Model Description

5.7.1 Base Model of Transmission

The model is a deterministic ordinary non-linear differential equation representation of the dynamics of the human population. In the model, the population is divided into nine compartments: the susceptible population (S), the asexual blood stage only (B_l and B_f) for locally and imported infections respectively and the infectious gametocyte stage (I_l and I_f) for locally and imported infections respectively. The blood stage and infectious stage compartments are further stratified according to whether the infection is treated or not. The liver stage of the infection is incorporated as a delay in the flow between the susceptible and blood stage compartments. As this is a low transmission environment, immunity and super-infection are rare and are excluded from this model. While the seasonal nature of transmission is incorporated in the model, the mosquito population is not modelled directly as it is assumed that the mosquito dynamics operate on a faster time-scale than the human dynamics and as such the mosquito population can be considered to be at equilibrium with respect to changes in the human population [66]. In the absence of sufficient data, asymptomatic infections and human migration are included indirectly in the model. The impact of the movement of infected individuals from external sources is captured through the parameter λ_f , the foreign force of infection i.e. the force of infection that generates imported infections. The impact of asymptomatic infections is captured by repeating the model analysis for a low assumption on the proportion seeking treatment.

This system is described by a set of non-linear differential equations of form:

$$\begin{aligned} \frac{dS}{dt} &= \mu N - \lambda_l[t - \sigma_1]seas_l[t]S - \lambda_f[t - \sigma_1]seas_f[t]S + \frac{1}{r + \tau}(B_{l,tr} + I_{l,tr} + B_{f,tr} + I_{f,tr}) + \\ &\quad \frac{1}{\delta}(I_{l,u} + I_{f,u}) - \mu S \\ \frac{dB_{l,tr}}{dt} &= p\lambda_l[t - \sigma_1]seas_l[t]S - \frac{1}{\sigma_2}B_{l,tr} - \frac{1}{r + \tau}B_{l,tr} - \mu B_{l,tr} \\ \frac{dI_{l,tr}}{dt} &= \frac{1}{\sigma_2}B_{l,tr} - \frac{1}{r + \tau}I_{l,tr} - \mu I_{l,tr} \\ \frac{dB_{l,u}}{dt} &= (1 - p)\lambda_l[t - \sigma_1]seas_l[t]S - \frac{1}{\sigma_2}B_{l,u} - \mu B_{l,u} \\ \frac{dI_{l,u}}{dt} &= \frac{1}{\sigma_2}B_{l,u} - \frac{1}{\delta}I_{l,u} - \mu I_{l,u} \\ \frac{dB_{f,tr}}{dt} &= p\lambda_f[t - \sigma_1]seas_f[t]S - \frac{1}{\sigma_2}B_{f,tr} - \frac{1}{r + \tau}B_{f,tr} - \mu B_{f,tr} \\ \frac{dI_{f,tr}}{dt} &= \frac{1}{\sigma_2}B_{f,tr} - \frac{1}{r + \tau}I_{f,tr} - \mu I_{f,tr} \\ \frac{dB_{f,u}}{dt} &= (1 - p)\lambda_f[t - \sigma_1]seas_f[t]S - \frac{1}{\sigma_2}B_{f,u} - \mu B_{f,u} \end{aligned}$$

$$\frac{dI_{f,u}}{dt} = \frac{1}{\sigma_2} B_{f,u} - \frac{1}{\delta} I_{f,u} - \mu I_{f,u}$$

where

$$\lambda_l = (1 - vc[t])\beta_l \times \frac{I_{l,u} + I_{l,tr} + I_{f,u} + I_{f,tr}}{N}$$

and subscript l refers to locally sourced infections, f : foreign sourced infections, u : untreated infections and tr : treated infections. Thus local transmission is a function of the force of infection λ , the annual number of mosquito bites per person \times proportion of bites testing positive for sporozoites (β_l), seasonality of transmission ($seas$) and vector control (vc). Data fitting produces an estimate for the scalar β_l and any modelled increases or decreases in the *level* of transmission are due to changes in vector control. Compartment descriptions are provided in Table 5.2.

5.7.2 Transmission model with interventions

In this model the following interventions are modelled: Mass Drug Administration, Focal Screen and Treat, Scale-up of Vector Control and Foreign Source Reduction. In the intervention model, it is further assumed that Mass Drug administration is subjected only once to members of the population during a particular MDA cycle. While, a prophylactic effect of drug is accounted for, it is still possible to be infected after the protective period but before the MDA cycle is completed. Should this be the case, the proportion of the population will not receive MDA in that cycle again, but will be subject to routine treatment as per the base model. FSAT is applied to new imported infections (arising from a foreign source of infection λ_f) as they enter Mpumalanga from the foreign source and are assumed to be infectious.

The following scenarios are tested:

- (a) Scale up Vector Control so as to decrease β_l by a further (i) 10% and (ii) 20%
- (b) Mass Drug Administration at 80% coverage over two months
 - (i) annually over the peak of the season
 - (ii) annually over the trough of the season
 - (iii) six consecutive rounds over twelve months
- (c) Focal Screen and Treat on imported infections at 70% coverage for six months over the malaria season
- (d) (b-iii) & annual rounds of (c)
- (e) (b-iii) & annual rounds of (c) & (a-i)

(f) Reducing the foreign source of infection by 70%

(g) (b-iii) & reducing the foreign source of infection by 100% (Hypothetical)

This system is described by a set of non-linear differential equations and is depicted in Figure 5.9:

$$\begin{aligned}
 \frac{dS}{dt} &= \mu N - \lambda_l[t - \sigma_1]seas_l[t]S - \lambda_f[t - \sigma_1]seas_f[t](1 - f_{sr}[t])S + \frac{1}{r + \tau}(B_{l,tr} + I_{l,tr} + B_{f,tr} + I_{f,tr}) + \\
 &\quad \frac{1}{\delta}(I_{l,u} + I_{f,u}) - \frac{1}{mrate[t]}S + \frac{1}{ass[t]}S_{mda} + \frac{1}{proFSAT[t]}S_{fsat} - \mu S \\
 \frac{dB_{l,tr}}{dt} &= p\lambda_l[t - \sigma_1]seas_l[t]S - \frac{1}{\sigma_2}B_{l,tr} - \frac{1}{r + \tau}B_{l,tr} - \frac{1}{mrate[t]}B_{l,tr} + \frac{1}{ass[t]}B_{mda,l,tr} - \mu B_{l,tr} \\
 \frac{dI_{l,tr}}{dt} &= \frac{1}{\sigma_2}B_{l,tr} - \frac{1}{r + \tau}I_{l,tr} - \frac{1}{mrate[t]}I_{l,tr} + \frac{1}{ass[t]}I_{mda,l,tr} - \mu I_{l,tr} \\
 \frac{dB_{l,u}}{dt} &= (1 - p)\lambda_l[t - \sigma_1]seas_l[t]S - \frac{1}{\sigma_2}B_{l,u} - \frac{1}{mrate[t]}B_{l,u} + \frac{1}{ass[t]}B_{mda,l,u} - \mu B_{l,u} \\
 \frac{dI_{l,u}}{dt} &= \frac{1}{\sigma_2}B_{l,u} - \frac{1}{\delta}I_{l,u} - \frac{1}{mrate[t]}I_{l,u} + \frac{1}{ass[t]}I_{mda,l,u} - \mu I_{l,u} \\
 \frac{dB_{f,tr}}{dt} &= p(1 - msprop[t])\lambda_f[t - \sigma_1]seas_f[t](1 - f_{sr}[t])S - \frac{1}{\sigma_2}B_{f,tr} - \frac{1}{r + \tau}B_{f,tr} - \frac{1}{mrate[t]}B_{f,tr} + \\
 &\quad \frac{1}{ass[t]}B_{mda,f,tr} - \mu B_{f,tr} \\
 \frac{dI_{f,tr}}{dt} &= \frac{1}{\sigma_2}B_{f,tr} - \frac{1}{r + \tau}I_{f,tr} - \frac{1}{mrate[t]}I_{f,tr} + \frac{1}{ass[t]}I_{mda,f,tr} - \mu I_{f,tr} \\
 \frac{dB_{f,u}}{dt} &= (1 - p)(1 - msprop[t])\lambda_f[t - \sigma_1]seas_f[t](1 - f_{sr}[t])S - \frac{1}{\sigma_2}B_{f,u} - \frac{1}{mrate[t]}B_{f,u} + \frac{1}{ass[t]}B_{mda,f,u} - \mu B_{f,u} \\
 \frac{dI_{f,u}}{dt} &= \frac{1}{\sigma_2}B_{f,u} - \frac{1}{\delta}I_{f,u} - \frac{1}{mrate[t]}I_{f,u} + \frac{1}{ass[t]}I_{mda,f,u} - \mu I_{f,u} \\
 \frac{dS_{mda}}{dt} &= \frac{1}{mrate[t]}S + adh * \frac{1}{proMDA[t]}(B_{mda} + I_{mda}) - \frac{1}{ass[t]}S_{mda} - \mu S_{mda} \\
 \frac{dB_{mda}}{dt} &= \frac{1}{mrate[t]}(B_{l,tr} + B_{l,u} + B_{f,tr} + B_{f,u}) - \frac{1}{\sigma_2}B_{mda} - adh * \frac{1}{proMDA[t]}B_{mda} - \mu B_{mda} \\
 \frac{dI_{mda}}{dt} &= \frac{1}{mrate[t]}(I_{l,tr} + I_{l,u} + I_{f,tr} + I_{f,u}) + \frac{1}{\sigma_2}B_{mda} - adh * \frac{1}{proMDA[t]}I_{mda} - \mu I_{mda} \\
 \frac{dS_{fsat}}{dt} &= adh * \frac{1}{r}I_{fsat} - \frac{1}{proFSAT[t]}S_{fsat} - \mu S_{fsat} \\
 \frac{dI_{fsat}}{dt} &= msprop[t]\lambda_f[t - \sigma_1]seas_f[t](1 - f_{sr}[t])S - adh * \frac{1}{r}I_{fsat} - \mu I_{fsat} \\
 \frac{dB_{mda,l,tr}}{dt} &= p\lambda_l[t - \sigma_1]seas_l[t]S_{mda} - \frac{1}{\sigma_2}B_{mda,l,tr} - \frac{1}{r + \tau}B_{mda,l,tr} - \frac{1}{ass[t]}B_{mda,l,tr} - \mu B_{mda,l,tr} \\
 \frac{dI_{mda,l,tr}}{dt} &= \frac{1}{\sigma_2}B_{mda,l,tr} - \frac{1}{r + \tau}I_{mda,l,tr} - \frac{1}{ass[t]}I_{mda,l,tr} - \mu I_{mda,l,tr} \\
 \frac{dB_{mda,l,u}}{dt} &= (1 - p)\lambda_l[t - \sigma_1]seas_l[t]S_{mda} - \frac{1}{\sigma_2}B_{mda,l,u} - \frac{1}{ass[t]}B_{mda,l,u} - \mu B_{mda,l,u}
 \end{aligned}$$

$$\begin{aligned}
 \frac{dI_{mda,l,u}}{dt} &= \frac{1}{\sigma_2} B_{mda,l,u} - \frac{1}{\delta} I_{mda,l,u} - \frac{1}{ass[t]} I_{mda,l,u} - \mu I_{mda,l,u} \\
 \frac{dB_{mda,f,tr}}{dt} &= p(1 - msprop[t])\lambda_f[t - \sigma_1]seas_f[t](1 - fsr[t])S_{mda} - \frac{1}{\sigma_2} B_{mda,f,tr} - \frac{1}{r + \tau} B_{mda,f,tr} \\
 &\quad - \frac{1}{ass[t]} B_{mda,f,tr} - \mu B_{mda,f,tr} \\
 \frac{dI_{mda,f,tr}}{dt} &= \frac{1}{\sigma_2} B_{mda,f,tr} - \frac{1}{r + \tau} I_{mda,f,tr} - \frac{1}{ass[t]} I_{mda,f,tr} - \mu I_{mda,f,tr} \\
 \frac{dB_{mda,f,u}}{dt} &= (1 - p)(1 - msprop[t])\lambda_f[t - \sigma_1]seas_f[t](1 - fsr[t])S_{mda} - \frac{1}{\sigma_2} B_{mda,f,u} \\
 &\quad - \frac{1}{ass[t]} B_{mda,f,u} - \mu B_{mda,f,u} \\
 \frac{dI_{mda,f,u}}{dt} &= \frac{1}{\sigma_2} B_{mda,f,u} - \frac{1}{\delta} I_{mda,f,u} - \frac{1}{ass[t]} I_{mda,f,u} - \mu I_{mda,f,u}
 \end{aligned}$$

where

$$\lambda_l = (1 - vc[t] - vc_{add}[t]) \beta_l \times \frac{I_{l,u} + I_{l,tr} + I_{f,u} + I_{f,tr} + I_{mda} + I_{fsat} + I_{mda,l,u} + I_{mda,l,tr} + I_{mda,f,u} + I_{mda,f,tr}}{N}$$

and subscript l refers to locally sourced infections, f : foreign sourced infections, u : untreated infections and tr : treated infections. Compartment descriptions are provided in Table 5.2.

Table 5.2: Model 1: Compartment Descriptions table

Compartment	Description
S	Susceptible Population
$B_{l,tr}$	Population with Blood Stage local Infections that are treated
$I_{l,tr}$	Population with Infectious Stage local Infections that are treated
$B_{l,u}$	Population with Blood Stage local Infections that are not treated
$I_{l,u}$	Population with Infectious Stage local Infections that are not treated
$B_{f,tr}$	Population with Blood Stage foreign Infections that are treated
$I_{f,tr}$	Population with Infectious Stage foreign Infections that are treated
$B_{f,u}$	Population with Blood Stage foreign Infections that are not treated
$I_{f,u}$	Population with Infectious Stage foreign Infections that are not treated
S_{mda}	Susceptible Population having received MDA in a given cycle
B_{mda}	Population with Blood stage infections having received MDA in a given cycle
I_{mda}	Population with Infectious stage infections having received MDA in a given cycle
S_{fsat}	Susceptible Population having received FSAT in a given cycle

I_{fsat}	Population with Blood and Infectious stage infections having received FSAT in a given cycle
$B_{mda,l,tr}$	Population (infected after MDA) with Blood Stage local Infections that are treated
$I_{mda,l,tr}$	Population (infected after MDA) with Infectious Stage local Infections that are treated
$B_{mda,l,u}$	Population (infected after MDA) with Blood Stage local Infections that are not treated
$I_{mda,l,u}$	Population (infected after MDA) with Infectious Stage local Infections that are not treated
$B_{mda,f,tr}$	Population (infected after MDA) with Blood Stage foreign Infections that are treated
$I_{mda,f,tr}$	Population (infected after MDA) with Infectious Stage foreign Infections that are treated
$B_{mda,f,u}$	Population (infected after MDA) with Blood Stage foreign Infections that are not treated
$I_{mda,f,u}$	Population (infected after MDA) with Infectious Stage foreign Infections that are not treated

Table 5.3: Full Parameter table

Parameter	Description	Value	Source
Base Model Parameters			
N	Population size	4×10^6	[125]
μ	Mortality Rate	$\frac{105}{10000}$	[90]
δ	Natural recovery period	26 weeks	[61, 86, 141]
σ_1	Period between liver stage and blood stage	7 days (5-10)	[19, 25, 33]
σ_2	Period between blood stage and onset of gametocytemia	1 week	[61, 134]
r	AL elimination half-life	6 days	[77]
τ	Time to seek treatment	1/2 week	Expert opinion
p	Proportion that receive treatment	0.95	[18, 58]
$seas_l$	Seasonal forcing function for locally sourced cases	Derived from data	[116]

$seas_f$	Seasonal forcing function for foreign sourced cases	Derived from data	[116]
β_l	Annual number of mosquito bites per person x proportion of bites testing positive for sporozoites	39.170 (38.894, 39.448)	Estimated from model fitting process
λ_f	Force of imported infections	0.002163 (0.002124, 0.002202)	Estimated from model fitting process
λ_l	Force of locally sourced infections	$(1 - vc[t])\beta_l \times \frac{I_{l,u} + I_{l,tr} + I_{f,u} + I_{f,tr}}{N}$	
Vector Control			
$vc[t]$	$vccov \times vceff$		
$vccov$	Vector Control Coverage	0.22-0.90	Derived from data
$vceff$	Effectiveness of vector control	0.9060 (0.8884, 0.9212)	Estimated from model-fitting process
$vc_{add}[t]$	Additional Vector Control Coverage	$vcaddon \times vcadd$	
$vcaddon$	Additional Vector Control Switch	Binary	
$vcadd$	Additional Vector Control Coverage	Scenario list	
Mass Drug Administration			
$mrate[t]$	Rate of MDA Take-up	$mdaon(-\log(1-mcov)/mdur)$	
$mdaon$	Mass Drug Administration Switch	Binary	
$mcov$	MDA coverage	80%	
$mdur$	Duration of MDA cycle	8 weeks	
$pro_{MDA}[t]$	Drug Protection period	4 weeks	[103]
adh	Adherence to Treatment	90%	[8]
$ass^{-1}[t]$	Rate of assimilation at the end of MDA cycle	Shift parameter	Modelling construct
Focal Screen and Treat			
$msprop[t]$	Proportion Screened and Treated through Border Control	$mson \times mscov$	

m_{son}	Focal Screen and Treat Switch	Binary	
m_{scov}	FSAT coverage	70%	
$pro_{FSAT}[t]$	Drug Protection period	4 weeks	[103]
Foreign Source Reduction			
$fsr[t]$	Proportion reduced of the force of imported infections	$fsron \times fsrprop$	
$fsron$	Foreign Source Reduction Switch	Binary	
$fsrprop[t]$	Proportional reduction	Scenario list	

5.7.3 Vector Control

Indoor Residual spraying is the primary vector control intervention employed in Mpumalanga. The data on the number of structures sprayed in Mpumalanga is provided by the Malaria Elimination Programme and has already been presented in Ngomane and de Jager (2012) and is depicted in Figure 5.10 [95]. Given that IRS is not 100% effective, a parameter on the effectiveness of IRS ($vceff$) has been estimated in the data-fitting process.

5.7.4 Asymptomatic Infections

As asymptomatic infections are common even in low transmission areas, it is important to consider their impact in this model [55, 98]. In the absence of any data on the prevalence of asymptomatic infections in Mpumalanga, their impact has been assessed by re-running the analysis reducing the probability of treatment from 95% to 50%. By re-fitting the model to the data and re-running the analysis, the model predicts that it is only through action that reduces imported infections like extreme source reduction that elimination (as defined by the threshold used in the model) is possible (Figure 5.11). This is in line with the results predicted by the base model.

5.7.5 Data Fitting Method

The model is fitted to weekly cases from 2002 to 2008, and then validated with data from 2009 to 2012. The model is run from 1990 to reach a steady state before being fitted to data from 2002. IRS coverage and drug treatment are included in the model for the data fitting. The model output (local and imported treated cases) are fitted to the data using the maximum likelihood approach assuming an underlying Poisson distribution with canonical parameter λ as the average

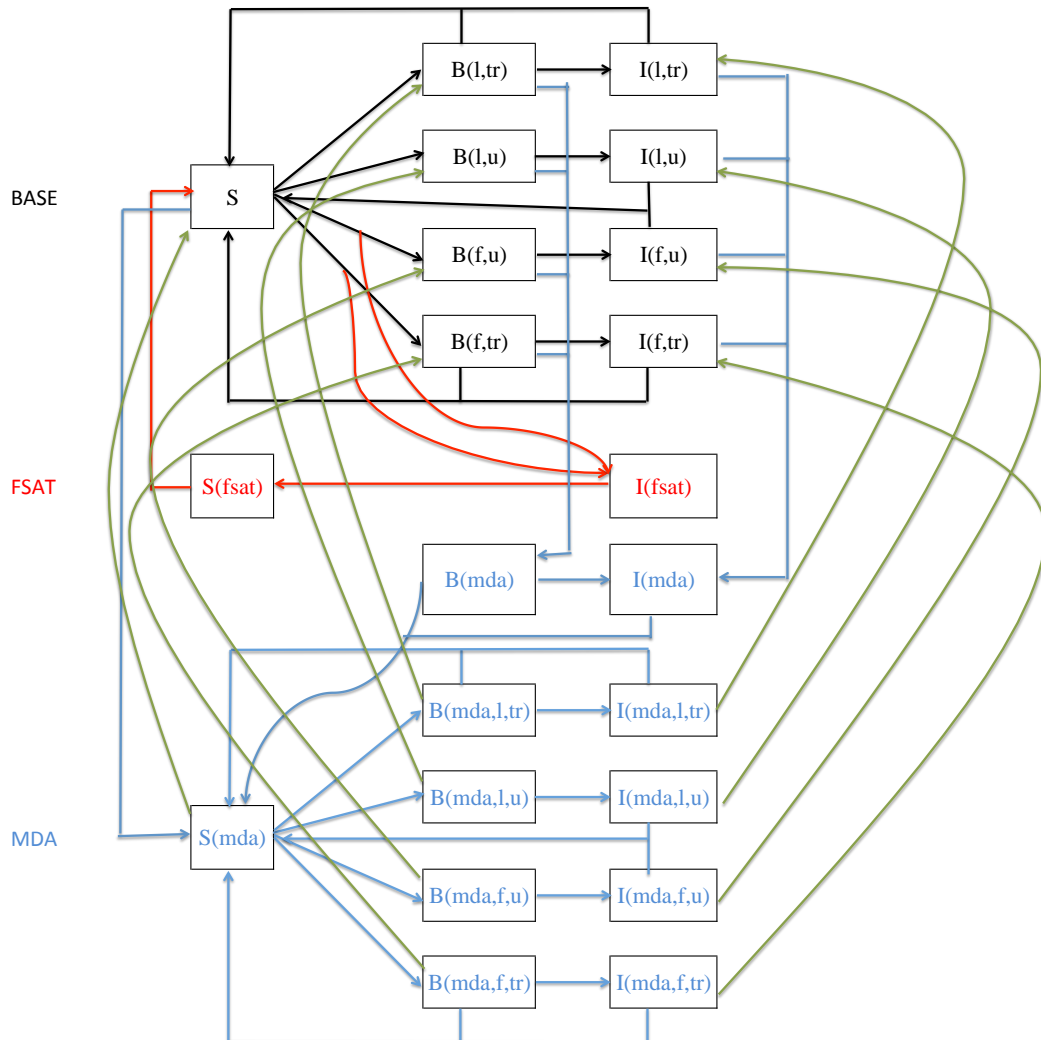


Figure 5.9: Model flow: Base Model (black) with interventions: FSAT(red), MDA(blue). The assimilation of the population having been subjected to MDA, but infected during the MDA cycle though after the prophylactic protection period of the drug, is represented in green. This is necessary as the duration of the MDA cycle is 8 weeks whereas the prophylactic period of the drug is only 4 weeks, so it is possible to get infected again within the 8 week period after being subjected to MDA. If these infections were accounted for in the base model compartments, it would be possible to receive MDA again, which is not usually the case.

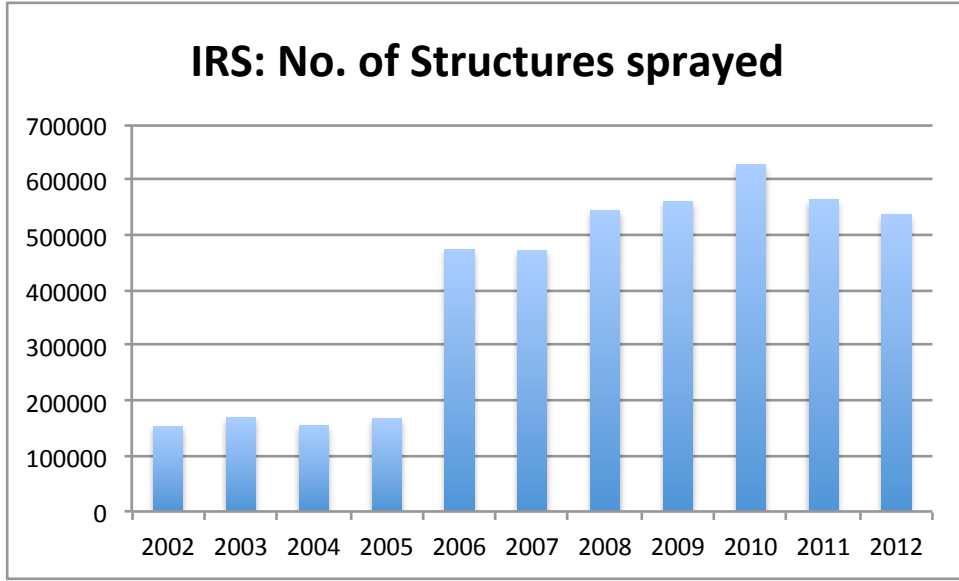


Figure 5.10: Number of structures sprayed in Mpumalanga between 2002 and 2012

number of treated cases per week. No reporting proportion is attached to the parameter λ as studies in Mpumalanga have highlighted the extremely high treatment seeking proportion and intention to do so within 24 hours [18, 58]. The population-level non-linear differential equation model is expressed in terms of average rates of movement between compartments.

The Poisson probability of observing x counts when the average is λ is given by

$$P(x|\lambda) = \frac{\lambda^x \exp^{-\lambda}}{x!}.$$

As the model is being fitted to time series data with N time bins, λ , the expected number of counts per bin is a function of time. Assuming the independence of data in each time bin reduces the likelihood to

$$L(\lambda_i|x_i) = \prod_{i=1}^N \frac{\lambda_i^{x_i} \exp^{-\lambda_i}}{x_i!}$$

and the log likelihood becomes

$$\ln(L(\lambda_i|x_i)) = \sum_{i=1}^N x_i \ln(\lambda_i) - \lambda_i - \ln(x_i!).$$

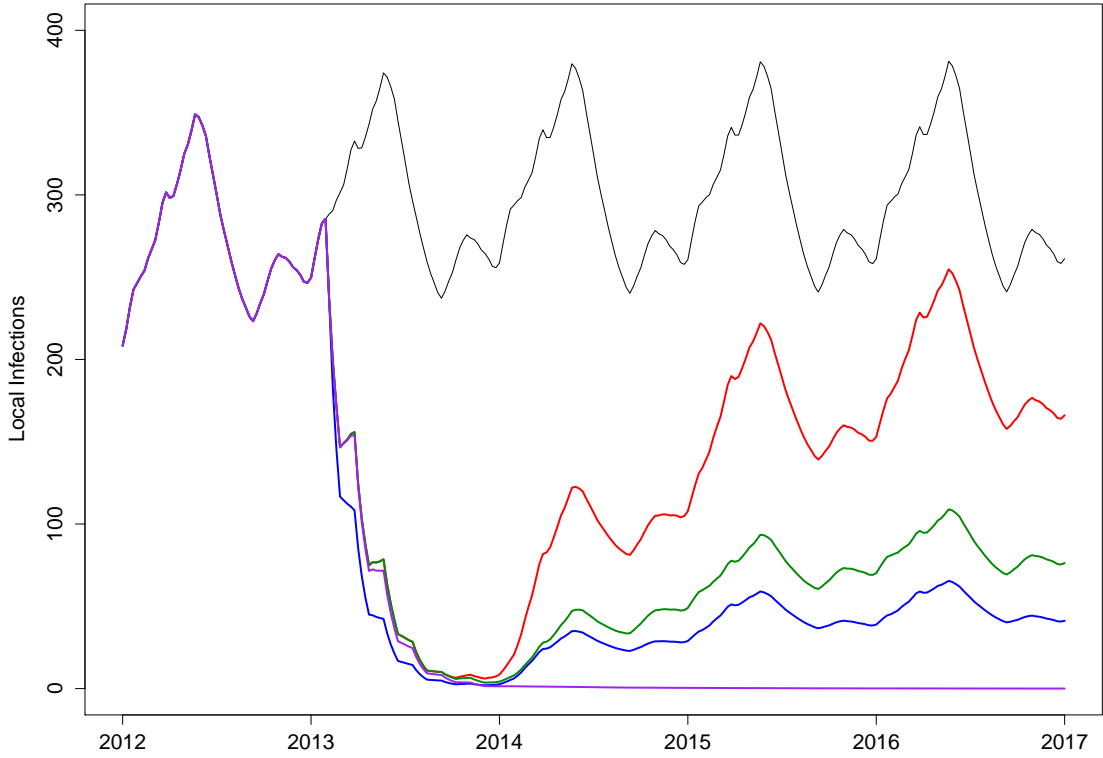


Figure 5.11: 50% probability of treatment: Predicted impact on local infections of combination of interventions on local infections: Black: No additional interventions, Red: 70% coverage of FSAT on local population with new imported infections following six consecutive two-monthly rounds of MDA at 80% coverage, Blue: same as red (MDA+FSAT) with increased vector control to decrease transmission by a further 20%, Green: six consecutive two-monthly rounds of MDA with increased vector control, and 70% decrease in the foreign force of infection, Purple: six consecutive two-monthly rounds of MDA with zero imported infections

The model output is fitted to two sets of data for each weekly time bin: locally sourced treated cases (l) and imported treated cases (f). Under the assumption of independence, the log likelihood to be maximised is

$$\ln(L(\lambda_{l,i}, \lambda_{f,i} | x_{l,i}, x_{f,i})) \propto \sum_{i=1}^n x_{l,i} \ln(\lambda_{l,i}) - \lambda_{l,i} + x_{f,i} \ln(\lambda_{f,i}) - \lambda_{f,i}$$

The log-likelihood is negated and minimised using the optim function implementing the Nelder and Mead algorithm in the R package Stats [94]. The parameters β_l , λ_f and $vceff$ are estimated

through this data fitting process. As the Nelder and Mead algorithm is a local search method, it is necessary to perform the optimisation from different starting points. The optimisation is performed 10000 times with starting values sampled from a Latin hypercube framework. The parameter estimates and their standard errors are retrieved from the optimisation output and are presented in Table 5.3. The model with the estimated parameter values is then run for a further 3 years (including IRS at comparative levels) to be further validated by comparison to data between 2009 and 2012.

Chapter 6

Model 2 - Metapopulation model of malaria transmission

Chapter 5's population level model of malaria transmission predicted that while all strategies (in isolation or combined) contributed to decreasing local infections, none was able to decrease local infections to zero due mainly to the continuous stream of imported infections highlighting the importance of cross-border collaborative initiatives. It was also noted that the model considers only the population of Mpumalanga and while population-level models are useful to assess aggregate effects, the entire population is treated as homogeneously affected by malaria transmission. Hence there is no scope to incorporate heterogeneous behaviour and spatial variation in the transmission model nor in the interventions themselves. Though imported infections play an important role in transmission dynamics in Mpumalanga, human migration is not explicitly modelled in Chapter 5. The metapopulation model presented in this chapter addresses this issue by modelling transmission in Ehlanzeni District, the district most affected by malaria in Mpumalanga and disaggregating the population of Ehlanzeni District into the five administrative municipalities. To explicitly incorporate human migration, an additional metapopulation representing Maputo Province is modelled. Each metapopulation (or patch, as it is also known) is further sub-divided into three populations: (1) the local population of the patch currently in the patch, (2) the local population of the patch having returned from travel to a foreign place (Maputo, if the patch is South African and vice versa) and (3) the population from the foreign place currently in the patch. In this way, migration between Mpumalanga and Maputo province is modelled. The SBI model presented is then used to model malaria transmission in each sub-patch. The SBI model structure differs from the population level model presented in Chapter 5 only in that infections are no longer stratified by source, as the metapopulation model structure incorporates source of infection already. The population level model in Chapter 5 was a deterministic one as it represented average behaviour in the malaria system. In choosing to

model only Ehlanzeni District and further disaggregating the population into smaller groups, it became necessary to introduce stochasticity into the metapopulation model as average effects may no longer be representative of the behaviour of small populations.

The metapopulation model presented in this chapter is developed to assess the impact of proposed elimination-focused policy interventions in Mpumalanga. This is the first study designed for this purpose in Mpumalanga and the first to do so in South Africa since the call for malaria elimination. The metapopulation structure is used to describe movement between five municipalities in the Ehlanzeni District (Thaba Chewu (TC), Mbombela (MB), Umjindi (UJ), Nkomazi (NK) and Bushbuckridge (BB)) on the eastern border of Mpumalanga and more importantly movement between these municipalities and Maputo Province (MP), Mozambique. A stochastic non-linear ordinary differential equation model fitted to the Mpumalanga and Maputo Province malaria case data, is used to predict the impact of the following interventions (alone and in combination): scale-up of Vector Control, Mass Drug Administration (MDA), a Focal Screen and treat campaign (FSAT) and foreign source reduction.

The model is fitted to weekly case data of treated cases from 2002 to 2008, and then validated with data from 2009 to 2012. The model predicts that while locally focused strategies (in isolation or combined) contribute to decreasing local infections, none is able to decrease local infections to zero. The greatest impact on local infections is predicted when source reduction through mass action or vector control is conducted in Maputo itself highlighting the importance of cross-border collaborative initiatives. The paper concludes that a regionally focused strategy may stand a better chance at achieving elimination in Mpumalanga and South Africa compared to a nationally focused one in the face of high visitation rates from neighbours in higher transmission regions. An additional file which contains detailed descriptions of the model fitting process and model equations is presented at the end of the chapter.

SPS wrote the paper and performed the mathematical model development and analysis. SPS and LJW conceptualised the mathematical model and analysis. FL, KIB and LJW reviewed the manuscript extensively. All authors have read and approved the manuscript.

We are grateful to the Malaria Elimination Programme of the Department of Health in Mpumalanga, South Africa for the provision of data and are particularly grateful to Aaron Mabuza and Gerdalize Kok from the Malaria Elimination Programme for their valuable input. This material is based upon work supported financially by the National Research Foundation in South Africa. We are grateful to the National Research Foundation in South Africa for financial support. Any opinion, findings and conclusions or recommendations expressed in this material are those of the authors and therefore the NRF does not accept any liability in regard thereto. Mahidol-Oxford Tropical Medicine Research Unit is funded by the Wellcome Trust.

Hitting a moving target: a model for malaria elimination in the presence of population movement

Sheetal Prakash Silal^{1,*}, Francesca Little¹, Karen I Barnes², Lisa J White^{3,4},

¹ Department of Statistical Sciences, University of Cape Town, Cape Town, South Africa

² Division of Clinical Pharmacology, Department of Medicine, University of Cape Town, Cape Town, South Africa

³ Mahidol-Oxford Tropical Medicine Research Unit, Mahidol University, Bangkok, Thailand

⁴ Centre for Tropical Medicine, Nuffield Department of Clinical Medicine, Churchill Hospital, University of Oxford, Oxford, UK

6.1 Abstract

South Africa is committed to eliminating malaria by 2018. Malaria elimination strategies may be unsuccessful if they focus only on the biology of vector, and ignore the mobility patterns of humans, particularly where the majority of infections are imported. In the first study in Mpumalanga Province in South Africa designed for this purpose, a meta-population model is developed to assess the impact of their proposed elimination-focused policy interventions. A stochastic non-linear ordinary differential equation model is fitted to malaria data from Mpumalanga and neighbouring Maputo Province in Mozambique. Further scaling-up of vector control is predicted to lead to a minimal reduction in local infections, while mass drug administration and focal screening and treatment at the Mpumalanga-Maputo border are predicted to have only a short-lived impact. Source reduction in Maputo Province is predicted to generate large reductions in local infections through stemming imported infections. The mathematical model predicts malaria elimination to be possible only when imported infections are treated before entry or eliminated at the source. To eliminate malaria by 2018, the government of South Africa will need to design and implement an elimination strategy tailored for a country with a high level of imported infections. A regionally focused strategy appears needed, for achieving malaria elimination in Mpumalanga and South Africa.

Under review at Science

6.2 Introduction

Mathematical modelling is an integral tool aiding our understanding of the dynamics of infectious diseases [2]. Mathematical models and their applications to malaria in particular, have a history that spans over 100 years [82]. Since the call in October 2007 for renewed efforts towards achieving global malaria eradication, more than 25 previously endemic countries are in the pre-elimination or elimination phase of the eradication effort [51, 108]. As South Africa (now in the pre-elimination phase - < 5 cases per 1000 people) is committed to eliminating malaria by 2018, efforts are increasing in the malaria-endemic provinces, including Mpumalanga, beyond those needed for malaria control [93]. With vector-borne diseases like malaria, strategies to eliminate may be unsuccessful if they focus only on the biology of vector and parasite, and ignore the mobility patterns of humans [3]. This is particularly true in areas where the majority of infections are imported, where the elimination strategy needs also to consider sources of infection in neighbouring regions, including mobility between regions and whether their control or elimination efforts are optimal. In this paper, a metapopulation non-linear, stochastic ordinary differential equation model is used to simulate malaria transmission in Mpumalanga and neighbouring Maputo Province in Mozambique, in order to assess the potential impact of implementing the policy changes that may be used to achieve malaria elimination in Mpumalanga.

Malaria prevalence and control in Mpumalanga has been documented extensively [11, 42, 88, 95, 113–115]. The five municipalities in the Ehlanzeni District bordering Maputo Province and Swaziland are those most affected by malaria in the province (Figure 6.1). Vector control through indoor residual spraying (IRS), the introduction of artemisinin-based combination therapy (ACT) policy of artesunate plus sulphadoxine-pyremethamine in 2003, followed by artemether-lumefantrine (AL) in 2006 and the Lubombo Spatial Development cross-border Initiative (LSDI) are all considered responsible for the substantial decrease in malaria cases and malaria deaths in Mpumalanga since 2000 [88]. Between 2002 and 2012, 40 650 cases were notified, with the proportion of cases imported increasing from 39% in 2002 to 87% in 2012. Of the cases imported in 2012, 13% were sourced in South Africa and 85% were sourced from Mozambique (with the remaining 2% sourced from other African and Asian countries). Malaria is considered the most important public health problem in Mozambique accounting for 29% of all deaths, followed closely by AIDS at 27% [105]. Maputo Province, which shares the eastern border of Mpumalanga, has also experienced a sharp decline in cases since 2002 but still has a substantially higher malaria incidence. The LSDI malaria control programme was a regional collaboration between South Africa, Swaziland and Mozambique that aimed to decrease malaria in the areas surrounding the Lubombo Mountains [70]. Interventions took place primarily in Mozambique's Maputo Province but were later extended to Gaza Province. The early termination of the LSDI in September 2010 and reduced IRS in Maputo Province thereafter, coincides with the increase observed in malaria cases in Maputo from 2011.

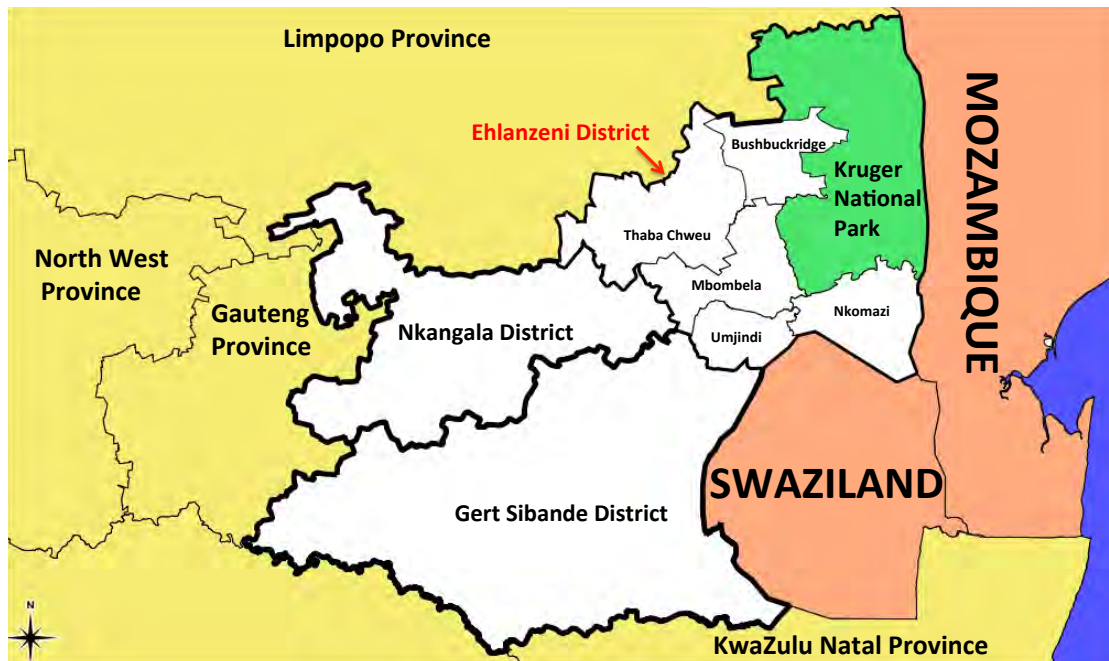


Figure 6.1: A map of Mpumalanga Province in relation to Mozambique and Swaziland (Source: Mpumalanga Malaria Elimination Programme (unpublished))

Metapopulation modelling is one method to describe movement between geographical areas with several applications in malaria and other infectious diseases. Ariey *et al.* used the metapopulation concept to examine the spread of chloroquine resistance, while Oluwagbemi *et al.*, Le Menach *et al.* and Smith *et al.* modelled malaria transmission assuming the migration of the mosquitoes only while Arino *et al.*, Zorom *et al.*, Auger *et al.*, and Rodriguez and Torres-Sorando accounted for only human migration [4, 5, 7, 67, 100, 109, 119, 152]. Mathematical modelling of malaria in Mpumalanga includes a climate-based fuzzy distribution model and an eco-hydrological model [26, 87]. Coleman *et al.* considered spatial heterogeneity by using the SaTScan methodology to detect local malaria clusters to guide the Mpumalanga Malaria Control Programme [24]. The metapopulation model presented in this paper is developed to assess the impact of proposed elimination-focused policy interventions in Mpumalanga. This is the first study in Mpumalanga designed for this purpose and the first to do so in South Africa since the call for malaria elimination. The metapopulation structure is used to describe movement between five municipalities in the Ehlanzeni District on the eastern border of Mpumalanga and more importantly, movement between these municipalities and Maputo Province (MP), Mozambique. A stochastic non-linear ordinary differential equation model fitted to the Mpumalanga and Maputo malaria case notification data, is used to predict the impact of the following interventions (alone and in combination): scale-up of Vector Control, Mass Drug Administration (MDA), a Focal Screen and Treat (FSAT) campaign and foreign source reduction.

6.3 Methods

6.3.1 Transmission Model

Metapopulation models divide a population into a number of discrete patches under the assumption that the sub-populations are well-mixed/homogenous. This structure allows for the modelling of transmission within and between different populations. The area under consideration is divided into six patches: five patches for the five municipalities in Ehlanzeni District (Thaba Chewu (TC), Mbombela (MB), Umjindi (UJ), Nkomazi (NK) and Bushbuckridge (BB)) and one patch for Maputo Province. Each patch is further divided into three sub-patches representing (1) the local population of the patch currently in the patch, (2) the local population of the patch having returned from travel to a foreign place (Maputo, if the patch is South African and vice versa) and (3) the population from the foreign place currently in the patch (Figure 6.2). In each sub-patch, the population is divided into five compartments representing the population susceptible to malaria (S), the population infected with asexual blood-stage malaria parasites (BT and BU) and the population at the infectious stage (IT and IU) i.e. those carrying gametocytes (Figure 6.2(a)). The blood and infectious stage compartments are further stratified according to whether the infection is treated (T) or not (U) and the latent liver stage of the infection is incorporated as a delay in the flow between the susceptible and blood stage compartments. Movement between compartments is governed by parameters described in Table 6.1. While the seasonal nature of transmission is incorporated in the model, the mosquito population is not modelled directly as it is assumed that the mosquito dynamics operate on a faster time-scale than the human dynamics and as such the mosquito population can be considered to be at equilibrium with respect to changes in the human population [66]. Human movements are incorporated in two ways. Local movements are allowed between the five Mpumalanga patches (from all five compartments in all three sub-patches). Foreign travel is allowed between the Maputo patch and any of the five Mpumalanga patches (from all five compartments) as illustrated in Figure 6.2(b). These movements are inversely weighted by distance. A full description of the model is presented in Additional File 2 at the end of the chapter.

6.3.2 Data Fitting

The metapopulation model is fitted to weekly case notification data of treated cases from Mpumalanga and Maputo from 2002 to 2008, and then validated with the data from 2009 to 2012. Ethical approval for use of the data was obtained from the Mpumalanga Department of Health and the University of Cape Town Human Research Ethics Committee. In Southern Africa, most malaria transmission occurs during the summer rainfall season between October and May. Silal *et al.* (2013) describes in detail the characteristic triple peaked pattern in the Mpumalanga case data with peaks occurring during October, December/January and April/-

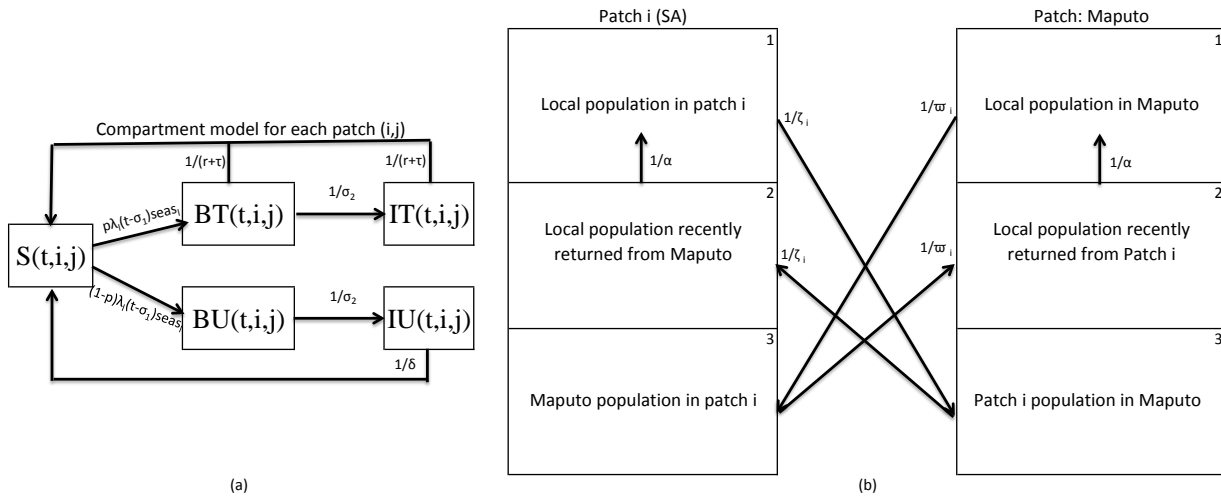


Figure 6.2: Metapopulation Model flow (a) Compartment transmission model for each sub-patch j (1-3) in patch i (1-6) at time step t with compartments S -Susceptible, BT - Blood stage and treated, BU - Blood stage and untreated, IT - Infectious and treated, and IU - Infectious, asymptomatic and untreated. (b) Metapopulation structure highlighting human movement between each local patch $i \in \{1, 2, 3, 4, 5\}$ and foreign patch 6. Movement between the five local patches is not shown. Other parameters are described in Table 6.1 and Additional file 2.

May while Maputo Province exhibited the December and April peaks only. The seasonal forcing functions that determine the behaviour of transmission for the six patches are derived from the data using Seasonal decomposition of Time series by LOESS (STL) methods for extracting time series components [22]. ACT drug therapy and IRS implemented between 2002 and 2008 are included in the model.

The model is run deterministically from 1990 to reach a steady state before being fitted to data from 2002. The model output (predicted weekly malaria cases treated) is fitted to the data from 2002 to 2008 using the maximum likelihood approach by assuming an underlying Poisson distribution with rate λ as the number of treated cases per week. Several parameters are estimated through the data fitting process using the particle swarm optimization routine, a population-based global search algorithm [32, 64]. The model with the estimated parameter values is then run for a further 3 years to be validated by comparison to data between 2009 and 2012. A full description of the data fitting method is presented in Additional File 2. Model development, fitting and subsequent analysis was performed in R v3.02 [106]. The particle swarm optimization routine was performed using the R package hydroPSO v0.3-3 [150, 151].

6.4 Results

6.4.1 Estimation of Parameters through data-fitting

Figure 6.3 shows the notified case data for the five municipalities and Maputo (black) with the model output from the fitting process (red) and the predicted model output for 2009 to 2012 (blue) for the five Mpumalanga municipalities and for Maputo Province. As the data was fitted to each sub-patch simultaneously, Figure 6.3 represents only a summation of the data fitting. The confidence band for Maputo is plotted but is not visible due to a low resolution y-axis. More detailed output on the data fitting is available in Additional File 2. The parameters driving the model and those estimated through data-fitting procedures are presented in Table 6.1.

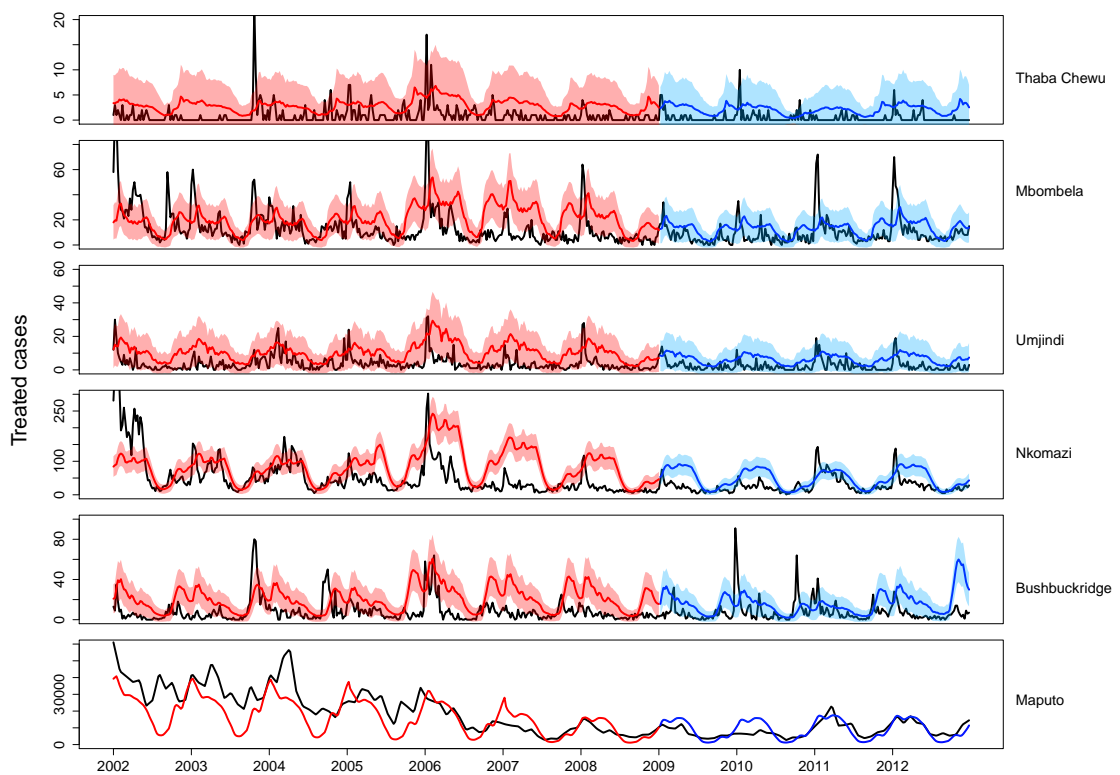


Figure 6.3: Predicted average weekly treated cases (blue: 2002 - 2008; red: 2009-2012) fitted to and validated with data (black). The 95% uncertainty range for weekly case predictions is shown.

Table 6.1: Values, descriptions and sources of the parameters driving the base metapopulation model of transmission. ($i = \{TC; MB; UJ; NK; BB; MP\}$)

Parameter	Description	Value	Source
N	Population size	4×10^6	[125]
μ	Mortality/birth Rate	$\frac{105}{10000}$	[90]
δ	Natural recovery period	26 weeks	[61, 86, 141]
σ_1	Period between liver stage and blood stage	7 days (5-10)	[19, 25, 33]
σ_2	Period between blood stage and onset of gametocytemia	1 week	[61, 134]
r	AL elimination half-life	6 days	[77]
τ	Time to seek treatment	1/2 week	Expert opinion
p	Proportion of local infected population receiving treatment	0.95	[18, 58]
pf_{yr}	Proportion of foreign infected population that receive treatment in a local patch	$pf_1 = 0.5655(0.5652, 0.5658)$ (pre April 2005) $pf_2 = 0.5500 (0.5494, 0.5506)$ (post April 2005)	Estimated from model fitting process
$seas_i$	Seasonal forcing function for foreign sourced cases	Derived from data	[116]
β_i	Annual number of mosquito bites per person x proportion of bites testing positive for sporozoites for patch i	$\beta_{TC} = 0.334 (0.244, 0.425)$ $\beta_{MB} = 2.178 (2.056, 2.300)$ $\beta_{UJ} = 0.805 (0.700, 0.910)$ $\beta_{NK} = 1.330 (1.310, 1.350)$ $\beta_{BB} = 8.304 (7.903, 8.705)$ $\beta_{MP} = 94.999 (93.327, 96.671)$	Estimated from model fitting process
$\frac{1}{\alpha}$	Rate of movement between sub-patch 2 and sub-patch 1	1.5 weeks^{-1}	Expert opinion
$\frac{1}{k}$	Rate of movement between 5 Mpumalanga municipalities	$1/48.603 (1/51.328, 1/45.787)$ weeks^{-1}	Estimated from model fitting process

$\frac{1}{v_y}$	Maputo residents: Rate of movement between Maputo and 5 Mpumalanga municipalities	Rate $\frac{1}{v_1} = 1/1258.828 \text{ weeks}^{-1}$ (1/1261.249, 1/1256.407) (pre-April 2005) $\frac{1}{v_2} = 1/319.042 \text{ weeks}^{-1}$ (1/322.796, 1/315.333) (post April 2005)	Estimated from model fitting process
$\frac{1}{z}$	Mpumalanga residents: Rate of movement between 5 Mpumalanga municipalities and Maputo	$\frac{1}{z} = 1/765.19 \text{ weeks}^{-1}$	Estimated from model fitting process
$fwgt$	Foreign movement weight intensity	8.385 (8.232, 8.537)	Estimated from model fitting process
$lwgt$	Local movement weight intensity	2.613 (2.607, 2.618)	Estimated from model fitting process
$vc[i, t]$ $vccov[i, t]$	$vccov[i, t] \times vef$ Vector Control Coverage	0.22-0.90	Derived from data
vef	Effectiveness of vector control	0.900 (0.897, 0.903)	Estimated from model fitting process

The proportion of infections treated varies widely across Africa with some estimates as low as 10% and others as high as 90% [45]. In South Africa and Mozambique, the proportion of the local infected population receiving treatment was informed by two studies [18, 58]. Castillo-Riquelme *et al.* (2008) conducted household surveys in Mozambique and South Africa between 2001 and 2002 to evaluate malaria-related treatment-seeking behaviour and found that 100% of respondents in Mpumalanga and 99% of respondents in Mozambique with recent malaria sought treatment. Hlongwana *et al.* (2011) conducted a study on malaria-related knowledge and practices in Bushbuckridge Municipality in 2008 and reported that 99% of respondents would seek malaria treatment (95% Confidence interval: 97.5- 99.5%). There are two rates each for the foreign treatment proportion and the rate of foreign movement. These are because in April 2005, the South African and Mozambican governments waived the short stay visa requirements for Mozambicans entering South Africa which subsequently led to increased movement between the two countries [97].

6.4.2 Interventions

Interventions are tested on a stochastic version of the fitted model with the same intervention applied to multiple runs of the model so that its impact on local infections can be described with a mean effect and a 95% confidence interval. The model is run stochastically by treating each flow between compartments at time t as a random realisation of a Poisson process with rate λ as the deterministic flow value at that time, and by simulating the parameter values from their 95% confidence intervals. The interventions to be tested include: scaling-up of vector control from current levels, mass drug administration in three local patches, a focal screen and treat campaign at the Mpumalanga-Maputo border, foreign source reduction through vector control and MDA in Maputo Province only and reducing vector control during the FSAT campaign.

Further Scaling up Vector Control

Vector control in Nkomazi and Bushbuckridge municipalities is achieved through high coverage IRS with larviciding at selected sites. Vector control is used less intensively in Mbombela and Umjindi municipalities and is not currently conducted in Thaba Chewu municipality. Assuming vector control remains at 2012 levels until 2020, the impact of vector control is modelled as a percentage decrease in β , the number of local human contacts with infectious mosquitos. Scaling up vector control in Nkomazi, Bushbuckridge and Mbombela municipalities so as to decrease β_i by a further 10% is predicted to result in a decrease in local infections in all municipalities including Umjindi where vector control was not scaled-up and Thaba Chewu where vector control was not conducted at all (Figure 6.4(1)). The decrease, though substantial in some municipalities, is not predicted to be enough to eliminate local malaria owing to the continued flow of imported infections into the province. While onward transmission from imported cases may be decreased by vector control, the inflow of imported cases is otherwise unhampered by increased vector control in the province. The seasonal decomposition of local cases suggests that they occur earlier in the season in Bushbuckridge municipality than the other municipalities [116]. Exploring the scenario of scaling up vector control first in Bushbuckridge followed by Nkomazi municipality is predicted to result in further decreases in local infections in the deterministic model, but these decreases were trivial in the stochastic model.

Mass Drug Administration

Mass Drug Administration is an intervention aimed at treating all individuals without screening and regardless of disease status. Though MDA may be targeted at certain populations, it is still improbable that every member of the population receives treatment and thus MDA is modelled with a coverage rate below 100%. The model predicts that when MDA coverage achieves at least 80% for three consecutive rounds of two months each in Nkomazi, Bushbuckridge and

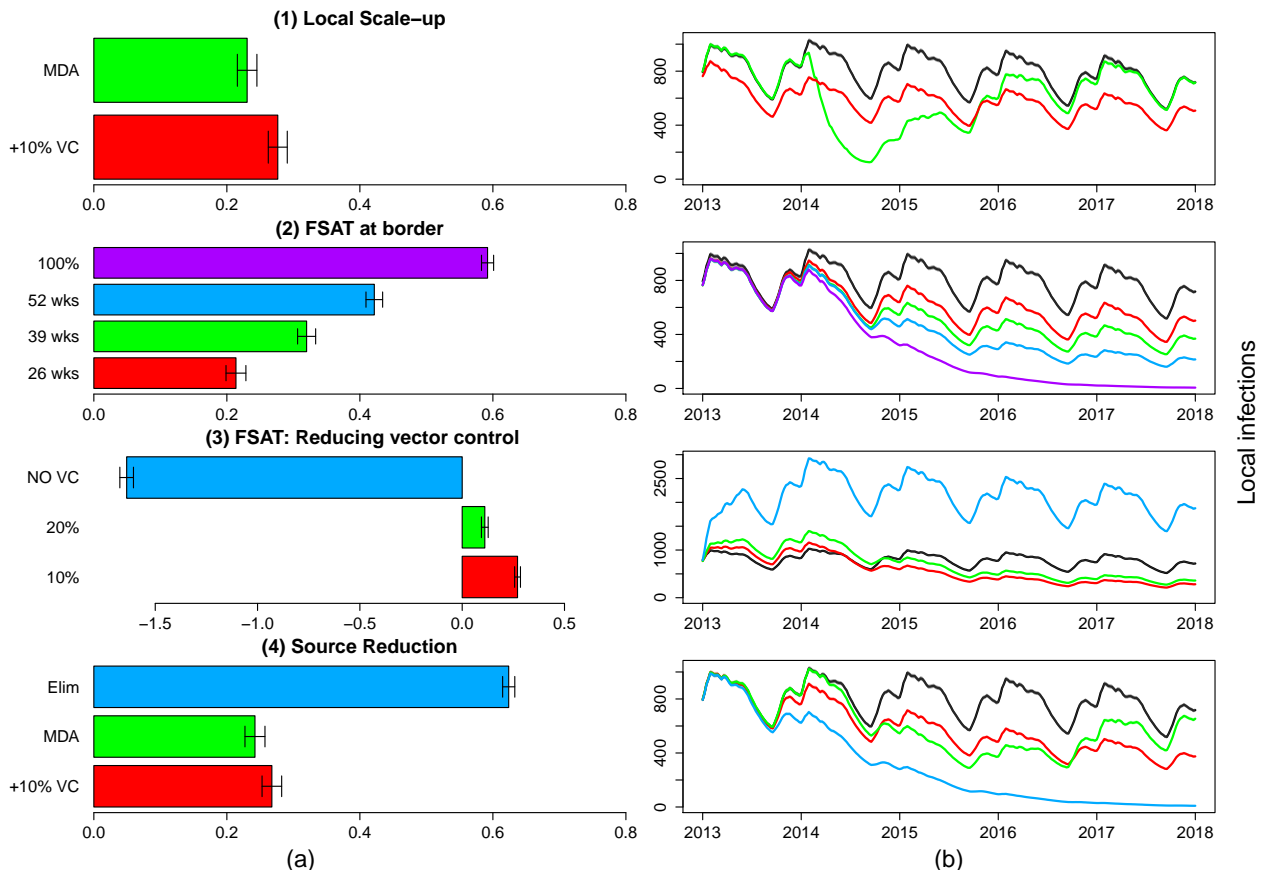


Figure 6.4: Predicted impact of interventions on the number of local infections in the Ehlanzeni district (summation of the five local patches). (a) shows the number of cases averted due to the interventions between 2013 and 2018 as a percentage of total local infections in the absence of interventions and (b) shows the impact of the interventions on local infections in Ehlanzeni district through time compared to the base case of no interventions (black). (1) Local Scale-up: Increase in local vector control so as to reduce the mosquito-human contact rate by a further 10% (red) & three consecutive two-monthly rounds of MDA in Mbombela, Nkomazi and Bushbuckridge Municipalities (green). (2) FSAT at the border: at 70% coverage for 26 weeks (red), 39 weeks (green), 52 weeks (blue) and 52 weeks at 100% coverage (purple). (3) Reducing Vector Control: FSAT at the border at 70% coverage administered all year round while simultaneously reducing vector control by 10% (red), 20% (green) and stopping vector control altogether (blue). (4) Source Reduction: 10% scale up of vector control in Maputo (red), three consecutive two-monthly rounds of MDA in Maputo (green) and eliminating malaria in Maputo (blue).

Mbombela municipalities, local infections decrease substantially in all five municipalities, though this decrease is not predicted to eliminate local malaria (Figure 6.4(1)). While this predicted decrease is substantial, it is short-lived with infections predicted to reach previous levels within three years. As MDA is administered regardless of the source of infection, foreign infections in the five municipalities are also predicted to decrease substantially during MDA but revert back to previous levels within 18 months of the end of the MDA as the subsequent inflow of imported infections remains unaffected.

Focal Screen and Treat Campaign at the Mpumalanga-Maputo Province border post

It is a resource-intensive exercise to treat all individuals regardless of disease status. Focal Screen and Treat campaigns include an additional stage of screening individuals, resulting in only those testing positive receiving treatment. However, FSAT campaigns are still resource intensive and are unlikely to achieve very high coverage in large target populations. A high coverage FSAT campaign is more feasible if focused on a subset of the population only. Figure 6.4(2) shows the predicted impact of administering FSAT (at different coverage rates and for different durations) at the border entry point between Maputo and Mpumalanga. The rationale for screening travellers and treating positive cases before entry into Mpumalanga is that imported cases now comprise the majority of Mpumalanga's malaria cases, with Mozambique being the most frequent source of infection. The advantage of the metapopulation structure of the model is that the impact of FSAT is modelled on both the foreign population entering Mpumalanga and the local population returning from travel to Maputo Province. FSAT is modelled at a 70% coverage rate to account for limitations in test sensitivity, illegal border crossing, and other forms of entry into the province. Vector control activities are assumed to continue at levels in 2012. Figure 6.4(2) shows the predicted impact of different FSAT schemes at the border on *local* infections i.e. the effect on onward transmission as result of fewer imported cases in the Mpumalanga patches. In particular FSAT is modelled at 70% coverage for six months from October to March (red), nine months from September to May (green), all year round (blue) and all year round at 100% coverage (purple) compared to no FSAT (black). The impact on local infections is predicted to be substantial regardless of the duration of FSAT. At 70% coverage, FSAT is predicted to be most effective when performed throughout the year (blue) as even a few imported cases over the non-malaria season may contribute to local transmission. Even when performed throughout the year at 70% coverage, FSAT is insufficient to eliminate local infections. Elimination is predicted if FSAT is performed continuously throughout the year at 100% coverage (purple). This is of course unrealistic but serves to illustrate the prediction that if imported infections are treated before entry into Mpumalanga (as opposed to being prevented altogether), elimination of local malaria becomes a possibility. Like MDA, FSAT has a short-lived benefit as the model predicts a reversion to previous levels approximately three years after the end of the intervention.

FSAT with Reducing Vector Control

Focal Screen and treat campaigns have been predicted to be effective in reducing infections substantially if sustained for a long period. In dedicating resources to this intervention, it may be tempting to reduce the vector control effort in an attempt to shift resources rather than procure additional resources. Figure 6.4(3) shows the impact of an FSAT campaign on the border between Maputo and Mpumalanga, at 70% coverage, administered all year round while simultaneously reducing the Mpumalanga vector control effort. The black line represents the model prediction if the only intervention is vector control at current levels. FSAT is then modelled while simultaneously reducing vector control by 10% (red), 20% (green) and stopping vector control all together (blue). The model predicts that the impact of a sustained FSAT programme is dampened by a reduction in vector control with the impact of FSAT being zero and local infections increasing substantially if vector control is abandoned all together.

Source Reduction

In 2012, 87% of all reported malaria cases in Mpumalanga were imported and Figure 6.4(2) shows that using FSAT to treat imported cases is predicted to decrease local infections substantially. Therefore source reduction is explored by assessing the effects of scaling up vector control and MDA in Maputo Province. Figure 6.4(4) shows the predicted impact of a scale up of vector control in Maputo Province such that the local human-infectious mosquito contact rate is decreased by 10% (red), three consecutive two-monthly rounds of MDA in Maputo Province (green) and eliminating malaria in Maputo Province (blue), on local infections in Mpumalanga. The scale up in vector control in Maputo Province is predicted to have a delayed but substantial impact on local infections in Mpumalanga through the decrease in the number of imported infections. Likewise, the impact of six months of MDA in Maputo Province is also predicted to decrease local infections substantially, though predicted local infections revert slowly to previous levels once the MDA in Maputo Province has stopped. If malaria is eventually eliminated in Maputo Province (blue) and vector control is continued in Mpumalanga at 2012 levels, the model predicts that local malaria will also be eliminated in Mpumalanga. This prediction is in line with the model prediction that treating all imported infections will also lead to the elimination of local infection in Figure 6.4(2).

6.5 Discussion

South Africa aims to achieve malaria elimination by 2018. A malaria elimination strategy should aim to interrupt the transmission cycle and prevent it from being re-established. An elimination strategy that employs ‘more of the same’ approach may decrease the malaria burden, but will

Highlights

The stochastic metapopulation transmission model developed to simulate transmission in Ehlanzeni District, Mpumalanga, and Maputo Province, Mozambique has made predictions that lead to the following conclusions:

- Scaling-up vector control will decrease prevalence but not eliminate malaria in the presence of imported infections.
- Mass interventions lead to large and immediate decreases in prevalence but will result in rebound in prevalence three years after the intervention has stopped.
- A smaller scale intervention such as FSAT at the border has the same large but short-lived impact of mass interventions and is most effective if conducted throughout the year as the presence of even a few imported infections, leads to onward transmission.
- Source reduction is likely to be effective in decreasing local prevalence, whether through better control or elimination at the source.
- Reducing vector control in favour of FSAT dampens the impact of FSAT, particularly in the long term.
- There is no "one size fits all" strategy to achieve malaria elimination and a tailored approach is needed to address linkages between populations. For example, in the case of Mpumalanga province, the high level of imported infections suggests that a regional approach to malaria elimination will be more successful than a nationally focused one.

be insufficient to eliminate it as the focus needs to shift from better overall control to the identification of residual transmission foci leading to the last few infections. The interruption of the transmission cycle and prevention of its re-establishment theoretically requires three elements: (1) the elimination of the mosquito vector to prevent onward transmission, (2) stopping the inflow of imported infections and (3) reduction of infections at their source [89]. The first element is operationally unfeasible and has not been recommended [80]. The second element could be achieved if borders were closed, or more realistically if imported infections were identified and treated at border entry points before they can contribute to the infectious reservoir locally. The third element would require regional collaboration with these sources of imported infections to reduce transmission in the region [89]. South Africa has employed consistent IRS and artemisinin-based combination therapy to control malaria. This paper has explored a range of additional interventions (scale-up of vector control, MDA, FSAT and source reduction) that speak to all three key elements of elimination.

Mass Drug Administration is an intervention that is resource intensive in terms of labour and the cost of drugs. It is also an intervention that needs to be acted out quickly and efficiently to achieve desired target coverage rates. In a single patch deterministic model of malaria in Mpumalanga, Silal *et al.* predicted that in the absence of imported infections, MDA applied in six consecutive two-monthly rounds at 80% coverage would be sufficient to eliminate local malaria, but even repeated annual rounds of MDA for seven years is insufficient to eliminate local malaria at the current level of imported infections because MDA does not interrupt the inflow of imported infections. The stochastic metapopulation model presented in this paper also

predicts that MDA applied in the three municipalities with the highest incidence has a large impact but this is short-lived because there is no impact on the flow of imported infections. A Focal Screen and Treat campaign focused on treating infections at the border control point between Maputo Province and Mpumalanga is also predicted to have a large impact, but is not enough to eliminate local malaria on its own unless the unlikely scenario of all imported infections being screened and treated is achieved. As soon as the FSAT campaign is stopped, infections revert to previous levels within three years. This suggests that screening and treating infections at the border would need to be intense over a long term to minimize the impact of imported infections on malaria transmission.

In Mpumalanga, vector control has been conducted using high-coverage IRS with dichlorodiphenyl-trichloroethane (DDT) and larviciding at identified breeding sites. Scaling-up vector control as an elimination intervention may include intensifying the already extensive spraying programme, increasing the distribution of insecticide-treated bednets and the identification and larviciding of additional breeding sites. The purpose of a scale-up in vector control would be to decrease the potential for onward local transmission, though it is impossible to reduce this to zero. While effective if the majority of infections are locally sourced, the model predicts that increasing vector control alone will not eliminate local infection if the stream of imported infections is left unchecked. These predictions are in line with the single patch model in Silal *et al.* (2014) but the metapopulation model has predicted that increasing vector control in Nkomazi, Mbombela and Bushbuckridge municipalities only also leads to a knock-on decrease in malaria cases in the other two municipalities. Another recent modelling study found that at low receptivity levels, case management alone could not reliably prevent the re-establishment of transmission in the presence of medium to high importation rates [28].

While scaling-up vector control alone in Mpumalanga may not be enough to interrupt transmission and prevent its re-establishment, vector control at the source of imported cases has a large effect. The model predicts that if vector control is continued at current levels in Mpumalanga, but is scaled up in Maputo, the related decrease in local infections in Mpumalanga will be substantial. This decrease results because a smaller proportion of the population that travels into Mpumalanga will be infected and hence the infectious reservoir in Mpumalanga is reduced. These knock-on decreases in local infections in Mpumalanga are also predicted if MDA is performed in Maputo Province, although infections revert to previous levels a few years after the end of the MDA campaign. The model also predicts that if malaria were to be eliminated in Maputo, malaria would also be eliminated in Mpumalanga. These predictions highlight the need for and pivotal importance of cross-border/regional collaboration. The Lubombo Spatial Development Initiative, a trilateral agreement between South Africa, Mozambique and Swaziland, was initiated in 1999 and successfully reduced malaria cases by 78 to 95% in the border areas of South Africa and Swaziland within five years of the start of IRS and then ACT deployment in Maputo Province [70]. In September 2010, the earlier than expected ending of LSDI support for IRS (when the Global Fund withdrew support) resulted in sub-optimal spraying in Maputo and

Gaza provinces. This coincides with the increase in malaria cases in Maputo Province from 2011 [105].

In allocating resources towards elimination-focused interventions, programme managers may wish to decrease routine activities to shift budgets towards elimination. It is important to remember that even in areas of very low transmission intensity (as seen in the pre-elimination phase), imported infections will augment the infectious reservoir, and since the vector remains present, imported infections may lead to onward transmission to the local population and a resurgence of malaria. The model predicted that the impact of FSAT could be dampened and even reduced to zero if current vector control efforts are reduced or stopped.

This paper presents the findings of a stochastic metapopulation non-linear differential equation model of five municipalities in Mpumalanga, South Africa and in neighbouring Maputo Province, Mozambique. While the current metapopulation structure allows for more disaggregated modelling than the model presented in Silal *et al.* (2014), mass interventions if administered, will most likely be performed in smaller hotspot areas within a municipality and may be more accurately modelled if patches are disaggregated further or agent-based modelling is used to incorporate heterogeneous behaviour among individuals. This metapopulation comprised six patches and while this methodology may theoretically be extended to any number of patches, several aspects must be taken into account. Computationally, extending the methodology to a large number of patches n with $\frac{n(n-1)}{2}$ links between patches (499 500 in the case of 1000 patches), will result in the equations becoming too numerous to be efficient. Further, depending on the size of the populations of interest and the available data, one could consider either agent-based modelling (disaggregating populations into individuals) or a simplified approach where for example, patches are linked using weights rather than flows. Future work also includes exploring the impact of border control through FSAT in greater detail and incorporating vector population dynamics in the model so that vector control activities such as indoor residual spraying and larviciding may be modelled explicitly and thereby allow for an exploration of post-elimination maintenance strategies to detect outbreaks and prevent the resurgence of local transmission.

6.6 Conclusion

To eliminate malaria by 2018, the government of South Africa will need to design and implement an elimination strategy tailored for a country with a high level of imported infections. A regionally focused strategy may stand a better chance at achieving elimination in Mpumalanga and South Africa compared to a nationally focused one in the face of frequent population movement between the pre-elimination area and neighbouring high transmission intensity regions [128]. Mathematical modelling has been used in this paper to predict the impact of elimination-focused strategies like scaled up vector control, MDA, FSAT at the border and foreign source

reduction). In this manner, mathematical modelling may be used to inform government policy to tailor a strategy that captures the malaria situation not just in South Africa, but also in the immediate region, in order to form feasible strategies to enable malaria elimination in the foreseeable future.

6.7 Additional File 2: Mathematical Model Description

6.7.1 Summary Equations: Metapopulation Model of Transmission

The model comprises six patches; five to represent Mpumalanga municipalities, and one for Maputo province, Mozambique. Each patch comprises three sub-patches: (1) the local population of patch i currently in patch i , (2) the local population of patch i having returned from travel to a foreign place (Maputo, if the patch is South African and vice versa) and (3) the population from the foreign place currently in patch i . In each sub-patch, the population is divided into five compartments representing the population susceptible to malaria (S), the population infected with malaria at the asexual blood-stage (B) and the population at the infectious stage (I). The blood and infectious stage compartments are further stratified according to whether the infection is treated (T) or not (U).

This system is described by a set of non-linear differential equations for which the compartment and parameter descriptions are given in Tables 6.2 and 6.3 respectively.

The force of infection $\lambda_i[t]$ for each patch i is a function of the level of vector control, the annual number of mosquito bites per person \times proportion of bites testing positive for sporozoites for patch i (β_i) and the proportion of infectiousness in the population lagged to reflect the infectiousness proportion at the time the mosquito was infected.

$$\lambda_i[t] = (1 - vc_i[t] * vef)\beta_i \times \frac{IT_{i,1}[t-4] + IU_{i,1}[t-4] + IT_{i,2}[t-4] + IU_{i,2}[t-4] + IT_{i,3}[t-4] + IU_{i,3}[t-4]}{N_i}.$$

Population migration between the different patches is characterised by three sets of movements:

1. Movement may occur between any two of the the five Mpumalanga patches i and j at a rate $\frac{1}{\kappa_{i,j}}$ where

$$\begin{aligned} \frac{1}{\kappa_{i,j}} &= \frac{1}{k} \times \frac{1}{\sum_{i=1}^5 \frac{1}{(1+\sqrt{(x_i-x_j)^2+(y_i-y_j)^2})^{twgt}}} && \text{if } i, j = 1, 2, 3, 4, 5 \text{ \& } i \neq j \\ &= 0 && \text{if } i \text{ or } j = 6 \text{ (local movement only)} \\ \frac{1}{\kappa_{i,j}} &= \frac{1}{\kappa_{j,i}} \end{aligned}$$

where (x_i, y_i) and (x_j, y_j) are the centroid coordinates for patches i and j respectively. This movement is weighted inversely by distance so that movement between South African patches that are closer together occurs at a higher rate than those further apart. The parameter $lwgt$ determines the degree of linkage between patches i and j .

2. Movement may occur when South African citizens cross the border into Maputo (from patch $i = 1 - 5$ in sub-patch 1 to patch 6 in sub-patch 3) and return (patch 6 in sub-patch 3 to patch $i = 1 - 5$ in sub-patch 2) at a rate of $\frac{1}{\zeta_{i,6}}$ where

$$\begin{aligned} \frac{1}{\zeta_{i,6}} &= \frac{1}{z} \times \frac{\frac{1}{(1+\sqrt{(x_i-x_6)^2+(y_i-y_6)^2})^{fwgt}}}{\sum_{i=1}^5 \frac{1}{(1+\sqrt{(x_i-x_6)^2+(y_i-y_6)^2})^{fwgt}}} & \text{if } i = 1, 2, 3, 4, 5 \\ &= 0 & \text{otherwise} \\ \frac{1}{\zeta_{i,6}} &= \frac{1}{\zeta_{6,i}} \end{aligned}$$

where (x_i, y_i) and (x_6, y_6) are the centroid coordinates for patches i and 6 respectively. This movement is weighted inversely by distance so that movement between the South African patches and Maputo that are closer together occurs at a higher rate than those further apart. The parameter $fwgt$ determines the degree of linkage between patches i and j .

3. Movement may also occur when Mozambican citizens cross the border into Mpumalanga (from patch 6 in sub-patch 1 to patch $j = 1 - 5$ in sub-patch 3) and return (patch $j = 1 - 5$ in sub-patch 3 to patch 6 in sub-patch 2) at a rate of $\frac{1}{\varpi_{6,j}}$ where

$$\begin{aligned} \frac{1}{\varpi_{6,j}} &= \frac{1}{v_{yr}} \times \frac{\frac{1}{(1+\sqrt{(x_6-x_j)^2+(y_6-y_j)^2})^{fwgt}}}{\sum_{i=1}^5 \frac{1}{(1+\sqrt{(x_6-x_j)^2+(y_6-y_j)^2})^{fwgt}}} & \text{if } j = 1, 2, 3, 4, 5 \text{ \& } yr = 1, 2 \\ &= 0 & \text{otherwise} \\ \frac{1}{\varpi_{6,j}} &= \frac{1}{\varpi_{j,6}} \end{aligned}$$

where (x_6, y_6) and (x_j, y_j) are the centroid coordinates for patches 6 and j respectively. This movement is weighted inversely by distance so that movement between the South African patches and Maputo that are closer together occurs at a higher rate than those further apart. The parameter $fwgt$ determines the degree of linkage between patches i and j .

This leads to the following set of differential equations. Footnotes have been added where needed to describe the flows between compartments. Footnotes appear at the first occurrence of each type of flow.

Sub-patch 1 (Local population): For each patch i moving to patch j ($i, j \in \{1, 2, \dots, 6\}, j \neq i$):

$$\begin{aligned} \frac{dS_{i,1}}{dt} &= \underbrace{\mu N_i}_{(1)} - \underbrace{\lambda_i[t - \sigma_1]seas_i[t]S_{i,1}}_{(2)} + \underbrace{\frac{1}{r + \tau}(BT_{i,1} + IT_{i,1})}_{(3)} + \underbrace{\frac{1}{\delta}IU_{i,1}}_{(4)} + \underbrace{\frac{1}{\alpha}S_{i,2}}_{(5)} + \underbrace{\sum_j \frac{1}{\kappa_{i,j}}(S_{j,1} - S_{i,1})}_{(6)} \\ &\quad - \underbrace{\frac{1}{\varpi_{i,j}}S_{i,1}}_{(7)} - \underbrace{\frac{1}{\zeta_{i,6}}S_{i,1}}_{(8)} - \underbrace{\mu S_{i,1}}_{(9)} \\ \frac{dBT_{i,1}}{dt} &= \underbrace{p\lambda_i[t - \sigma]seas_i[t](S_{i,1} + S_{i,2})}_{(10)} - \underbrace{\frac{1}{\sigma_2}BT_{i,1}}_{(11)} - \frac{1}{r + \tau}BT_{i,1} + \frac{1}{\alpha}BT_{i,2} + \sum_j \frac{1}{\kappa_{i,j}}(BT_{j,1} - BT_{i,1}) \\ &\quad - \frac{1}{\varpi_{i,j}}BT_{i,1} - \frac{1}{\zeta_{i,6}}BT_{i,1} - \mu BT_{i,1} \\ \frac{dIT_{i,1}}{dt} &= \frac{1}{\sigma_2}BT_{i,1} - \frac{1}{r + \tau}IT_{i,1} + \frac{1}{\alpha}IT_{i,2} + \sum_j \frac{1}{\kappa_{i,j}}(IT_{j,1} - IT_{i,1}) - \frac{1}{\varpi_{i,j}}IT_{i,1} - \frac{1}{\zeta_{i,6}}IT_{i,1} - \mu IT_{i,1} \end{aligned}$$

$$\begin{aligned} \frac{dBU_{i,1}}{dt} &= \underbrace{(1 - p)\lambda_i[t - \sigma_1]seas_i[t](S_{i,1} + S_{i,2})}_{(12)} - \frac{1}{\sigma_2}BU_{i,1} + \frac{1}{\alpha}BU_{i,2} + \sum_j \frac{1}{\kappa_{i,j}}(BU_{j,1} - BU_{i,1}) \\ &\quad - \frac{1}{\varpi_{i,j}}BU_{i,1} - \frac{1}{\zeta_{i,6}}BU_{i,1} - \mu BU_{i,1} \\ \frac{dIU_{i,1}}{dt} &= \frac{1}{\sigma_2}BU_{i,1} - \frac{1}{\delta}IU_{i,1} + \frac{1}{\alpha}IU_{i,2} + \sum_j \frac{1}{\kappa_{i,j}}(IU_{j,1} - IU_{i,1}) - \frac{1}{\varpi_{i,j}}IU_{i,1} - \frac{1}{\zeta_{i,6}}IU_{i,1} - \mu IU_{i,1} \end{aligned}$$

- (1) Births in patch i
- (2) Local incidence arising from sub-patch 1
- (3) Recovery of treated blood and infectious stage infections at a rate dependent on the time to seek treatment and the time to recovery
- (4) Recovery of untreated infections at a rate dependent on the duration of natural recovery
- (5) Assimilation of population in sub-patch 2 (locals having returned from foreign travel) back into sub-patch 1 from whence they originated.
- (6) Movement between local patches (1-5) out of and into the compartment

- (7) Movement of local patch i population to foreign patch j when $i=6$ and $j = 1-5$; $=0$ for all other values of i as this rate is particular to movement of Maputo population (patch 6)
- (8) Movement of local patch i population to foreign patch 6 when $i=1-5$; $=0$ for $i=6$ as this rate is particular to movement of the Mpumalanga population to and from Maputo (patches 1-5)
- (9) Deaths in patch i from this compartment
- (10) New infections destined to be treated having arisen from susceptible populations in sub-patch 1 (local population) and sub-patch 2 (local population having returned from foreign travel) as these are infections due to local transmission.
- (11) Development of infectiousness at a rate dependent on the duration of the blood stage
- (12) New infections destined to remain untreated (having arisen from susceptible populations in sub-patch 1 (local population) and sub-patch 2 (local population having returned from foreign travel) as these are infections due to local transmission.

Sub-patch 2 (Local population returning from foreign travel) : For each patch i moving to patch j ($i, j \in \{1, 2, \dots, 6\}, j \neq i$)

$$\frac{dS_{i,2}}{dt} = - \underbrace{\lambda_i [t - \sigma_1] \text{seas}_i [t] S_{i,2}}_{(13)} + \frac{1}{r + \tau} (BT_{i,2} + IT_{i,2}) + \frac{1}{\delta} IU_{i,2} - \underbrace{\frac{1}{\alpha} S_{i,2}}_{(14)} + \underbrace{\sum_j \frac{1}{\kappa_{i,j}} (S_{j,2} - S_{i,2})}_{(15)}$$

$$\underbrace{\sum_j \frac{1}{\varpi_{i,j}} S_{j,3}}_{(16)} + \underbrace{\frac{1}{\zeta_{i,6}} S_{6,3}}_{(17)} - \mu S_{i,2}$$

$$\frac{dBT_{i,2}}{dt} = -\frac{1}{\sigma_2} BT_{i,2} - \frac{1}{r + \tau} BT_{i,2} - \frac{1}{\alpha} BT_{i,2} + \sum_j \frac{1}{\kappa_{i,j}} (BT_{j,2} - BT_{i,2}) + \sum_j \frac{1}{\varpi_{i,j}} BT_{j,3} + \frac{1}{\zeta_{i,6}} BT_{j,3} - \mu BT_{i,2}$$

$$\frac{dIT_{i,2}}{dt} = \frac{1}{\sigma_2} BT_{i,2} - \frac{1}{r + \tau} IT_{i,2} - \frac{1}{\alpha} IT_{i,2} + \sum_j \frac{1}{\kappa_{i,j}} (IT_{j,2} - IT_{i,2}) + \sum_j \frac{1}{\varpi_{i,j}} IT_{j,3} + \frac{1}{\zeta_{i,6}} IT_{j,3} - \mu IT_{i,2}$$

$$\frac{dBU_{i,2}}{dt} = -\frac{1}{\sigma_2} BU_{i,2} - \frac{1}{\alpha} BU_{i,2} + \sum_j \frac{1}{\kappa_{i,j}} (BU_{j,2} - BU_{i,2}) + \sum_j \frac{1}{\varpi_{i,j}} BU_{j,3} + \frac{1}{\zeta_{i,6}} BU_{j,3} - \mu BU_{i,2}$$

$$\frac{dIU_{i,2}}{dt} = \frac{1}{\sigma_2} BU_{i,2} - \frac{1}{\delta} IU_{i,2} - \frac{1}{\alpha} IU_{i,2} + \sum_j \frac{1}{\kappa_{i,j}} (IU_{j,2} - IU_{i,2}) + \sum_j \frac{1}{\varpi_{i,j}} IU_{j,3} + \frac{1}{\zeta_{i,6}} IU_{j,3} - \mu IU_{i,2}$$

- (13) New infections arising from sub-patch 2 due to local transmission and not infections contracted while travelling
- (14) Assimilation of population in sub-patch 2 (locals having returned from foreign travel) back into sub-patch 1 from whence they originated.
- (15) Movement between local patches (1-5) out of and into the compartment

- (16) Movement of patch 6 population from foreign patch j , sub-patch 3 back into patch 6 but in sub-patch 2, when $i=6$ and $j = 1-5$; $=0$ for all other values of i as this rate is particular to movement of Maputo population (patch 6)
- (17) Movement of patch i population from foreign patch 6 sub-patch 3 back into patch i , sub-patch 2, when $i=1-5$; $=0$ for $j=6$ as this rate is particular to movement of the Mpumalanga population to and from Maputo (patches 1-5)

Sub-patch 3 (Foreign population): For each patch i moving to patch j ($i, j \in \{1, 2, \dots, 6\}, j \neq i$):

$$\frac{dS_{i,3}}{dt} = - \underbrace{\lambda_i [t - \sigma_1] seas_i [t] S_{i,3}}_{(18)} + \frac{1}{r + \tau} (BT_{i,3} + IT_{i,3}) + \frac{1}{\delta} IU_{i,3} + \underbrace{\sum_j \frac{1}{\kappa_{i,j}} (S_{j,3} - S_{i,3})}_{(19)}$$

$$+ \underbrace{\frac{1}{\varpi_{i,j}} (S_{j,1} - S_{i,3})}_{(20)} + \underbrace{\sum_j \frac{1}{\zeta_{i,j}} (S_{j,1} - S_{i,3})}_{(21)} - \mu S_{i,3}$$

$$\frac{dBT_{i,3}}{dt} = pf_y \lambda_i [t - \sigma_1] seas_i [t] S_{i,3} - \frac{1}{\sigma_2} BT_{i,3} - \frac{1}{r + \tau} BT_{i,3} + \sum_j \frac{1}{\kappa_{i,j}} (BT_{j,3} - BT_{i,3})$$

$$+ \frac{1}{\varpi_{i,j}} (BT_{j,1} - BT_{i,3}) + \sum_j \frac{1}{\zeta_{i,j}} (BT_{j,1} - BT_{i,3}) - \mu BT_{i,3}$$

$$\frac{dIT_{i,3}}{dt} = \frac{1}{\sigma_2} BT_{i,3} - \frac{1}{r + \tau} IT_{i,3} + \sum_j \frac{1}{\kappa_{i,j}} (IT_{j,3} - IT_{i,3}) + \frac{1}{\varpi_{i,j}} (IT_{j,1} - IT_{i,3}) + \sum_j \frac{1}{\zeta_{i,j}} (IT_{j,1} - IT_{i,3}) - \mu IT_{i,3}$$

$$\frac{dBU_{i,3}}{dt} = (1 - pf_y) \lambda_i [t - \sigma_1] seas_i [t] S_{i,3} - \frac{1}{\sigma_2} BU_{i,3} + \sum_j \frac{1}{\kappa_{i,j}} (BU_{j,3} - BU_{i,3}) + \frac{1}{\varpi_{i,j}} (BU_{j,1} - BU_{i,3})$$

$$+ \sum_j \frac{1}{\zeta_{i,j}} (BU_{j,1} - BU_{i,3}) - \mu BU_{i,3}$$

$$\frac{dIU_{i,3}}{dt} = \frac{1}{\sigma_2} BU_{i,3} - \frac{1}{\delta} IU_{i,3} + \sum_j \frac{1}{\kappa_{i,j}} (IU_{j,3} - IU_{i,3}) + \frac{1}{\varpi_{i,j}} (IU_{j,1} - IU_{i,3}) + \sum_j \frac{1}{\zeta_{i,j}} (IU_{j,1} - IU_{i,3}) - \mu IU_{i,3}$$

- (18) New infections arising from sub-patch 3 due to local transmission and not infections contracted from patch of origin
- (19) Movement between local patches (1-5) out of and into the compartment
- (20) Movement of patch 6 population from patch 6, sub-patch 1 into patch i , sub-patch 3, when $i=1-5$ and $j = 6$ and movement from patch i , sub-patch 3 back into to patch 6, sub-patch 2. This rate $=0$ for all other values of j as it is particular to movement of Maputo population (patch 6)
- (21) Movement of patch j population from patch j , sub-patch 1, into patch 6 sub-patch 3 when $i=6$ and $j=1-5$ and movement from patch 6, sub-patch 3 back into patch j , sub-patch 2 ; This rate $=0$ for $j=6$ as it is particular to movement of the Mpumalanga population (patches 1-5) to and from Maputo

Table 6.2: Model 2: Compartment Descriptions

Compartment	Description
$S_{i,k}$	Susceptible Population in patch i and sub-patch k
$BT_{i,k}$	Population with Blood Stage Infections in patch i and sub-patch k that are treated
$IT_{i,k}$	Population with Infectious Stage Infections in patch i and sub-patch k that are treated
$BU_{i,k}$	Population with Blood Stage Infections in patch i and sub-patch k that are not treated
$IU_{i,k}$	Population with Infectious Stage infections in patch i and sub-patch k that are not treated
$Smda_{i,k}$	Susceptible Population in patch i and sub-patch k receiving MDA
$Bmda_{i,k}$	Population with Blood stage infections in patch i and sub-patch k receiving MDA
$Imda_{i,k}$	Population with Infectious stage infections in patch i and sub-patch k receiving MDA
$Sfsat_{i,k}$	Susceptible Population in patch i and sub-patch k receiving FSAT
$Bfsat_{i,k}$	Population with Blood stage infections in patch i and sub-patch k receiving FSAT
$Ifsat_{i,k}$	Population with Infectious stage infections in patch i and sub-patch k receiving FSAT
$BT(mda)_{i,k}$	Population having already received MDA, with Blood Stage Infections in patch i and sub-patch k that are treated
$IT(mda)_{i,k}$	Population having already received MDA, with Infectious Stage Infections in patch i and sub-patch k that are treated
$BU(mda)_{i,k}$	Population having already received MDA, with Blood Stage Infections in patch i and sub-patch k that are not treated
$IU(mda)_{i,k}$	Population having already received MDA, with Infectious Stage infections in patch i and sub-patch k that are not treated

Table 6.3: Full Parameter table

Parameter	Description	Value	Source
Base Model Parameters			
N	Population size	4×10^6	[125]
μ	Mortality/birth Rate	$\frac{105}{10000}$	[90]
δ	Natural recovery period	26 weeks	[61, 86, 141]
σ_1	Period between liver stage and blood stage	7 days (5-10)	[19, 25, 33]
σ_2	Period between blood stage and onset of gametocytemia	1 week	[61, 134]
r	AL elimination half-life	6 days	[77]
τ	Time to seek treatment	1/2 week	Expert opinion
p	Proportion of local infected population receiving treatment	0.95	[18, 58]

pf_y	Proportion of foreign infected population that receive treatment in a local patch	$pf_1 = 0.5655(0.5652, 0.5658)$ (pre April 2005) $pf_2 = 0.5500 (0.5494, 0.5506)$ (post April 2005)	Estimated from model fitting process
$seas_i$	Seasonal forcing function for foreign sourced cases	Derived from data	[116]
β_i	Annual number of mosquito bites per person x proportion of bites testing positive for sporozoites for patch i	$\beta_{TC} = 0.334 (0.244, 0.425)$ $\beta_{MB} = 2.178 (2.056, 2.300)$ $\beta_{UJ} = 0.805 (0.700, 0.910)$ $\beta_{NK} = 1.330 (1.310, 1.350)$ $\beta_{BB} = 8.304 (7.903, 8.705)$ $\beta_{MP} = 94.999 (93.327, 96.671)$	Estimated from model fitting process
$\frac{1}{\alpha}$	Rate of movement between sub-patch 2 and sub-patch 1	1.5 weeks^{-1}	Expert opinion
$\frac{1}{k}$	Rate of movement between 5 Mpumalanga municipalities	$1/48.603 (1/51.328, 1/45.787)$ weeks^{-1}	Estimated from model fitting process
$\frac{1}{v_y}$	Maputo residents: Rate of movement between Maputo and 5 Mpumalanga municipalities	$\frac{1}{v_1} = 1/1258.828 \text{ weeks}^{-1}$ $(1/1/1261.249, 1/1256.407)$ (pre April 2005) $\frac{1}{v_2} = 1/319.042 \text{ weeks}^{-1}$ $(1/322.796, 1/315.333)$ (post April 2005)	Estimated from model fitting process
$\frac{1}{z}$	Mpumalanga residents: Rate of movement between 5 Mpumalanga municipalities and Maputo	$\frac{1}{z} = 1/765.19 \text{ weeks}^{-1}$	Estimated from model fitting process
$fwgt$	Foreign movement weight intensity	$8.385 (8.232, 8.537)$	Estimated from model fitting process
$lwgt$	Local movement weight intensity	$2.613 (2.607, 2.618)$	Estimated from model fitting process
$vc[i, t]$ $vccov[i, t]$	$vccov[i, t] \times vef$ Vector Control Coverage	$0.22-0.90$	Derived from data

vef	Effectiveness of vector control	0.900 (0.897, 0.903)	Estimated from model fitting process
Scale up of Vector Control			
$add_i[t]$	Additional Vector Control	$vcaddon \times vcadd_i$	
$vcaddon$	Additional Vector Control Switch	Binary	
$vcadd_i$	Additional Vector Control Coverage in patch i	10%, 20%	
Mass Drug Administration			
$mrate[t]^{-1}$	Rate of MDA Take-up	$mdaon(-\log(1-mcov)/mdur)$	
$mdaon$	Mass Drug Administration Switch	Binary	
$mcov$	MDA coverage	80%	
$mdur$	Duration of MDA cycle	8 weeks	
$pro_{MDA}[t]$	Drug Protection period	8 weeks	
Focal Screen and Treat			
$msprop[t]$	Proportion Screened and Treated through Border Control	$mson \times mscov$	
$fsaton$	Focal Screen and Treat Switch	Binary	
$mscov$	FSAT coverage \times effectiveness	70%	
$pro_{FSAT}[t]$	Drug Protection period	8 weeks	

6.7.2 Summary Equations: Metapopulation Transmission model with interventions

Mass Drug Administration, Focal Screen and Treat, Scale-up of Vector Control

The base metapopulation model is expanded to include the impact of interventions, in particular, mass drug administration, focal screen and treat and a scale up of vector control (Figure 6.5). Scaling up vector control is modelled as an additional decrease to β_i . As described in the paper, the FSAT campaign is focused at a border entry point, where both the local and foreign populations are subject to a screening and treating campaign. Hence three compartments are introduced into the model in sub-patches 2 and 3 of each patch to account for locals and foreign travel into Mpumalanga. Sfsat, Bfsat and Ifsat represent the Susceptible, Blood and Infectious stages for a population that has received treatment through an FSAT campaign. To include

MDA, three compartments are introduced into the model in each sub-patch of each patch. S_{mda} , B_{mda} and I_{mda} represent the Susceptible, Blood and Infectious stages for a population that has received treatment through an MDA cycle. As MDA is subjected to a population regardless of disease status, all stages of infection must be accounted for. The period of chemoprophylaxis (the drug protection period) is often shorter than the duration of the MDA cycle, and given that individuals in the population can expect to receive MDA only once per cycle, it is necessary to allow for new infections during the MDA cycle for the population who has already received MDA, but are reinfected as the drug protection period has lapsed. $BT(mda)$, $IT(mda)$, $BU(mda)$ and $IU(mda)$ are included to account for these infections.

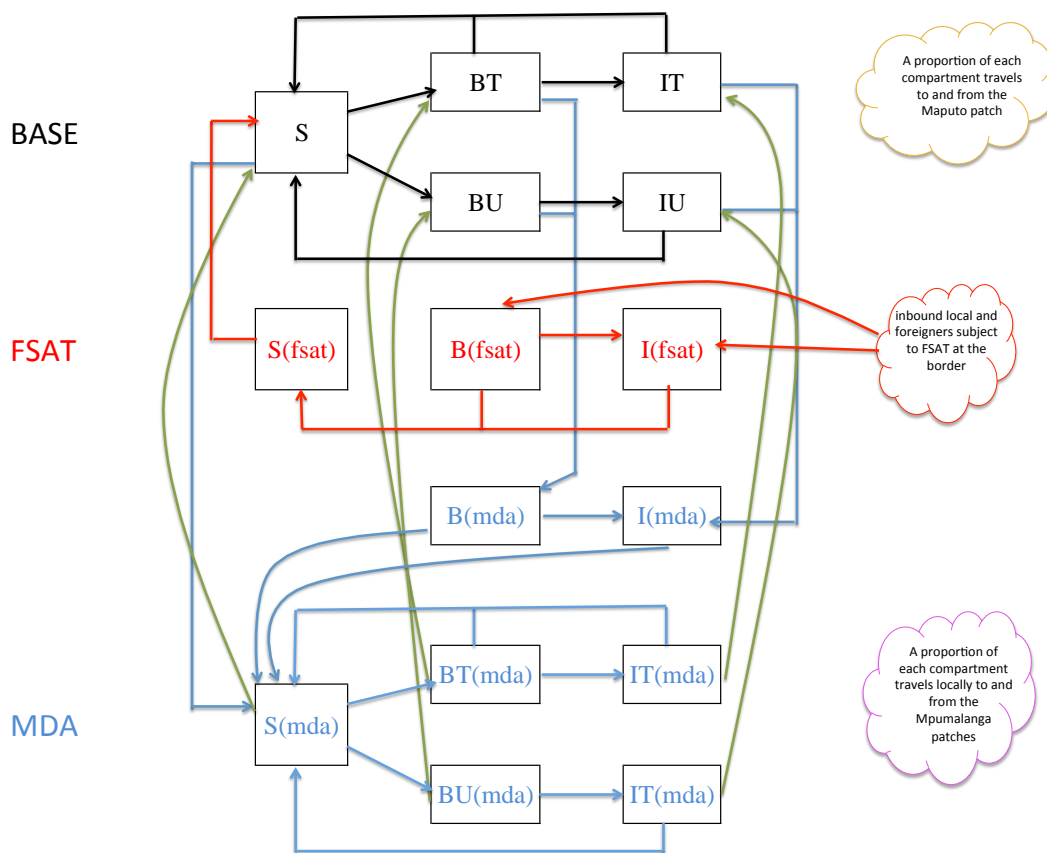


Figure 6.5: Transmission model with interventions for a single patch. Migration flows between patches are not shown. Note that the full model may be depicted as this single patch model, replicated 18 times, with migration flows between the 18 patches as described in the paper.

This leads to the following set of differential equations.

Sub-patch 1 (Local population): For each patch i moving to patch j ($i, j \in \{1, 2, \dots, 6\}, j \neq i$):

$$\begin{aligned}
 \frac{dS_{i,1}}{dt} &= \mu N_i - \lambda_i [t - \sigma_1] seas_i[t] S_{i,1} + \frac{1}{r + \tau} (BT_{i,1} + IT_{i,1}) + \frac{1}{\delta} IU_{i,1} + \frac{1}{\alpha} S_{i,2} + \sum_j \frac{1}{\kappa_{i,j}} (S_{j,1} - S_{i,1}) \\
 &\quad - \frac{1}{\varpi_{i,j}} S_{i,1} - \frac{1}{\zeta_{i,6}} S_{i,1} - \underbrace{\frac{1}{mrate[t]} S_{i,1}}_{(22)} + \underbrace{\frac{1}{promDA[t]} Smda_{i,1}}_{(23)} - \mu S_{i,1} \\
 \frac{dBT_{i,1}}{dt} &= p \lambda_i [t - \sigma_1] seas_i[t] (S_{i,1} + S_{i,2}) - \frac{1}{\sigma_2} BT_{i,1} - \frac{1}{r + \tau} BT_{i,1} + \frac{1}{\alpha} BT_{i,2} + \sum_j \frac{1}{\kappa_{i,j}} (BT_{j,1} - BT_{i,1}) \\
 &\quad - \frac{1}{\varpi_{i,j}} BT_{i,1} - \frac{1}{\zeta_{i,6}} BT_{i,1} - \frac{1}{mrate[t]} BT_{i,1} + \underbrace{\frac{1}{promDA[t]} BT(mda)_{i,1}}_{(24)} - \mu BT_{i,1} \\
 \frac{dIT_{i,1}}{dt} &= \frac{1}{\sigma_2} BT_{i,1} - \frac{1}{r + \tau} IT_{i,1} + \frac{1}{\alpha} IT_{i,2} + \sum_j \frac{1}{\kappa_{i,j}} (IT_{j,1} - IT_{i,1}) - \frac{1}{\varpi_{i,j}} IT_{i,1} - \frac{1}{\zeta_{i,6}} IT_{i,1} \\
 &\quad - \frac{1}{mrate[t]} IT_{i,1} + \frac{1}{promDA[t]} IT(mda)_{i,1} - \mu IT_{i,1} \\
 \frac{dBU_{i,1}}{dt} &= (1 - p) \lambda_i [t - \sigma_1] seas_i[t] (S_{i,1} + S_{i,2}) - \frac{1}{\sigma_2} BU_{i,1} + \frac{1}{\alpha} BU_{i,2} + \sum_j \frac{1}{\kappa_{i,j}} (BU_{j,1} - BU_{i,1}) \\
 &\quad - \frac{1}{\varpi_{i,j}} BU_{i,1} - \frac{1}{\zeta_{i,6}} BU_{i,1} - \frac{1}{mrate[t]} BU_{i,1} + \frac{1}{promDA[t]} BU(mda)_{i,1} - \mu BU_{i,1} \\
 \frac{dIU_{i,1}}{dt} &= \frac{1}{\sigma_2} BU_{i,1} - \frac{1}{\delta} IU_{i,1} + \frac{1}{\alpha} IU_{i,2} + \sum_j \frac{1}{\kappa_{i,j}} (IU_{j,1} - IU_{i,1}) - \frac{1}{\varpi_{i,j}} IU_{i,1} - \frac{1}{\zeta_{i,6}} IU_{i,1} \\
 &\quad - \frac{1}{mrate[t]} IU_{i,1} + \frac{1}{promDA[t]} IU(mda)_{i,1} - \mu IU_{i,1} \\
 \frac{dSmda_{i,1}}{dt} &= -\lambda_i [t - \sigma_1] seas_i[t] Smda_{i,1} + \frac{1}{mrate[t]} S_{i,1} + \underbrace{\frac{1}{r} (Bmda_{i,1} + Imda_{i,1})}_{(25)} - \frac{1}{promDA[t]} Smda_{i,1} \\
 &\quad - \mu Smda_{i,1} \\
 \frac{dBmda_{i,1}}{dt} &= \frac{1}{mrate[t]} (BT_{i,1} + BU_{i,1}) - \frac{1}{\sigma_2} Bmda_{i,1} - \frac{1}{r} Bmda_{i,1} - \mu Bmda_{i,1} \\
 \frac{dImda_{i,1}}{dt} &= \frac{1}{mrate[t]} (IT_{i,1} + IU_{i,1}) + \frac{1}{\sigma_2} Bmda_{i,1} - \frac{1}{r} Imda_{i,1} - \mu Imda_{i,1} \\
 \frac{dSfsat_{i,1}}{dt} &= \underbrace{0}_{(26)} \\
 \frac{dBfsat_{i,1}}{dt} &= \underbrace{0}_{(26)} \\
 \frac{dIfsat_{i,1}}{dt} &= \underbrace{0}_{(26)}
 \end{aligned}$$

$$\begin{aligned}
\frac{dBT(mda)_{i,1}}{dt} &= p\lambda_i[t - \sigma_1]seas_i[t](Smda_{i,1} + Smda_{i,2}) - \frac{1}{\sigma_2}BT(mda)_{i,1} - \frac{1}{r + \tau}BT(mda)_{i,1} + \frac{1}{\alpha}BT(mda)_{i,2} + \\
&\quad \sum_j \frac{1}{\kappa_{i,j}}(BT(mda)_{j,1} - BT(mda)_{i,1}) - \frac{1}{\varpi_{i,j}}BT(mda)_{i,1} - \frac{1}{\zeta_{i,6}}BT(mda)_{i,1} - \frac{1}{pro_{MDA}[t]}BT(mda)_{i,1} \\
&\quad - \mu BT(mda)_{i,1} \\
\frac{dIT(mda)_{i,1}}{dt} &= \frac{1}{\sigma_2}BT(mda)_{i,1} - \frac{1}{r + \tau}IT(mda)_{i,1} + \frac{1}{\alpha}IT(mda)_{i,2} + \sum_j \frac{1}{\kappa_{i,j}}(IT(mda)_{j,1} - IT(mda)_{i,1}) \\
&\quad - \frac{1}{\varpi_{i,j}}IT(mda)_{i,1} - \frac{1}{\zeta_{i,6}}IT(mda)_{i,1} - \frac{1}{pro_{MDA}[t]}IT(mda)_{i,1} - \mu IT(mda)_{i,1} \\
\frac{dBU(mda)_{i,1}}{dt} &= (1 - p)\lambda_i[t - \sigma_1]seas_i[t](Smda_{i,1} + Smda_{i,2}) - \frac{1}{\sigma_2}BU(mda)_{i,1} + \frac{1}{\alpha}BU(mda)_{i,2} \\
&\quad + \sum_j \frac{1}{\kappa_{i,j}}(BU(mda)_{j,1} - BU(mda)_{i,1}) - \frac{1}{\varpi_{i,j}}BU(mda)_{i,1} - \frac{1}{\zeta_{i,6}}BU(mda)_{i,1} \\
&\quad - \frac{1}{pro_{MDA}[t]}BU(mda)_{i,1} - \mu BU(mda)_{i,1} \\
\frac{dIU(mda)_{i,1}}{dt} &= \frac{1}{\sigma_2}BU(mda)_{i,1} - \frac{1}{\delta}IU(mda)_{i,1} + \frac{1}{\alpha}IU(mda)_{i,2} + \sum_j \frac{1}{\kappa_{i,j}}(IU(mda)_{j,1} - IU(mda)_{i,1}) \\
&\quad - \frac{1}{\varpi_{i,j}}IU(mda)_{i,1} - \frac{1}{\zeta_{i,6}}IU(mda)_{i,1} - \frac{1}{pro_{MDA}[t]}IU(mda)_{i,1} - \mu IU(mda)_{i,1}
\end{aligned}$$

(22) Take-up of MDA at a rate dependent on duration of the MDA cycle and the target coverage

(23) Assimilation back into the Susceptible population after MDA cycle is complete

(24) Recovery of infections treated during MDA

(25) Assimilation back into the Blood stage treated population after MDA cycle is complete

(26) As FSAT is modelled to be conducted at the Mpumalanga-Maputo border, only locals returning from Maputo (movement from sub-patch 3 to sub-patch 2) or foreigners entering Mpumalanga (movement from sub-patch 1 to sub-patch 3) are affected. Thus residents of sub-patch 1 are not affected by FSAT.

Sub-patch 2 (Local population returning from foreign travel): For each patch i moving to patch j ($i, j \in \{1, 2, \dots, 6\}, j \neq i$)

$$\begin{aligned}
\frac{dS_{i,2}}{dt} &= -\lambda_i[t - \sigma_1]seas_i[t]S_{i,2} + \frac{1}{r + \tau}(BT_{i,2} + IT_{i,2}) + \frac{1}{\delta}IU_{i,2} - \frac{1}{\alpha}S_{i,2} + \sum_j \frac{1}{\kappa_{i,j}}(S_{j,2} - S_{i,2}) \\
&\quad + \sum_j \frac{1}{\varpi_{i,j}}S_{j,3} + \frac{1}{\zeta_{i,6}}S_{j,3} - \frac{1}{mrate[t]}S_{i,2} + \frac{1}{pro_{MDA}[t]}Smda_{i,2} + \underbrace{\frac{1}{pro_{FSAT}[t]}Sf_{sat_{i,2}}}_{(27)} - \mu S_{i,2}
\end{aligned}$$

$$\begin{aligned}
 \frac{dBT_{i,2}}{dt} &= -\frac{1}{\sigma_2}BT_{i,2} - \frac{1}{r+\tau}BT_{i,2} - \frac{1}{\alpha}BT_{i,2} + \underbrace{\sum_j \frac{1}{\kappa_{i,j}}(BT_{j,2} - BT_{i,2}) + (1 - fsaton * mscov[t]) * \frac{1}{\zeta_{i,6}}BT_{j,3}}_{(28)} \\
 &\quad + \underbrace{\sum_j \frac{1}{\varpi_{i,j}}BT_{j,3} - \frac{1}{mrate[t]}BT_{i,2} + \frac{1}{promDA[t]}BT(mda)_{i,2} - \mu BT_{i,2}}_{(29)} \\
 \frac{dIT_{i,2}}{dt} &= \frac{1}{\sigma_2}BT_{i,2} - \frac{1}{r+\tau}IT_{i,2} - \frac{1}{\alpha}IT_{i,2} + \sum_j \frac{1}{\kappa_{i,j}}(IT_{j,2} - IT_{i,2}) + (1 - fsaton * mscov[t]) * \frac{1}{\zeta_{i,6}}IT_{j,3} \\
 &\quad \sum_j \frac{1}{\varpi_{i,j}}IT_{j,3} - \frac{1}{mrate[t]}IT_{i,2} + \frac{1}{promDA[t]}IT(mda)_{i,2} - \mu IT_{i,2} \\
 \frac{dBU_{i,2}}{dt} &= -\frac{1}{\sigma_2}BU_{i,2} - \frac{1}{\alpha}BU_{i,2} + \sum_j \frac{1}{\kappa_{i,j}}(BU_{j,2} - BU_{i,2}) + (1 - fsaton * mscov[t]) * \frac{1}{\zeta_{i,6}}BU_{j,3} \\
 &\quad \sum_j \frac{1}{\varpi_{i,j}}BU_{j,3} - \frac{1}{mrate[t]}BU_{i,2} + \frac{1}{promDA[t]}BU(mda)_{i,2} - \mu BU_{i,2} \\
 \frac{dIU_{i,2}}{dt} &= \frac{1}{\sigma_2}BU_{i,2} - \frac{1}{\delta}IU_{i,2} - \frac{1}{\alpha}IU_{i,2} + \sum_j \frac{1}{\kappa_{i,j}}(IU_{j,2} - IU_{i,2}) + (1 - fsaton * mscov[t]) * \frac{1}{\zeta_{i,6}}IU_{j,3} \\
 &\quad \sum_j \frac{1}{\varpi_{i,j}}IU_{j,3} - \frac{1}{mrate[t]}IU_{i,2} + \frac{1}{promDA[t]}IU(mda)_{i,2} - \mu IU_{i,2} \\
 \frac{dSmda_{i,2}}{dt} &= -\lambda_i[t - \sigma_1]seas_i[t]Smda_{i,2} + \frac{1}{mrate[t]}S_{i,2} + \frac{1}{r}(Bmda_{i,2} + Imda_{i,2}) - \frac{1}{promDA[t]}Smda_{i,2} \\
 &\quad - \mu Smda_{i,2} \\
 \frac{dBmda_{i,2}}{dt} &= \frac{1}{mrate[t]}(BT_{i,2} + BU_{i,2}) - \frac{1}{\sigma_2}Bmda_{i,2} - \frac{1}{r}Bmda_{i,2} - \mu Bmda_{i,2} \\
 \frac{dImda_{i,2}}{dt} &= \frac{1}{mrate[t]}(IT_{i,2} + IU_{i,2}) + \frac{1}{\sigma_2}Bmda_{i,2} - \frac{1}{r}Imda_{i,2} - \mu Imda_{i,2} \\
 \frac{dSfsat_{i,2}}{dt} &= \underbrace{\frac{1}{r}(Bfsat_{i,2} + Ifsat_{i,2})}_{(30)} - \frac{1}{promFSAT[t]}Sfsat_{i,2} - \mu Sfsat_{i,2} \\
 \frac{dBfsat_{i,2}}{dt} &= \underbrace{fsaton * mscov[t] * \left(\frac{1}{\zeta_{i,6}}BT_{j,3} + \frac{1}{\zeta_{i,6}}BU_{j,3} \right)}_{(31)} - \frac{1}{r}Bfsat_{i,2} - \frac{1}{\sigma_2}Bfsat_{i,2} - \mu Bfsat_{i,2} \\
 \frac{dIfsat_{i,2}}{dt} &= fsaton * mscov[t] * \left(\frac{1}{\zeta_{i,6}}IT_{j,3} + \frac{1}{\zeta_{i,6}}IU_{j,3} \right) + \frac{1}{\sigma_2}Bfsat_{i,2} - \frac{1}{r}Ifsat_{i,2} - \mu Ifsat_{i,2} \\
 \frac{dBT(mda)_{i,2}}{dt} &= -\frac{1}{\sigma_2}BT(mda)_{i,2} - \frac{1}{r+\tau}BT(mda)_{i,2} - \frac{1}{\alpha}BT(mda)_{i,2} + \sum_j \frac{1}{\kappa_{i,j}}(BT(mda)_{j,2} - BT(mda)_{i,2}) \\
 &\quad + \underbrace{(1 - fsaton * mscov[t]) * \frac{1}{\zeta_{i,6}}BT(mda)_{j,3}}_{(28)} + \underbrace{\sum_j \frac{1}{\varpi_{i,j}}BT(mda)_{j,3} - \frac{1}{promDA[t]}BT(mda)_{i,2}}_{(29)} \\
 &\quad - \mu BT(mda)_{i,2}
 \end{aligned}$$

$$\begin{aligned}
 \frac{dIT(mda)_{i,2}}{dt} &= \frac{1}{\sigma_2} BT(mda)_{i,2} - \frac{1}{r + \tau} IT(mda)_{i,2} - \frac{1}{\alpha} IT(mda)_{i,2} + \sum_j \frac{1}{\kappa_{i,j}} (IT(mda)_{j,2} - IT(mda)_{i,2}) \\
 &+ (1 - fsaton * mscov[t]) * \frac{1}{\zeta_{i,6}} IT(mda)_{j,3} + \sum_j \frac{1}{\varpi_{i,j}} IT(mda)_{j,3} - \frac{1}{proMDA[t]} IT(mda)_{i,2} \\
 &- \mu IT(mda)_{i,2} \\
 \frac{dBU(mda)_{i,2}}{dt} &= -\frac{1}{\sigma_2} BU(mda)_{i,2} - \frac{1}{\alpha} BU(mda)_{i,2} + \sum_j \frac{1}{\kappa_{i,j}} (BU(mda)_{j,2} - BU(mda)_{i,2}) + \\
 &(1 - fsaton * mscov[t]) * \frac{1}{\zeta_{i,6}} BU(mda)_{j,3} + \sum_j \frac{1}{\varpi_{i,j}} BU(mda)_{j,3} - \frac{1}{proMDA[t]} BU(mda)_{i,2} \\
 &- \mu BU(mda)_{i,2} \\
 \frac{dIU(mda)_{i,2}}{dt} &= \frac{1}{\sigma_2} BU(mda)_{i,2} - \frac{1}{\delta} IU(mda)_{i,2} - \frac{1}{\alpha} IU(mda)_{i,2} + \sum_j \frac{1}{\kappa_{i,j}} (IU(mda)_{j,2} - IU(mda)_{i,2}) \\
 &+ (1 - fsaton * mscov[t]) * \frac{1}{\zeta_{i,6}} IU(mda)_{j,3} + \sum_j \frac{1}{\varpi_{i,j}} IU(mda)_{j,3} - \frac{1}{proMDA[t]} IU(mda)_{i,2} \\
 &- \mu IU(mda)_{i,2}
 \end{aligned}$$

- (27) Assimilation back into the Susceptible population after MDA cycle is complete
- (28) Movement of patch i population **not subjected to FSAT** from foreign patch 6 sub-patch 3 back into patch i, sub-patch 2, when i=1-5; =0 for j=6 as this rate is particular to movement of the Mpumalanga population to and from Maputo (patches 1-5)
- (29) Movement of patch 6 population from foreign patch j, sub-patch 3 back into patch 6 but in sub-patch 2, when i=6 and j = 1-5; =0 for all other values of i as this rate is particular to movement of Maputo population (patch 6)
- (30) Recovery of infections treated during FSAT
- (31) Take-up of FSAT (of locals entering Mpumalanga) at a rate dependent on duration of the FSAT cycle and the target coverage

Sub-patch 3 (Foreign population): For each patch i moving to patch j ($i, j \in \{1, 2, \dots, 6\}, j \neq i$):

$$\begin{aligned}
 \frac{dS_{i,3}}{dt} &= -\lambda_i [t - \sigma_1] seas_i[t] S_{i,3} + \frac{1}{r + \tau} (BT_{i,3} + IT_{i,3}) + \frac{1}{\delta} IU_{i,3} + \sum_j \frac{1}{\kappa_{i,j}} (S_{j,3} - S_{i,3}) \\
 &+ \underbrace{\frac{1}{\varpi_{i,j}} (S_{j,1} - S_{i,3})}_{(32)} + \underbrace{\sum_j \frac{1}{\zeta_{i,j}} (S_{j,1} - S_{i,3})}_{(33)} - \frac{1}{mrate[t]} S_{i,3} + \frac{1}{proMDA[t]} Smda_{i,3} - \mu S_{i,3} \\
 \frac{dBT_{i,3}}{dt} &= pf_y \lambda_i [t - \sigma_1] seas_i[t] S_{i,3} - \frac{1}{\sigma_2} BT_{i,3} - \frac{1}{r + \tau} BT_{i,3} + \sum_j \frac{1}{\kappa_{i,j}} (BT_{j,3} - BT_{i,3})
 \end{aligned}$$

$$\begin{aligned}
 & + \underbrace{(1 - fsaton * mscov[t]) * \frac{1}{\varpi_{i,j}} BT_{j,1}}_{(34)} - \underbrace{\frac{1}{\varpi_{i,j}} BT_{i,3}}_{(35)} + \sum_j \frac{1}{\zeta_{i,j}} (BT_{j,1} - BT_{i,3}) - \frac{1}{mrate[t]} BT_{i,3} + \\
 & \frac{1}{proMDA[t]} BT(mda)_{i,3} - \mu BT_{i,3} \\
 \frac{dIT_{i,3}}{dt} & = \frac{1}{\sigma_2} BT_{i,3} - \frac{1}{r + \tau} IT_{i,3} + \sum_j \frac{1}{\kappa_{i,j}} (IT_{j,3} - IT_{i,3}) + (1 - fsaton * mscov[t]) * \frac{1}{\varpi_{i,j}} IT_{j,1} \\
 & - \frac{1}{\varpi_{i,j}} IT_{i,3} + \sum_j \frac{1}{\zeta_{i,j}} (IT_{j,1} - IT_{i,3}) - \frac{1}{mrate[t]} IT_{i,3} + \frac{1}{proMDA[t]} IT(mda)_{i,3} - \mu IT_{i,3} \\
 \frac{dBU_{i,3}}{dt} & = (1 - pf_y) \lambda_i [t - \sigma_1] seas_i[t] S_{i,3} - \frac{1}{\sigma_2} BU_{i,3} + \sum_j \frac{1}{\kappa_{i,j}} (BU_{j,3} - BU_{i,3}) + \\
 & (1 - fsaton * mscov[t]) * \frac{1}{\varpi_{i,j}} BU_{j,1} - \frac{1}{\varpi_{i,j}} BU_{i,3} + \sum_j \frac{1}{\zeta_{i,j}} (BU_{j,1} - BU_{i,3}) - \frac{1}{mrate[t]} BU_{i,3} + \\
 & \frac{1}{proMDA[t]} BU(mda)_{i,3} - \mu BU_{i,3} \\
 \frac{dIU_{i,3}}{dt} & = \frac{1}{\sigma_2} BU_{i,3} - \frac{1}{\delta} IU_{i,3} + \sum_j \frac{1}{\kappa_{i,j}} (IU_{j,3} - IU_{i,3}) + (1 - fsaton * mscov[t]) * \frac{1}{\varpi_{j,i}} IU_{j,1} \\
 & - \frac{1}{\varpi_{j,i}} IU_{i,3} + \sum_j \frac{1}{\zeta_{j,i}} (IU_{j,1} - IU_{i,3}) - \frac{1}{mrate[t]} IU_{i,3} + \frac{1}{proMDA[t]} IU(mda)_{i,3} - \mu IU_{i,3} \\
 \frac{dSmda_{i,3}}{dt} & = -\lambda_i [t - \sigma_1] seas_i[t] S(mda)_{i,3} + \frac{1}{mrate[t]} S_{i,3} + \frac{1}{r} (Bmda_{i,3} + Imda_{i,3}) - \frac{1}{proMDA[t]} Smda_{i,3} \\
 & - \mu Smda_{i,3} \\
 \frac{dBmda_{i,3}}{dt} & = \frac{1}{mrate[t]} (BT_{i,3} + BU_{i,3}) - \frac{1}{\sigma_2} Bmda_{i,3} - \frac{1}{r} Bmda_{i,3} - \mu Bmda_{i,3} \\
 \frac{dImda_{i,3}}{dt} & = \frac{1}{mrate[t]} (IT_{i,3} + IU_{i,3}) + \frac{1}{\sigma_2} Bmda_{i,3} - \frac{1}{r} Imda_{i,3} - \mu Imda_{i,3} \\
 \frac{dSfsat_{i,3}}{dt} & = \frac{1}{r} (Bfsat_{i,3} + Ifsat_{i,3}) - \frac{1}{proFSAT[t]} Sfsat_{i,3} - \mu Sfsat_{i,3} \\
 \frac{dBfsat_{i,3}}{dt} & = fsaton * mscov[t] * \underbrace{\left(\frac{1}{\varpi_{i,j}} BT_{j,1} + \frac{1}{\varpi_{i,j}} BU_{j,1} \right)}_{(36)} - \frac{1}{r} Bfsat_{i,3} - \frac{1}{\sigma_2} Bfsat_{i,3} - \mu Bfsat_{i,3} \\
 \frac{dIfsat_{i,3}}{dt} & = fsaton * mscov[t] * \left(\frac{1}{\varpi_{i,j}} IT_{j,1} + \frac{1}{\varpi_{i,j}} IU_{j,1} \right) + \frac{1}{\sigma_2} Bfsat_{i,3} - \frac{1}{r} Ifsat_{i,3} - \mu Ifsat_{i,3} \\
 \frac{dBT(mda)_{i,3}}{dt} & = pf_y \lambda_i [t - \sigma_1] seas_i[t] S(mda)_{i,3} - \frac{1}{\sigma_2} BT(mda)_{i,3} - \frac{1}{r + \tau} BT(mda)_{i,3} + \\
 & \sum_j \frac{1}{\kappa_{i,j}} (BT(mda)_{j,3} - BT(mda)_{i,3}) + \underbrace{(1 - fsaton * mscov[t]) * \frac{1}{\varpi_{i,j}} BT(mda)_{j,1}}_{(34)} \\
 & - \underbrace{\frac{1}{\varpi_{i,j}} BT(mda)_{i,3}}_{(35)} + \sum_j \frac{1}{\zeta_{i,j}} (BT(mda)_{j,1} - BT(mda)_{i,3}) - \frac{1}{proMDA[t]} BT(mda)_{i,3}
 \end{aligned}$$

$$\begin{aligned}
 & - \mu BT(mda)_{i,3} \\
 \frac{dIT(mda)_{i,3}}{dt} &= \frac{1}{\sigma_2} BT(mda)_{i,3} - \frac{1}{r + \tau} IT(mda)_{i,3} + \sum_j \frac{1}{\kappa_{i,j}} (IT(mda)_{j,3} - IT(mda)_{i,3}) + \\
 & (1 - fsaton * mscov[t]) * \frac{1}{\varpi_{i,j}} IT(mda)_{j,1} - \frac{1}{\varpi_{i,j}} IT(mda)_{i,3} + \sum_j \frac{1}{\zeta_{i,j}} (IT(mda)_{j,1} - IT_{i,3}) \\
 & - \frac{1}{pro_{MDA}[t]} IT(mda)_{i,3} - \mu IT(mda)_{i,3} \\
 \frac{dBU(mda)_{i,3}}{dt} &= (1 - pfy) \lambda_i [t - \sigma_1] seas_i[t] S(mda)_{i,3} - \frac{1}{\sigma_2} BU(mda)_{i,3} + \sum_j \frac{1}{\kappa_{i,j}} (BU(mda)_{j,3} - BU(mda)_{i,3}) \\
 & + (1 - fsaton * mscov[t]) * \frac{1}{\varpi_{i,j}} BU(mda)_{j,1} - \frac{1}{\varpi_{i,j}} BU(mda)_{i,3} \\
 & + \sum_j \frac{1}{\zeta_{i,j}} (BU(mda)_{j,1} - BU(mda)_{i,3}) - \frac{1}{pro_{MDA}[t]} BU(mda)_{i,3} - \mu BU(mda)_{i,3} \\
 \frac{dIU(mda)_{i,3}}{dt} &= \frac{1}{\sigma_2} BU(mda)_{i,3} - \frac{1}{\delta} IU(mda)_{i,3} + \sum_j \frac{1}{\kappa_{i,j}} (IU(mda)_{j,3} - IU(mda)_{i,3}) + \\
 & (1 - fsaton * mscov[t]) * \frac{1}{\varpi_{j,i}} IU(mda)_{j,1} - \frac{1}{\varpi_{j,i}} IU(mda)_{i,3} + \sum_j \frac{1}{\zeta_{j,i}} (IU(mda)_{j,1} - IU_{i,3}) \\
 & - \frac{1}{pro_{MDA}[t]} IU(mda)_{i,3} - \mu IU(mda)_{i,3}
 \end{aligned}$$

- (32) Movement of patch 6 population from patch 6, sub-patch 1 into patch i, sub-patch 3, when i=1-5 and j = 6 and movement from patch i, sub-patch 3 back into to patch 6, sub-patch 2. This rate =0 for all other values of j as it is particular to movement of Maputo population (patch 6)
- (33) Movement of patch j population from patch j, sub-patch 1, into patch 6 sub-patch 3 when i=6 and j=1-5 and movement from patch 6, sub-patch 3 back into patch j, sub-patch 2 ; This rate=0 for j=6 as it is particular to movement of the Mpumalanga population (patches 1-5) to and from Maputo
- (34) Movement of patch 6 population **not subjected to FSAT** from patch 6, sub-patch 1 into patch i, sub-patch 3, when i=1-5 and j = 6. This rate =0 for all other values of j as it is particular to movement of Maputo population (patch 6)
- (35) Movement from patch i, sub-patch 3 back into to patch 6, sub-patch 2 when i=1-5 and j = 6. This rate =0 for all other values of j as it is particular to movement of Maputo population (patch 6)
- (36) Take-up of FSAT (of foreigners entering Mpumalanga) at a rate dependent on duration of the FSAT cycle and the target coverage

where the force of infection is given by

$$\lambda_i[t] = (1 - vc_i[t] * vef) \beta_i \times \frac{\sum_{k=1}^3 (IT_{i,k}[t - 4] + IU_{i,k} + Imda_{i,k}[t - 4] + Ifsat_{i,k}[t - 4])}{N_i}$$

6.7.3 Vector Control

Indoor Residual spraying is the primary vector control intervention employed in Mpumalanga. The data on the number of structures sprayed in Mpumalanga is provided by the Malaria Elimination Programme and has already been presented in Ngomane and de Jager (2012) and is depicted in Figure 6.6 [95]. Given that IRS is not 100% effective, a parameter on the effectiveness of IRS (vef) has been estimated in the data-fitting process.

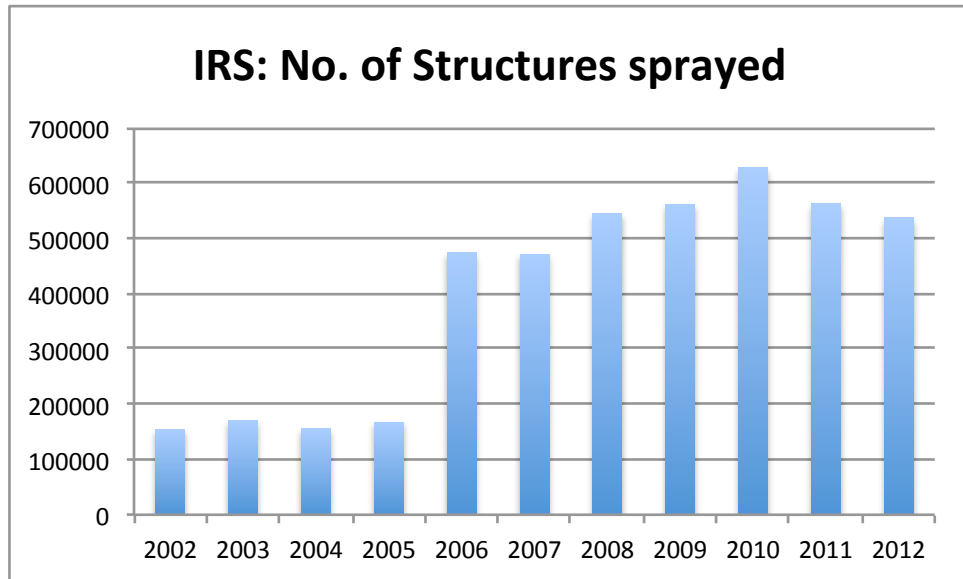


Figure 6.6: Number of structures sprayed in Mpumalanga between 2002 and 2012

6.7.4 Data Fitting Method

The model is fitted to weekly incidence data of treated cases from 2002 to 2008, and then validated with data from 2009 to 2012. The model is run from 1990 to reach a steady state before being fitted to data from 2002. IRS coverage and drug treatment are included in the model for the data fitting. The number of treated cases in each sub-patch k are fitted to the data using the maximum likelihood approach assuming an underlying Poisson distribution with canonical parameter λ as the average number of treated cases per week. The metapopulation non-linear differential equation model is expressed in terms of average rates of movement between compartments, thus λ is a function of the parameters to be estimated (listed in Table 6.3)

The Poisson probability of observing x counts when the average number of counts per week is λ

given by

$$P(x|\lambda) = \frac{\lambda^x \exp^{-\lambda}}{x!}.$$

As the model is being fitted to time series data with N time bins, λ , the expected number of counts per bin is a function of time. Assuming the independence of data from different time bins, the likelihood reduces to

$$L(\lambda_i|x_i) = \prod_{i=1}^N \frac{\lambda_i^{x_i} \exp^{-\lambda_i}}{x_i!}$$

and the log likelihood becomes

$$\ln(L(\lambda_i|x_i)) = \sum_{i=1}^N x_i \ln(\lambda_i) - \lambda_i - \ln(x_i!).$$

The model is fitted to 16 sets of data for each weekly time bin: treated cases for three sub-patches in five Mpumalanga municipalities and treated cases for Maputo. Under the assumption of independence, the log likelihood to be maximised is

$$\ln(L(\lambda_{s,i}|x_{s,i})) \propto \sum_{i=1}^N \sum_{s=1}^{16} x_{s,i} \ln(\lambda_{s,i}) - \lambda_{s,i}$$

The log-likelihood is negated and minimised using the hydroPSO function implementing a version of the Particle Swarm Optimisation algorithm in the R package hydroPSO v0.3-3 [150, 151]. Particle Swarm Optimisation is a global stochastic optimisation technique initially inspired by social behaviour of birds and fish [32, 64]. It shares similarities with evolutionary optimisation techniques like Genetic Algorithms (GA) but explores the multi-dimensional solution space on the basis of individual and global best-known particle positions without evolution operators. Problems are optimised by moving particles (the population of candidate solutions) around the search-space based on the particles' position and velocity. Particle movements are a function of local best positions and other best particle positions in the search-space. Thus the particles "swarm" towards the best solutions in the search-space.

The parameters estimated through the model fitting process are presented in Table 6.3. The

model with the estimated parameter values is run for a further 3 years to be further validated by comparison to data between 2009 and 2012. Figure 6.7 shows the data fitting and validation for all 16 sets of data with 95% confidence intervals. The differential equation model predicts the *average* number of treated cases per time point, whereas the data is one observation in time. Running the model several times, sampling parameter estimates from their 95% confidence ranges and treating model flows as a random realisation of a Poisson distribution, the average prediction at each time point is computed and plotted (solid red and blue lines). The shaded envelope around the average prediction is a 95% pseudo confidence interval for an individual prediction (computed by averaging the lower and upper bounds over each of the 95% confidence intervals calculated for every model run) as opposed to an interval for the average prediction. The latter, by default, would be narrower. The model fits the data in sub-patches 1 and 2 well, capturing the level and timing of transmission. Sub-patch 3 data is over-estimated before 2006 and captured relatively well thereafter for all municipalities except Nkomazi, where the prediction of infections is over-estimated. Sub-patch 3 for Bushbuckridge appears to be over-estimated, but as the scale of the graph is small compared to Nkomazi, this is less of an "over"-estimation. Both the timing and level of malaria transmission in Maputo is captured by the model fitting process.

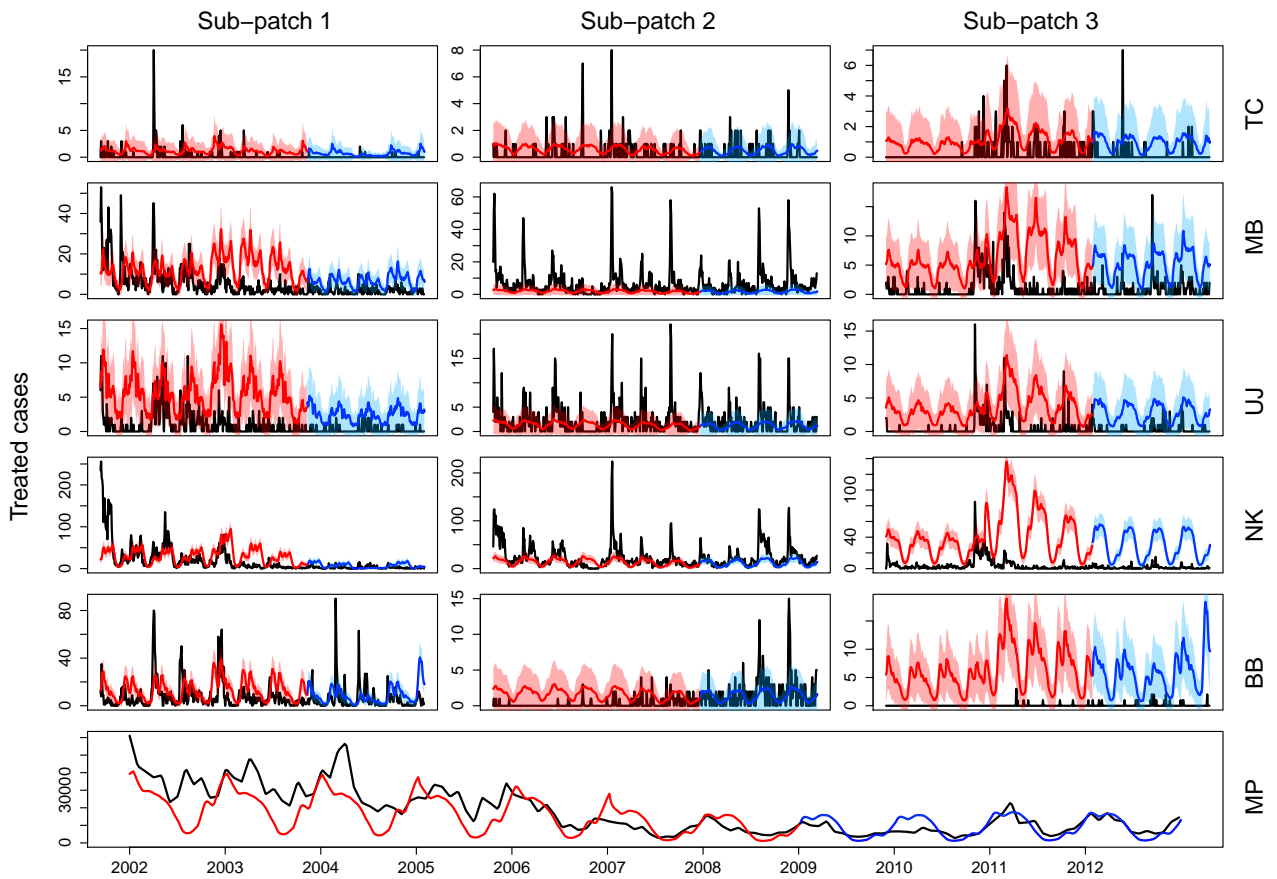


Figure 6.7: Model fit and validation with 95% uncertainty range for individual predictions

Chapter 7

Model 3 - A Hybrid Metapopulation DE-IBM model of malaria transmission

The models presented in Chapters 5 and 6 have predicted that while *locally focused* strategies (in isolation or combined) contributed to decreasing local infections, none was able to decrease local infections to zero due mainly to the continuous stream of imported infections. The greatest impact on local infections is predicted when source reduction is conducted in Maputo Province itself. An intervention that may assist in stemming the inflow of imported infections is a Focal Screen and Treat campaign at the Mpumalanga-Maputo border. The metapopulation model presented in the last chapter modelled this intervention at a broad level, predicting average effects while accounting for uncertainty in predictions by running the model stochastically. Adequately predicting the impact of an FSAT intervention like this, requires modelling to capture the coverage achieved, the diagnostic tools available and in use and the level of take-up by border-crossers, among other things. Individual based models are ideally suited for this purpose as they can incorporate individual variation in behaviour e.g. individual parasite loads and take up probabilities. Thus a metapopulation model is used to simulate malaria transmission in the five administrative municipalities and Maputo Province and the IBM model is used to simulate an FSAT campaign for locals returning to and foreigners entering Mpumalanga (at rates predicted by the metapopulation model), making this a hybrid metapopulation DE-IBM model.

The metapopulation model presented in this chapter incorporates human migration, in the same way as the model in Chapter 6. The compartment model used to model malaria transmission in each sub-patch has a different structure to that of Chapter 6. The structure differs in that the blood stage is incorporated along with the liver stage as a delay in the flow between the

susceptible population and the infectious population. This is because the infectious stage of untreated infections is subdivided into three groups: clinical untreated infections, asymptomatic patent untreated infections and asymptomatic sub-patent untreated infections. The reason for this subdivision is to account for the contribution of sub-patent infections to the infectious reservoir when they are missed by FSAT at the border by diagnostic tools with a low sensitivity. Thus the model is simplified in one aspect (incorporating the blood stage as a delay) and made more complex in another aspect (subdividing the infectious population) to suit the FSAT focus of the model.

The hybrid DE-IBM model presented in this paper is developed to simulate the impact of FSAT at the Mpumalanga-Maputo border as a means to inhibit the inflow of imported infections. This is the first study designed for this purpose in Mpumalanga and the first to do so in South Africa since the call for malaria elimination. To the author's knowledge, the hybrid metapopulation nested DE-IBM structure developed in Model 3 is a first simulation study of screening and treating malaria infections at a border control point and the first study to nest the IBM structure within the differential equation structure by *interrupting the flows of the DE model*. The impact of an FSAT campaign at the Maputo-Mpumalanga border is predicted for a variety of scenarios with respect to coverage levels, thresholds of detection, take-up proportion of individuals, target levels and typical diagnostic tools.

The model is fitted to weekly case data of treated cases from 2002 to 2008, and then validated with data from 2009 to 2012. The model predicts that the various scenarios of FSAT considered in this paper will not eliminate malaria for a number of reasons including low coverage at the border, due to other forms of entry into the province and the lack of resources to adequately screen and treat all individuals passing through the border. Diagnostic tools with high thresholds are likely to miss sub-patent infections resulting in untreated infectious individuals moving into Mpumalanga to contribute to onward infections. A low take up rate (in a non-mandatory FSAT campaign) is predicted to be another reason for failure of the intervention to eliminate. The paper concludes that a strategy focusing on preventing the inflow of imported infections through both FSAT and source reduction may stand a better chance at achieving elimination in Mpumalanga and South Africa compared to a nationally focused one in the face of high visitation rates from neighbours in higher transmission regions. An additional file which contains detailed descriptions of the model fitting process and model equations is presented at the end of the chapter.

SPS conceived the study, performed the mathematical model development and analysis and wrote the paper. SPS and LJW conceptualised the mathematical model and analysis. FL, KIB and LJW reviewed the manuscript extensively. All authors have read and approved the manuscript.

We are grateful to the Malaria Elimination Programme of the Department of Health in Mpumalanga, South Africa for the provision of data and are particularly grateful to Aaron Mabuza and Gerdalize Kok from the Malaria Elimination Programme and Jaishree Raman and John Frean from the National Institute for Communicable Diseases for their valuable input. This material is based

upon work supported financially by the National Research Foundation in South Africa. We are grateful to the National Research Foundation in South Africa for financial support. Any opinion, findings and conclusions or recommendations expressed in this material are those of the authors and therefore the NRF does not accept any liability in regard thereto. Mahidol-Oxford Tropical Medicine Research Unit is funded by the Wellcome Trust.

Predicting the impact of border control on malaria transmission: A Simulated Focal Screen and Treat campaign

Sheetal Prakash Silal^{1,*}, Francesca Little¹, Karen I Barnes², Lisa J White^{3,4},

¹ Department of Statistical Sciences, University of Cape Town, Cape Town, South Africa

² Division of Clinical Pharmacology, Department of Medicine, University of Cape Town, Cape Town, South Africa

³ Mahidol-Oxford Tropical Medicine Research Unit, Mahidol University, Bangkok, Thailand

⁴ Centre for Tropical Medicine, Nuffield Department of Clinical Medicine, Churchill Hospital, University of Oxford, Oxford, UK

7.1 Abstract

South Africa is one of many countries committed to malaria elimination with a target of achieving it by 2018 and all malaria-endemic provinces, including Mpumalanga, are increasing efforts towards this ambitious goal. Mathematical models have provided a valuable framework for analysing the dynamics of malaria transmission with a primary benefit being the ability to enact exogenous change on the modelled system to predict the impact of interventions without committing any real resources. A metapopulation, non-linear stochastic ordinary differential equation model is used to simulate malaria transmission in Mpumalanga and Maputo province, Mozambique to predict the impact of a Focal Screen and Treat campaign at the Mpumalanga-Maputo border. This campaign is simulated by nesting an Individual-Based Model for the Focal Screen and Treat campaign within the metapopulation transmission model. The model predicts that such a campaign, simulated for feasible levels of resources, coverage and take-up rates with different screening tools, will not eliminate malaria on its own, but will reduce transmission substantially and hence may form part of an integrated elimination strategy where a variety of interventions are employed together to achieve malaria elimination.

Under review at Malaria Journal

7.2 Background

Since the call for renewed efforts towards global malaria eradication in 2007, it has been acknowledged that new tools will be required to achieve this ambitious goal [129–133]. Drugs will need to be developed for a variety of purposes including use in elimination-focused strategies like Mass Drug Administration (MDA) and Mass Screen and Treat (MSAT) campaigns, prophylactic use and transmission prevention [131]. New insecticides and formulations will need to be developed considering varied vector biology and habits [133]. Importantly, diagnostic tools that are easily implemented with increased sensitivity and a decreased processing time will be necessary to quickly and successfully diagnose both patent and sub-patent infections [130]. This is particularly important as the impact of MSAT is dependent on the screening tool. South Africa is one of many countries committed to achieving malaria elimination with a target set at 2018 and all malaria-endemic provinces, including Mpumalanga province, are increasing efforts towards this ambitious goal. A malaria elimination strategy should aim to interrupt the transmission cycle and prevent it from being re-established. A successful interruption of malaria transmission ideally requires three elements: (1) the elimination of the vector, (2) the blockade of imported infections and (3) the reduction of these imported infections at their source [89]. Silal *et al.* and Model 2 in Chapter 6 have simulated interventions in Mpumalanga using mathematical modelling techniques aimed towards elements (1) and (3) ([117]). The reduction of imported infections was dealt with at a broad level through the simulation of a Focal Screen and Treat (FSAT) campaign at the Mpumalanga-Maputo border in Chapter 6. This paper focuses in more detail on the proposed FSAT campaign at the Mpumalanga-Maputo border using a hybrid metapopulation differential equation and individual based modelling (DE-IBM) approach.

Malaria in Mpumalanga has been documented extensively [11, 42, 75, 88, 95, 113–116]. Currently, malaria transmission occurs primarily in Ehlanzeni District on the border of both Maputo in Mozambique and Swaziland. The five municipalities in Ehlanzeni District are most affected by malaria in the province (Figure 7.1). The sharp decline in malaria incidence and malaria-related deaths in the province between 2002 and 2012 has been attributed to a series of policy interventions including intense vector control through indoor residual spraying (IRS), the introduction of artemisinin-based combination therapy (ACT) policy of artesunate plus sulphadoxine-pyremethamine in 2003, followed by artemether-lumefantrine (AL) in 2006 and the Lubombo Spatial Development cross-border Initiative (LSDI) between Mozambique, Swaziland and South Africa [88]. The LSDI malaria programme focused its activities primarily in Maputo Province in Mozambique and was later extended to Gaza Province resulting in substantial decreases in prevalence [70]. However the programme was terminated early in September 2010 and the resultant reduced IRS in Maputo thereafter correlates with increased malaria incidence observed from 2011 [105]. Between 2002 and 2012, 40 650 cases were notified, with the proportion of imported cases increasing from 39% in 2002 to 87% in 2012. Of the cases imported in 2012, 13% were sourced in South Africa and 85% were sourced from Mozambique (with the remaining 2%

sourced from other African and Asian countries).



Figure 7.1: A map of Mpumalanga Province in relation to Mozambique and Swaziland (Source: Mpumalanga Malaria Elimination Programme (unpublished))

Compartment models and their applications in malaria in particular, have a history that spans more than 100 years [82]. Increases in computing power have led to the increased use of Individual Based Models in recent years [139]. Metapopulation compartment models are an extension of compartment models where the population under consideration is sub-divided into patches. A compartment model is run in each patch and the patches are linked together, usually along geographical lines [112]. There have been several metapopulation compartment model applications in malaria [4, 5, 7, 67, 100, 109, 119, 152]. There have also been several applications of IBMs in malaria [46, 76, 99, 122]. With regards to screening and treating, Crowell *et al.* [27] modelled the cost effectiveness of MSAT as a disease reduction tool, Griffin modelled the impact of MSAT in an African setting at various transmission intensities, Maude *et al.* [84] modelled the impact of MSAT in the face of artemisinin resistance and White *et al.* [141] modelled the impact of MSAT in a comparison of simple and complex mathematical models. Applications of mathematical modelling of malaria in Mpumalanga have included a climate-based fuzzy distribution model [26], an eco-hydrological model for malaria outbreaks [87] and a cluster detection model [24]. Silal *et al.* [117] investigated the impact of FSAT and other interventions to achieve malaria elimination in Mpumalanga using a population level compartment model and Model 2 in Chapter 6 extended this application to a metapopulation model of the five municipalities in Ehlanzeni district and Maputo province. The hybrid metapopulation DE-IBM model presented

in this paper is developed to simulate the impact of FSAT at the Mpumalanga-Maputo border as a means to decrease the inflow of imported infections. This is the first model designed for this purpose in Mpumalanga and the first to do so since the call for malaria elimination in South Africa.

7.3 Methods

7.3.1 Transmission Model

The model presented in this paper is based on a model described in Chapter 6. The malaria transmission model has a metapopulation structure where the population of interest is divided into discrete patches under the assumption that individuals in these patches exhibit homogenous behaviour. Rather than modelling transmission in these patches in isolation, a metapopulation structure allows for transmission in a particular patch to be influenced by transmission in other patches. In this study, the area of interest is divided into six geographical patches: five patches for the five municipalities in Ehlanzeni District (Thaba Chewu (TC), Mbombela (MB), Umjindi (UJ), Nkomazi (NK) and Bushbuckridge (BB)) and one patch for Maputo province (MP). Each patch is further sub-divided into three sub-patches representing (1) the local population currently in the patch, (2) the local population having returned from travel to a foreign place (Maputo, if the patch is South African and vice versa) and (3) the population from the foreign place currently in the patch (Figure 7.2b). A malaria transmission model is developed for each sub-patch where the sub-patch population is divided into six compartments representing the population susceptible to malaria (S), the population at the infectious stage that receives treatment (I), the untreated symptomatic population at the infectious stage (C), the untreated asymptomatic population at the infectious stage (A), the untreated asymptomatic, sub-patent (< 100 parasites/ μ L) infectious population (M) and the population susceptible to malaria, but with prior asymptomatic infection (P) (Figure 7.2a). The liver and blood stage of the infection are incorporated as a delay in the flow between the susceptible and infectious stage compartments. Flows between compartments are governed by parameters described in Table 7.1. While the seasonal nature of transmission is incorporated in the model using forcing functions, the mosquito population is not modelled directly as it is assumed that the mosquito dynamics operate on a faster time-scale than the human dynamics and hence the mosquito population may be considered to be at equilibrium with respect to changes in the human population [66].

Human movements between patches are modelled in two ways. Local travel may occur between the five Mpumalanga patches (from all five compartments in all three sub-patches). Foreign travel may occur between the Maputo patch and the five Mpumalanga patches (from all five compartments) as illustrated in Figure 7.2b. These movements are inversely weighted by distance so that movements between patches that are closer together are more likely than movements

between patches that are further apart. A full description of the metapopulation transmission model is presented in Additional File 3 at the end of the chapter.

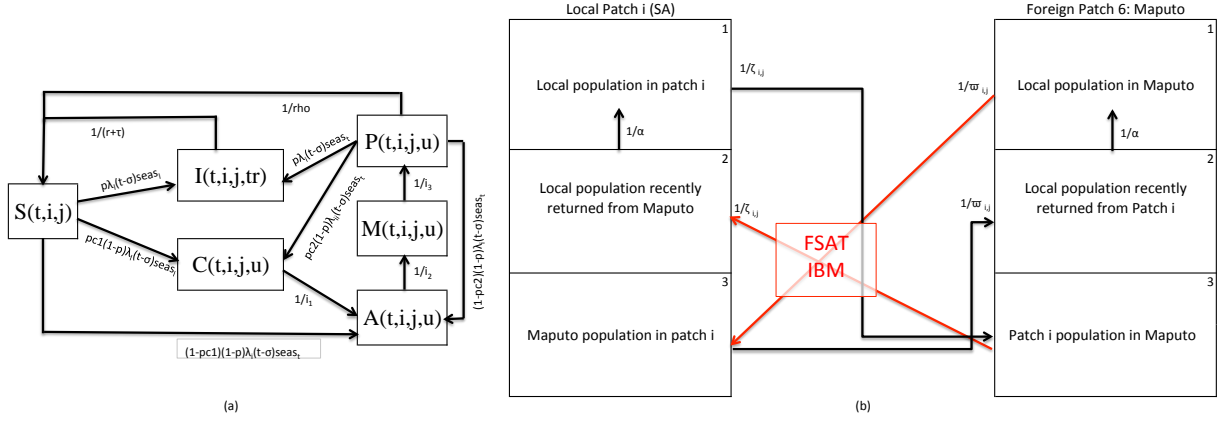


Figure 7.2: Hybrid Metapopulation DE-IBM Model flow (a) Compartment transmission model for each patch i (1-6) with sub-patch j (1-3) at time step t with compartments S -Susceptible, I - Infectious and treated (tr), C - Infectious, symptomatic and untreated (u), A - Infectious, asymptomatic and untreated, M - Infectious, sub-patent and untreated and P - Susceptible with prior asymptomatic infection. (b) Metapopulation structure highlighting human movement between each local patch $i \in \{1, 2, 3, 4, 5\}$ and foreign patch 6. Other parameters are described in Table 7.1 and Additional file 3.

Table 7.1: Values, descriptions and sources of the parameters driving the base metapopulation model of transmission. ($i = \{TC; MB; UJ; NK; BB; MP\}$)

Parameter	Description	Value	Source
N	Population size	4×10^6	[125]
μ	Mortality/birth Rate	$\frac{105}{10000}$	[90]
σ	Period between liver stage and onset of gametocytemia	2 weeks	[19, 25, 33, 134]
r	Artemether Lumefantrine elimination half-life	6 days	[77]
τ	Time to seek treatment	1/2 week	Expert opinion
ptf	Probability of treatment failure	0.01	[8]
p	Proportion of local infected population receiving treatment	0.95	[18, 58]

pf_{yr}	Proportion of foreign infected population that receive treatment in a local patch	$pf_1 = 0.6797$ (0.6795, 0.6800) (pre April 2005) $pf_2 = 0.6750$ (0.6742, 0.6758) (post April 2005)	Estimated from model fitting process
i_1	Duration of clinical infection before becoming asymptomatic	2.776 (2.688, 2.866) weeks	Estimated from model fitting process
i_2	Duration of asymptomatic infection before becoming sub-patent	11.063 (11.011, 11.114) weeks	Estimated from model fitting process
i_3	Duration of sub-patent infection	26.963 (26.912, 27.014) weeks	Estimated from model fitting process
ρ	Duration of clinical immunity	5 years	[35]
pc_1	Probability of clinical infection from naive individuals	0.9997 (0.9756, 0.9999)	[25, 45]
pc_2	Probability of clinical infection from partially immune individuals	0.902 (0.896, 0.901)	Estimated from data
$seas_i$	Seasonal forcing function for foreign sourced cases	Derived from data	[116]
β_i	Annual number of mosquito bites per person x proportion of bites testing positive for sporozoites for patch i	$\beta_{TC} = 3.996$ (3.623, 4.369) $\beta_{MB} = 0.016$ (0.013, 0.019) $\beta_{UJ} = 0.0003$ (0.00012, 0.00051) $\beta_{NK} = 2.563$ (2.509, 2.616) $\beta_{BB} = 9.983$ (9.592, 10.374) $\beta_{MP} = 92.728$ (92.571, 92.885)	Estimated from model fitting process
$\lambda_i(t)$	Force of infection	see Additional file 3	
$\frac{1}{\alpha}$	Rate of assimilation of population in sub-patch 2 (locals having returned from foreign travel) back into sub-patch 1 from whence they originated	1.5 weeks ⁻¹	Expert opinion
$\frac{1}{k}$	Rate of movement between 5 Mpumalanga municipalities	1/4.156 (1/4.075, 1/4.237) weeks ⁻¹	Estimated from model fitting process

$\frac{1}{v_{yr}}$	Maputo residents: Rate of movement between Maputo and 5 Mpumalanga municipalities	$\frac{1}{v_1} = 1/2289.789 \text{ weeks}^{-1}$ (1/2279.096, 1/2300.482) (pre April 2005) $\frac{1}{v_2} = 1/1363.792 \text{ weeks}^{-1}$ (1/1341.792, 1/1386.683) (post April 2005)	Estimated from model fitting process
$\frac{1}{\varpi_{i,j}}$	Maputo residents: Rate of movement between Maputo and 5 Mpumalanga municipalities based on $\frac{1}{v_{yr}}$ and distance between patches	see Additional file 1	
$\frac{1}{z}$	Mpumalanga residents: Rate of movement between 5 Mpumalanga municipalities and Maputo	$\frac{1}{z} = 1/298.781 \text{ weeks}^{-1}$ (1/296.953, 1/300.622)	Estimated from model fitting process
$\frac{1}{\zeta_{i,j}}$	Mpumalanga residents: Rate of movement between 5 Mpumalanga municipalities and Maputo based on $\frac{1}{z}$ and distance between patches	see Additional file 1	
$fwgt$	Foreign movement weight intensity	2.000 (1.944, 2.055)	Estimated from model fitting process
$lwgt$	Local movement weight intensity	13.693 (13.503, 13.885)	Estimated from model fitting process
vef	Effectiveness of vector control	0.9785 (0.9783, 0.9787)	Estimated from model fitting process
$vc_i[t]$	Vector Control Coverage in patch $i \times$ efficiency	Derived from data	

7.3.2 FSAT model

Figure 7.2b shows that only movement of the local Mpumalanga population returning from Maputo (patch 6, sub-patch 3 to patches 1-5, sub-patch 2) and the foreign population travelling

to Mpumalanga from Maputo (patch 6, sub-patch 1 to patches 1-5, sub-patch 3) are subject to the FSAT campaign as the purpose of the campaign is to prevent infections from entering Mpumalanga. The FSAT model has an individual-based model structure so that individual characteristics of the participants may be taken into account. Figure 7.3 depicts the algorithm applied to individuals in the FSAT model. The flow of local and foreign populations from Maputo into Mpumalanga at each time step (week) is captured and geographical destination patch, the sub-patch and disease status (susceptible, infectious, sub-patent etc) are stored for each individual in that flow. The first step is to simulate a parasite count for each individual dependent on their disease status. The log-normal distribution was selected with distribution parameters in Table 7.2 as it captures the skewness of parasite count distribution. To test the impact of take-up proportion, the campaign is modelled as being optional. Should an individual not wish to be part of the campaign, their disease status is maintained and the simulation is stopped. Depending on the diagnostic tool used, the processing times and hence the number of tests able to be performed per week will differ. Should capacity be available and an individual agrees to participate in the campaign, the individual is screened. A positive screen occurs if the individual's simulated parasite load is greater than the detection threshold of the diagnostic tool in use. A positive screen will result in the individual being treated. As the treatment is likely to be a multiple-dose regimen, there is a chance that the individual may not adhere to the full course and may run the risk of failing treatment. In the event of successful treatment, the individual's disease status is updated (e.g. Infectious to "Infectious having received FSAT" where the individual is cured from malaria at a rate of recovery dependent on the parasite clearance time of the drug) and the simulation stops. The model parameters governing this IBM algorithm are displayed in Table 7.2.

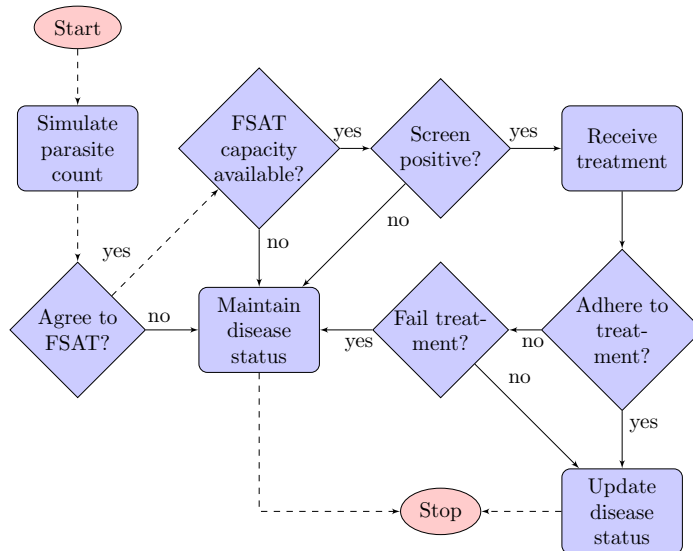


Figure 7.3: FSAT IBM algorithm

Table 7.2: Values, descriptions and sources of the parameters driving the FSAT Individual Based Model.

Parameter	Description	Value	Source
f_{son}	Focal Screen and Treat Switch	Binary	
cov	FSAT coverage	25; 50; 75; 100%	values to be tested
	Baseline FSAT coverage	70%	assumed
$f_{sprop}[t]$	Proportion Screened and Treated through Border Control	$f_{son} \times cov$	
opt	Take-up proportion for FSAT	25; 50; 75; 100%	values to be tested
adh	Probability of adherence	0.90	[8]
$fail$	Probability of treatment failure	0.01	[8]
rep	Number of screens tests performed simultaneously	3	assumed
μ_C	Geometric mean of log-normal parasite distribution for clinical infections	25000	[57, 149]
σ_C	Log standard deviation of log-normal parasite distribution for clinical infections	1.3	[57, 149]
μ_A	Geometric mean of log-normal parasite distribution for asymptomatic infections	1000	[123, 149]
σ_A	Log standard deviation of log-normal parasite distribution for asymptomatic infections	1.5	[123, 149]
μ_S	Geometric mean of log-normal parasite distribution for sub-patent infections	50	[91]
σ_S	Log standard deviation of log-normal parasite distribution for sub-patent infections	0.75	assumed

7.3.3 Hybrid metapopulation DE-IBM model

The metapopulation DE model and the IBM model are linked such that the IBM model is nested in the DE model. At each time step, the DE model generates flows of a population that leave one compartment and enter another compartment (in the various sub-patches and patches). The IBM model takes the flow value at each time step once it has been negated from a compartment, discretises it into individuals in a population, executes the IBM algorithm, re-groups the individuals back into a population flow, and adds the flow to its destination compartment. In this application, only the flows of local and foreign people entering the five Mpumalanga patches from Maputo are interrupted to perform FSAT using the IBM model. Further details on this hybrid modelling approach are available in the Additional File 3.

7.3.4 Data Fitting

The metapopulation transmission model is fitted to weekly case notification data from Mpumalanga and Maputo Province from 2002 to 2008, and then validated with data from 2009 to 2012. Ethical approval for use of this secondary data was obtained from the Mpumalanga Department of Health and the University of Cape Town Human Research Ethics Committee. The Mpumalanga case data displays a characteristic triple peaked pattern in the malaria season with peaks occurring in September/October, December/January and April/May while the Maputo Province malaria season exhibited peaks in December and April only [116]. The seasonal forcing functions, used to determine seasonal variation in transmission, for the six patches are derived from the data using Seasonal decomposition of Time series by LOESS (STL) methods for extracting time series components [22]. ACT drug therapy and the impact of IRS implemented between 2002 and 2008 are also included in the model. In order to reach a steady state the model is run deterministically from 1990 before being fitted to data from 2002. The model output (predicted weekly treated cases) is fitted to the data from 2002 to 2008 using the maximum likelihood approach by assuming an underlying Poisson distribution with rate λ as the number of treated cases per week. Several parameters as detailed in Table 7.1 are estimated through the data fitting process using the population-based global search algorithm of particle swarm optimisation [32, 64]. The model with the estimated parameter values is then validated with a further 3 years of data (2009 to 2012). A full description of the data fitting method is presented in Additional file 3. All model development, fitting and subsequent analysis was performed in R v3.02 [106]. The particle swarm optimisation routine was performed using the R package hydroPSO v0.3-3 [150, 151].

7.4 Results

The estimation of parameters through data fitting is presented first followed by the results of a simulated FSAT campaign at varied coverage levels, target levels and thresholds of detection.

7.4.1 Estimation of Parameters through data-fitting

Weekly case data for the five Mpumalanga patches and Maputo (black) along with the model output from the data-fitting process (red) and predicted model output for 2009 to 2012 (blue) is shown in Figure 7.4. Figure 7.4 is a summation of the data fitting results in each patch, as data was fitted to each sub-patch simultaneously. Both the peak and timing of the malaria season in Ehlanzeni District and Maputo Province are captured well by the model prediction and the uncertainty range. Additional file 3 contains more detailed output from the data-fitting procedure. The parameters estimated through data-fitting and other parameters driving

the transmission model are presented in Table 7.1. There are two rates each for the foreign treatment proportion and the rate of foreign movement. This is due to the waiver of short stay visa requirements between Mozambique and South Africa in April 2005, resulting in increased cross-border movement [97]. Very little data exists on the duration of asymptomatic and sub-patent infections; hence the need to estimate these parameters from the data-fitting process.

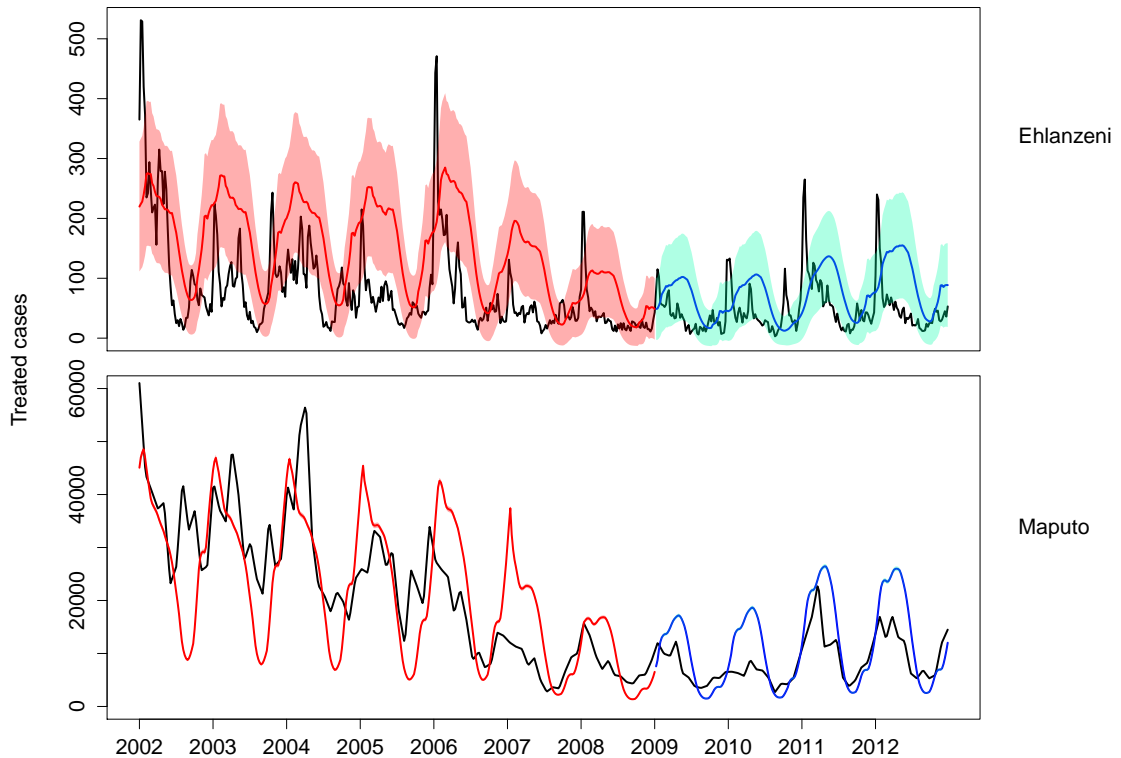


Figure 7.4: Predicted weekly treated cases (blue: 2002 - 2008; red: 2009-2012) fitted to and validated with data (black). The 95% uncertainty range for weekly case predictions is shown.

7.4.2 Simulated FSAT

The predicted impact of an FSAT campaign at the Mpumalanga-Maputo border is presented below with respect to coverage levels, thresholds of detection, take-up proportions, target levels and typical diagnostic tools. To facilitate accurate comparison of coverage levels, targets, thresholds and diagnostic tools, the take-up proportion of FSAT is assumed to be 100%. The impact of a less than 100% take-up proportion is also explored. The FSAT campaign is assumed to run for eight hours a day, seven days a week with a maximum of three tests being conducted simultane-

ously. This number of simultaneous tests is also considered at different levels in the simulation. As malaria elimination is defined by the World Health Organisation as zero incidence of locally contracted cases, the impact of the simulated FSAT campaign is measured as the decrease in local infections as result of the campaign [80]. This impact is a function of the change in onward transmission resulting from fewer imported infections entering Mpumalanga (due to FSAT). All results are compared to the base case of no FSAT, depicted in black in all figures. Each scenario was run 100 times so that results presented are the mean local infections per week with a 95% confidence interval shaded around the mean. In many cases, the shading is not visible due to either narrow confidence intervals or a low resolution y-axis.

Diagnostic tools

Diagnosing malaria at a border point ideally requires a diagnostic tool that is both sensitive, specific and has a short processing time. Several tools have been considered for this simulation (Table 7.3). The Rapid Diagnostic Test (RDT) currently in use at South African public health facilities has a theoretical detection threshold of 200 parasites/ μL and a maximum processing time of 20 minutes. Microscopy in experienced hands may exhibit a sensitivity of 50 parasites/ μL but is more likely to have a sensitivity in the region of 100 parasites/ μL . Real-time quantitative polymerase chain reaction (qPCR) and Loop-mediated isothermal DNA Amplification (LAMP) are very sensitive tools with qPCR needing sophisticated equipment for a processing time of three hours. LAMP on the other hand is a less complex technique with a one hour processing time [47]. These diagnostic tools are also compared to a highly sensitive hypothetical RDT with a standard process time of 20 minutes and a detection threshold of 5 parasites/ μL .

Table 7.3: Descriptions of diagnostic tools used in FSAT model

Tool	Detection Threshold	Process Time	Target per week (tests per/hr \times 3 reps \times 8 hrs \times 7 days)	Source
RDT	200 parasites/ μL	0.33 hours	504 tests	[47]
Microscopy	100 parasites/ μL	2.25 hours	75 tests	Expert opinion, [47]
qPCR	1 parasites/ μL	3 hours	63 tests	[47]
LAMP	5 parasites/ μL	1 hour	168 tests	[59, 104]
Hypothetical RDT	5 parasites/ μL	0.33 hours	504 tests	

The model predicts that at a baseline FSAT coverage of 70%, microscopy and qPCR do not substantially decrease local infections due to their long processing time (Figure 7.5). LAMP is predicted to lead to a larger decrease in local infections though this decrease is small in comparison to that predicted for the RDT with a detection threshold of 200 parasites/ μL . While LAMP is more likely to detect asymptomatic and sub-patent infections than the RDT, the three times longer turnaround time results in only a third of the tests being performed compared to

the RDT. The hypothetical RDT that is as sensitive as LAMP is predicted to perform the best as it combines a high sensitivity with a short processing time.

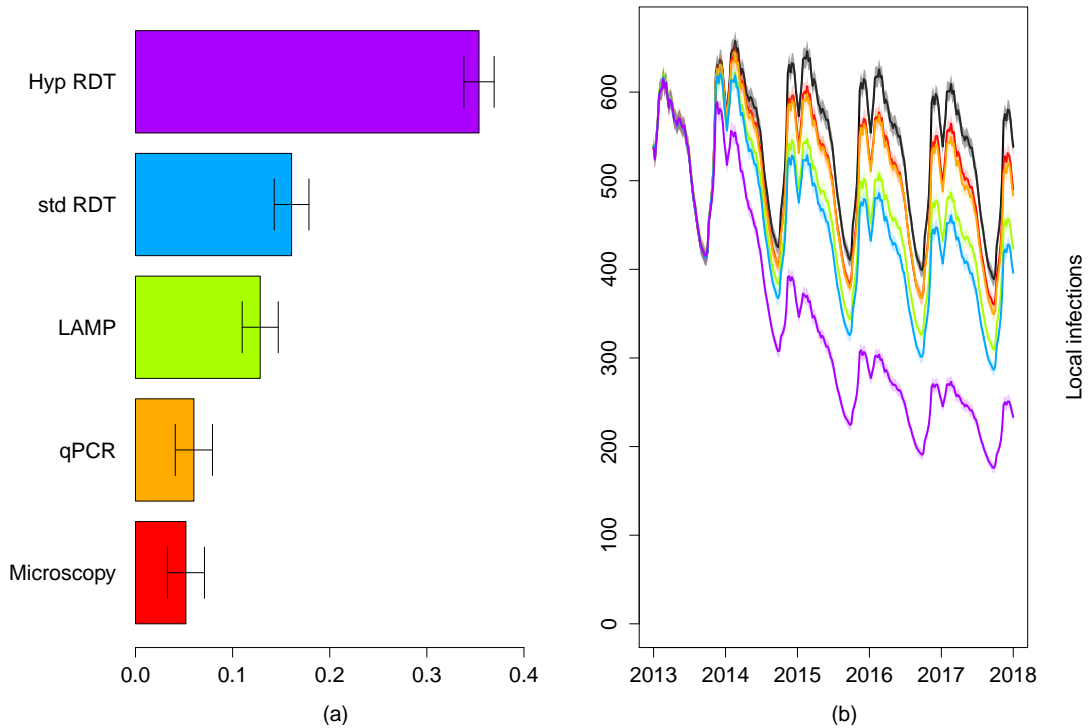


Figure 7.5: Predicted impact due to FSAT between 2014 and 2018 using the following diagnostic tools: microscopy (red), qPCR (orange), LAMP (green), RDT (blue) and a hypothetical RDT (purple). (a) shows the percentage decrease in local infections due to the FSAT and (b) shows the impact of FSAT on local infections in Ehlanzeni district through time compared to the base case of no interventions (black).

Coverage, detection thresholds, take-up proportions and target levels

Coverage levels refer to the proportion of cross-border movements reached by the FSAT campaign. This proportion is generally less than 100% to account for other forms of entry into the province e.g. illegal entry. FSAT at various coverage levels is simulated using the characteristics of the RDT currently in use in South Africa (theoretical detection threshold of 200 parasites/ μL and a process time of 20 minutes). Figure 7.6(1) shows that even at 25% coverage, a substantial decrease in local infections is predicted. The marginal impact on local infections decreases to the point where local infections at 75% and 100% FSAT coverage are non-distinguishable with overlapping confidence intervals for the expected decrease in local infections. This occurs because though coverage may be very high, infections with less than 200 parasites/ μL will remain



Figure 7.6: Predicted impact due to FSAT between 2014 and 2018. (a) shows the percentage decrease in local infections due to the FSAT and (b) shows the impact of FSAT on local infections in Ehlanzeni district through time compared to the base case of no interventions (black). The impact of FSAT is predicted for different (1) coverage proportions, (2) thresholds of detections for the diagnostic tool used (parasites / μ L), (3) take-up proportions, (4) coverage proportions for Mass Drug Administration and (5) weekly targets (capacity) keeping all other variables constant. 95% Confidence Intervals are depicted for the average percentage decrease.

undetected by a standard RDT. In simulating the impact of detection thresholds alone, coverage is kept at its baseline value of 70%. Figure 7.6(2) shows that the predicted impact on local infections of using an RDT at any threshold is substantial. The greatest decrease in local infections is predicted with the most sensitive RDT. The impact of take-up proportion is such that a low proportion of only 25% does not substantially decrease local infections compared to the extreme of 100% take-up i.e. mandatory participation (Figure 7.6(3)). The local infections predicted by mandatory participation may be further decreased if a more sensitive tool was used, or coverage was higher. If mandatory participation is a viable option, a government could consider a Mass Drug Administration instead of FSAT. Figure 7.6(4) suggests that at even 50% coverage, the impact of MDA is higher than FSAT at 100% coverage as sub-patent infections are being captured by the intervention. A baseline assumption is that three screenings may be performed simultaneously. If this capacity is increased, the number of tests that may be performed per week will also increase. Comparing different weekly target levels suggests that any target below 250 people is not predicted to substantially decrease local infections (Figure 7.6(5)).

7.5 Discussion

In the last decade, a policy shift to ACTs, source reduction through the LSDI malaria programme and a strong IRS strategy have contributed to decreasing malaria prevalence in Mpumalanga to the low levels experienced today. In shifting focus from control to elimination, the goal to interrupt transmission and prevent its reestablishment implies that a "more of the same" approach will not work [89]. The early termination of the LSDI programme and the associated subsequent rise in cases in Maputo Province and Mpumalanga demonstrate the importance of regional collaboration and urgency to collaborate further. Chapter 6 assessed the impact of source reduction in Maputo on malaria incidence in Mpumalanga using a metapopulation model of transmission. That model predicted that the largest decrease in local infections was achieved when source reduction interventions were simulated. Of the three ideal elements of an elimination strategy highlighted in the introduction of this paper, the prevention of imported infections is not addressed by a strong IRS focus as IRS will limit onward transmission of all infections but is not targeted at imported infections. The implementation of FSAT at the border is one strategy to inhibit the inflow of local and foreign individuals with malaria infections sourced elsewhere. Successful implementation of this strategy requires among other things, decisions on when to conduct the campaign, the choice of diagnostic tool and drug and the level of resources and man-power available. Model 2 in Chapter 6 predicts that FSAT conducted at the Mpumalanga-Maputo border over the peak of the season only is not as effective in decreasing local infections because imported infections resume previous high levels as soon as FSAT is stopped. Sustained decreases were predicted when FSAT was conducted at the border throughout the year.

The choice of diagnostic tool is a critical one for several reasons. Firstly, the tool should be highly

sensitive to effectively screen and treat all infections. If a tool with a low to medium sensitivity is used, it is likely that sub-patent infections will be missed by FSAT and enter Mpumalanga to contribute to infectious reservoir and thus to onward transmission. Okell *et al.* estimated that in very low prevalence settings, sub-patent infections comprise 70-80% of all malaria infections and are responsible for 20-50% of all human-to-mosquito infections [98]. Without addressing these sub-patent infections, it is likely that these low density infections will sustain malaria transmission [91]. Secondly, the diagnostic tool should take into account existing man-power and resources. Some tools such as qPCR require specialised equipment and highly trained operators while other tools like RDTs and LAMP have protocols that require minimal instrumentation and expertise [47]. Thirdly, the processing time of the tools will directly impact the usefulness of the tool in FSAT. Tools with long turnaround times are not feasible as it is unlikely that travellers would be willing to wait at a border-post for a result that takes a long time to process. In simulating the choice of diagnostic tool, the model predicted that microscopy and qPCR, though more sensitive than RDTs performed worse than LAMP and RDTs owing to the long processing times. LAMP may be an ideal tool for FSAT when the population of interest is able to wait for an hour to receive results, but this is most likely not the case for individuals passing through a border-post. The best performing tool was predicted to be a hypothetical RDT that had the standard processing time of 20 minutes with the sensitivity of LAMP. Modelling this hypothetical tool resulting in a capacity of 504 tests per week. The same target would be reached if increased resources resulted in nine LAMP tests being performed simultaneously instead of the baseline three tests.

From a provider perspective, the success of a FSAT strategy depends critically on the allocated capital and labour resources. Resources will influence the length of the FSAT campaign, the choice of tool and the labour assigned to the execution of the campaign. The model has predicted that processing a small proportion of individuals passing through the border results in small decreases in local infection. To optimise the impact of a FSAT campaign, the choice of tool and labour assigned to implement the tool should together seek to maximise the number of tests possible. From a participant perspective, the success of a FSAT campaign depends on the willingness to participate in the campaign and after a positive test result, the adherence of the participant to complete the drug regimen. The first line of malaria treatment in South Africa is a three day regimen of artemether-lumefantrine where only the first dose is supervised [93]. The issue of drug adherence may only be addressed adequately when a single dose cure of malaria is available. The model predicts that a high willingness to participate results in substantially larger decreases in local infections. One method to guarantee participation is to make the FSAT campaign mandatory. This approach would most likely require extensive resources to cope with the workload and enable efficient passing through the border, but may also be against the ethos of the South African and Mozambican governments. Yet even with mandatory FSAT, sub-patent infections may be missed depending on the screening tool employed. On the other hand, the model predicted that MDA at a low coverage in place of FSAT leads to large decreases in local

infections as low sensitivity of screening tools is no longer an issue. Given recent estimates that 70-80% of all infections in a low transmission setting are sub-patent, MDA at the border becomes a suitable intervention [98]. An alternative way to view MDA at border entry points, is mandatory prophylaxis for travellers. Many countries require proof of vaccinations against yellow fever, typhoid, influenza and other diseases and infections. Proof of recent malaria prophylaxis can then effectively become a "lower cost" mass drug administration campaign for all travellers (local and foreign) entering a malaria-endemic country. If this becomes policy, the MDA campaign is effectively extended to all ports of entry into a country, not just the few selected for a traditional MDA/FSAT campaign.

The model has predicted that the various scenarios of FSAT considered in this paper will not eliminate malaria. This is in line with findings from Silal *et al* and Chapter 6 [117]. Von Seidlein [140] lists both the inability of FSAT to detect and treat all infections (using RDTs), and hence the inability to prevent reinfection as reasons why screening and treating failed in trials conducted at a school level [52]. These studies all suggest that as long as the reservoir of sub-patent infections endures, FSAT on its own will not be able to eliminate malaria. The model has predicted through various scenarios of FSAT that it may still be successful in reducing local malaria incidence, even if it cannot reduce it to zero. In this manner, FSAT may still form part of an integrated elimination strategy where a variety of interventions are employed together to achieve malaria elimination. This paper presented a hybrid DE-IBM model where a metapopulation level, non-linear stochastic ordinary differential equation model was used to simulate malaria transmission in Mpumalanga and Maputo so that Individual-Based Modelling techniques may be used to predict the impact of FSAT at the Mpumalanga-Maputo border. Future work includes adding an economic cost component to the FSAT IBM model in an attempt to optimise the impact on local infections based on a suite of potential diagnostic tools and the resources required to implement them.

7.6 Conclusion

Malaria incidence and related mortality has declined since 2002 to a point where South Africa is in the pre-elimination phase (< 5 cases per 1000 people). In this time the proportion of annual imported cases has increased from 39% in 2002 to 87% in 2012. The reduction of imported cases will be vital to any future malaria control or elimination strategy. Mathematical modelling has been used in this paper to estimate the impact of FSAT at a border control point under a variety of scenarios, as a means to reduce the inflow of imported infections in an environment where imported cases far exceed local cases. In this manner, mathematical modelling of FSAT may be used to inform a strategy with a strong regional focus aimed at interrupting local transmission so that malaria elimination may one day become a reality.

7.7 Additional File 3: Mathematical Model Description

7.7.1 Summary Equations: Metapopulation Model of Transmission

The model presented in this paper is based on a model described in Chapter 6. The model comprises six patches; five to represent Mpumalanga municipalities, and one for Maputo province, Mozambique. Each patch comprises three sub-patches: (1) the local population of patch i currently in patch i , (2) the local population of patch i having returned from travel to a foreign place (Maputo, if the patch is South African and vice versa) and (3) the population from the foreign place currently in patch i . A malaria transmission model is developed for each sub-patch where the sub-patch population is divided into six compartments representing the population susceptible to malaria (S), the population at the infectious stage that receives treatment (I), the untreated symptomatic population at the infectious stage (C), the untreated asymptomatic population at the infectious stage (A), the untreated asymptomatic, sub-patent (< 100 parasites/ μ L) infectious population (M) and the population susceptible to malaria, but with prior asymptomatic infection (P). The liver and blood stage of the infection is incorporated as a delay in the flow between the susceptible and infectious stage compartments.

Descriptions of the compartments and parameters governing the flows between compartments are provided in Tables 7.4 and 7.5 respectively. This model structure differs from that presented in Chapter 6 in two ways. Firstly, given that the purpose of this paper is to predict the impact of FSAT, it is necessary to model infectious stage infections in more detail. The sensitivity of diagnostic screening tools is such that sub-patent infections, i.e. infections with a low parasite count, may often be missed. These infections then remain untreated and continue to contribute to the infectious reservoir in the area. For this reason, the untreated infectious stage compartment in Chapter 6 is decomposed into the C, A and M compartments described earlier. Secondly, the blood stage of infection is incorporated as a delay in the flow between the susceptible and infectious stage compartments in order to simplify the model structure given the addition of asymptomatic and sub-patent infection compartments. Chapter 4 describes the sensitivity of predictions to model structure and shows that this sensitivity is reduced substantially if the models are fitted to data. Given that this model and the one presented in Chapter 6 are fitted to data, the change in model structure is justified.

The force of infection $\lambda_i[t]$ for each patch i is a function of the level of vector control, the annual number of mosquito bites per person \times proportion of bites testing positive for sporozoites for patch i (β_i) and the proportion of infectiousness in the population lagged to reflect the infectiousness proportion at the time the mosquito was infected.

$$\lambda_i[t] = (1 - vc_i[t] * vef)\beta_i \times \frac{\sum_{k=1}^3 (I_{i,k}[t-4] + C_{i,k}[t-4] + A_{i,k}[t-4] + M_{i,k}[t-4])}{N_i[t-4]}.$$

Population migration between the different patches is characterised by three sets of movements: These movements have been reported in Chapter 6, but are reported here again for the sake of completion.

1. Movement may occur between any two of the the five Mpumalanga patches i and j at a rate $\frac{1}{\kappa_{i,j}}$ where

$$\begin{aligned} \frac{1}{\kappa_{i,j}} &= \frac{1}{k} \times \frac{\frac{1}{(1+\sqrt{(x_i-x_j)^2+(y_i-y_j)^2})^{lwg t}}}{\sum_{i=1}^5 \frac{1}{(1+\sqrt{(x_i-x_j)^2+(y_i-y_j)^2})^{lwg t}}} && \text{if } i, j = 1, 2, 3, 4, 5 \text{ \& } i \neq j \\ &= 0 && \text{if } i \text{ or } j = 6 \text{ (local movement only)} \\ \frac{1}{\kappa_{i,j}} &= \frac{1}{\kappa_{j,i}} \end{aligned}$$

where (x_i, y_i) and (x_j, y_j) are the centroid coordinates for patches i and j respectively. This movement is weighted inversely by distance so that movement between South African patches that are closer together occurs at a higher rate than those further apart.

2. Movement may occur when South African citizens cross the border into Maputo (from patch $i = 1 - 5$ in sub-patch 1 to patch 6 in sub-patch 3) and return (patch 6 in sub-patch 3 to patch $i = 1 - 5$ in sub-patch 2) at a rate of $\frac{1}{\zeta_{i,6}}$ where

$$\begin{aligned} \frac{1}{\zeta_{i,6}} &= \frac{1}{z} \times \frac{\frac{1}{(1+\sqrt{(x_i-x_6)^2+(y_i-y_6)^2})^{fwg t}}}{\sum_{i=1}^5 \frac{1}{(1+\sqrt{(x_i-x_6)^2+(y_i-y_6)^2})^{fwg t}}} && \text{if } i = 1, 2, 3, 4, 5 \\ &= 0 && \text{otherwise} \\ \frac{1}{\zeta_{i,6}} &= \frac{1}{\zeta_{6,i}} \end{aligned}$$

where (x_i, y_i) and (x_6, y_6) are the centroid coordinates for patches i and 6 respectively. This movement is weighted inversely by distance so that movement between the South African patches and Maputo that are closer together occurs at a higher rate than those further apart.

3. Movement may also occur when Mozambican citizens cross the border into Mpumalanga (from patch 6 in sub-patch 1 to patch $j = 1 - 5$ in sub-patch 3) and return (patch $j = 1 - 5$

in sub-patch 3 to patch 6 in sub-patch 2) at a rate of $\frac{1}{\varpi_{6,j}}$ where

$$\begin{aligned} \frac{1}{\varpi_{6,j}} &= \frac{1}{v_{yr}} \times \frac{1}{\sum_{i=1}^5 \frac{1}{(1+\sqrt{(x_6-x_j)^2+(y_6-y_j)^2})^{f_w g t}}} && \text{if } j = 1, 2, 3, 4, 5 \text{ \& } yr = 1, 2 \\ &= 0 && \text{otherwise} \\ \frac{1}{\varpi_{6,j}} &= \frac{1}{\varpi_{j,6}} \end{aligned}$$

where (x_6, y_6) and (x_j, y_j) are the centroid coordinates for patches 6 and j respectively. This movement is weighted inversely by distance so that movement between the South African patches and Maputo that are closer together occurs at a higher rate than those further apart.

This leads to the following set of differential equations.

Sub-patch 1 (Local population): For each patch i with population movement (local or foreign) to patch j ($i, j \in \{1, 2, \dots, 6\}, j \neq i$):

$$\begin{aligned} \frac{dS_{i,1}}{dt} &= \underbrace{\mu N_i}_{(1)} - \underbrace{\lambda_i[t - \sigma]seas_i[t]S_{i,1}}_{(2)} + \underbrace{\frac{1}{r + \tau}I_{i,1}}_{(3)} + \underbrace{\frac{1}{\rho}P_{i,1}}_{(4)} + \underbrace{\frac{1}{\alpha}S_{i,2}}_{(5)} + \underbrace{\sum_j \frac{1}{\kappa_{i,j}}(S_{j,1} - S_{i,1})}_{(6)} - \underbrace{\frac{1}{\varpi_{i,j}}S_{i,1}}_{(7)} - \underbrace{\frac{1}{\zeta_{i,6}}S_{i,1}}_{(8)} - \underbrace{\mu S_{i,1}}_{(9)} \\ \frac{dI_{i,1}}{dt} &= \underbrace{p\lambda_i[t - \sigma]seas_i[t](S_{i,1} + S_{i,2})}_{(10)} + \underbrace{p\lambda_i[t - \sigma]seas_i[t](P_{i,1} + P_{i,2})}_{(11)} - \frac{1}{r + \tau}I_{i,1} + \frac{1}{\alpha}I_{i,2} + \sum_j \frac{1}{\kappa_{i,j}}(I_{j,1} - I_{i,1}) \\ &\quad - \frac{1}{\varpi_{i,j}}I_{i,1} - \frac{1}{\zeta_{i,6}}I_{i,1} - \mu I_{i,1} \\ \frac{dC_{i,1}}{dt} &= \underbrace{pc_1(1 - p)\lambda_i[t - \sigma]seas_i[t](S_{i,1} + S_{i,2})}_{(12)} + \underbrace{pc_2(1 - p)\lambda_i[t - \sigma]seas_i[t](P_{i,1} + P_{i,2})}_{(13)} - \underbrace{\frac{1}{i_1}C_{i,1}}_{(14)} + \frac{1}{\alpha}C_{i,2} + \\ &\quad \sum_j \frac{1}{\kappa_{i,j}}(C_{j,1} - C_{i,1}) - \frac{1}{\varpi_{i,j}}C_{i,1} - \frac{1}{\zeta_{i,6}}C_{i,1} - \mu C_{i,1} \\ \frac{dA_{i,1}}{dt} &= \underbrace{(1 - pc_1)(1 - p)\lambda_i[t - \sigma]seas_i[t](S_{i,1} + S_{i,2})}_{(15)} + \underbrace{(1 - pc_2)(1 - p)\lambda_i[t - \sigma]seas_i[t](P_{i,1} + P_{i,2})}_{(16)} + \frac{1}{i_1}C_{i,1} \\ &\quad - \underbrace{\frac{1}{i_2}A_{i,1} + \frac{1}{\alpha}A_{i,2}}_{(17)} + \sum_j \frac{1}{\kappa_{i,j}}(A_{j,1} - A_{i,1}) - \frac{1}{\varpi_{i,j}}A_{i,1} - \frac{1}{\zeta_{i,6}}A_{i,1} - \mu A_{i,1} \\ \frac{dM_{i,1}}{dt} &= \frac{1}{i_2}A_{i,1} - \frac{1}{i_3}M_{i,1} + \frac{1}{\alpha}M_{i,2} + \sum_j \frac{1}{\kappa_{i,j}}(M_{j,1} - M_{i,1}) - \frac{1}{\varpi_{i,j}}M_{i,1} - \frac{1}{\zeta_{i,6}}M_{i,1} - \mu M_{i,1} \end{aligned}$$

$$\begin{aligned} \frac{dP_{i,1}}{dt} = & \underbrace{\frac{1}{i_3} M_{i,1} - \lambda_i [t - \sigma] seas_i [t] (P_{i,1} + P_{i,2})}_{(18)} - \frac{1}{\rho} P_{i,1} + \frac{1}{\alpha} P_{i,2} + \sum_j \frac{1}{\kappa_{i,j}} (P_{j,1} - P_{i,1}) - \frac{1}{\varpi_{i,j}} P_{i,1} \\ & - \frac{1}{\zeta_{i,6}} P_{i,1} - \mu P_{i,1} \end{aligned}$$

- (1) Births in patch i
- (2) Local incidence arising from sub-patch 1
- (3) Recovery of treated infectious stage infections at a rate dependent on the time to seek treatment and the time to recovery
- (4) Return to full susceptibility at a rate determined by the duration of clinical immunity
- (5) Assimilation of population in sub-patch 2 (locals having returned from foreign travel) back into sub-patch 1 from whence they originated.
- (6) Movement between local patches (1-5) out of and into the compartment
- (7) Movement of local patch i population to foreign patch j when i=6 and j = 1-5; =0 for all other values of i as this rate is particular to movement of Maputo population (patch 6)
- (8) Movement of local patch i population to foreign patch 6 when i=1-5; =0 for i=6 as this rate is particular to movement of the Mpumalanga population to and from Maputo (patches 1-5)
- (9) Deaths in patch i from this compartment
- (10) New infections destined to be treated having arisen from susceptible populations in sub-patch 1 (local population) and sub-patch 2 (local population having returned from foreign travel) as these are infections due to local transmission.
- (11) New infections destined to be treated having arisen from susceptible population with prior asymptomatic infection in sub-patches 1 and 2
- (12) New clinical infections destined to remain untreated having arisen from susceptible populations in sub-patches 1 and 2
- (13) New clinical infections destined to remain untreated having arisen from susceptible population with prior asymptomatic infection in sub-patches 1 and 2
- (14) Development of clinical untreated infections to asymptomatic infections at a rate dependent on the duration of clinical untreated infections
- (15) New asymptomatic infections destined to remain untreated having arisen from susceptible populations in sub-patches 1 and 2
- (16) New asymptomatic infections destined to remain untreated having arisen from susceptible population with prior asymptomatic infection in sub-patches 1 and 2
- (17) Development of asymptomatic to sub-patent infections at a rate dependent on the duration of asymptomatic infections
- (18) Recovery of sub-patent infections at a rate dependent on the duration of sub-patent infections

Sub-patch 2 (Local population returning from foreign travel) : For each patch i moving to patch j ($i, j \in \{1, 2, \dots, 6\}, j \neq i$)

$$\begin{aligned}
 \frac{dS_{i,2}}{dt} &= - \underbrace{\lambda_i[t - \sigma]seas_i[t]S_{i,2}}_{(19)} + \frac{1}{r + \tau}I_{i,2} + \frac{1}{\rho}P_{i,2} - \underbrace{\frac{1}{\alpha}S_{i,2}}_{(20)} + \underbrace{\sum_j \frac{1}{\kappa_{i,j}}(S_{j,2} - S_{i,2})}_{(21)} \\
 &\quad + \underbrace{\sum_j \frac{1}{\varpi_{i,j}}S_{j,3}}_{(22)} + \underbrace{\frac{1}{\zeta_{i,6}}S_{6,3}}_{(23)} - \mu S_{i,2} \\
 \frac{dI_{i,2}}{dt} &= -\frac{1}{r + \tau}I_{i,2} - \frac{1}{\alpha}I_{i,2} + \sum_j \frac{1}{\kappa_{i,j}}(I_{j,2} - I_{i,2}) + \sum_j \frac{1}{\varpi_{i,j}}I_{j,3} + \frac{1}{\zeta_{i,6}}I_{j,3} - \mu I_{i,2} \\
 \frac{dC_{i,2}}{dt} &= -\frac{1}{i_1}C_{i,2} - \frac{1}{\alpha}C_{i,2} + \sum_j \frac{1}{\kappa_{i,j}}(C_{j,2} - C_{i,2}) + \sum_j \frac{1}{\varpi_{i,j}}C_{j,3} + \frac{1}{\zeta_{i,6}}C_{j,3} - \mu C_{i,2} \\
 \frac{dA_{i,2}}{dt} &= \frac{1}{i_1}I_{i,2} - \frac{1}{i_2}A_{i,2} - \frac{1}{\alpha}A_{i,2} + \sum_j \frac{1}{\kappa_{i,j}}(A_{j,2} - A_{i,2}) + \sum_j \frac{1}{\varpi_{i,j}}A_{j,3} + \frac{1}{\zeta_{i,6}}A_{j,3} - \mu A_{i,2} \\
 \frac{dM_{i,2}}{dt} &= \frac{1}{i_2}A_{i,2} - \frac{1}{i_3}M_{i,2} - \frac{1}{\alpha}M_{i,2} + \sum_j \frac{1}{\kappa_{i,j}}(M_{j,2} - M_{i,2}) + \sum_j \frac{1}{\varpi_{i,j}}M_{j,3} + \frac{1}{\zeta_{i,6}}M_{j,3} - \mu M_{i,2} \\
 \frac{dP_{i,2}}{dt} &= \frac{1}{i_3}M_{i,2} - \underbrace{\lambda_i[t - \sigma]seas_i[t](P_{i,2} + P_{i,2})}_{(24)} - \frac{1}{\rho}P_{i,2} - \frac{1}{\alpha}P_{i,2} + \sum_j \frac{1}{\kappa_{i,j}}(P_{j,2} - P_{i,2}) + \sum_j \frac{1}{\varpi_{i,j}}P_{j,3} \\
 &\quad + \frac{1}{\zeta_{i,6}}P_{j,3} - \mu P_{i,2}
 \end{aligned}$$

- (19) New infections arising from sub-patch 2 due to local transmission and not infections contracted while travelling
- (20) Assimilation of population in sub-patch 2 (locals having returned from foreign travel) back into sub-patch 1 from whence they originated.
- (21) Movement between local patches (1-5) out of and into the compartment
- (22) Movement of patch 6 population from foreign patch j, sub-patch 3 back into patch i but in sub-patch 2, when $i=6$ and $j = 1-5$; $=0$ for all other values of i as this rate is particular to movement of Maputo population (patch 6)
- (23) Movement of patch i population from foreign patch 6 sub-patch 3 back into patch i , sub-patch 2, when $i=1-5$; $=0$ for $j=6$ as this rate is particular to movement of the Mpumalanga population to and from Maputo (patches 1-5)
- (24) New infections arising from the susceptible population with a prior asymptomatic infection in sub-patch 2

Sub-patch 3 (Foreign population) : For each patch i moving to patch j ($i, j \in \{1, 2, \dots, 6\}, j \neq i$)

$$\begin{aligned}
 \frac{dS_{i,3}}{dt} &= - \underbrace{\lambda_i[t - \sigma]seas_i[t]S_{i,3}}_{(25)} + \frac{1}{r + \tau}I_{i,3} + \frac{1}{\rho}P_{i,3} + \underbrace{\sum_j \frac{1}{\kappa_{i,j}}(S_{j,3} - S_{i,3})}_{(26)} + \underbrace{\frac{1}{\varpi_{i,j}}(S_{j,1} - S_{i,3})}_{(27)} \\
 &+ \underbrace{\sum_j \frac{1}{\zeta_{i,j}}(S_{j,1} - S_{i,3})}_{(28)} - \mu S_{i,3} \\
 \frac{dI_{i,3}}{dt} &= \underbrace{pf_{yr}\lambda_i[t - \sigma]seas_i[t]S_{i,3}}_{(29)} + \underbrace{pf_{yr}\lambda_i[t - \sigma]seas_i[t]P_{i,3}}_{(30)} - \frac{1}{r + \tau}I_{i,3} + \sum_j \frac{1}{\kappa_{i,j}}(I_{j,3} - I_{i,3}) + \\
 &\frac{1}{\varpi_{i,j}}(I_{j,1} - I_{i,3}) + \sum_j \frac{1}{\zeta_{i,j}}(I_{j,1} - I_{i,3}) - \mu I_{i,3} \\
 \frac{dC_{i,3}}{dt} &= \underbrace{pc_1(1 - pf_{yr})\lambda_i[t - \sigma]seas_i[t]S_{i,3}}_{(31)} + \underbrace{pc_2(1 - pf_{yr})\lambda_i[t - \sigma]seas_i[t]P_{i,3}}_{(32)} - \frac{1}{i_1}C_{i,3} \\
 &+ \sum_j \frac{1}{\kappa_{i,j}}(C_{j,3} - C_{i,3}) + \frac{1}{\varpi_{i,j}}(C_{j,1} - C_{i,3}) + \sum_j \frac{1}{\zeta_{i,j}}(C_{j,1} - C_{i,3}) - \mu C_{i,3} \\
 \frac{dA_{i,3}}{dt} &= \underbrace{(1 - pc_1)(1 - pf_{yr})\lambda_i[t - \sigma]seas_i[t]S_{i,3}}_{(33)} + \underbrace{(1 - pc_2)(1 - pf_{yr})\lambda_i[t - \sigma]seas_i[t]P_{i,3}}_{(34)} + \frac{1}{i_1}C_{i,3} - \frac{1}{i_2}A_{i,3} \\
 &+ \sum_j \frac{1}{\kappa_{i,j}}(A_{j,3} - A_{i,3}) + \frac{1}{\varpi_{i,j}}(A_{j,1} - A_{i,3}) + \sum_j \frac{1}{\zeta_{i,j}}(A_{j,1} - A_{i,3}) - \mu A_{i,3} \\
 \frac{dM_{i,3}}{dt} &= \frac{1}{i_2}A_{i,3} - \frac{1}{i_3}M_{i,3} + \sum_j \frac{1}{\kappa_{i,j}}(M_{j,3} - M_{i,3}) + \frac{1}{\varpi_{i,j}}(M_{j,1} - M_{i,3}) + \sum_j \frac{1}{\zeta_{i,j}}(M_{j,1} - M_{i,3}) - \mu M_{i,3} \\
 \frac{dP_{i,3}}{dt} &= \frac{1}{i_3}M_{i,3} - \underbrace{\lambda_i[t - \sigma]seas_i[t]P_{i,3}}_{(35)} - \frac{1}{\rho}P_{i,3} + \sum_j \frac{1}{\kappa_{i,j}}(P_{j,3} - P_{i,3}) + \frac{1}{\varpi_{i,j}}(P_{j,1} - P_{i,3}) \\
 &+ \sum_j \frac{1}{\zeta_{i,j}}(P_{j,1} - P_{i,3}) - \mu P_{i,3}
 \end{aligned}$$

(25) New infections arising from sub-patch 3 due to local transmission and not infections contracted from patch of origin

(26) Movement between local patches (1-5) out of and into the compartment

(27) Movement of patch 6 population from patch 6, sub-patch 1 into patch i , sub-patch 3, when $i=1-5$ and $j = 6$ and movement from patch i , sub-patch 3 back into to patch 6, sub-patch 2. This rate =0 for all other values of j as it is particular to movement of Maputo population (patch 6)

(28) Movement of patch j population from patch j , sub-patch 1, into patch 6 sub-patch 3 when $i=6$ and $j=1-5$ and movement from patch 6, sub-patch 3 back into patch j , sub-patch 2 ; This rate=0

for $j=6$ as it is particular to movement of the Mpumalanga population (patches 1-5) to and from Maputo

- (29) New infections destined to be treated having arisen from susceptible population in sub-patch 3
- (30) New infections destined to be treated having arisen from susceptible population with prior asymptomatic infection in sub-patches 3
- (31) New clinical infections destined to remain untreated having arisen from susceptible population in sub-patch 3
- (32) New clinical infections destined to remain untreated having arisen from susceptible population with prior asymptomatic infection in sub-patch 3
- (33) New asymptomatic infections destined to remain untreated having arisen from susceptible population in sub-patch 3
- (34) New asymptomatic infections destined to remain untreated having arisen from susceptible population with prior asymptomatic infection in sub-patch 3
- (35) New infections arising from the susceptible population with a prior asymptomatic infection in sub-patch 3

Table 7.4: Compartment Descriptions

Compartment	Description
$S_{i,k}$	Susceptible Population in patch i and sub-patch k
$I_{i,k}$	Infectious Treated Population in patch i and sub-patch k
$C_{i,k}$	Symptomatic Infectious Untreated Population in patch i and sub-patch k
$A_{i,k}$	Asymptomatic Infectious Untreated Population in patch i and sub-patch k
$M_{i,k}$	Infectious Population with Untreated Sub-patent Infectious in patch i and sub-patch k
$P_{i,k}$	Susceptible Population with prior asymptomatic infection in patch i and sub-patch k

Table 7.5: Values, descriptions and sources of the parameters driving the base metapopulation model of transmission. ($i = \{TC; MB; UJ; NK; BB; MP\}$)

Parameter	Description	Value	Source
N	Population size	4×10^6	[125]
μ	Mortality/birth Rate	$\frac{105}{10000}$	[90]
σ	Period between liver stage and onset of gametocytemia	2 weeks	[19, 25, 33, 134]
r	Artemether Lumefantrine elimination half-life	6 days	[77]
τ	Time to seek treatment	1/2 week	Expert opinion
ptf	Probability of treatment failure	0.01	[8]

p	Proportion of local infected population receiving treatment	0.95	[18, 58]
pf_{yr}	Proportion of foreign infected population that receive treatment in a local patch	$pf_1 = 0.6797$ (0.6795, 0.6800) (pre April 2005) $pf_2 = 0.6750$ (0.6742, 0.6758) (post April 2005)	Estimated from model fitting process
i_1	Duration of clinical infection before becoming asymptomatic	2.776 (2.688, 2.866) weeks	Estimated from model fitting process
i_2	Duration of asymptomatic infection before becoming sub-patent	11.063 (11.011, 11.114) weeks	Estimated from model fitting process
i_3	Duration of sub-patent infection	26.963 (26.912, 27.014) weeks	Estimated from model fitting process
ρ	Duration of clinical immunity	5 years	[35]
pc_1	Probability of clinical infection from naive individuals	0.9997 (0.9756, 0.9999)	[25, 45]
pc_2	Probability of clinical infection from partially immune individuals	0.902 (0.896, 0.901)	Estimated from data
$seas_i$	Seasonal forcing function for foreign sourced cases	Derived from data	[116]
β_i	Annual number of mosquito bites per person x proportion of bites testing positive for sporozoites for patch i	$\beta_{TC} = 3.996$ (3.623, 4.369) $\beta_{MB} = 0.016$ (0.013, 0.019) $\beta_{UJ} = 0.0003$ (0.00012, 0.00051) $\beta_{NK} = 2.563$ (2.509, 2.616) $\beta_{BB} = 9.983$ (9.592, 10.374) $\beta_{MP} = 92.728$ (92.571, 92.885)	Estimated from model fitting process
$\frac{1}{\alpha}$	Rate of assimilation of population in sub-patch 2 (locals having returned from foreign travel) back into sub-patch 1 from whence they originated	1.5 weeks ⁻¹	Expert opinion

$\frac{1}{k}$	Rate of movement between 5 Mpumalanga municipalities	1/4.156 (1/4.075, 1/4.237) weeks ⁻¹	Estimated from model fitting process
$\frac{1}{v_{yr}}$	Maputo residents: Rate of movement between Maputo and 5 Mpumalanga municipalities	$\frac{1}{v_1} = 1/2289.789$ weeks ⁻¹ (1/2279.096, 1/2300.482) (pre April 2005) $\frac{1}{v_2} = 1/1363.792$ weeks ⁻¹ (1/1341.792, 1/1386.683) (post April 2005)	Estimated from model fitting process
$\frac{1}{\varpi_{i,j}}$	Maputo residents: Rate of movement between Maputo and 5 Mpumalanga municipalities based on $\frac{1}{v_{yr}}$ and distance between patches	see Additional file 1	
$\frac{1}{z}$	Mpumalanga residents: Rate of movement between 5 Mpumalanga municipalities and Maputo	$\frac{1}{z} = 1/298.781$ weeks ⁻¹ (1/296.953, 1/300.622)	Estimated from model fitting process
$\frac{1}{\zeta_{i,j}}$	Mpumalanga residents: Rate of movement between 5 Mpumalanga municipalities and Maputo based on $\frac{1}{z}$ and distance between patches	see Additional file 1	
<i>fwgt</i>	Foreign movement weight intensity	2.000 (1.944, 2.055)	Estimated from model fitting process
<i>lwgt</i>	Local movement weight intensity	13.693 (13.503, 13.885)	Estimated from model fitting process
<i>vef</i>	Effectiveness of vector control	0.9785 (0.9783, 0.9787)	Estimated from model fitting process
<i>vc_i[t]</i>	Vector Control Coverage in patch <i>i</i> × efficiency	Derived from data	

7.7.2 Hybrid metapopulation DE-IBM model

The metapopulation DE model and the IBM model are linked in an unusual way in that the IBM model is nested in the DE model. At each time step, the DE model generates flows of a population that leave one compartment and enter another compartment (in the various sub-patches and patches). The IBM model takes the flow value at each time step once it has been negated from a compartment, discretises it into individuals in a population, executes the IBM algorithm, re-groups the individuals back into a population flow, and adds it into its destination compartment.

The metapopulation DE transmission model predicts (among other things) the number of local and foreign people entering the five Mpumalanga patches from the Maputo patch. These flows of the proportion of the population leaving compartments in the Maputo patch are interrupted before they enter the Mpumalanga patches. The proportion of the population is multiplied by the population size and discretised into individual people. These individual people are then subject to the individually-based FSAT model described earlier. The FSAT IBM algorithm is applied. Once all individuals have passed through the algorithm, they are grouped once again into populations per patch, sub-patch and compartment and the flow into Mpumalanga is completed and the transmission model continues processing as normal. For example, if the flow between Maputo and Nkomazi patch is 0.002 from the Susceptible compartment and 0.01 from the Infected compartment, then in a population of 1000 people, this translates to 2 susceptible individuals and 10 infected individuals passing through the border. Applying the FSAT IBM algorithm to these individuals may result in only 1 susceptible and 8 infected individuals agreeing to be screened. The detectable threshold may be such that of the 8 infected individuals, only 6 test positive for malaria. Thus 6 receive treatment but perhaps only 4 adhere to the regimen and of the two that do not adhere to treatment, one fails treatment. In the absence of FSAT, two susceptible individuals and ten infected individuals would have been added to population of Nkomazi. The result of the FSAT campaign is that the 2 susceptible individuals remain malaria free, 5 of the 12 individuals are cured of their malaria and will be added to the susceptible population in Nkomazi. The 2 infected individuals who did not participate in the FSAT campaign and the one who failed treatment will be added to the infected population in Nkomazi. The 2 infected individuals who were screened but did not test positive will be added to the sub-patent infected population in Nkomazi. Thus the IBM model is completely nested in the metapopulation DE model.

7.7.3 Data Fitting Method

The model is fitted to weekly treated case data from 2002 to 2008, and then validated with data from 2009 to 2012. The model is run from 1990 to reach a steady state before being fitted to data from 2002. IRS coverage and drug treatment are included in the model for the data fitting. The

number of treated cases in each sub-patch k are fitted to the data using the maximum likelihood approach assuming an underlying Poisson distribution with canonical parameter λ as the average number of treated cases per week. The metapopulation non-linear differential equation model is expressed in terms of average rates of movement between compartments, thus λ is a function of the parameters to be estimated (listed in Table 7.4)

The Poisson probability of observing x counts when the average number of counts per week is λ given by

$$P(x|\lambda) = \frac{\lambda^x \exp^{-\lambda}}{x!}.$$

As the model is being fitted to time series data with N time bins, λ , the expected number of counts per bin is a function of time. Assuming the independence of data from different time bins, the likelihood reduces to

$$L(\lambda_i|x_i) = \prod_{i=1}^N \frac{\lambda_i^{x_i} \exp^{-\lambda_i}}{x_i!}$$

and the log likelihood becomes

$$\ln(L(\lambda_i|x_i)) = \sum_{i=1}^N x_i \ln(\lambda_i) - \lambda_i - \ln(x_i!).$$

The model is fitted to 16 sets of data for each weekly time bin: treated cases for three sub-patches in five Mpumalanga municipalities and treated cases for Maputo. Under the assumption of independence, the log likelihood to be maximised is

$$\ln(L(\lambda_{s,i}|x_{s,i})) \propto \sum_{i=1}^N \sum_{s=1}^{16} x_{s,i} \ln(\lambda_{s,i}) - \lambda_{s,i}$$

The log-likelihood is negated and minimised using the hydroPSO function implementing a version of the Particle Swarm Optimisation algorithm in the R package hydroPSO v0.3-3 [150, 151]. Particle Swarm Optimisation is a global stochastic optimisation technique initially inspired by social behaviour of birds and fish [32, 64]. It shares similarities with evolutionary optimisation techniques like Genetic Algorithms (GA) but explores the multi-dimensional solution space on

the basis of individual and global best-known particle positions without evolution operators. Problems are optimised by moving particles (the population of candidate solutions) around the search-space based on the particles' position and velocity. Particle movements are a function of local best positions and other best particle positions in the search-space. Thus the particles "swarm" towards the best solutions in the search-space.

The parameters estimated through the model fitting process are presented in Table 7.4. The model with the estimated parameter values is run for a further 3 years to be further validated by comparison to data between 2009 and 2012. Figure 7.7 shows the data fitting and validation for all 16 sets of data. The model fits the data in sub-patches 1 and 2 well, capturing the level and timing of transmission. Sub-patch 3 data is over-estimated before 2006 (with the exception of Nkomazi Municipality) and captured relatively well thereafter given that the level of infections is low for the other four municipalities. Both the timing and level of malaria transmission in Maputo is captured by the model fitting process.

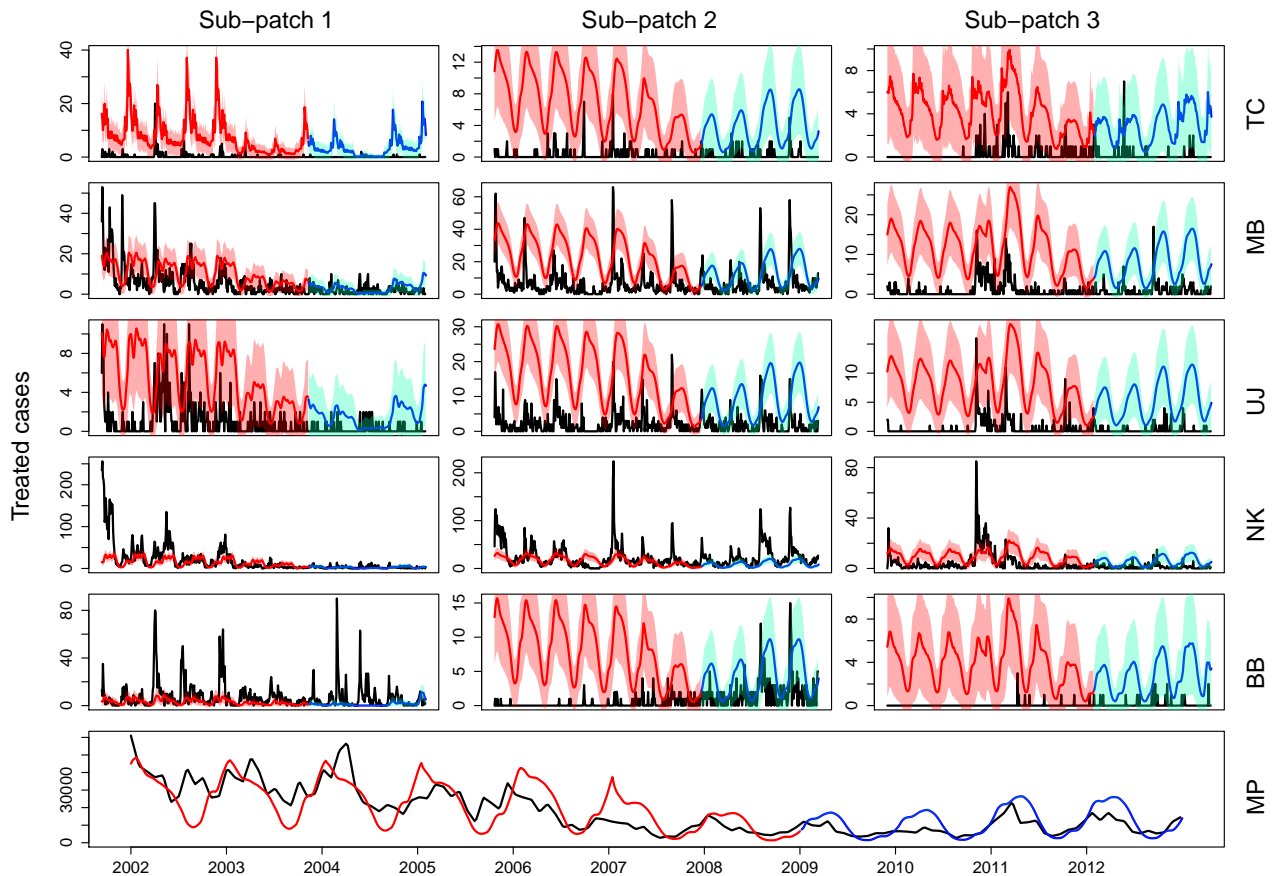


Figure 7.7: Model fit and validation with 95% uncertainty range

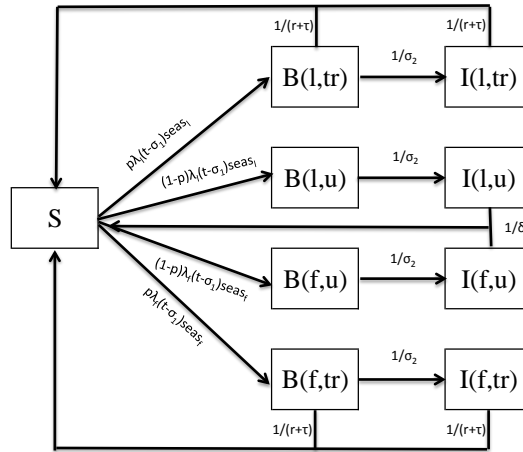
Chapter 8

Discussion and Conclusions

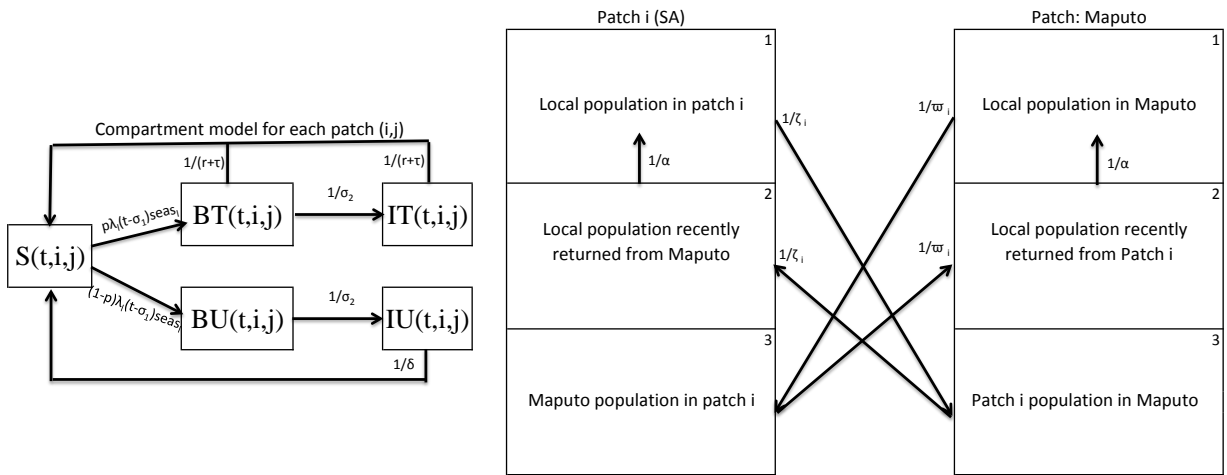
8.1 Mathematical models of malaria

Mathematical modelling is an integral tool aiding our understanding of the dynamics of infectious diseases and mathematical models and their applications to malaria in particular, have a history that spans over 100 years [2, 82]. The mathematical models developed in this study combined the theory of ordinary differential equations, metapopulation differential equation models and individual-based simulation models (Figure 8.1). Given the range of mathematical models for malaria highlighted in Chapter 2, the choice of model structure is pivotal. The analysis on the sensitivity to model structure for a selection of compartment models presented in Chapter 4 suggested that models with only small differences in structure may produce very different estimates of the same phenomenon but this sensitivity may be reduced by fitting the models to data. It was discussed that while this may be an argument for selecting simple models over complex ones, model structure (and its complexity) needs to be chosen carefully depending on the focus of the model and the use to which it will be put.

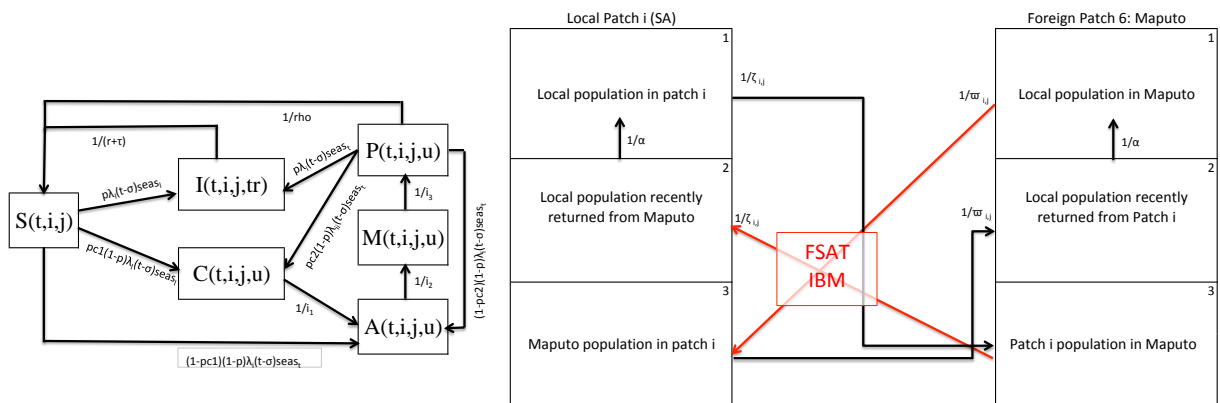
Model 1 was based on a model from Chapter 4 but replicated once to model both local and imported infections. In the metapopulation framework of Model 2, the same basic structure (condensed so that the latent liver stage of malaria was incorporated as a delay in a flow, rather than as a compartment) was replicated 18 times for the 18 sub-patches, and migration flows between all compartments in all sub-patches were modelled. This very complex structure allowed for interventions to be modelled explicitly. For example, in Model 1, FSAT at the border was modelled by decreasing the average incidence of imported infections by the FSAT coverage proportion where as in Model 2, FSAT was modelled on the average inflow of locals and foreigners entering Mpumalanga. Given that the focus in Model 3 was to model FSAT only, the intervention was modelled in a more complex manner by incorporating individual-



(a)



(b)



(c)

Figure 8.1: Mathematical models of transmission

based modelling where FSAT is applied to individuals rather than the average number of people entering Mpumalanga. In this manner, each of the three models structures were chosen to suit the focus of the model and the suite of interventions to be simulated.

Several methods were used to fit models to data in this study. In Chapter 4, given that simulated data was fitted to very simple models, a least squares approach was employed, minimising the squared distance between the data values and the model output. Model 1 required that two sets of data were fitted simultaneously (local and imported infections) and given that the data exhibited several sharp peaks, a likelihood approach was selected in favour of a cost-minimising one. The log-likelihood was maximised using the Nelder-Mead multi-dimensional, unconstrained direct search method [94]. Given that this is not a global maximisation routine and the technique is known to be affected by the initial parameter values, several fits were performed by starting points randomised in a latin hypercube design.

The Nelder-Mead algorithm was not chosen as the data-fitting algorithm for Models 2 and 3 as the algorithm is known to make large improvements in the first few iterations, but requires a large number of iterations to make further improvements. Models 2 and 3 required the simultaneous fitting of 16 datasets and the complexity of the models were such that a global optimisation routine that could be computed in parallel was selected in favour of the Nelder-Mead algorithm. A parallelised version of Particle swarm optimisation was thus employed to fit data to Models 2 and 3. The uncertainty in parameter estimates were assessed by computing the standard errors from the hessian matrix derived from the log likelihood. Models 2 and 3 were run stochastically by simulating the fitted parameter values from their 95% confidence intervals. Given that differential equation models predict average behaviour whereas the weekly case data represents a single occurrence, the models were made doubly stochastic by also treating predicted weekly case data as a random realisation of a Poisson process using the simulated average weekly case data as the average of the Poisson distribution. In this manner, the uncertainty of parameter estimates and the difference in the predicted averages and the data have been accounted for. Given that model parameters were estimated from the data simultaneously (in all three models), there is a chance that there are several choices for parameter sets that maximise the likelihood. Running the models stochastically by varying parameter values between the lower and upper bounds of their 95% confidence intervals accounted for the variability of these parameter estimates. Further, estimating the parameters from different starting points in Model 1 and recording the best parameter set after every iteration of the PSO algorithm in Models 2 and 3, allowed one to monitor the stability of the parameter estimates that best fitted the data.

The metapopulation structure of Models 2 and 3 comprised 18 individual patches/metapopulations and while this structure may theoretically be extended to any number of patches, several aspects must be taken into account. Computationally, extending the methodology to a large number of patches n with $\frac{n(n-1)}{2}$ links between patches (499 500 in the case of 1000 patches) will result in the equations becoming too numerous to be efficient. The number of parameters to

be estimated will increase with the increase in patches and fitting a model of this complexity to data (if such data are available at this level of disaggregation) is likely to be extremely computationally intensive. Further, depending on the size of the populations of interest and the available data, one could consider either individual based modelling (by disaggregating populations into individuals) or a simplified approach where for example, patches are linked using weights rather than flows. With computational advances in parallel computing in recent years, it is tempting to select individual based modelling in favour of any aggregated modelling approach. However, if there is no data to support the model at an individual level, it is likely that data will still be fitted to aggregated model output. The increasing availability of Big Data may lead to increased usage of IBMs but given that malaria is a disease associated with poverty, it is likely that mathematical modellers of infectious diseases will continue to be faced with a "no-data" problem in the foreseeable future.

8.2 Malaria elimination in Mpumalanga

A malaria elimination strategy should aim to interrupt the transmission cycle and prevent it from being re-established. An elimination strategy that employs "more of the same" approach may decrease the malaria burden, but will be insufficient to eliminate it as the focus needs to shift from better overall control to the identification of residual transmission foci leading to the last few infections. The interruption of the transmission cycle and prevention of its re-establishment theoretically requires three elements: (1) the elimination of the mosquito vector to prevent onward transmission, (2) stopping the inflow of imported infections and (3) reduction of infections at their source [89]. The first element is operationally unfeasible and has not been recommended [80]. The second element could be achieved if borders were closed, or more realistically if imported infections were identified and treated at border entry points before they can contribute to the infectious reservoir locally. The third element would require regional collaboration with these sources of imported infections to reduce transmission in the region [89].

This study aimed to use mathematical models to simulate malaria transmission in Mpumalanga in order to test a variety of elimination-focused tools on the models to assess the impact on local malaria prevalence and whether these tools may be used to achieve and maintain malaria elimination. This led to four fundamental research questions:

1. What is the temporal pattern of malaria transmission in Mpumalanga and what are the drivers of this pattern?
2. How long will it take to eliminate malaria with a strategy of maintaining current interventions at current levels?
3. How long will it take to eliminate malaria with a strategy of scaling up current interventions?

4. What alternative/additional interventions should be considered to make the elimination efforts more effective?

To answer these questions, a statistical analysis of case data was performed and three mathematical models of malaria transmission were developed. The analysis of the case notification data in Chapter 3 revealed a triple-peaked pattern of transmission with high levels of imported infections arising primarily from Mozambique. It was found that though malaria transmission in Mpumalanga may be low, it is also unstable and a change in climate and the level of imported infections may lead to a spike in local infections and generally a modification of the incidence pattern. The population of interest in the first model (a) spanned the entire province of Mpumalanga only, incorporating both local and imported infections without modelling migration or the source of infection explicitly. Instead the foreign force of infection, the instantaneous rate of acquiring an imported infection, was estimated from the data and used thereafter to generate imported infections. The second model (b) focused on a smaller population, the five municipalities most affected by malaria and neighbouring Maputo Province in Mozambique. The stochastic metapopulation model allowed for transmission in both the local and foreign sources of infection to be modelled and incorporated explicit movement between patches. The third model (c), also a stochastic metapopulation model, aimed at simulating in more detail the impact of a Focal Screen and Treat Campaign at the Mpumalanga-Maputo border. The FSAT campaign was nested in the differential equation model and simulated using Individual-based modelling.

The question of the possibility of malaria elimination through maintaining interventions at current levels was answered using both Models 1 and 2. The base case scenarios in both these models show that if routine drug therapy and vector control through IRS continues at current levels, malaria elimination will not be achieved as the level of imported infections is so high, that current vector control efforts are insufficient to decrease the receptivity of Mpumalanga to prevent onward infection. The same conclusion was reached when migration was modelled implicitly (Model 1) and explicitly (Model 2). While malaria elimination is not predicted to be possible through routine drug therapy and vector control at current levels in Mpumalanga, it is responsible for keeping malaria cases at the low levels required, to be in the pre-elimination phase.

To answer the question of the possibility of malaria elimination through scaling-up current interventions, one needs to assess the feasibility of scaling-up routine treatment and vector control. Studies in Mpumalanga have already suggested that the malaria-related treatment seeking probabilities are very high: 100% [18] and 99% (95% confidence interval: 97.5% - 99.5%) [58] though a marginally lower treatment probability of 95% was used in all models. Scaling-up routine drug therapy further would require increasing the treatment seeking probability above 95%. This may be infeasible as there will always be segments of a population that will not access the health system for treatment. For example, asymptomatic carriers of infection may not exhibit clinical symptoms and therefore feel no need to seek treatment and marginalised groups such as the

homeless may also not actively seek treatment for fear of authority. For this reason, scaling-up current interventions would imply increasing vector control efforts in Mpumalanga. This may include intensifying the already extensive spraying programme, increasing the distribution of insecticide-treated bednets and the identification and larviciding of additional breeding sites. The purpose of a scale-up in vector control would be to decrease the potential for onward local transmission, though it is impossible to reduce this to zero. While effective if the majority of infections are locally sourced, both Models 1 and 2 predict that increasing vector control alone will result in decreases in local infections but will not eliminate them if the stream of imported infections is left unchecked. Model 2's metapopulation structure has allowed it to further predict that increasing vector control in Nkomazi, Mbombela and Bushbuckridge municipalities only also leads to a knock-on decreases in malaria cases in the other two municipalities. These findings are also supported by another recent modelling study that found that at low receptivity levels, case management alone could not reliably prevent the re-establishment of transmission in the presence of medium to high importation rates [28].

Answering the third question required an assessment of various other tools that may be deployed to decrease malaria incidence to achieve malaria elimination. Between the three models, the following general interventions were considered: Mass Drug Administration, Source Reduction, and Focal Screen and Treat campaigns.

Models 1 and 2 predicted that Mass Drug Administration is an intervention with an immediate and large impact. Yet in countries with a large migrant population or populations with sub-optimal coverage, these interventions can fail because of the reintroduction of parasites and their impact may be short-lived [41]. Given the large proportion of imported cases in Mpumalanga, the models predict that when such a mass intervention targeting all infections (local and imported) is stopped, both local and imported infection levels revert back to pre-intervention levels within three years. This is because forces within Mpumalanga do not determine the level of imported infections; it is determined by the prevalence of malaria in the source country itself. Model 1 predicted that in the absence of imported infections, MDA applied in six consecutive two-monthly rounds at 80% coverage would be sufficient to eliminate local malaria, but even repeated annual rounds of MDA for seven years is insufficient to eliminate local malaria at the current level of imported infections.

As the interruption of the transmission cycle requires the reduction of transmission at the source itself, source reduction was assessed in Model 2 in the Maputo Province patch by simulating an increase in vector control activities and an MDA campaign. Model 2 predicts that if vector control is continued at current levels in Mpumalanga, but is scaled up in Maputo, the related decrease in local infections in Mpumalanga will be substantial because a smaller proportion of the population that travels into Mpumalanga will be infected and hence the infectious reservoir in Mpumalanga is reduced. These knock-on decreases in local infections in Mpumalanga are also predicted if MDA is performed in Maputo Province, although infections revert to previous levels

a few years after the end of the MDA campaign.

All three models predicted the impact of FSAT at the Mpumalanga-Maputo border. Model 1 simulated the campaign indirectly (without incorporating migration explicitly), Model 2 applied modelled the average impact of FSAT on migration flows into Mpumalanga and Model 3 incorporated individual-based simulation to disaggregate the migration flows to individuals, run an FSAT algorithm on the individuals, and re-group them for aggregation into the differential equation model. The results of all three models concurred where FSAT at a high, but imperfect coverage level is unable to eliminate malaria but has a substantial knock-on decrease in local infections through the decrease in imported infections in Mpumalanga. Even this reduction is dependent on achieving high coverage, getting border-crossers to agree to participate in the campaign and importantly, obtaining a diagnostic tool that is sensitive enough to detect low levels of parasitaemia without deterring border-crossers with long processing times. Mass drug administration at the border may be an option to achieve decreases in local infections without the sensitivity and processing time issues with screening tools. Implementing MDA as mandatory malaria prophylaxis for local and foreign travellers entering South Africa, extends the campaign beyond the Mpumalanga-Maputo border, while saving resources simultaneously. In allocating resources towards elimination-focused interventions, programme managers may wish to decrease routine activities to shift budgets towards elimination. In this regard, Model 2 predicted that the impact of FSAT could be dampened and even reduced to zero and malaria prevalence increased if current vector control efforts are reduced or stopped altogether. Thus, even in areas of very low transmission intensity (e.g. pre-elimination phase), imported infections will augment the infectious reservoir, and since the vector remains present, imported infections may lead to onward transmission to the local population and a resurgence of malaria.

There were very few scenarios where malaria elimination was predicted to occur. Model 1 predicted that the elimination of local infections would occur if the foreign force of infection (the instantaneous probability of generating an imported infection) was decreased to zero and Model 2 predicted the elimination of local malaria to occur if FSAT were to achieve an unlikely 100% coverage and when malaria in Maputo Province was itself eliminated. These predictions suggest that elimination is possible if either the foreign source of infection is eliminated entirely or, if the source of infection persists, all infections from this source need to be treated before entering the local region. While both of these scenarios may be beyond the capabilities of the local government, they highlight the need for and pivotal importance of cross-border/regional collaboration. One such example was the Lubombo Spatial Development Initiative, a trilateral agreement between South Africa, Mozambique and Swaziland, initiated in 1999, that successfully reduced malaria cases by 78% to 95% in the border areas of South Africa and Swaziland within five years of the start of IRS and subsequent ACT deployment in Maputo Province [70]. In September 2010, the earlier than expected ending of LSDI support for IRS (when the Global Fund withdrew support) resulted in sub-optimal spraying in Maputo and Gaza provinces which coincided with the increase in malaria cases in Maputo Province from 2011 thereafter [105].

In a review on the historical and current definitions of malaria, Cohen *et al.* defines three states of malaria transmission to be controlled low-endemic malaria, elimination and controlled non-endemic malaria. This third state describes the situation where the interruption of endemic transmission has occurred but there is still malaria resulting from onward transmission from imported infections and this onward transmission is sufficiently high that elimination has not yet been achieved [23]. This implies that if all onward infection from imported infections could be prevented, elimination of malaria would follow naturally. The results from the three models suggest that Mpumalanga is in this third state of transmission as elimination of malaria is only predicted to be possible with unrealistic, resource-intensive interventions that result in drastic reductions in imported infections. For countries in this state, it may be the case that a new definition of malaria elimination is required, as mathematical modelling suggests resources geared towards local interventions will result in only a limited decrease in local incidence. At the current rate of imported infections, the models suggest that it is not possible to reach elimination by intervening locally, using WHO's definition i.e achieve *zero* local cases. A new definition of elimination for countries in this third state will assist policy makers in setting realistic targets and optimising the elimination strategy.

8.3 Conclusion

This study is the first mathematical modelling study to be designed for this purpose in Mpumalanga and the first to do so in South Africa since the call for malaria elimination in 2007. It has contributed to the malaria elimination knowledge base in South Africa by predicting the impact of several elimination-focused interventions in the face of large rates of imported infections. The models themselves are tools with which the impact of other proposed interventions may be predicted. The models and the results may be used to inform future malaria-related policies. To the author's knowledge, the hybrid metapopulation nested DE-IBM structure developed in Model 3 is a first simulation study of screening and treating malaria infections at a border control point and the first study to nest the IBM structure within the differential equation structure by interrupting the flows of the DE model.

Future work in this area includes adding an economic cost component to the existing models and extending the metapopulation structure to the other malaria-endemic provinces in South Africa and eventually to the rest of Southern Africa (particularly, all of Mozambique, Zimbabwe, Botswana and Namibia) to consider the feasibility of a regional approach to malaria elimination. The extension of the models to such a large geographical area will bring with it computational challenges in model development and statistical challenges in fitting such a complex model to several sets of data. In this study, mathematical modelling has been used to develop models of malaria transmission to predict the impact of elimination-focused strategies such as a scale-up in current interventions, FSAT at the border and foreign source reduction.

To eliminate malaria by 2018, the government of South Africa will need to design and implement an elimination strategy tailored for a country with a high level of imported infections. The results from all three models presented in this dissertation suggest that a regionally-focused strategy will stand a better chance at achieving elimination in Mpumalanga and South Africa compared to a nationally-focused one, particularly in the face of frequent population movement between the pre-elimination area and neighbouring high transmission intensity regions. In this manner, mathematical models can form an integral part of the research, planning and evaluation of elimination-focused strategies so that malaria elimination is possible in the foreseeable future.

Bibliography

1. Alexander, N., Sutherland, C., Roper, C., Cissé, B. and Schellenberg, D. [2007], ‘Modelling the impact of intermittent preventive treatment for malaria on selection pressure for drug resistance’, *Malaria Journal* **6**(9).
2. Anderson, R. M. and May, R. M. [1992], *Infectious Diseases of Humans: Dynamics and Control*, Oxford University Press.
3. Aragón, L. and Espinal, C. [1992], ‘Expansión de la frontera, expansión de la enfermedad: movilidad geográfica y salud en la amazonia’, *Enfoque Integral de la Salud Humana en la Amazonia* pp. 429–456.
4. Ariey, F., Duchemin, J.-B. and Robert, V. [2003], ‘Metapopulation concepts applied to falciparum malaria and their impacts on the emergence and spread of chloroquine resistance.’, *Infection, genetics and evolution : Journal of molecular epidemiology and evolutionary genetics in infectious diseases* **2**(3), 185–92.
URL: <http://www.ncbi.nlm.nih.gov/pubmed/12797980>
5. Arino, J., Ducrot, A. and Zongo, P. [2012], ‘A metapopulation model for malaria with transmission-blocking partial immunity in hosts.’, *Journal of Mathematical Biology* **64**(3), 423–48.
URL: <http://www.ncbi.nlm.nih.gov/pubmed/21442182>
6. Aron, J. L. [1988], ‘Acquired Immunity dependent upon exposure in an SIRS epidemic model’, *Mathematical Biosciences* **88**, 37–47.
7. Auger, P., Kouokam, E., Sallet, G., Tchuenté, M. and Tsanou, B. [2008], ‘The Ross-Macdonald model in a patchy environment.’, *Mathematical Biosciences* **216**(2), 123–31.
URL: <http://www.ncbi.nlm.nih.gov/pubmed/18805432>
8. Barnes, K. I., Durrheim, D. N., Little, F., Jackson, A., Mehta, U., Allen, E., Dlamini, S. S., Tsoka, J., Bredenkamp, B., Mthembu, D. J. et al. [2005], ‘Effect of artemether-lumefantrine policy and improved vector control on malaria burden in Kwazulu-Natal, South Africa’, *PLoS Medicine* **2**(11), e330.

BIBLIOGRAPHY

9. Barnes, K. I., Little, F., Mabuza, A., Mngomezulu, N., Govere, J., Durrheim, D., Roper, C., Watkins, B. and White, N. J. [2008], 'Increased gametocytemia after treatment: an early parasitological indicator of emerging sulfadoxine-pyrimethamine resistance in falciparum malaria.', *The Journal of Infectious Diseases* **197**(11), 1605–13.
URL: <http://www.ncbi.nlm.nih.gov/pubmed/18471066>
10. Berg, B. A. [2004], *Markov Chain Monte Carlo Simulations And Their Statistical Analysis: With Web-based Fortran Code*, World Scientific.
11. Blumberg, L. and Frean, J. [2007], 'Malaria control in South Africa - challenges and successes', *South African Medical Journal* **97**(11), 1193.
URL: <http://www.samj.org.za/index.php/samj/article/view/304>
12. Bosman, M., Wentzel, M., Mabitsela, M., Marais, J., Nkai, D., Viljoen, J. and Vennekens, A. [2000], Causes of cross-border migration between South Africa and respectively Mozambique and Zimbabwe, Technical report, Human Sciences Research Council, South Africa.
URL: <http://www.hsrc.ac.za/en/research-outputs/view/806>
13. Brauer, F. [2001], 'Models for transmission of disease with immigration of infectives', *Mathematical Biosciences* **171**(2), 143–154.
URL: <http://linkinghub.elsevier.com/retrieve/pii/S0025556401000578>
14. Brauer, F., van den Driessche, P. and Wu, J., eds [2008], *Mathematical Epidemiology*, number 1945, 1 edn, Springer.
URL: <http://books.google.com/books?id=gcP5l1a22rQC&pgis=1>
15. Brockwell, P. J. and Davis, R. A. [2009], *Time Series: Theory and Methods*, Springer Series in Statistics, Springer.
URL: <http://www.amazon.com/Time-Series-Methods-Springer-Statistics/dp/1441903194>
16. Cairns, M., Ghani, A., Okell, L., Gosling, R., Carneiro, I., Anto, F., Asoala, V., Owusu-Agyei, S., Greenwood, B., Chandramohan, D. et al. [2011], 'Modelling the protective efficacy of alternative delivery schedules for intermittent preventive treatment of malaria in infants and children', *PloS one* **6**(4), e18947.
17. Carneiro, I., Smith, L., Ross, A., Roca-Feltrer, A., Greenwood, B., Schellenberg, J. A., Smith, T. and Schellenberg, D. [2010], 'Intermittent preventive treatment for malaria in infants: a decision-support tool for sub-Saharan Africa', *Bulletin of the World Health Organization* **88**(11), 807–814.
18. Castillo-Riquelme, M., McIntyre, D. and Barnes, K. [2008], 'Household burden of malaria in South Africa and Mozambique: is there a catastrophic impact?', *Tropical medicine and International health* **13**(1), 108–22.
URL: <http://www.ncbi.nlm.nih.gov/pubmed/18291009>

19. Chitnis, N., Hyman, J. M. and Cushing, J. M. [2008], ‘Determining important parameters in the spread of malaria through the sensitivity analysis of a mathematical model.’, *Bulletin of Mathematical Biology* **70**(5), 1272–96.
URL: <http://www.ncbi.nlm.nih.gov/pubmed/18293044>
20. Chitnis, N., Schapira, A., Smith, T. and Steketee, R. [2010], ‘Comparing the effectiveness of malaria vector-control interventions through a mathematical model’, *The American journal of Tropical Medicine and Hygiene* **83**(2), 230–240.
21. Chubb, M. C. and Jacobsen, K. H. [2010], ‘Mathematical modeling and the epidemiological research process.’, *European Journal of Epidemiology* **25**(1), 13–9.
URL: <http://www.ncbi.nlm.nih.gov/pubmed/19859816>
22. Cleveland, R. B. [1990], ‘STL: A seasonal-trend decomposition procedure based on LOESS’, *Journal of Official Statistics* **6**(1).
URL: <http://cs.wellesley.edu/cs315/Papers/stl%20statistical%20model.pdf>
23. Cohen, J. M., Moonen, B., Snow, R. W. and Smith, D. L. [2010], ‘How absolute is zero? An evaluation of historical and current definitions of malaria elimination.’, *Malaria Journal* **9**, 213.
URL: <http://www.malariajournal.com/content/9/1/213>
24. Coleman, M., Coleman, M., Mabuza, A. M., Kok, G., Coetzee, M. and Durrheim, D. N. [2009], ‘Using the SaTScan method to detect local malaria clusters for guiding malaria control programmes.’, *Malaria Journal* **8**(1), 68.
URL: <http://www.malariajournal.com/content/8/1/68>
25. Collins, W. E. and Jeffery, G. M. [1999], ‘A retrospective examination of sporozoite- and trophozoite-induced infections with *Plasmodium falciparum*: development of parasitologic and clinical immunity during primary infection.’, *The American Journal of Tropical Medicine and Hygiene* **61**(1 Suppl), 4–19.
URL: <http://www.ncbi.nlm.nih.gov/pubmed/10432041>
26. Craig, M., Snow, R. and le Sueur, D. [1999], ‘A Climate-based Distribution Model of Malaria Transmission in Sub-Saharan Africa’, *Parasitology Today* **15**(3), 105–111.
URL: [http://dx.doi.org/10.1016/S0169-4758\(99\)01396-4](http://dx.doi.org/10.1016/S0169-4758(99)01396-4)
27. Crowell, V., Briët, O. J. T., Hardy, D., Chitnis, N., Maire, N., Di Pasquale, A. and Smith, T. A. [2013], ‘Modelling the cost-effectiveness of mass screening and treatment for reducing *Plasmodium falciparum* malaria burden.’, *Malaria Journal* **12**(1), 4.
URL: <http://www.malariajournal.com/content/12/1/4>
28. Crowell, V., Hardy, D., Briët, O., Chitnis, N., Maire, N. and Smith, T. [2012], ‘Can we depend on case management to prevent re-establishment of *P. falciparum* malaria, after

- local interruption of transmission?', *Epidemics* **4**(1), 1–8.
URL: <http://www.sciencedirect.com/science/article/pii/S1755436511000442>
29. Dietz, K. [1980], Models for vector-borne parasitic diseases, in 'Vito Volterra Symposium on Mathematical Models in Biology', Springer, pp. 264–277.
30. Doolan, D. L., Dobano, C. and Baird, J. K. [2009], 'Acquired immunity to malaria.', *Clinical microbiology reviews* **22**(1), 13–36.
URL: <http://cmr.asm.org/content/22/1/13>
31. Dowdle, W. R. [1998], 'The principles of disease elimination and eradication.', *Bulletin of the World Health Organization* **76 Suppl 2**, 22–5.
32. Eberhart, R. and Kennedy, J. [1995], A new optimizer using particle swarm theory, in 'MHS'95. Proceedings of the Sixth International Symposium on Micro Machine and Human Science', IEEE, pp. 39–43.
URL: <http://ieeexplore.ieee.org/articleDetails.jsp?arnumber=494215>
33. Eyles, D. E. and Young, M. D. [1951], 'The duration of untreated or inadequately treated *Plasmodium falciparum* infections in the human host.', *Journal of National Malaria Society (U.S.)* **10**(4), 327–36.
URL: <http://www.ncbi.nlm.nih.gov/pubmed/14908561>
34. Ferrer, J., Albuquerque, J., Prats, C., Lopez, D. and Valls, J. [2012], Agent-based Models in malaria elimination strategy design, in 'EMCSR 2012'.
URL: <http://www.emcsr-conference.org/2012/paper/view/21>
35. Filipe, J. A. N., Riley, E. M., Drakeley, C. J., Sutherland, C. J. and Ghani, A. C. [2007], 'Determination of the processes driving the acquisition of immunity to malaria using a mathematical transmission model.', *PLoS Computational Biology* **3**(12), e255.
URL: <http://dx.plos.org/10.1371/journal.pcbi.0030255>
36. Gething, P. W., Smith, D. L., Patil, A. P., Tatem, A. J., Snow, R. W. and Hay, S. I. [2010], 'Climate change and the global malaria recession.', *Nature* **465**(7296), 342–5.
URL: <http://dx.doi.org/10.1038/nature09098>
37. *Global Malaria Action Plan for a malaria-free world* [2014].
URL: <http://www.rbm.who.int/gmap/2-3.html>
38. *Global malaria control and elimination. Report of a technical review* [2009], Technical report, World Health Organization.
URL: <http://www.who.int/malaria/publications/atoz/9789241596756/en/>
39. Gosling, R., Carneiro, I. and Chandramohan, D. [2009], 'Intermittent preventive treatment of malaria in infants: how does it work and where will it work?', *Tropical Medicine & International Health* **14**(9), 1003–1010.

-
40. Gosling, R. D., Ghani, A. C., Deen, J. L., von Seidlein, L., Greenwood, B. M. and Chandramohan, D. [2008], ‘Can changes in malaria transmission intensity explain prolonged protection and contribute to high protective efficacy of intermittent preventive treatment for malaria in infants’, *Malaria Journal* **7**, 54.
41. Gosling, R. D., Okell, L., Mosha, J. and Chandramohan, D. [2011], ‘The role of antimalarial treatment in the elimination of malaria.’, *Clinical microbiology and infection* **17**(11), 1617–23.
URL: <http://www.ncbi.nlm.nih.gov/pubmed/21951597>
42. Govere, J., Durrheim, D., Coetzee, M. and Hunt, R. H. [2001], ‘Malaria in Mpumalanga, South Africa, with special reference to the period 1987-1999’, *South African Journal of Science* **97**, 55–58.
43. Govere, J., Durrheim, D. N., Coetzee, M., Hunt, R. H. and la Grange, J. J. [2000], ‘Captures of mosquitoes of the *Anopheles gambiae* complex (Diptera: Culicidae) in the Lowveld Region of Mpumalanga Province, South Africa.’, *African Entomology* **8**(1), 91–99.
URL: <http://reference.sabinet.co.za/webx/access/journal-archive/10213589/283.pdf>
44. Greenwood, B. [2010], ‘Anti-malarial drugs and the prevention of malaria in the population of malaria endemic areas.’, *Malaria journal* **9 Suppl 3**(Suppl 3), S2.
URL: <http://www.malariajournal.com/content/9/S3/S2>
45. Griffin, J. T., Ferguson, N. M. and Ghani, A. C. [2014], ‘Estimates of the changing age-burden of *Plasmodium falciparum* malaria disease in sub-saharan africa’, *Nature Communications* **5**.
46. Griffin, J. T., Hollingsworth, T. D., Okell, L. C., Churcher, T. S., White, M., Hinsley, W., Bousema, T., Drakeley, C. J., Ferguson, N. M., Basáñez, M.-G. and Ghani, A. C. [2010], ‘Reducing *Plasmodium falciparum* Malaria Transmission in Africa: A Model-Based Evaluation of Intervention Strategies.’, *PLoS Medicine* **7**(8).
URL: <http://www.ncbi.nlm.nih.gov/pubmed/20711482>
47. Grueninger, H. and Hamed, K. [2013], ‘Transitioning from malaria control to elimination: the vital role of ACTs.’, *Trends in Parasitology* **29**(2), 60–4.
URL: <http://www.ncbi.nlm.nih.gov/pubmed/23228225>
48. Guerin, P. J., Olliaro, P., Nosten, F., Druilhe, P., Laxminarayan, R., Binka, F., Kilama, W. L., Ford, N. and White, N. J. [2002], ‘Malaria: current status of control, diagnosis, treatment, and a proposed agenda for research and development.’, *The Lancet Infectious Diseases* **2**(9), 564–73.
URL: <http://www.ncbi.nlm.nih.gov/pubmed/12206972>

BIBLIOGRAPHY

49. *Guidelines for the treatment of malaria in South Africa: 2010* [2010], Technical report, South African National Department of Health.
URL: <http://www.doh.gov.za/docs/facts-f.html>
50. *Guidelines on Prevention of the Reintroduction of Malaria* [2007], Technical report, World Health Organisation.
URL: <http://books.google.com/books?id=BoHPq6KqqqMC&pgis=1>
51. Hall, B. F. and Fauci, A. S. [2009], ‘Malaria control, elimination, and eradication: the role of the evolving biomedical research agenda.’, *The Journal of Infectious Diseases* **200**(11), 1639–43.
URL: <http://jid.oxfordjournals.org/content/200/11/1639.full#ref-2>
52. Halliday, K. E., Okello, G., Turner, E. L., Njagi, K., Mcharo, C., Kengo, J., Allen, E., Dubeck, M. M., Jukes, M. C. H. and Brooker, S. J. [2014], ‘Impact of intermittent screening and treatment for malaria among school children in Kenya: a cluster randomised trial.’, *PLoS Medicine* **11**(1), e1001594.
URL: <http://dx.plos.org/10.1371/journal.pmed.1001594>
53. Halloran, M. E., Struchiner, C. J. and Spielman, A. [1989], ‘Modeling malaria vaccines ii: Population effects of stage-specific malaria vaccines dependent on natural boosting’, *Mathematical Biosciences* **94**(1), 115–149.
54. Hansen, P. C., Pereyra, V. and Scherer, G. [2012], *Least Squares Data Fitting with Applications*, JHU Press.
55. Harris, I., Sharrock, W. W., Bain, L. M., Gray, K.-A., Bobogare, A., Boaz, L., Lilley, K., Krause, D., Vallely, A., Johnson, M.-L., Gatton, M. L., Shanks, G. D. and Cheng, Q. [2010], ‘A large proportion of asymptomatic *Plasmodium* infections with low and sub-microscopic parasite densities in the low transmission setting of Temotu Province, Solomon Islands: challenges for malaria diagnostics in an elimination setting.’, *Malaria Journal* **9**, 254.
URL: <http://espace.library.uq.edu.au/view/UQ:218971>
56. Hay, S. I., Cox, J., Rogers, D. J., Randolph, S. E., Stern, D. I., Shanks, G. D., Myers, M. F. and Snow, R. W. [2002], ‘Climate change and the resurgence of malaria in the East African highlands.’, *Nature* **415**(6874), 905–9.
URL: <http://dx.doi.org/10.1038/415905a>
57. Hendriksen, I. C. E., White, L. J., Veenemans, J., Mtove, G., Woodrow, C., Amos, B., Saiwaew, S., Gesase, S., Nadjm, B., Silamut, K., Joseph, S., Chotivanich, K., Day, N. P. J., von Seidlein, L., Verhoef, H., Reyburn, H., White, N. J. and Dondorp, A. M. [2013], ‘Defining *falciparum*-malaria-attributable severe febrile illness in moderate-to-high transmission settings on the basis of plasma PfHRP2 concentration.’, *The Journal of Infectious Diseases*

- 207(2), 351–61.
URL: <http://www.ncbi.nlm.nih.gov/pubmed/23136222>
58. Hlongwana, K. W., Zitha, A., Mabuza, A. M. and Maharaj, R. [2011], ‘Knowledge and practices towards malaria amongst residents of Bushbuckridge, Mpumalanga, South Africa’, *African Journal of Primary Health Care & Family Medicine* **3**(1).
URL: <http://www.phcfm.org/index.php/phcfm/article/view/257>
59. Hopkins, H., Gonzalez, I. J., Polley, S. D., Angutoko, P., Ategeka, J., Asiiimwe, C., Agaba, B., Kyabayinze, D. J., Sutherland, C. J., Perkins, M. D. and Bell, D. [2013], ‘Highly sensitive detection of malaria parasitemia in a malaria-endemic setting: performance of a new loop-mediated isothermal amplification kit in a remote clinic in Uganda.’, *The Journal of Infectious Diseases* **208**(4), 645–52.
URL: <http://jid.oxfordjournals.org/content/early/2013/05/31/infdis.jit184.full>
60. Jacquez, J. A. [1996], *Compartmental analysis in biology and medicine*, BioMedware.
URL: <http://books.google.com/books?id=U81qAAAAMAAJ&pgis=1>
61. Jeffery, G. M. and Eyles, D. E. [1955], ‘Infectivity to mosquitoes of *Plasmodium falciparum* as related to gametocyte density and duration of infection.’, *The American journal of Tropical Medicine and Hygiene* **4**(5), 781–9.
URL: <http://www.ncbi.nlm.nih.gov/pubmed/13259002>
62. Juan, Z. [2006], ‘Global dynamics of an SEIR epidemic model with immigration of different compartments’, *Acta Mathematica Scientia* **26**(3), 551–567.
URL: <http://linkinghub.elsevier.com/retrieve/pii/S0252960206600817>
63. *Keep Your Head Down: Unprotected Migrants in South Africa: Background* [2007].
URL: <http://www.hrw.org/reports/2007/southafrica0207/6.htm>
64. Kennedy, J. and Eberhart, R. [n.d.], Particle swarm optimization, in ‘Proceedings of ICNN’95 - International Conference on Neural Networks’, Vol. 4, IEEE, pp. 1942–1948.
URL: <http://ieeexplore.ieee.org/articleDetails.jsp?arnumber=488968>
65. Killeen, G. F., Knols, B. G. and Gu, W. [2003], ‘Taking malaria transmission out of the bottle: implications of mosquito dispersal for vector-control interventions’, *The Lancet Infectious Diseases* **3**(5), 297–303.
66. Koella, J. C. and Antia, R. [2003], ‘Epidemiological models for the spread of anti-malarial resistance’, *Malaria Journal* **2**(3).
67. Le Menach, A., McKenzie, F. E., Flahault, A. and Smith, D. L. [2005], ‘The unexpected importance of mosquito oviposition behaviour for malaria: non-productive larval habitats can be sources for malaria transmission.’, *Malaria Journal* **4**(1), 23.
URL: <http://www.malariajournal.com/content/4/1/23>

BIBLIOGRAPHY

68. L'Hospital, G. [1696], *Analyse des infiniment petits pour l'intelligence des lignes courbes*, L'imprimerie Royale, Paris.
69. *Life cycle of the malaria parasite* [2014].
URL: <http://www.malariavaccine.org/malvac-lifecycle.php>
70. *Lubombo Spatial Development Initiative* [2014].
URL: <http://www.malaria.org.za/lodi/home.html>
71. Luz, P. M., Struchiner, C. J. and Galvani, A. P. [2010], 'Modeling transmission dynamics and control of vector-borne neglected tropical diseases.', *PLoS Neglected Tropical Diseases* **4**(10), e761.
URL: <http://www.ncbi.nlm.nih.gov/pubmed/21049062>
72. Mabaso, M. L. H., Sharp, B. and Lengeler, C. [2004], 'Historical review of malarial control in southern Africa with emphasis on the use of indoor residual house-spraying.', *Tropical Medicine and International health* **9**(8), 846–56.
URL: <http://www.ncbi.nlm.nih.gov/pubmed/15303988>
73. Mabuza, A., Govere, J., Grange, K., Mngomezulu, N., Allen, E., Zitha, A., Mbokazi, F. and Barnes, K. [2005], 'Therapeutic efficacy of sulfadoxine-pyrimethamine for *Plasmodium falciparum* malaria: A study 5 years after implementation of combination therapy in Mpumalanga', *South African Medical Journal* **95**(5).
74. Maharaj, R., Morris, N., Seocharan, I., Kruger, P., Moonasar, D., Mabuza, A., Raswiswi, E. and Raman, J. [2012], 'The feasibility of malaria elimination in South Africa.', *Malaria Journal* **11**(1), 423.
URL: <http://www.malariajournal.com/content/11/1/423>
75. Maharaj, R., Raman, J., Morris, N., Moonasar, D., Durrheim, D. N., Seocharan, I., Kruger, P., Shandukani, B. and Kleinschmidt, I. [2013], 'Epidemiology of malaria in South Africa: From control to elimination', *South African Medical Journal* **103**(10), 779–783.
URL: <http://www.samj.org.za/index.php/samj/article/view/7441/5461>
76. Maire, N., Smith, T., Ross, A., Owusu-Agyei, S., Dietz, K. and Molineaux, L. [2006], 'A Model for natural immunity to asexual blood stages of *Plasmodium falciparum* malaria in endemic areas', *American Journal of Tropical Medicine and Hygiene* **75**(2), 19–31.
URL: http://www.ajtmh.org/content/75/2_suppl/19.abstract
77. Makanga, M. and Krudsood, S. [2009], 'The clinical efficacy of artemether/lumefantrine (Coartem).', *Malaria Journal* **8**(Suppl 1).
URL: <http://www.malariajournal.com/content/8/S1/S5>

-
78. *Making up the Numbers: Measuring "Illegal Immigration" to South Africa* [2001], Technical report, Southern African Migration Project, Canada.
URL: <http://www.queensu.ca/samp/forms/form1.html>
79. *Malaria* [2014].
URL: <http://www.niaid.nih.gov/topics/malaria/pages/lifecycle.aspx>
80. *Malaria elimination. A field manual for low and moderate endemic countries* [2007], Technical report, World Health Organisation, Geneva.
URL: <http://www.who.int/malaria/publications/atoz/9789241596084/en/>
81. *Malaria Site: Life Cycle of Malaria Parasite; Sexual Phase, Sporogony; Asexual phase, Schizogony* [2014].
URL: <http://www.malariasite.com/malaria/LifeCycle.htm>
82. Mandal, S., Sarkar, R. R. and Sinha, S. [2011], 'Mathematical models of malaria-a review.', *Malaria Journal* **10**(1), 202.
URL: <http://www.malariajournal.com/content/10/1/202>
83. Martens, P., Kovats, R., Nijhof, S., Devries, P., Livermore, M., Bradley, D., Cox, J. and McMichael, A. [1999], 'Climate change and future populations at risk of malaria', *Global Environmental Change* **9**, 89–107.
URL: [http://dx.doi.org/10.1016/S0959-3780\(99\)00020-5](http://dx.doi.org/10.1016/S0959-3780(99)00020-5)
84. Maude, R. J., Pontavornpinyo, W., Saralamba, S., Aguas, R., Yeung, S., Dondorp, A. M., Day, N. P. J., White, N. J. and White, L. J. [2009], 'The last man standing is the most resistant: eliminating artemisinin-resistant malaria in Cambodia.', *Malaria Journal* **8**.
URL: <http://www.malariajournal.com/content/8/1/31>
85. Maude, R. J., Socheat, D., Nguon, C., Saroth, P., Dara, P., Li, G., Song, J., Yeung, S., Dondorp, A. M., Day, N. P., White, N. J. and White, L. J. [2012], 'Optimising strategies for *Plasmodium falciparum* malaria elimination in Cambodia: primaquine, mass drug administration and artemisinin resistance.', *PloS one* **7**(5).
URL: <http://dx.plos.org/10.1371/journal.pone.0037166>
86. Miller, M. J. [1958], 'Observations on the natural history of malaria in the semi-resistant West African.', *Transactions of the Royal Society of Tropical Medicine and Hygiene* **52**, 152–68.
URL: <http://www.ncbi.nlm.nih.gov/pubmed/13543904>
87. Montosi, E., Manzoni, S., Porporato, A. and Montanari, A. [2012], 'An ecohydrological model of malaria outbreaks', *Hydrology and Earth System Sciences* **16**(8), 2759–2769.
URL: <http://www.hydrol-earth-syst-sci.net/16/2759/2012/hess-16-2759-2012.html>

BIBLIOGRAPHY

88. Moonasar, D., Nuthulaganti, T., Kruger, P. S., Mabuza, A., Rasiswi, E. S., Benson, F. G. and Maharaj, R. [2012], ‘Malaria control in South Africa 2000-2010: beyond MDG6.’, *Malaria Journal* **11**(1), 294.
URL: <http://www.malariajournal.com/content/11/1/294>
89. Moonen, B., Cohen, J. M., Snow, R. W., Slutsker, L., Drakeley, C., Smith, D. L., Abeyasinghe, R. R., Rodriguez, M. H., Maharaj, R., Tanner, M. and Targett, G. [2010], ‘Operational strategies to achieve and maintain malaria elimination.’, *Lancet* **376**(9752), 1592–603.
URL: [http://www.thelancet.com/journals/lancet/article/PIIS0140-6736\(10\)61269-X/fulltext](http://www.thelancet.com/journals/lancet/article/PIIS0140-6736(10)61269-X/fulltext)
90. *Mortality and causes of death in South Africa, 2010: Findings from death notification* [2013], Technical report, Statistics South Africa, Pretoria.
URL: <http://www.statssa.gov.za/publications/p03093/p030932010.pdf>
91. Mosha, J. F., Sturrock, H. J. W., Greenhouse, B., Greenwood, B., Sutherland, C. J., Gadalla, N., Atwal, S., Drakeley, C., Kibiki, G., Bousema, T., Chandramohan, D. and Gosling, R. [2013], ‘Epidemiology of subpatent *Plasmodium falciparum* infection: implications for detection of hotspots with imperfect diagnostics.’, *Malaria Journal* **12**(1), 221.
URL: <http://www.malariajournal.com/content/12/1/221>
92. Murray, J. [2003], *Mathematical Biology II*, Vol. 18, Springer.
URL: <http://www.amazon.com/Mathematical-Biology-II-J-D-Murray/dp/0387952284>
93. *National Malaria Elimination Strategy 2011–2018* [2011], Technical report, South African National Department of Health, Pretoria.
94. Nelder, J. A. and Mead, R. [1965], ‘A Simplex Method for Function Minimization’, *The Computer Journal* **7**(4), 308–313.
URL: <http://comjnl.oxfordjournals.org/content/7/4/308.abstract>
95. Ngomane, L. and de Jager, C. [2012], ‘Changes in malaria morbidity and mortality in Mpumalanga Province, South Africa (2001- 2009): a retrospective study’, *Malaria Journal* **11**(1), 19.
URL: <http://www.malariajournal.com/content/11/1/19>
96. O’Connell, K. A., Samandari, G., Phok, S., Phou, M., Dysoley, L., Yeung, S., Allen, H. and Littrell, M. [2012], ‘“Souls of the ancestor that knock us out” and other tales. A qualitative study to identify demand-side factors influencing malaria case management in Cambodia.’, *Malaria journal* **11**(1), 335.
URL: <http://www.malariajournal.com/content/11/1/335>

-
97. of Home Affairs, D. [2005], South africa and mozambique sign a visa waiver agreement, Technical report, Department of Home Affairs.
98. Okell, L. C., Bousema, T., Griffin, J. T., Ouédraogo, A. L., Ghani, A. C. and Drakeley, C. J. [2012], ‘Factors determining the occurrence of submicroscopic malaria infections and their relevance for control.’, *Nature Communications* **3**, 1237.
URL: <http://dx.doi.org/10.1038/ncomms2241>
99. Okell, L. C., Griffin, J. T., Kleinschmidt, I., Hollingsworth, T. D., Churcher, T. S., White, M. J., Bousema, T., Drakeley, C. J. and Ghani, A. C. [2011], ‘The potential contribution of mass treatment to the control of *Plasmodium falciparum* malaria.’, *PloS one* **6**(5).
URL: <http://www.plosone.org/article/info%3Adoi%2F10.1371%2Fjournal.pone.0020179>
100. Oluwagbemi, O. O., Fornadel, C. M., Adebisi, E. F., Norris, D. E. and Rasgon, J. L. [2013], ‘ANOSPEX: a stochastic, spatially explicit model for studying *Anopheles* metapopulation dynamics.’, *PloS one* **8**(7).
URL: <http://www.plosone.org/article/info:doi/10.1371/journal.pone.0068040#pone-0068040-g004>
101. O’Meara, W. P., Smith, D. L. and McKenzie, F. E. [2006], ‘Potential impact of intermittent preventive treatment (IPT) on spread of drug-resistant malaria’, *PLoS Medicine* **3**(5), e141.
102. Pankratz, A. [1991], *Forecasting with Dynamic Regression Models*, Wiley-Interscience.
URL: <http://www.amazon.com/Forecasting-Dynamic-Regression-Models-Pankratz/dp/0471615285>
103. Phiri, K., Esan, M., van Hensbroek, M. B., Khairallah, C., Faragher, B. and ter Kuile, F. O. [2012], ‘Intermittent preventive therapy for malaria with monthly artemether–lumefantrine for the post-discharge management of severe anaemia in children aged 4–59 months in southern malawi: a multicentre, randomised, placebo-controlled trial’, *The Lancet Infectious Diseases* **12**, 191–200.
104. Polley, S. D., Gonzalez, I. J., Mohamed, D., Daly, R., Bowers, K., Watson, J., Mewse, E., Armstrong, M., Gray, C., Perkins, M. D., Bell, D., Kanda, H., Tomita, N., Kubota, Y., Mori, Y., Chiodini, P. L. and Sutherland, C. J. [2013], ‘Clinical evaluation of a loop-mediated amplification kit for diagnosis of imported malaria.’, *The Journal of Infectious Diseases* **208**(4), 637–44.
URL: <http://jid.oxfordjournals.org/content/early/2013/04/30/infdis.jit183.abstract?keytype=ref>
105. President’s Malaria Initiative [2013], Mozambique malaria operational plan financial year: 2013, Technical report, President’s Malaria Initiative.
106. R Core Group [2013].
URL: www.r-project.org

BIBLIOGRAPHY

107. Rahmandad, H. and Sterman, J. [2008], ‘Heterogeneity and Network Structure in the Dynamics of Diffusion: Comparing Agent-Based and Differential Equation Models’, *Management Science* **54**(5), 998–1014.
URL: <http://mansci.journal.informs.org/content/54/5/998.abstract>
108. Roberts, L. and Enserink, M. [2007], ‘Malaria. Did they really say ... eradication?’, *Science* **318**(5856), 1544–5.
URL: <http://www.sciencemag.org/content/318/5856/1544.short>
109. Rodriguez, D. J. and Torres-Sorando, L. [2001], ‘Models of infectious diseases in spatially heterogeneous environments.’, *Bulletin of Mathematical Biology* **63**(3), 547–71.
URL: <http://www.ncbi.nlm.nih.gov/pubmed/11374305>
110. Ross, R. [1911], *The Prevention of Malaria*, John Murray, Albemarle Street.
URL: <http://books.google.com/books?id=GDUzAQAAMAAJ&pgis=1>
111. Sachs, J. and Malaney, P. [2002], ‘The economic and social burden of malaria.’, *Nature* **415**(6872), 680–5.
URL: <http://dx.doi.org/10.1038/415680a>
112. Sattenspiel, L. and Lloyd, A. [2009], *The geographic spread of infectious diseases: models and applications*, Princeton University Press, Princeton.
URL: http://books.google.com/books?id=jtGP_qwD1MgC&pgis=1
113. Sharp, B., Craig, M., Mnzava, A., Curtis, B., Maharaj, R. and Kleinschmidt, I. [2001], Review of Malaria in South Africa, Technical report, Health Systems Trust.
114. Sharp, B. L., Kleinschmidt, I., Streat, E., Maharaj, R., Barnes, K. I., Durrheim, D. N., Ridl, F. C., Morris, N., Seocharan, I., Kunene, S., La-Grange, J. J. P., Mthembu, J. D., Maartens, F., Martin, C. L. and Barreto, A. [2007], ‘Seven years of regional malaria control collaboration - Mozambique, South Africa and Swaziland’, *American Journal of Tropical Medicine and Hygiene* **76**(1), 42–47.
115. Sharp, B. L. and le Sueur, D. [1996], ‘Malaria in South Africa—the past, the present and selected implications for the future.’, *South African Medical Journal* **86**(1), 83–90.
URL: <http://www.ncbi.nlm.nih.gov/pubmed/8685790>
116. Silal, S. P., Barnes, K. I., Kok, G., Mabuza, A. and Little, F. [2013], ‘Exploring the seasonality of reported treated malaria cases in Mpumalanga, South Africa.’, *PloS one* **8**(10), e76640.
URL: <http://www.plosone.org/article/info%3Adoi%2F10.1371%2Fjournal.pone.0076640>
117. Silal, S. P., Little, F., Barnes, K. I. and White, L. J. [2014], ‘Towards malaria elimination in Mpumalanga, South Africa: A population-level mathematical modeling approach’, *Malaria Journal* **13**(297).
URL: <http://www.malariajournal.com/content/pdf/1475-2875-13-297.pdf>

-
118. Slater, H. C., Walker, P. G., Bousema, T., Okell, L. C. and Ghani, A. C. [2014], ‘The potential impact of adding ivermectin to a mass treatment intervention to reduce malaria transmission: a modelling study’, *Journal of Infectious Diseases* p. 351.
119. Smith, D. L., Dushoff, J. and McKenzie, F. E. [2004], ‘The risk of a mosquito-borne infection in a heterogeneous environment.’, *PLoS Biology* **2**(11).
URL: <http://dx.plos.org/10.1371/journal.pbio.0020368>
120. Smith, T., Killeen, G. F., Maire, N., Ross, A., Molineaux, L., Tediosi, F., Hutton, G., Utzinger, J., Dietz, K. and Tanner, M. [2006], ‘Mathematical modeling of the impact of malaria vaccines on the clinical epidemiology and natural history of *Plasmodium falciparum* malaria: Overview’, *The American Journal of Tropical Medicine and Hygiene* **75**(2 suppl), 1–10.
121. Smith, T., Maire, N., Dietz, K., Killeen, G. F., Vounatsou, P., Molineaux, L. and Tanner, M. [2006], ‘Relationship between the entomologic inoculation rate and the force of infection for *Plasmodium falciparum* malaria’, *The American Journal of Tropical Medicine and Hygiene* **75**(2 suppl), 11–18.
122. Smith, T., Maire, N., Ross, a., Penny, M., Chitnis, N., Schapira, a., Studer, a., Genton, B., Lengeler, C., Tediosi, F., de Savigny, D. and Tanner, M. [2008], ‘Towards a comprehensive simulation model of malaria epidemiology and control.’, *Parasitology* **135**(13), 1507–16.
URL: <http://www.ncbi.nlm.nih.gov/pubmed/18694530>
123. Starzengruber, P., Fuehrer, H.-P., Ley, B., Thriemer, K., Swoboda, P., Habler, V. E., Jung, M., Graninger, W., Khan, W. A., Haque, R. and Noedl, H. [2014], ‘High prevalence of asymptomatic malaria in south-eastern Bangladesh.’, *Malaria Journal* **13**, 16.
URL: <http://www.malariajournal.com/content/13/1/16>
124. *STATA: Data Analysis and Statistical Software* [2013].
URL: www.stata.com
125. *Statistical release Mid-year population estimates* [2011], Technical report, Statistics South Africa.
URL: <http://www.statssa.gov.za/publications/P0302/P03022011.pdf>
126. Struchiner, C. J., Halloran, M. E. and Spielman, A. [1989], ‘Modeling malaria vaccines i: new uses for old ideas’, *Mathematical Biosciences* **94**(1), 87–113.
127. Tanser, F. C., Sharp, B. and le Sueur, D. [2003], ‘Potential effect of climate change on malaria transmission in Africa.’, *Lancet* **362**(9398), 1792–8.
URL: [http://dx.doi.org/10.1016/S0140-6736\(03\)14898-2](http://dx.doi.org/10.1016/S0140-6736(03)14898-2)

BIBLIOGRAPHY

128. Tatem, A. J. and Smith, D. L. [2010], ‘International population movements and regional *Plasmodium falciparum* malaria elimination strategies.’, *Proceedings of the National Academy of Sciences of the United States of America* **107**(27), 12222–7.
URL: <http://www.pnas.org/content/107/27/12222.short>
129. The malERA Consultative Group on Basic Science and Enabling [2011], ‘A research agenda for malaria eradication: basic science and enabling technologies.’, *PLoS Medicine* **8**(1).
URL: <http://www.plosmedicine.org/article/info%3Adoi%2F10.1371%2Fjournal.pmed.1000399>
130. The malERA Consultative Group on Diagnoses [2011], ‘A Research Agenda for Malaria Eradication: Diagnoses and Diagnostics’, *PLoS Medicine* **8**(1).
URL: <http://www.plosmedicine.org/article/info%3Adoi%2F10.1371%2Fjournal.pmed.1000396>
131. The malERA Consultative Group on Drugs [2011], ‘A research agenda for malaria eradication: drugs.’, *PLoS medicine* **8**(1).
URL: <http://www.plosmedicine.org/article/info%3Adoi%2F10.1371%2Fjournal.pmed.1000402>
132. The malERA Consultative Group on Modeling [2011], ‘A research agenda for malaria eradication: modeling.’, *PLoS medicine* **8**(1).
URL: <http://www.plosmedicine.org/article/info%3Adoi%2F10.1371%2Fjournal.pmed.1000403>
133. The malERA Consultative Group on Vector Control [2011], ‘A research agenda for malaria eradication: vector control.’, *PLoS medicine* **8**(1).
URL: <http://www.plosmedicine.org/article/info%3Adoi%2F10.1371%2Fjournal.pmed.1000401>
134. Thomson, D. [1911], *A Research Into the Production, Life and Death of Crescents in Malignant Tertian Malaria, in Treated and Untreated Cases, by an Enumerative Method; The Leucocytes in Malarial Fever: A Method of Diagnosing Malaria Long After it is Apparently Cured*, University Press.
135. Torres-Sorando, L. and Rodriguez, D. J. [1997], ‘Models of spatio-temporal dynamics in malaria’, *Ecological Modelling* **104**(2-3), 231–240.
URL: [http://dx.doi.org/10.1016/S0304-3800\(97\)00135-X](http://dx.doi.org/10.1016/S0304-3800(97)00135-X)
136. Tumwiine, J., Mugisha, J. and Luboobi, L. [2010], ‘A host-vector model for malaria with infective immigrants’, *Journal of Mathematical Analysis and Applications* **361**(1), 139–149.
URL: <http://linkinghub.elsevier.com/retrieve/pii/S0022247X09007185>
137. *Use of Antimalarials to Reduce Malaria Transmission* [2014].
URL: <http://www.cdc.gov/malaria/malaria-worldwide/reduction/mda-mft.html>
138. *Vector control: methods for use by individuals and communities* [1997], Technical report, World Health Organization.
URL: <http://www.who.int/malaria/publications/atoz/9241544945/en/index.html>

139. Vittorini, P. and di Orio, F. [2013], *7th International Conference on Practical Applications of Computational Biology & Bioinformatics*, Vol. 222 of *Advances in Intelligent Systems and Computing*, Springer International Publishing, Heidelberg.
URL: <http://link.springer.com/10.1007/978-3-319-00578-2>
140. von Seidlein, L. [2014], ‘The failure of screening and treating as a malaria elimination strategy.’, *PLoS Medicine* **11**(1).
URL: <http://dx.plos.org/10.1371/journal.pmed.1001595>
141. White, L. J., Maude, R. J., Pongtavornpinyo, W., Saralamba, S., Aguas, R., Van Effelterre, T., Day, N. P. J. and White, N. J. [2009], ‘The role of simple mathematical models in malaria elimination strategy design.’, *Malaria Journal* **8**, 212.
URL: <http://www.malariajournal.com/content/8/1/212>
142. White, N. J. [2008], ‘The role of anti-malarial drugs in eliminating malaria.’, *Malaria Journal* **7**(Suppl 1).
URL: <http://www.malariajournal.com/content/7/S1/S8>
143. WHO — *Factsheet on the World Malaria Report 2012* [2012], Technical report, World Health Organisation.
URL: http://www.who.int/malaria/media/world_malaria_report_2012_facts/en/index.html
144. WHO — *Factsheet on the World Malaria Report 2013* [n.d.], Technical report, World Health Organization.
URL: http://www.who.int/malaria/media/world_malaria_report_2013/en/
145. WHO — *Malaria* [2014].
URL: <http://www.who.int/topics/malaria/en/>
146. Worrall, E., Basu, S. and Hanson, K. [2005], ‘Is malaria a disease of poverty? A review of the literature.’, *Tropical medicine and International Health* **10**(10), 1047–59.
URL: <http://www.ncbi.nlm.nih.gov/pubmed/16185240>
147. Yang, H. M. [2000], ‘Malaria transmission model for different levels of acquired immunity and temperature-dependent parameters (vector).’, *Revista de saude publica* **34**(3), 223–31.
URL: <http://www.ncbi.nlm.nih.gov/pubmed/10920443>
148. Yang, H. M. and Ferreira, M. U. [2000], ‘Assessing the effects of global warming and local social and economic conditions on the malaria transmission.’, *Revista de saude publica* **34**(3), 214–22.
URL: <http://www.ncbi.nlm.nih.gov/pubmed/10920442>
149. Zaloumis, S., Humberstone, A., Charman, S. A., Price, R. N., Moehrle, J., Gamo-Benito, J., McCaw, J., Jansen, K. M., Smith, K. and Simpson, J. A. [2012], ‘Assessing the utility

- of an anti-malarial pharmacokinetic-pharmacodynamic model for aiding drug clinical development.', *Malaria Journal* **11**(1).
URL: <http://www.malariajournal.com/content/11/1/303>
150. Zambrano-Bigiarini, M. and Rojas, R. [2013], *hydroPSO: Particle Swarm Optimisation, with focus on Environmental Models*. R package version 0.3-3 — For new features, see the 'NEWS' file (on CRAN, rforge or the package source).
URL: <http://www.rforge.net/hydroPSO>, <http://cran.r-project.org/web/packages/hydroPSO>
151. Zambrano-Bigiarini, M., Rojas and R. [2013], 'A model-independent particle swarm optimisation software for model calibration', *Environmental Modelling and Software* **43**, 5–25.
URL: <http://dx.doi.org/10.1016/j.envsoft.2013.01.004>
152. Zorom, M., Zongo, P., Barbier, B. and Somé, B. [2012], 'Optimal control of a spatio-temporal model for malaria: Synergy treatment and prevention', *Journal of Applied Mathematics* .

BIBLIOGRAPHY

Appendix A

Model Code

A.1 Model 1 - Population model of malaria transmission

```
#Packages
library(foreign)
library(lhs)
library(optimx)

#Data import
#casem<-read.dta("/Volumes/SHEETAL PHD/PhD/Data/MPM data/Case data/casesmonth.dta")
#casem<-data.frame(casem)
alldata<-read.dta("/Volumes/SHEETAL PHD/PhD/Data/MPM data/Case data/onep.dta")
fitdata<-read.dta("/Volumes/SHEETAL PHD/PhD/Data/MPM data/Case data/onep2002-2008.dta")
fitdata<-data.frame(fitdata)

#Time set up
N<- 4500000 # population size
dt<- 1/52 #time step
stoptime<- 2020
starttime<- 1992

tsteps<-(stoptime - starttime)/dt
time<- (1:tsteps+1)*dt - dt
time2<-array(0,c(tsteps+1))
time2[2:(tsteps+1)]=starttime+time
time2[1]=starttime
```

APPENDIX A. MODEL CODE

```
#Interventions
#10\% additional vector control
vcaddlon=0

#10\% ITN coverage control
itnon=0
itn<-array(0,(tsteps+1))
for (i in 1094:(tsteps+1)) {itn[i]=0.3}

#MDA/MSAT
mdaon=0
msaton=0
dlfon=0
dlfp = 0
vcaddon=0

#####
#Deterministic One Patch Model

dim<-22 # no of stocks
nf<-75 #no of flows

parms<- c(betapl=12.54, lambdaf=0.003046,p=0.8)

onep<-function(parms,time) {

  #Parameters
  betapl=parms[1] # local contact rate
  #betapf=parms[2] # foreign contact rate
  lambdafp=parms[2] #foreign contact *foreign prop infectiousness
  p=parms[3] #Pr(trt)
  #pl=parms[3] # Pr(local trt)
  #pf=parms[4] # Pr(for trt)
  #finv=parms[5] # Prop foreign infectiousness
  mu<-0.0175 # natural mortality rate
  delta=1/(26/52) # natural recovery rate for naive pop
  sigma1=1 #time to latency (weeks)
  sigma2=1/(2/52) # gametocytemia
  q=(1/(1.5/52)) #clearance +seek trt
  #flag=parms[5]
  #llag=parms[7]
  totstr=699100
```

```

#amp=parms[4]
#peak=0
adh=0.9 #ref barnes:2005

#Interventions
# Mass Drug Administration
mstart=1094 # week of the year when mda is started
mdur=8/52 #
mcure=1/(4/52) # cure rate for mda drug +protective effect
mpoc<-array(0,c(tsteps+1)) # prophylactic effect of mda drug vector
mpocp=0 #poc parameter
mcov=0.8 #mda coverage
mrounds=6 # no. of rounds
mspace=8 #time between rounds
mrate<-array(0,c(tsteps+1))
for (j in 1:mrounds) {
for (i in ((mstart+4+26*w+(j-1)*mspace):(mstart+26*w+(j-1)*mspace+(mdur*52-1)))) \\
    {mrate[i]= mdaon*(-log(1-mcov)/mdur)}
mpoc[(mstart+4+26*w+(j-1)*mspace+(mdur*52)):(mstart+26*w+(j-1)*mspace+(mdur*52)+
    mpocp)]
    =1/(0.0000144/52) }

# Changing lambda_f - foreigners
lfstart=1094+4 # week of the year when msat is started
lfdur=52/52 # msat duration
dlf<-array(0,(tsteps+1))
lfrounds=7 # no. of rounds
lfspace= 52 #time between rounds
lfrate<-array(0,c(tsteps+1))
for (j in 1:lfrounds) {
    for (i in ((lfstart+26*w+(j-1)*lfspace):(lfstart+26*w+(j-1)*lfspace+(lfdur*52-1)
    )))
        {dlf[i]= dlfon*dlfp}}

# Mass Screen and Treat - foreigners
msstart=1094+4#1137 # week of the year when msat is started
msdur=26/52 # msat duration
mscure=1/(0.5/52) # cure rate for mda/msat drug
mspoc<-array(0,c(tsteps+1)) # prophylactic effect of mda/msat drug vector
mspocp=1/(3/52) #poc parameter (ref: phiri 2012)
mscov=0.7 #msat coverage

```

APPENDIX A. MODEL CODE

```

msrounds=7 # no. of rounds
msspace= 52 #time between rounds
mseff = 1 # sensitivity of screening
msprop<-array(0,c(tsteps+1)) #prop treated with msat
msrate<-array(0,c(tsteps+1))
for (j in 1:msrounds) {
  #for (i in ((msstart+26*w+(j-1)*msspace):(msstart+26*w+(j-1)*msspace+(msdur*52-1)
    )))\\
    { msrate[i]= msaton*(-log(1-mscov*mseff)/msdur) }
  #mspoc[(msstart+26*w+(j-1)*msspace+(msdur*52-1)):
    (msstart+26*w+(j-1)*msspace+(msdur*52-1)+mspocp)]=1/(0.0000144/52)
  msprop[(msstart+26*w+(j-1)*msspace):(msstart+26*w+(j-1)*msspace+((msdur*52)-1))
    ]\\
    =mseff*mscov }

# Vector Control
vcon=1 # switch on vec con
tvc = 469 # week when vc starts
vceff=0.92 # vc efficacy
vcadd1<-array(0,(tsteps+1))
for (i in 1094+4:(tsteps+1)) {vcadd1[i]=2/9}
vc <-array(0,c(tsteps+1))
vccov<-array(0,(tsteps+1))
for (i in 468:520){vccov[i]=168400/(52*totstr)*i-9*168400/totstr} #2001
for (i in 521:572) {vccov[i]=154070/totstr} #2002
for (i in 573:624) {vccov[i]=170313/totstr} #2003
for (i in 625:676) {vccov[i]=155644/totstr} #2004
for (i in 677:728) {vccov[i]=167762/totstr} #2005
for (i in 729:780) {vccov[i]=474174/totstr} #2006
for (i in 781:832) {vccov[i]=471624/totstr}#2007
for (i in 833:885) {vccov[i]=544654/totstr} #2008
for (i in 886:937) {vccov[i]=561597/totstr} #2009
for (i in 938:989) {vccov[i]=627684/totstr} #2010
for (i in 990:1041) {vccov[i]=563587/totstr} #2011
for (i in 1042:1093) {vccov[i]=537206/totstr} #2012
for (i in 1094:(tsteps+1)) {vccov[i]=537506/totstr} #2013:2020
for (i in 468:(tsteps+1)){ vc[i]=(vccov[i]+vcadd1on*vcadd1[i])*vceff}

#Information matrices
v<- array(0, c(dim,tsteps+1))
betal<-array(0, c(tsteps+1))

```

```
betaf<-array(0, c(tsteps+1))
pop<- array(0, c(tsteps+1))
tib1p<-array(0,c(tsteps+1))
loc1p<-array(0,c(tsteps+1))
for1p<-array(0,c(tsteps+1))
trtfor<-array(0,c(tsteps+1))
trtloc<-array(0,c(tsteps+1))
seas<- array(0, c(tsteps+1))
seasl<- array(0, c(tsteps+1))
seasf<- array(0, c(tsteps+1))
lambda<-array(0, c(tsteps+1))
lambdaf<-array(0, c(tsteps+1))
plambda<-array(0, c(tsteps+1))
nplambda<-array(0, c(tsteps+1))
plambdaf<-array(0, c(tsteps+1))
nplambdaf<-array(0, c(tsteps+1))
mdaplambdaf<-array(0, c(tsteps+1))
mdanplambda<-array(0, c(tsteps+1))
mdaplambdaf<-array(0, c(tsteps+1))
mdanplambdaf<-array(0, c(tsteps+1))
msplambdaf<-array(0, c(tsteps+1))
msnplambdaf<-array(0, c(tsteps+1))
sus<-array(0, c(tsteps+1))
inf<-array(0, c(tsteps+1))
infts<-array(0, c(tsteps+1))
tot<-array(0, c(tsteps+1))
trt1p<-array(0,c(tsteps+1))
casel1p<-array(0,c(tsteps+1))
casel1p<-array(0,c(tsteps+1))
casef1p<-array(0,c(tsteps+1))
cinc1p<-array(0,c(tsteps+1))
ctr1p<-array(0,c(tsteps+1))
cp1p<-array(0,c(tsteps+1))
rxl<-array(0,c(tsteps+1))
for (i in 1:(tsteps+1)){rxl[i]=p}
rxl<-array(0,c(tsteps+1))
for (i in 1:(tsteps+1)){rxl[i]=p}
mflow<-array(0, c(tsteps+1))
mstock<-array(0, c(tsteps+1))
msus<-array(0, c(tsteps+1))
msflow<-array(0, c(tsteps+1))
msstock<-array(0, c(tsteps+1))
mssus<-array(0, c(tsteps+1))
```

APPENDIX A. MODEL CODE

```
msinf<-array(0, c(tsteps+1))
msinfect<-array(0, c(tsteps+1))

# seasonality
tscase=ts(alldata$caseweekall, start=2002, frequency=52)
tssourcel = ts(alldata$sourcetotl, start=2002, frequency=52)
tssourcef = ts(alldata$sourcetotf, start=2002, frequency=52)
stlcase<-stl(tscase, "per")
stlf<-stl(tssourcef, "per")
stll<-stl(tssourcel, "per")
s<-as.vector(stlcase$time.series[,1])
f<-as.vector(stlf$time.series[,1])
l<-as.vector(stll$time.series[,1])
ss=(s-min(s))/(max(s)-min(s))
sf=(f-min(f))/(max(f)-min(f))
sl=(l-min(l))/(max(l)-min(l))
seas=rep(ss[1:52], (stoptime-starttime) )
seasl=rep(sl[1:52], (stoptime-starttime) )
seasf=rep(sf[1:52], (stoptime-starttime) )

#Initial Conditions
v11<-4499324 #449324
v21<-145
v31<-145
v41<-100
v51<-100
v61<-38
v71<-38
v81<-50

v[1,1]= v11 # Susceptibles (450000 - sum of rest = 449324)
v[2,1]= v21 # 20 # Infected & Treated (Local)
v[3,1]= v31 #100 # Infectious & Treated (Local) (v12+v13 = 290)
v[4,1]= v41 # 56 # Infected & Not treated (Local)
v[5,1]= v51 # 100 # Infectious & Not Treated (Local)
v[6,1]= v61 #100 # Infected & Treated (Foreign)
v[7,1]= v71 #40 # Infectious & Treated (Foreign) (v2+v4 = 76)
v[8,1]= v81 #250 # Infected & Not treated (Foreign)
v[9,1]= N - (v[1,1]+v[2,1]+ v[3,1]+v[4,1]+v[5,1]+ v[6,1] +v[7,1] +v[8,1])
#100 #Infectious & Not Treated (foreign)
v[10,1]=0 # Susceptible MDA
```

```

v[11,1]=0 # Infected MDA
v[12,1]=0 # Infectious MDA
v[13,1]=0 # Susceptible MSAT-f
v[14,1]=0 # Infected/Infectious MSAT-f
v[15,1]=0 # 20 # POST MDA Infected & Treated (Local)
v[16,1]= 0 #100 # POST MDA Infectious & Treated (Local) (v12+v13 = 290)
v[17,1]= 0 # 56 # POST MDAInfected & Not treated (Local)
v[18,1]= 0 # 100 #POST MDA Infectious & Not Treated (Local)
v[19,1]= 0 #100 # POST MDAInfected & Treated (Foreign)
v[20,1]= 0 #40 # POST MDAInfectious & Treated (Foreign) (v2+v4 = 76)
v[21,1]= 0 #250 #POST MDA Infected & Not treated (Foreign)
v[22,1]= 0 #100 #POST MDA Infectious & Not Treated (foregin)

pop[1]= sum(v[,1])
tib1p[1]=pop[1] - (v[1,1]+v[10,1]+v[13,1])
case1p[1] = tib1p[1]

#Model

for (t in 2:(tsteps+1)) {

#seasl = amp*cos(2*pi*(time-peak))

betal[1]=betapl*(0.05+seasl[1])
if (vcon==1) betal[t]=betapl*(1-itnon*itn[t])*(0.05+seasl[t])*(1-(vc[t])) \\
else betal[t]=betapl*(1-itnon*itn[t])*(0.05+seasl[t])
lambdaf[1]=lambdafp*(seasf[1])
lambdaf[t]=lambdafp*(seasf[t])

lambda[1]= betal[1]*((v[3,1]+v[5,1]+v[7,1]+v[9,1]+v[16,1]+v[18,1]+v[20,1]+v
[22,1]) \\
/pop[1])
lambda[t] = betal[t]*((v[3,t-1]+v[5,t-1]+v[7,t-1]+v[9,t-1]+v[16,t-1]+v[18,t-1]\\
+v[20,t-1]+v[22,t-1])/pop[t-1])
plambda[1] = rxl[1]*lambda[1]
plambda[t] = rxl[t]*lambda[t]
nplambda[1] = (1-rxl[1])*lambda[1]
nplambda[t] = (1-rxl[t])*lambda[t]
plambdaf[1] = rxf[1]*(1-msaton*msprop[1])*lambdaf[1]*(1-dlf[1])
plambdaf[t] = rxf[t]*(1-msaton*msprop[t])*lambdaf[t]*(1-dlf[t])
nplambdaf[1] = (1-rxf[1])*(1-msaton*msprop[1])*lambdaf[1]*(1-dlf[1])
nplambdaf[t] = (1-rxf[t])*(1-msaton*msprop[t])*lambdaf[t]*(1-dlf[t])

```

```

if (mrate[t]>0) {
mdaplambd[1] = rxl[1]*lambda[1]
mdaplambd[t] = rxl[t]*lambda[t]
mdanplambd[1] = (1-rxl[1])*lambda[1]
mdanplambd[t] = (1-rxl[t])*lambda[t]
mdaplambdaf[1] = rxf[1]*(1-msaton*msprop[1])*lambdaf[1]*(1-dlf[1])
mdaplambdaf[t] = rxf[t]*(1-msaton*msprop[t])*lambdaf[t]*(1-dlf[t])
mdanplambdaf[1] = (1-rxf[1])*(1-msaton*msprop[1])*lambdaf[1]*(1-dlf[1])
mdanplambdaf[t] = (1-rxf[t])*(1-msaton*msprop[t])*lambdaf[t]*(1-dlf[t]) }

#MSAT flows
msplambdaf[1] = rxf[1]*(msaton*msprop[1])*lambdaf[1]*(1-dlf[1])
msplambdaf[t] = rxf[t]*(msaton*msprop[t])*lambdaf[t]*(1-dlf[t])
msnplambdaf[1] = (1-rxf[1])*(msaton*msprop[1])*lambdaf[1]*(1-dlf[1])
msnplambdaf[t] = (1-rxf[t])*(msaton*msprop[t])*lambdaf[t]*(1-dlf[t])

#flow matrix
# f<-(parameter, out, in)
f<-rbind(c(mu,1,1), c(mu,2,1), c(mu,3,1), c(mu,4,1), c(mu,5,1), c(mu,6,1),c(mu
,7,1),
c(mu,8,1),c(mu,9,1),c(mu,10,1),c(mu,11,1),c(mu,12,1),c(mu,13,1),c(mu,14,1),c(
mu,15,1),
c(mu,16,1),c(mu,17,1),c(mu,18,1), c(mu,19,1),c(mu,20,1),c(mu,21,1),c(mu
,22,1),
c(plambd[t-sigma1],1,2), c(nplambd[t-sigma1],1,4), c(plambdaf[t-sigma1
],1,6),
c(nplambdaf[t-sigma1],1,8),c(mdaplambd[t-sigma1],10,15), c(mdanplambd[t-
sigma1],10,17),
c(mdaplambdaf[t-sigma1],10,19), c(mdanplambdaf[t-sigma1],10,21), c(sigma2
,2,3),
c(sigma2, 4,5), c(sigma2,6,7), c(sigma2, 8,9), c(sigma2,15,16),c(sigma2,
17,18),
c(sigma2,19,20), c(sigma2, 20,21),c(q,2,1), c(q,3,1), c(q,6,1), c(q,7,1),c(q
,15,10),
c(q,16,10), c(q,19,10), c(q,20,10), c(delta,5,1), c(delta, 9,1),c(delta
,18,10), c(delta, 22,10),
c(sigma2,11,12), c(adh*mcure,11,10), c(adh*mcure,12,10), c(adh*mscure,14,13),
c(mpoc[t],10,1),c(mspocp,13,1),c(mpoc[t],15,2), c(mpoc[t],16,3),c(mpoc[t
],17,4),c(mpoc[t],18,5),
c(mpoc[t],19,6),c(mpoc[t],20,7),c(mpoc[t],21,8),c(mpoc[t],22,9),c(mrate[t
],1,10), c(mrate[t],2,11),
c(mrate[t],4,11), c(mrate[t],6,11),c(mrate[t],8,11),c(mrate[t],3,12),c(mrate[
t],5,12),

```

```

c(mrate[t],7,12),c(mrate[t],9,12), c(msplambdaf[t],1,14),c(msnplambdaf[t
],1,14))

flow<- array(0,c(1,nf))
for (g in 1:nf) {
  flow[g]<-v[f[g,2],t-1]*(1-exp(-f[g,1]*dt)) }

v[,t] = v[,t-1]
for (g in 1:nf) {
  v[f[g,2],t] = v[f[g,2],t]- flow[g]
  v[f[g,3],t] = v[f[g,3],t]+ flow[g]
} #end g

pop[t]= sum(v[,t])
tib1p[t]= pop[t]- (v[1,t]+v[10,t] +v[13,t])
loc1p[t]= v[2,t] +v[3,t]+v[4,t]+v[5,t] +v[15,t] +v[16,t]+v[17,t]+v[18,t]
for1p[t]= v[6,t] +v[7,t]+v[8,t]+v[9,t] +v[14,t] +v[19,t] +v[20,t]+v[21,t]+v[22,t]
sus[t]= v[1,t]+v[10,t] +v[13,t]
inf[t]= v[2,t]+ v[4,t]+v[6,t]+ v[7,t]+v[11,t]+ v[15,t]+v[17,t]+ v[19,t]+v[21,t]
inf1s[t]=v[3,t]+v[5,t]+v[7,t]+ v[9,t]+v[12,t] +v[14,t]+ v[16,t]+v[18,t]+ v[20,t]+
v[22,t]
trtfor[t]=flow[41]+flow[42]+flow[45]+flow[46]
trtloc[t]=flow[39]+flow[40]+flow[43]+flow[44]
tot[t]=sus[t]+inf[t]+inf1s[t]
case1p[t] = flow[23]+flow[24]+flow[25]+flow[26]+flow[27]+flow[28]+flow[29]+flow
[30]
case1p[t] = flow[23]+flow[24]+flow[27]+flow[28]
case1p[t] =flow[25]+flow[26]+flow[29]+flow[30]
trt1p[t] = trtfor[t]+trtloc[t]
cinc1p[t] = cinc1p[t-1]+case1p[t]
ctr1p[t] = ctr1p[t-1]+trt1p[t]
cp1p[t] = ctr1p[t]/cinc1p[t]
mflow[t]=flow[65]+flow[66]+flow[67]+flow[68]+flow[69]+flow[70]+flow[71]+flow[72]+
flow[73]
mstock[t]=v[10,t]+v[11,t]+v[12,t]
msus[t]= v[10,t]
msflow[t]=flow[74]+flow[75]
mstock[t]=v[13,t]+v[14,t]
mssus[t]= v[13,t]
msinf[t] = v[14,t]

} # end t

```

```
return(as.vector(list(vc=vc, pop=pop, plambda=plambda, nplambda=nplambda, \\
  plambdaf=plambdaf, nplambdaf=nplambdaf, betal=betal, betaf=betaf, seas=seas, \\
  seasl=seasl, seasf=seasf, sus=sus, inf=inf, infts=infts, trtloc=trtloc, trtfor=
  trtfor, \\
  tib1p=tib1p, loc1p=loc1p, for1p=for1p, case1p=case1p, case1p=case1p, \\
  casef1p=casef1p, trt1p=trt1p, cinclp=cinclp, ctrt1p=ctrt1p, cptrt1p=cptrt1p
  , \\
  mflow=mflow, mstock=mstock, \\msus=msus, msflow=msflow, msstock=msstock, \\
  mssus=mssus, msinf=msinf, msinfect=msinfect)))
} #end function
```

A.2 Model 2 - Metapopulation model of malaria transmission

```

library(foreign)
library(optimx)
library(hydroPSO)
library(parallel)
library(multicore)
library(sp)
library(maptools)
library(rgeos)
library(gplots)
library(doParallel)
registerDoParallel(cores=23)

lm<-read.dta("/Users/sheetalprakashsilal/Desktop/Modelfit/Multipatch2/2002-2012-EDM-
wide-full.dta")
map<-read.dta("/Users/sheetalprakashsilal/Desktop/Modelfit/Multipatch2/maputo.dta")
spray<-read.csv("/Users/sheetalprakashsilal/Desktop/Modelfit/Multipatch2/SprayMP.csv
")

tslm=ts(lm, start=2002, frequency=52)
tsmap = ts(map, start=2002, frequency=12)
c2<-rbind(c(32.45049, -25.54154), c(32.94872, -26.01871), \
c(32.72298, -25.84556), c(32.91575, -25.97316)) #map centroids
c1<-rbind(c(30.57137, -25.06539), c(31.12738, -25.33060), c(31.00102, -25.74883), \
c(31.73014, -25.50319), c(31.52450, -24.55777)) # loc centroids
popdata<-c(98000,590000,70000, 390000, 540000)

#Time & Space set up
n<-popdata # population size
dt<- 1/52 #time step
stoptime<- 2020
starttime<- 1992
dim<-15 # no of stocks
nf<-2424 #1356 #no of flows
np<-6 #no of patches (5 local + 1 foreign) (TC, MB, UJ, NK, BB, MP)
nsp<-3 #no of sub-patches 1 - local in patch, 2 - local back from travel, 3 - foreign
visiting patch

tsteps<-(stoptime - starttime)/dt
time<- (1:(tsteps+4))*dt - dt
time2<-array(0, c(tsteps+4))

```

```

time2[4:(tsteps+4)]=starttime+time
time2[3]=starttime-dt
time2[2]=starttime-2*dt
time2[1]=starttime-3*dt

year<-array(starttime:stoptime,c(stoptime-starttime))
month<-array(1:((stoptime-starttime)*13),c((stoptime-starttime)*13))

seasl<-array(0,c(tsteps+4,np))
stlTC1=stl(tslm[,1],"per")$time.series[,1]
stlMB1=stl(tslm[,4],"per")$time.series[,1]
stlUJ1=stl(tslm[,7],"per")$time.series[,1]
stlNK1=stl(tslm[,10],"per")$time.series[,1]
stlBBR1=stl(tslm[,13],"per")$time.series[,1]
sTC1=(stlTC1-min(stlTC1))/(max(stlTC1)-min(stlTC1))
sMB1=(stlMB1-min(stlMB1))/(max(stlMB1)-min(stlMB1))
sUJ1=(stlUJ1-min(stlUJ1))/(max(stlUJ1)-min(stlUJ1))
sNK1=(stlNK1-min(stlNK1))/(max(stlNK1)-min(stlNK1))
sBBR1=(stlBBR1-min(stlBBR1))/(max(stlBBR1)-min(stlBBR1))
seasl[5:(tsteps+4),1]=rep(sTC1[1:52],(stoptime-starttime))
seasl[5:(tsteps+4),2]=rep(sMB1[1:52],(stoptime-starttime))
seasl[5:(tsteps+4),3]=rep(sUJ1[1:52],(stoptime-starttime))
seasl[5:(tsteps+4),4]=rep(sNK1[1:52],(stoptime-starttime))
seasl[5:(tsteps+4),5]=rep(sBBR1[1:52],(stoptime-starttime))
stlmap = stl(tsmmap[,12],"per")$time.series[,1]
x=1:13
m1<-approx(x,stlmap[1:13],method="linear",n=52)
sMP =(m1$y - min(m1$y))/(max(m1$y)- min(m1$y))
seasl[5:(tsteps+4),6]=rep(sMP[1:52],(stoptime-starttime))
seasl[1:4,]=seasl[53:56,]

#Stochastic Model
#best week fit
w=0
mdaon=0
vcadd=array(0,c(tsteps+4,np))
msstart=1136 # week of the year when msat is started
msdur=26/52 # msat duration
mstart=1148 # week of the year when mda is started
mdur=8/52 #

```

```

mcure=1/(4/52) # cure rate for mda drug + protective period Phiri 2010
mpoc<-array(0,c(tsteps+4))
#mpoc<-array(0,c(tsteps+4, np, 8)) # prophylactic effect of mda drug vector
mpocp=0 #poc parameter
mcov=0.8 #mda coverage
mrounds=3 # no. of rounds
mspace=8 #time between rounds
mrate<-array(0,c(tsteps+4,np))
for (j in 1:mrounds) {
  for (i in ((mstart+26*w+(j-1)*mspace):(mstart+26*w+(j-1)*mspace+(mdur*52-1)))) {
mrate[i,2]= mdaon*(-log(1-mcov)/mdur)
mrate[i,4]= mdaon*(-log(1-mcov)/mdur)
mrate[i,5]= mdaon*(-log(1-mcov)/mdur)
# mrate[i,6]= mdaon*(-log(1-mcov)/mdur)
mpoc[(mstart+26*w+(j-1)*mspace+(mdur*52)):(mstart+26*w+(j-1)*mspace+mdur*52)+mpocp)
  ]=\\
1/(0.00144/52) }}

```

```

Params<-cbind(c(betaplTC=(0.3344071),
betaplMB=(2.1783218),
betaplUJ=(0.8050481),
betapK=(1.3303331),
betaplBBR=(8.3041098),
betaplMP=(94.9994004),
vceff=(0.90),
kappap=(48.6032236),
varpip1=(1258.828),
tsf1=(0.5654939),
varpip2=(319.042397),
zetap=(728.2441934),
fwgt=8.3849044,
tsf2=0.55,
lwgt=2.612637))

```

```

metap<-function(Parms,time,fmvton=1,lmvton=1,vcon=1,vcaddlon=0,msaton=0,mscov
=0.7, mdaon=0, w=0) {

```

```

#Movement and Distance
x1<-c1[,1]
y1<-c1[,2]
x2<-c2[,1]

```

```

y2<-c2[,2]

dis<-array(0, c(np, np))
for (d in 1:(np-1)) {
  for (od in 1:(np-1)) {
    dis[d,od]= 1/(1+(((x1[d]-x1[od])^2+(y1[d]-y1[od])^2)^0.5))^Parms[15]
    dis[d,d] = 0}}
lwgt=dis/rowSums(dis)
lwgt[6,]=0
lwgt[,6]=0

fdis<-array(0, c(np-1))
for (d in 1:(np-1)) {
  fdis[d]=1/(1+(((x1[d]-x2[1])^2+(y1[d]-y2[1])^2)^0.5))^Parms[13]}
fwgt = fdis/sum(fdis)
fwgt[6]=0

#Parameters
betapl=(Parms[1:6])
mu<-0.0105 # natural mortality rate
delta=1/(26/52) # natural recovery rate for naive pop
sigma1=1 #time to latency (weeks)
sigma2=1/(2/52) # gametocytemia
q=(1/(1.5/52)) #clearance +seek trt
m = 0.5 #mvt scaling factor
adh=0.9 #ref barnes:2005

# Vector Control
vceff=(Parms[7]) # vc efficacy
vc <-array(0,c(tsteps+4,np))
totstr=c(200, 100000, 5000, 300000, 260000, 1)
vccov<-array(0,c(tsteps+4,np))
for (i in 1:np) {vccov[1:(tsteps+4),i]=spray[1:(tsteps+4),(i+2)]/totstr[i]} #2001
for (i in 1:(tsteps+4)){ for(j in 1:np) { vc[i,j]=(vccov[i,j]+vcaddlon*vcadd[i,j])*
  vceff} }

# Mass Screen and Treat - foreigners
# msstart=1132 # week of the year when msat is started
# msdur=52/52 # msat duration
mscure=1/(0.5/52) # cure rate for mda/msat drug
mspoc<-array(0,c(tsteps+4)) # prophylactic effect of mda/msat drug vector
mspocp=1/(3.5/52) #poc parameter Protective period - cure time

```

```

#mscov=0.7 #msat coverage
msrounds=7 # no. of rounds
msspace= 52 #time between rounds
msprop<-array(0,c(tsteps+4)) #prop treated with msat
msrate<-array(0,c(tsteps+4))
for (j in 1:msrounds) {
  msprop[(msstart+26*w+(j-1)*msspace):(msstart+26*w+(j-1)*msspace+((msdur*52)-1))]=
    mscov }

# Mass Drug Administration

# mstart=1148 # week of the year when mda is started
#mdur=8/52 #
#mcure=1/(0.5/52) # cure rate for mda drug
#mpoc<-array(0,c(tsteps+4))
#mpoc<-array(0,c(tsteps+4, np, 8)) # prophylactic effect of mda drug vector
#mpocp=0 #poc parameter
#mcov=0.8 #mda coverage
# mrounds=3 # no. of rounds
#mspace=8 #time between rounds
#mrate<-array(0,c(tsteps+4,np))

#for (j in 1:mrounds) {
  # for (i in ((mstart+26*w+(j-1)*mspace):(mstart+26*w+(j-1)*mspace+(mdur*52-1))) {
    #mrate[i,2]= mdaon*(-log(1-mcov)/mdur)
    #mrate[i,4]= mdaon*(-log(1-mcov)/mdur)
    #mrate[i,5]= mdaon*(-log(1-mcov)/mdur)
    # mrate[i,6]= mdaon*(-log(1-mcov)/mdur)
    # mpoc[(mstart+26*w+(j-1)*mspace+(mdur*52)):(mstart+26*w+(j-1)*mspace+mdur*52)+
      mpocp] \\ =1/(0.00144/52) }}

#lay out mda strategies for p/w
stratmda<-array(0,c(tsteps+4, np, 8))
#strat1 = MB, NK, BBR @same time
stratmda[,2,1]=1
stratmda[,4,1]=1
stratmda[,5,1]=1
#strat2 = seq -B, M, N
stratmda[(mstart+26*w):(mstart+26*w+(mdur*52-1)),5,2]=1
stratmda[(mstart+26*w+mspace):(mstart+26*w+mspace+(mdur*52-1)),2,2]=1
stratmda[(mstart+26*w+2*mspace):(mstart+26*w+2*mspace+(mdur*52-1)),4,2]=1

```

```

#strat3 = seq -B, N, M
stratmda [( mstart+26*w):( mstart+26*w+(mdur*52-1)) ,5,3]=1
stratmda [( mstart+26*w+mspace):( mstart+26*w+mspace+(mdur*52-1)) ,4,3]=1
stratmda [( mstart+26*w+2*mspace):( mstart+26*w+2*mspace+(mdur*52-1)) ,2,3]=1
#strat4 = seq -N, M, B
stratmda [( mstart+26*w):( mstart+26*w+(mdur*52-1)) ,4,4]=1
stratmda [( mstart+26*w+mspace):( mstart+26*w+mspace+(mdur*52-1)) ,2,4]=1
stratmda [( mstart+26*w+2*mspace):( mstart+26*w+2*mspace+(mdur*52-1)) ,5,4]=1
#strat5 = seq -N, B,M
stratmda [( mstart+26*w):( mstart+26*w+(mdur*52-1)) ,4,5]=1
stratmda [( mstart+26*w+mspace):( mstart+26*w+mspace+(mdur*52-1)) ,5,5]=1
stratmda [( mstart+26*w+2*mspace):( mstart+26*w+2*mspace+(mdur*52-1)) ,2,5]=1
#strat6 = seq -M, B,N
stratmda [( mstart+26*w):( mstart+26*w+(mdur*52-1)) ,2,6]=1
stratmda [( mstart+26*w+mspace):( mstart+26*w+mspace+(mdur*52-1)) ,5,6]=1
stratmda [( mstart+26*w+2*mspace):( mstart+26*w+2*mspace+(mdur*52-1)) ,4,6]=1
#strat7 = seq -M, N,B
stratmda [( mstart+26*w):( mstart+26*w+(mdur*52-1)) ,2,7]=1
stratmda [( mstart+26*w+mspace):( mstart+26*w+mspace+(mdur*52-1)) ,4,7]=1
stratmda [( mstart+26*w+2*mspace):( mstart+26*w+2*mspace+(mdur*52-1)) ,5,7]=1

# for (j in 1:mrounds) {
#   for (i in (( mstart+26*w+(j-1)*mspace):( mstart+26*w+(j-1)*mspace+(mdur*52-1)))) {
#     for (k in 1:np) {mrate[i,k,]= mdaon*stratmda[i,k,]*(-log(1-mcov)/mdur)}
#     mpoc[( mstart+26*w+(j-1)*mspace+(mdur*52)):( mstart+26*w+(j-1)*mspace+mdur*52)+
#           mpocp),k,]= \\
1/(0.0000144/52) }}

#Information matrices
v<- array(0, c(dim,tsteps+4,np,nsp))
init<- array(0, c(dim,np))
pop<- array(0, c(tsteps+4,np,nsp))
beta<-array(0, c(tsteps+4,np))
N<- array(0, c(tsteps+4))
tibnsp<-array(0,c(tsteps+4,np,nsp))
tib<-array(0,c(tsteps+4))
trtnsp<-array(0,c(tsteps+4,np,nsp))
lambda<-array(0, c(tsteps+4,np))
plambda<-array(0, c(tsteps+4,np,nsp))
nplambda<-array(0, c(tsteps+4,np,nsp))
sus<-array(0, c(tsteps+4,np,nsp))

```

```

inf<-array(0, c(tsteps+4,np, nsp))
infts<-array(0, c(tsteps+4,np, nsp))
infi<-array(0, c(tsteps+4,np, nsp))
tot<-array(0, c(tsteps+4,np, nsp))
casensp<-array(0, c(tsteps+4,np, nsp))
p<-array(0, c(tsteps+4, np, nsp))
p[,1:6,1:2]=0.95 # Marianella's paper says 100% care seekign
p[1:731,1:6,3]= (Parms[10]) # fit - trt seeking for foreigners in a country
p[732:(tsteps+4),1:6,3]= (Parms[14]) # fit - trt seeking for foreigners in a
country
locmv<-array(0, c(tsteps+4, np))
formv<-array(0, c(tsteps+4, np))

# mvt
alpha<-array(0, c(np, nsp))
alpha[,2]<-(1/(2/52)) # nsp 2 moving back to nsp 1

zeta<-array(0, c(tsteps+4,np))
for (j in 1:np) {zeta[,j]=fmvton*1/(Parms[12]/52)*fwgt[j] }#foreign travel for
locals

varpi<-array(0, c(tsteps+4,np))
for (j in 1:np) {
varpi[1:731,j]=fmvton*1/(Parms[9]/52)*fwgt[j] # foreign travel
varpi[732:(tsteps+4),j]=fmvton*1/(Parms[11]/52)*fwgt[j] } # foreign travel for
foreigners

kappa<- 1/(Parms[8]/52) # FIT!!! local travel
lmvt<-lmvton*kappa*lwgt #mvt between local provinces

#Initial Values DATA
init=cbind(c(97999,0,0,0,0), # TC nsp 1
c(589942,18,18,0,0), #MB nsp 1
c(69988,3,3,0,0), #UJ nsp 1
c(389719,117,118,0,0), #NK nsp 1
c(539987,6,7,0,0), #BBR nsp 1
c(839800,100,100,0,0), #MP nsp 1
c(0,0,1,0,0), #TC nsp 2
c(0,0,20,0,0), #MB nsp 2
c(0,0,4,0,0), #UJ nsp 2
c(0,0,46,0,0), #NK nsp 2

```

```

        c(0,0,0,0,0), #BBR nsp 2
        c(0,0,0,0,0), #MP nsp 2
        c(0,0,0,0,0), #FC nsp 3
        c(0,0,2,0,0), #MB nsp 3
        c(0,0,2,0,0), #UJ nsp 3
        c(0,0,0,0,0), #NK nsp 3
        c(0,0,13,0,0), #BBR nsp 3
        c(0,0,0,0,0) #MP nsp 3
for(t in 1:4) {for (i in 1:np) {
  # Sub-patch 1 (local - local)
  v[1,t,i,1]= init[1,i] # Susceptibles
  v[2,t,i,1]= init[2,i] # Infected & Treated
  v[3,t,i,1]= init[3,i] # Infectious & Treated (v12+v13 = 290)
  v[4,t,i,1]= init[4,i] # Infected & Not treated
  v[5,t,i,1]= init[5,i] # 100 # Infectious & Not Treated
  #MDA stocks
  v[6,t,i,1]= 0 # MDA Susceptibles
  v[7,t,i,1]= 0 # MDA Infected
  v[8,t,i,1]= 0 # MDA Infectious
  #MSAT stocks
  v[9,t,i,1]= 0 # MSAT Susceptibles
  v[10,t,i,1]= 0 # MSAT Infected
  v[11,t,i,1]= 0 # MSAT Infectious
  #MDA-2nd level stocks
  v[12,t,i,1]= 0 # MDA Infected & Treated
  v[13,t,i,1]= 0 # MDA Infectious & Treated (v12+v13 = 290)
  v[14,t,i,1]= 0 # MDA Infected & Not treated
  v[15,t,i,1]= 0 # MDA 100 # Infectious & Not Treated
  # Sub-patch 2 (local - foreign)
  v[1,t,i,2]= init[1,i+6] # Susceptibles
  v[2,t,i,2]= init[2,i+6] # Infected & Treated
  v[3,t,i,2]= init[3,i+6] # Infectious & Treated (v12+v13 = 290)
  v[4,t,i,2]= init[4,i+6] # Infected & Not treated
  v[5,t,i,2]= init[5,i+6] # 100 # Infectious & Not Treated
  #MDA stocks
  v[6,t,i,2]= 0 # MDA Susceptibles
  v[7,t,i,2]= 0 # MDA Infected
  v[8,t,i,2]= 0 # MDA Infectious
  #MSAT stocks
  v[9,t,i,2]= 0 # MSAT Susceptibles
  v[10,t,i,2]= 0 # MSAT Infected
  v[11,t,i,2]= 0 # MSAT Infectious
  #MDA-2nd level stocks

```

```

v[12,t,i,2]= 0 # MDA Infected & Treated
v[13,t,i,2]= 0 # MDA Infectious & Treated (v12+v13 = 290)
v[14,t,i,2]= 0 # MDA Infected & Not treated
v[15,t,i,2]= 0 # MDA 100 # Infectious & Not Treated
# Sub-patch 3 (foreign)
v[1,t,i,3]= init[1,i+12] # Susceptibles
v[2,t,i,3]= init[2,i+12] # Infected & Treated
v[3,t,i,3]= init[3,i+12] # Infectious & Treated (v12+v13 = 290)
v[4,t,i,3]= init[4,i+12] # Infected & Not treated
v[5,t,i,3]= init[5,i+12] # 100 # Infectious & Not Treated
#MDA stocks
v[6,t,i,3]= 0 # MDA Susceptibles
v[7,t,i,3]= 0 # MDA Infected
v[8,t,i,3]= 0 # MDA Infectious
#MSAT stocks
v[9,t,i,3]= 0 # MSAT Susceptibles
v[10,t,i,3]= 0 # MSAT Infected
v[11,t,i,3]= 0 # MSAT Infectious
#MDA-2nd level stocks
v[12,t,i,3]= 0 # MDA Infected & Treated
v[13,t,i,3]= 0 # MDA Infectious & Treated (v12+v13 = 290)
v[14,t,i,3]= 0 # MDA Infected & Not treated
v[15,t,i,3]= 0 # MDA 100 # Infectious & Not Treated
}}

for (t in 1:4) {for (i in 1:np) { for (k in 1:nsp) {
  pop[t,i,k]= sum(v[,t,i,k])
  tibnsp[t,i,k]=pop[t,i,k]-v[1,t,i,k]
  beta[t,i]=betapl[i]*(seasl[t,i]+0.05)
  lambda[t,i]= beta[t,i]*(sum(v[3,t,i,1]+v[5,t,i,1]+v[3,t,i,2]+v[5,t,i,2]+v[3,t,i,3])\
    +v[5,t,i,3])/sum(pop[t,i,]))
  plambda[t,i,k] = p[t,i,k]*lambda[t,i]
  nplambda[t,i,k] = (1-p[t,i,k])*lambda[t,i]
  N[t]=sum(pop[t, ,])
  tib[t]= sum(tibnsp[t, ,])
} }}

#model

for (t in 5:(tsteps+4)) { #time
  #for (t in 5:6) { #time

```

```

#flow matrix
# f<-(parameter, v-out, patch(out), subp(out), v-in, patch(in), subp(in))
f<-c()
for (i in 1:np) {      # patch i
  for (k in 1:nsp) {  # subpatch k

    if (vcon==1) beta[t,i]=betapl[i]*(seasl[t,i]+0.05)*(1-(vc[t,i])) \\
    else beta[t,i]=betapl[i]*(seasl[t,i]+0.05)
    lambda[t,i] = beta[t,i]*(sum(v[3,t-4,i,1]+v[5,t-4,i,1]+v[3,t-4,i,2]+v[5,t-4,i,2]+ \\
    v[3,t-4,i,3]+v[5,t-4,i,3]+ v[13,t-4,i,1]+v[15,t-4,i,1]+v[13,t-4,i,2]+v[15,t-4,i,2]+ \\
    v[13,t-4,i,3]+v[15,t-4,i,3])/sum(pop[t-4,i,]))
    plambda[t,i,k] = p[t,i,k]*lambda[t,i]
    nplambda[t,i,k] = (1-p[t,i,k])*lambda[t,i]
    for (j in 1:np) {      #patch j

f<-rbind(f, c(lmvt[i,j],1,i,k,1,j,k), c(lmvt[i,j],2,i,k,2,j,k), c(lmvt[i,j],3,i,k,3,j,k),
,k),
          c(lmvt[i,j],4,i,k,4,j,k), c(lmvt[i,j],5,i,k,5,j,k),
          c(lmvt[i,j],6,i,k,6,j,k), c(lmvt[i,j],12,i,k,12,j,k), c(lmvt[i,j],13,i,k,13,j,k),
          c(lmvt[i,j],14,i,k,14,j,k), c(lmvt[i,j],15,i,k,15,j,k)) } # end j

f<-rbind(f,
          c(mu,1,i,k,1,i,k), c(mu,2,i,k,1,i,k), c(mu,3,i,k,1,i,k), c(mu,4,i,k,1,i,k),
          c(mu,5,i,k,1,i,k), c(mu,6,i,k,1,i,k), c(mu,7,i,k,1,i,k), c(mu,8,i,k,1,i,k),
          c(mu,9,i,k,1,i,k), c(mu,10,i,k,1,i,k), c(mu,11,i,k,1,i,k),
          c(mu,12,i,k,1,i,k), c(mu,13,i,k,1,i,k), c(mu,14,i,k,1,i,k),
          c(mu,15,i,k,1,i,k),
          c(sigma2,2,i,k,3,i,k), c(sigma2,4,i,k,5,i,k), c(sigma2,7,i,k,8,i,k),
          c(sigma2,10,i,k,11,i,k), c(sigma2,12,i,k,13,i,k), c(sigma2,14,i,k,15,i,k),
          c(q,2,i,k,1,i,k), c(q,3,i,k,1,i,k), c(q,12,i,k,6,i,k), c(q,13,i,k,6,i,k),
          c(delta,5,i,k,1,i,k), c(delta,15,i,k,6,i,k),
          c(alpha[i,k],1,i,k,1,i,k), c(alpha[i,k],2,i,k,2,i,k),
          c(alpha[i,k],3,i,k,3,i,k), c(alpha[i,k],4,i,k,4,i,k), c(alpha[i,k],5,i,k,5,i,k),
          c(alpha[i,k],6,i,k,6,i,k), c(alpha[i,k],12,i,k,12,i,k), c(alpha[i,k],13,i,k,13,i,k),

```

```

c(alpha[i,k],14,i,k,14,i,k), c(alpha[i,k],15,i,k,15,i,k),
c(mrate[t,i],1,i,k,6,i,k), c(mrate[t,i],2,i,k,7,i,k), c(mrate[t,i],
  ],3,i,k,8,i,k),
c(mrate[t,i],4,i,k,7,i,k), c(mrate[t,i],5,i,k,8,i,k), c(adh*mcure,7,
  i,k,6,i,k),
c(adh*mcure,8,i,k,6,i,k), c(mpoc[t],6,i,k,1,i,k), c(mpoc[t],12,i,k,2,
  i,k),
c(mpoc[t],13,i,k,3,i,k), c(mpoc[t],14,i,k,4,i,k), c(mpoc[t],15,i,k,5,
  i,k),
c(adh*mscure,10,i,k,9,i,k), c(adh*mscure,11,i,k,9,i,k), c(mspocp,9,i,
  k,1,i,k)
} # end k

f<-rbind(f,c(plambda[t-sigma1,i,k],1,i,1,2,i,1), c(nplambda[t-sigma1,i,k],1,i,1,4,i
,1),
c(plambda[t-sigma1,i,k],1,i,3,2,i,3), c(nplambda[t-sigma1,i,k],1,i
,3,4,i,3),
c(plambda[t-sigma1,i,k],1,i,2,2,i,1), c(nplambda[t-sigma1,i,k],1,i
,2,4,i,1),
c(plambda[t-sigma1,i,k],6,i,1,12,i,1), c(nplambda[t-sigma1,i,k],6,i
,1,14,i,1),
c(plambda[t-sigma1,i,k],6,i,3,12,i,3), c(nplambda[t-sigma1,i,k],6,i
,3,14,i,3),
c(plambda[t-sigma1,i,k],6,i,2,12,i,1), c(nplambda[t-sigma1,i,k],6,i
,2,14,i,1),

c(zeta[t,i],1,i,1,1,6,3), c(zeta[t,i],2,i,1,2,6,3), c(zeta[t,i],3,i
,1,3,6,3),
c(zeta[t,i],4,i,1,4,6,3), c(zeta[t,i],5,i,1,5,6,3), c(zeta[t,i],6,i
,1,6,6,3),
c(zeta[t,i],12,i,1,12,6,3), c(zeta[t,i],13,i,1,13,6,3), c(zeta[t,i],14,
i,1,14,6,3),
c(zeta[t,i],15,i,1,15,6,3),

c(zeta[t,i],1,6,3,1,i,2), c((1-msaton*msprop[t])*zeta[t,i],2,6,3,2,i
,2),
c((1-msaton*msprop[t])*zeta[t,i],3,6,3,3,i,2),
c((1-msaton*msprop[t])*zeta[t,i],4,6,3,4,i,2),
c((1-msaton*msprop[t])*zeta[t,i],5,6,3,5,i,2),
c((1-msaton*msprop[t])*zeta[t,i],6,6,3,6,i,2), c(zeta[t,i],12,6,3,12,i
,2),
c((1-msaton*msprop[t])*zeta[t,i],13,6,3,13,i,2),
c((1-msaton*msprop[t])*zeta[t,i],14,6,3,14,i,2),

```

```

c((1-msaton*msprop[t])*zeta[t,i],15,6,3,15,i,2),

c(msaton*msprop[t]*zeta[t,i],2,6,3,10,i,2), c(msaton*msprop[t]*zeta[t,
i],3,6,3,11,i,2),
c(msaton*msprop[t]*zeta[t,i],4,6,3,10,i,2), c(msaton*msprop[t]*zeta[t,i
],5,6,3,11,i,2),
c(msaton*msprop[t]*zeta[t,i],12,6,3,10,i,2), c(msaton*msprop[t]*zeta[t
,i],13,6,3,11,i,2),
c(msaton*msprop[t]*zeta[t,i],14,6,3,10,i,2), c(msaton*msprop[t]*zeta[t,
i],15,6,3,11,i,2),

c(varpi[t,i],1,i,3,1,6,2), c(varpi[t,i],2,i,3,2,6,2), c(varpi[t,i],3,i
,3,3,6,2),
c(varpi[t,i],4,i,3,4,6,2), c(varpi[t,i],5,i,3,5,6,2),
c(varpi[t,i],6,i,3,6,6,2), c(varpi[t,i],12,i,3,12,6,2),
c(varpi[t,i],13,i,3,13,6,2),
c(varpi[t,i],14,i,3,14,6,2), c(varpi[t,i],15,i,3,15,6,2),

c(varpi[t,i],1,6,1,1,i,3), c((1-msaton*msprop[t])*varpi[t,i],2,6,1,2,i
,3),
c((1-msaton*msprop[t])*varpi[t,i],3,6,1,3,i,3),
c((1-msaton*msprop[t])*varpi[t,i],4,6,1,4,i,3),
c((1-msaton*msprop[t])*varpi[t,i],5,6,1,5,i,3),
c(varpi[t,i],6,6,1,6,i,3), c((1-msaton*msprop[t])*varpi[t,i
],12,6,1,12,i,3),
c((1-msaton*msprop[t])*varpi[t,i],13,6,1,13,i,3),
c((1-msaton*msprop[t])*varpi[t,i],14,6,1,14,i,3),
c((1-msaton*msprop[t])*varpi[t,i],15,6,1,15,i,3),

c(msaton*msprop[t]*varpi[t,i],2,6,1,10,i,3),
c(msaton*msprop[t]*varpi[t,i],3,6,1,11,i,3),
c(msaton*msprop[t]*varpi[t,i],4,6,1,10,i,3),
c(msaton*msprop[t]*varpi[t,i],5,6,1,11,i,3),
c(msaton*msprop[t]*varpi[t,i],12,6,1,10,i,3),
c(msaton*msprop[t]*varpi[t,i],13,6,1,11,i,3),
c(msaton*msprop[t]*varpi[t,i],14,6,1,10,i,3),
c(msaton*msprop[t]*varpi[t,i],15,6,1,11,i,3))

} #end i

```

```

flow<- array(0,c(1,nf))
rflow<- array(0,c(1,nf))
for (g in 1:nf) {
  flow[g]<-v[f[g,2],t-1,f[g,3],f[g,4]]*(1-exp(-f[g,1]*dt))
  rflow[g]<-rpois(1,flow[g])
}

v[,t,]=v[,t-1,]

for (g in 1:nf) {
  v[f[g,2],t,f[g,3],f[g,4]] = max(0,v[f[g,2],t,f[g,3],f[g,4]] - rflow[g])
  v[f[g,5],t,f[g,6],f[g,7]] = max(0,v[f[g,5],t,f[g,6],f[g,7]] + rflow[g])
} #end g

for (i in 1:np) {      # patch i
  for (k in 1:nsp) { # subpatch k
    trtnsp[t,i,k] = sum(flow[which(f[,1]==q &f[,3]==i &f[,4]==k)]) }
}

for (i in 1:np) {      # patch i
  for (k in 1:nsp) { # subpatch k

    pop[t,i,k]= sum(v[,t,i,k])
    N[t]=sum(pop[t, ,])
    tibnsp[t,i,k]= pop[t,i,k] - (v[1,t,i,k]+v[6,t,i,k]+v[9,t,i,k])
    tib[t]= sum(tibnsp[t,1:5,])
    sus[t,i,k]= v[1,t,i,k]
    inf[t,i,k]= v[2,t,i,k]+ v[4,t,i,k]
    infts[t,i,k]=v[3,t,i,k]+v[5,t,i,k]
    tot[t,i,k]=sus[t,i,k]+inf[t,i,k]+infts[t,i,k]
  } #end k
} #end i
} # end t
return(as.vector(list(N=N,v=v,pop=pop,plambda=plambda,nplambda=nplambda,lambda=
lambda,\\
betapl=betapl, seasl=seasl,sus=sus,inf=inf, infts=infts, trtnsp=trtnsp,tibnsp=tibnsp
,\\
casensp=casensp,locmv=locmv,formv=formv)))
} #end function

```

A.3 Model 3 - Hybrid Metapopulation DE-IBM model of malaria transmission

```
library(foreign)
library(optimx)
library(hydroPSO)
library(parallel)
library(multicore)
library(doParallel)
library(maptools)
library(rgeos)
library(sp)
registerDoParallel(cores=23)

lm<-read.dta("/Users/sheetalprakashsilal/Dropbox/2002-2012-EDM-wide-full.dta")
map<-read.dta("/Users/sheetalprakashsilal/Dropbox/maputo.dta")
#spray<-read.csv("/Users/sheetalprakashsilal/Dropbox/SprayMP.csv")
spray<-read.csv("/Users/sheetalprakashsilal/Desktop/Modelfit/Multipatch2/SprayMP.csv")
  ")

tslm=ts(lm, start=2002, frequency=52)
tsmap = ts(map, start=2002, frequency=12)
c2<-rbind(c(32.45049, -25.54154), c(32.94872, -26.01871), c(32.72298, -25.84556), \\
c(32.91575, -25.97316)) #map centroids
c1<-rbind(c(30.57137, -25.06539), c(31.12738, -25.33060), c(31.00102, -25.74883), \\
c(31.73014, -25.50319), c(31.52450, -24.55777)) # loc centroids
popdata<-c(98000,590000,70000, 390000, 540000)

#Time & Space set up
n<-popdata # population size
dt<- 1/52 #time step
stoptime<- 2020
starttime<- 1992
dim<-9 # no of stocks
nf<-1482 #no of flows
np<-6 #no of patches (5 local + 1 foreign) (TC, MB, UJ, NK, BB, MP)
nsp<-3 #no of sub-patches 1 - local in patch, 2 - local back from travel, \\
3 - foreign visiting patch
```

```

tsteps<-(stoptime - starttime)/dt
time<- (1:(tsteps+4))*dt - dt
time2<-array(0,c(tsteps+4))
time2[4:(tsteps+4)]=starttime+time
time2[3]=starttime-dt
time2[2]=starttime-2*dt
time2[1]=starttime-3*dt

year<-array(starttime:stoptime,c(stoptime-starttime))
month<-array(1:((stoptime-starttime)*13),c((stoptime-starttime)*13))

seasl<- array(0,c(tsteps+4,np))
stlTC1=stl(tslm[,1], "per")$time.series[,1]
stlMB1=stl(tslm[,4], "per")$time.series[,1]
stlUJ1=stl(tslm[,7], "per")$time.series[,1]
stlNK1=stl(tslm[,10], "per")$time.series[,1]
stlBBR1=stl(tslm[,13], "per")$time.series[,1]
sTC1=(stlTC1-min(stlTC1))/(max(stlTC1)-min(stlTC1))
sMB1=(stlMB1-min(stlMB1))/(max(stlMB1)-min(stlMB1))
sUJ1=(stlUJ1-min(stlUJ1))/(max(stlUJ1)-min(stlUJ1))
sNK1=(stlNK1-min(stlNK1))/(max(stlNK1)-min(stlNK1))
sBBR1=(stlBBR1-min(stlBBR1))/(max(stlBBR1)-min(stlBBR1))
seasl[5:(tsteps+4),1]=rep(sTC1[1:52],(stoptime-starttime))
seasl[5:(tsteps+4),2]=rep(sMB1[1:52],(stoptime-starttime))
seasl[5:(tsteps+4),3]=rep(sUJ1[1:52],(stoptime-starttime))
seasl[5:(tsteps+4),4]=rep(sNK1[1:52],(stoptime-starttime))
seasl[5:(tsteps+4),5]=rep(sBBR1[1:52],(stoptime-starttime))
stlmap = stl(tsmmap[,12], "per")$time.series[,1]
x=1:13
m1<-approx(x,stlmap[1:13], method="linear",n=52)
sMP =(m1$y - min(m1$y))/(max(m1$y)- min(m1$y))
seasl[5:(tsteps+4),6]=rep(sMP[1:52],(stoptime-starttime))
seasl[1:4,]=seasl[53:56,]

#Stochastic Model
#best week fit

vcadd=array(0,c(tsteps+4,np))

Parms<-cbind(c(betaplTC=(3.996202),
               betaplMB=(0.0162165),

```

```

betaplUJ=(0.0003163905),
betapK=(2.562793),
betaplBBR=(9.983371),
betaplMP1=(92.728167),
vceff=(0.9785401),
kappap=(4.156166),
varpip1=(2289.789),
tsf1=(0.6797384),
varpip2=(1363.792),
zetap=(297.4116),
fwgt=2.000148,
tsf2=0.675,
i1=2.775852,
i2=11.0625,
i3=26.96343,
lwgt=13.69267,
pc1=0.99977,
pc2=0.9021748,
percdecMP2=0.9899145))

```

```

metap<-function(Parms,time,fmvton=1,lmvton=1,vcon=1,vcaddlon=0,w=0,msaton=0,mscov
=0.7,\\
opt=0.5,adherence=0.9,rxfail=0.01,threshold=200,tgton=1,target=100) {

```

```

#Movement and Distance

```

```

x1<-c1[,1]
y1<-c1[,2]
x2<-c2[,1]
y2<-c2[,2]

```

```

dis<-array(0,c(np,np))
for(d in 1:(np-1)) {
  for(od in 1:(np-1)) {
    dis[d,od]= 1/(1+(((x1[d]-x1[od])^2+(y1[d]-y1[od])^2)^0.5))^Parms[18]
    dis[d,d] = 0}}
lwgt=dis/rowSums(dis)
lwgt[6,]=0
lwgt[,6]=0

```

```

fdis<-array(0,c(np-1))

```

```

for (d in 1:(np-1)) {
  fdis [d]=1/(1+(((x1 [d]-x2 [1]) ^2+(y1 [d]-y2 [1]) ^2) ^0.5)) ^Parms [13]}
fwgt = fdis/sum(fdis)
fwgt [6]=0

#Parameters
betapl=(Parms [1:6])
mu<-0.0105 # natural mortality rate
delta1=1/(26/52) # rate of becoming sub-patent
delta2=1/(26/52) # natural recovery rate for sub-patent pop
sigma=2 # time to gametocytemia
q=(1/(3/52)) #clearance +seek trt
rho=(1/(260/52)) #protective period
ptf=0.01 # probablility of treatment failure
pc1=Parms [19] # probability of naive clinical case
pc2 = Parms [20] # probabilityof a naive clinical case
i1=(1/(Parms [15]/52)) # rate of clinical untreated becoming asymptomatic
i2=(1/(Parms [16]/52)) # rate of asymptomatic becoming sub-patent
i3=(1/(Parms [17]/52)) # natural recovery rate for sub-patent

# Vector Control
vceff= (Parms [7]) # vc efficacy
vcadd1<-array (0,c (tsteps+4, np))
vc <-array (0,c (tsteps+4,np))
totstr=c (200, 100000, 5000, 350000, 260000, 1)
vccov<-array (0,c (tsteps+4,np))
for (i in 1:np) {vccov [1:(tsteps+4),i]=spray [1:(tsteps+4),(i+2)]/totstr [i]} #2001
for (i in 1:(tsteps+4)){ for(j in 1:np) { vc [i,j]=(vccov [i,j]+vcadd1on*vcadd [i,j])*
  vceff} }

# Mass Screen and Treat - foreigners
msstart=1132 # week of the year when msat is started
msdur=52/52 # msat duration
mcure1=1/(0.5/52) # cure rate for mda/msat drug
mcure2=1/(4/52) # cure rate for mda/msat drug
mspoc<-array (0,c (tsteps+4)) # prophylactic effect of mda/msat drug vector
mspocp=1/(4/52) #poc parameter
#mscov=0.7 #msat coverage
msrounds=7 # no. of rounds
msspace= 52 #time between rounds
msprop<-array (0,c (tsteps+4)) #prop treated with msat
msrate<-array (0,c (tsteps+4))
for (j in 1:msrounds) {

```

APPENDIX A. MODEL CODE

```
msprop[(msstart+26*w+(j-1)*msspace):(msstart+26*w+(j-1)*msspace+((msdur*52)-1))]=
  mscov }

#Information matrices
v<- array(0, c(dim, tsteps+4, np, nsp))
init<- array(0, c(dim, np))
pop<- array(0, c(tsteps+4, np, nsp))
beta<-array(0, c(tsteps+4, np))
N<- array(0, c(tsteps+4))
tibnsp<-array(0, c(tsteps+4, np, nsp))
tib<-array(0, c(tsteps+4))
trtnsp<-array(0, c(tsteps+4, np, nsp))
lambda<-array(0, c(tsteps+4, np))
plambda<-array(0, c(tsteps+4, np, nsp))
nplambda<-array(0, c(tsteps+4, np, nsp))
sus<-array(0, c(tsteps+4, np, nsp))
infts<-array(0, c(tsteps+4, np, nsp))
tot<-array(0, c(tsteps+4, np, nsp))
casensp<-array(0, c(tsteps+4, np, nsp))
p<-array(0, c(tsteps+4, np, nsp))
p[,1:6,1:2]=0.95 # % care seeking
p[1:697,1:6,3]= (Parms[10]) # fit - trt seeking for foreigners in a country
p[698:(tsteps+4),1:6,3]= (Parms[14]) # fit - trt seeking for foreigners in a
  country
locmv<-array(0, c(tsteps+4, np, nsp))
formv<-array(0, c(tsteps+4, np, nsp))

# mvt
alpha<-array(0, c(np, nsp))
alpha[,2]<-(1/(2/52)) # nsp 2 moving back to nsp 1

zeta<-array(0, c(tsteps+4, np))
for (j in 1:np) {zeta[,j]=fmvton*1/(Parms[12]/52)*fwgt[j] }# foreign travel for
  locals

varpi<-array(0, c(tsteps+4, np))
for (j in 1:np) {
  varpi[1:697, j]=fmvton*1/(Parms[9]/52)*fwgt[j] # FIT!! foreign travel
  varpi[698:(tsteps+4), j]=fmvton*1/(Parms[11]/52)*fwgt[j] } #foreign travel for
  foreigners
```

```

#fmvt<-fmvton*varpi # visit/return from nsp 1 to nsp 3 fit

kappa<- 1/(Parms[8]/52) # FIT!!! local travel
lmvt<-lmvton*kappa*lwgt #mvt between local provinces

#Initial Values DATA
init=cbind(c(97999,0,0,0,0), # TC nsp 1
           c(589942,36,0,0,0), #MB nsp 1
           c(69988,6,0,0,0), #UJ nsp 1
           c(389719,235,0,0,0), #NK nsp 1
           c(539987,13,0,0,0), #BBR nsp 1
           c(839800,200,0,0,0), #MP nsp 1
           c(0,1,0,0,0), #IC nsp 2
           c(0,20,0,0,0), #MB nsp 2
           c(0,4,0,0,0), #UJ nsp 2
           c(0,46,0,0,0), #NK nsp 2
           c(0,0,0,0,0), #BBR nsp 2
           c(0,0,0,0,0), #MP nsp 2
           c(0,0,0,0,0), #IC nsp 3
           c(0,2,0,0,0), #MB nsp 3
           c(0,2,0,0,0), #UJ nsp 3
           c(0,0,0,0,0), #NK nsp 3
           c(0,13,0,0,0), #BBR nsp 3
           c(0,0,0,0,0)) #MP nsp 3
for(t in 1:4) {for (i in 1:np) {
  # Sub-patch 1 (local - local)
  v[1,t,i,1]= init[1,i] # Susceptibles
  v[2,t,i,1]= init[2,i] # Infectious & Treated
  v[3,t,i,1]= init[3,i] # Infectious, Clinical & Not treated
  v[4,t,i,1]= init[4,i] # Infectious, Asymptomatic & Not treated
  v[5,t,i,1]= init[5,i] # Infectious, Sub-patent
  v[6,t,i,1]= 0 # Susceptible with prior infection; partial clinical immunity
  #MSAT stocks
  v[7,t,i,1]= 0 # MSAT Susceptibles
  v[8,t,i,1]= 0 # MSAT Infectious
  v[9,t,i,1]= 0 # MSAT Fail

  # Sub-patch 2 (local - foreign)
  v[1,t,i,2]= init[1,i+6] # Susceptibles
  v[2,t,i,2]= init[2,i+6] # Infectious & Treated
  v[3,t,i,2]= init[3,i+6] # Infectious, Clinical & Not treated
  v[4,t,i,2]= init[4,i+6] # Infectious, Asymptomatic & Not treated
  v[5,t,i,2]= init[5,i+6] # Infectious, Sub-patent

```

APPENDIX A. MODEL CODE

```

v[6,t,i,2]= 0 # Susceptible with prior infection; partial clinical immunity
#MSAT stocks
v[7,t,i,2]= 0 # MSAT Susceptibles
v[8,t,i,2]= 0 # MSAT Infectious
v[9,t,i,2]= 0 # MSAT Fail

# Sub-patch 3 (foreign)
v[1,t,i,3]= init[1,i+12] # Susceptibles
v[2,t,i,3]= init[2,i+12] # Infectious & Treated
v[3,t,i,3]= init[3,i+12] # Infectious, Clinical & Not treated
v[4,t,i,3]= init[4,i+12] # Infectious, Asymptomatic & Not treated
v[5,t,i,3]= init[5,i+12] # Infectious, Sub-patent
v[6,t,i,3]= 0 # Susceptible with prior infection; partial clinical immunity
#MSAT stocks
v[7,t,i,3]= 0 # MSAT Susceptibles
v[8,t,i,3]= 0 # MSAT Infectious
v[9,t,i,3]= 0 }# MSAT Fail

for (t in 1:4) {for (i in 1:np) { for (k in 1:nsp) {
  pop[t,i,k]= sum(v[,t,i,k])
  tibnsp[t,i,k]=pop[t,i,k]-v[1,t,i,k]-v[6,t,i,k]
  beta[t,i]=betapl[i]*(seasl[t,i]+0.05)
  lambda[t,i]= beta[t,i]*(sum(v[3,t,i,1]+v[5,t,i,1]+v[2,t,i,1]+v[4,t,i,1]+v[3,t,i,2]+v[5,t,i,2]+
    v[2,t,i,2]+v[4,t,i,2]+v[3,t,i,3]+v[5,t,i,3]+v[2,t,i,3]+v[4,t,i,3])/
    sum(pop[t,i,]))
  plambda[t,i,k] = p[t,i,k]*lambda[t,i]
  nplambda[t,i,k] = (1-p[t,i,k])*lambda[t,i]
  N[t]=sum(pop[t, ,])
  tib[t]= sum(tibnsp[t, ,])
} }}

#model

for (t in 5:(tsteps+4)) { #time

#flow matrix
# f<-(parameter, v-out, patch(out), subp(out), v-in, patch(in), subp(in))
f<-c()
f1<-c()
f2<-c()
f3<-c()

```

```

f4<-c()
for (i in 1:np) {      # patch i
  for (k in 1:nsp) {  # subpatch k

if (vcon==1) beta[t,i]=betapl[i]*(seasl[t,i]+0.05)*(1-(vc[t,i])) \\
  else beta[t,i]=betapl[i]*(seasl[t,i]+0.05)
if (t>641) beta[t,6]=Parms[21]*(beta[t,6]) else beta[t,6]=beta[t,6]
lambda[t,i] = beta[t,i]*(sum(v[3,t-2,i,1]+v[5,t-2,i,1]+v[2,t-2,i,1]+v[4,t-2,i,1]+v[3,
t-2,i,2]\\
+v[5,t-2,i,2]+v[2,t-2,i,2]+v[4,t-2,i,2]+v[3,t-2,i,3]+v[5,t-2,i,3]+v[2,t-2,i
,3]+v[4,t-2,i,3])
/sum(pop[t-2,i,]))
plambda[t,i,k] = p[t,i,k]*lambda[t,i]
nplambda[t,i,k] = (1-p[t,i,k])*lambda[t,i]
plambdalag=plambda[t-sigma,i,k]
nplambdalag=nplambda[t-sigma,i,k]
for (j in 1:np) {      #patch j

f<-rbind(f, c(lmvt[i,j],1,i,k,1,j,k), c(lmvt[i,j],2,i,k,2,j,k), c(lmvt[i,j],3,i,k,3,j
,k),
          c(lmvt[i,j],4,i,k,4,j,k), c(lmvt[i,j],5,i,k,5,j,k), c(lmvt[i,j],6,
i,k,6,j,k))
} #end j

f<-rbind(f,
c(mu,1,i,k,1,i,k), c(mu,2,i,k,1,i,k), c(mu,3,i,k,1,i,k), c(mu,4,i,k
,1,i,k),
c(mu,5,i,k,1,i,k), c(mu,6,i,k,1,i,k),c(mu,7,i,k,1,i,k), c(mu,8,i,k
,1,i,k),
c(mu,9,i,k,1,i,k), c((1-ptf)*q,2,i,k,6,i,k), c(rho,6,i,k,1,i,k),
c(i1,3,i,k,4,i,k), c(i2,4,i,k,5,i,k), c(i3,5,i,k,6,i,k),
c(alpha[i,k],1,i,k,1,i,k), c(alpha[i,k],2,i,k,2,i,k), c(alpha[i,k
],3,i,k,3,i,k),
c(alpha[i,k],4,i,k,4,i,k), c(alpha[i,k],5,i,k,5,i,k), c(alpha[i,k
],6,i,k,6,i,k),
c(mcure1,8,i,k,7,i,k), c(mcure2,9,i,k,7,i,k), c(mspocp,7,i,k,1,i,k))
} # end k
f<-rbind(f,
c(plambda[t-sigma,i,k],1,i,1,2,i,1), c(pc1*nplambda[t-sigma,i,k],1,i
,1,3,i,1),
c((1-pc1)*nplambda[t-sigma,i,k],1,i,1,4,i,1),
c(plambda[t-sigma,i,k],1,i,2,2,i,1), c(pc1*nplambda[t-sigma,i,k],1,i
,2,3,i,1),

```

```

c((1-pc1)*nplambda[t-sigma,i,k],1,i,2,4,i,1),
  c(plambda[t-sigma,i,k],1,i,3,2,i,3), c(pc1*nplambda[t-sigma,i,k],1,i
    ,3,3,i,3),
c((1-pc1)*nplambda[t-sigma,i,k],1,i,3,4,i,3),
  c(plambda[t-sigma,i,k],6,i,1,2,i,1), c(pc2*nplambda[t-sigma,i,k],6,i
    ,1,3,i,1),
c((1-pc2)*nplambda[t-sigma,i,k],6,i,1,4,i,1),
  c(plambda[t-sigma,i,k],6,i,2,2,i,1), c(pc2*nplambda[t-sigma,i,k],6,i
    ,2,3,i,1),
c((1-pc2)*nplambda[t-sigma,i,k],6,i,2,4,i,1),
  c(plambda[t-sigma,i,k],6,i,3,2,i,3), c(pc2*nplambda[t-sigma,i,k],6,i
    ,3,3,i,3),
c((1-pc2)*nplambda[t-sigma,i,k],6,i,3,4,i,3),

  c(zeta[t,i],1,i,1,1,6,3), c(zeta[t,i],2,i,1,2,6,3),c(zeta[t,i],3,i
    ,1,3,6,3),
  c(zeta[t,i],4,i,1,4,6,3),c(zeta[t,i],5,i,1,5,6,3),c(zeta[t,i],6,i
    ,1,6,6,3),
  c((1-msaton*msprop[t])*zeta[t,i],1,6,3,1,i,2),
c((1-msaton*msprop[t])*zeta[t,i],2,6,3,2,i,2),
  c((1-msaton*msprop[t])*zeta[t,i],3,6,3,3,i,2),
c((1-msaton*msprop[t])*zeta[t,i],4,6,3,4,i,2),
  c((1-msaton*msprop[t])*zeta[t,i],5,6,3,5,i,2),
c((1-msaton*msprop[t])*zeta[t,i],6,6,3,6,i,2),
  c(varpi[t,i],1,i,3,1,6,2), c(varpi[t,i],2,i,3,2,6,2),c(varpi[t,i],3,i
    ,3,3,6,2),
  c(varpi[t,i],4,i,3,4,6,2),c(varpi[t,i],5,i,3,5,6,2),c(varpi[t,i],6,i
    ,3,6,6,2),
  c((1-msaton*msprop[t])*varpi[t,i],1,6,1,1,i,3),
c((1-msaton*msprop[t])*varpi[t,i],2,6,1,2,i,3),
  c((1-msaton*msprop[t])*varpi[t,i],3,6,1,3,i,3),
c((1-msaton*msprop[t])*varpi[t,i],4,6,1,4,i,3),
  c((1-msaton*msprop[t])*varpi[t,i],5,6,1,5,i,3),
c((1-msaton*msprop[t])*varpi[t,i],6,6,1,6,i,3))
} #end i

for (i in 1:np) {      # patch i

f1<-rbind(f1,c(msaton*msprop[t]*zeta[t,i],1,6,3,1,i,2),
c(msaton*msprop[t]*zeta[t,i],2,6,3,2,i,2),
c(msaton*msprop[t]*zeta[t,i],3,6,3,3,i,2),
  c(msaton*msprop[t]*zeta[t,i],4,6,3,4,i,2),
c(msaton*msprop[t]*zeta[t,i],5,6,3,5,i,2),

```

```

c(msaton*msprop[t]*zeta[t,i],6,6,3,6,i,2))
  } #end i

for (i in 1:np) {

f2<-rbind(f2,c(msaton*msprop[t]*varpi[t,i],1,6,1,1,i,3),
c(msaton*msprop[t]*varpi[t,i],2,6,1,2,i,3),
c(msaton*msprop[t]*varpi[t,i],3,6,1,3,i,3),
          c(msaton*msprop[t]*varpi[t,i],4,6,1,4,i,3),
c(msaton*msprop[t]*varpi[t,i],5,6,1,5,i,3),
c(msaton*msprop[t]*varpi[t,i],6,6,1,6,i,3))
  } #end i

for (i in 1:np) {      # patch i local msat

f3<-rbind(f3,c(0,2,6,3,8,i,2),c(0,3,6,3,8,i,2), c(0,4,6,3,8,i,2),c(0,5,6,3,8,i,2),
          c(0,2,6,3,9,i,2),c(0,3,6,3,9,i,2), c(0,4,6,3,9,i,2),c(0,5,6,3,9,i,2))
  } #end i

for (i in 1:np) { #foreign msat movement
  f4<-rbind(f4,c(0,2,6,1,8,i,3),c(0,3,6,1,8,i,3), c(0,4,6,1,8,i,3),c(0,5,6,1,8,i,
    3),
          c(0,2,6,1,9,i,3),c(0,3,6,1,9,i,3), c(0,4,6,1,9,i,3),c(0,5,6,1,9,i,3))
  } #end i

f<-rbind(f,f1,f2,f3,f4)

flow<- array(0,c(1,nf))
rflow<- array(0,c(1,nf))
for (g in 1:nf) {
  flow[g]<-v[f[g,2],t-1,f[g,3],f[g,4]]*(1-exp(-f[g,1]*dt))
  rflow[g]<-rpois(1,flow[g])
}
  rflow1=rflow

# Add in IBM
inds=NULL
if (msaton==1 & msprop[t]>0) {
  size=tgtton*target # f arg changes for each tool

# 1. Define individual matrix
f1=round(rflow[1315:1350])

```

```
ff=round(rflow[1351:1386])# lmvf=flow[1315:1350] fmvf=flow[1351:1386]
profilel=cbind(fl, patch=f1[,6], state=f1[,2], loc=1)
profilef=cbind(ff, patch=f2[,6], state=f2[,2], loc=0)
profilel=profilel[which(profilel[,1]!=0),]
profilef=profilef[which(profilef[,1]!=0),]
for(g in 1:dim(profilef)[1]){ for(i in 1:profilef[g,1])
{inds <- data.frame(rbind(inds, profilef[g,]))}}
for(g in 1:dim(profilel)[1]){ for(i in 1:profilel[g,1])
{inds <- data.frame(rbind(inds, profilel[g,]))}}
case=rep(1:dim(inds)[1])

# 2. Assign Parasite loads
for(i in 1:dim(inds)[1]) {
  if((inds$state[i]==1|inds$state[i]==6)) inds$para[i]=0
  if(inds$state[i]==2) inds$para[i]=rlnorm(1,10.1266311,1.3)
  if(inds$state[i]==3) inds$para[i]=rlnorm(1,10.1266311,1.3)
  if(inds$state[i]==4) inds$para[i]=rlnorm(1, 6.9077552, 1.5)
  if(inds$state[i]==5) inds$para[i]=rlnorm(1, 3.91, 0.75) #subpatent
}

# 3. Apply optional argument
for(i in 1:dim(inds)[1]) {
  if(runif(1)<opt) inds$opt[i]=1 else inds$opt[i]=0
}

# 4. Sample for target possible for each technique
potentials=case[which(inds$opt==1)]
if(length(potentials)<=size) s=potentials else s=sample(potentials, size)
for(i in 1:dim(inds)[1]) {inds$sample[i]=sum(s==i)}

# 5. Apply threshold
inds$msat=0
for(i in 1:dim(inds)[1]) {
  if(inds$sample[i]==1 & inds$para[i]<threshold) inds$msat[i]=0
  if(inds$sample[i]==1 & inds$para[i]>=threshold) inds$msat[i]=1
}

# 6. Apply adherence
inds$fail=0
for(i in 1:dim(inds)[1]) {
  if(runif(1)<adherence & inds$msat[i]==1) inds$adherence[i]=1 else
  inds$adherence[i]=0
```

```

    if (inds$adherence[i]==1 & inds$msat[i]==1) inds$fail[i]=0
    if (inds$adherence[i]==0 & inds$msat[i]==1 & runif(1)>rxfail) inds$fail[i]=0
    if (inds$adherence[i]==0 & inds$msat[i]==1 & runif(1)<rxfail) inds$fail[i]=1
  }

# 7. Assign new state values
for (i in 1:dim(inds)[1]) {
  if (inds$state[i]==1 | inds$state[i]==6) inds$newstate[i]=inds$state[i]
  if (inds$state[i] >=2 & inds$state[i]<=5 & inds$msat[i]==0)
    inds$newstate[i]=inds$state[i]
  if (inds$state[i] >=2 & inds$state[i]<=5 & inds$msat[i]==0 & inds$para[i]
    <200)
    inds$newstate[i]=5
  if (inds$state[i] >=2 & inds$state[i]<=5 & inds$msat[i]==1 & inds$fail[i]==0)
    inds$newstate[i]=8
  if (inds$state[i] >=2 & inds$state[i]<=5 & inds$msat[i]==1 & inds$fail[i]==1)
    inds$newstate[i]=9
}

# 8. Total up
flow0=array(0,c(dim(f1)[1]+dim(f2)[1]+dim(f3)[1]+dim(f4)[1]))
loc=array(0,c(dim(f1)[1]+dim(f2)[1]+dim(f3)[1]+dim(f4)[1]))
newstate=array(0,c(dim(f1)[1]+dim(f2)[1]+dim(f3)[1]+dim(f4)[1]))
patch=array(0,c(dim(f1)[1]+dim(f2)[1]+dim(f3)[1]+dim(f4)[1]))

newflow=cbind(flow0,loc,newstate,patch)

#f1: local no msat
newflow[1:36,2]=1
newflow[1:36,3]=rep(1:6,6)
newflow[1:36,4]=rep(1:6,each=6)
for (j in 1:36) {
  newflow[j,1]=sum(inds$loc==newflow[j,2] & inds$newstate==newflow[j,3]
& inds$state==newflow[j,3] & inds$patch==newflow[j,4])
}

#f2: foreign no msat
newflow[37:72,2]=0
newflow[37:72,3]=rep(1:6,6)
newflow[37:72,4]=rep(1:6,each=6)
for (j in 37:72) {
  newflow[j,1]=sum(inds$loc==newflow[j,2] & inds$newstate==newflow[j,3]
& inds$state==newflow[j,3] & inds$patch==newflow[j,4])
}

```

```
}

#f3: local msat
newflow[73:120,2]=1
newflow[73:120,3]=rep(rep(8:9, each=4),6)
newflow[73:120,4]=rep(1:6, each=8)
for (j in 73:120) {
  newflow[j,1]=sum(inds$loc==newflow[j,2] & inds$newstate==newflow[j,3]
&inds$patch==newflow[j,4])
}

#f4: foreign msat
newflow[121:168,2]=0
newflow[121:168,3]=rep(rep(8:9, each=4),6)
newflow[121:168,4]=rep(1:6, each=8)
for (j in 121:168) {
  newflow[j,1]=sum(inds$loc==newflow[j,2] & inds$newstate==newflow[j,3]
&inds$patch==newflow[j,4])
}
rflow1[1315:1482]=newflow[,1]
}
# End IBM

v[,t,,] = v[,t-1,,]

for (g in 1:nf) {
  v[f[g,2],t,f[g,3],f[g,4]] = max(0,v[f[g,2],t,f[g,3],f[g,4]] - rflow[g])
  v[f[g,5],t,f[g,6],f[g,7]] = max(0,v[f[g,5],t,f[g,6],f[g,7]] + rflow1[g])
} #end g

for (i in 1:np) { # patch i
  for (k in 1:nsp) { # subpatch k
    trtnsp[t,i,k] = sum(rflow[which(f[,1]==(1-ptf)*q &f[,3]==i &f[,4]==k)]) }}

for (i in 1:np) { # patch i
  for (k in 1:nsp) { # subpatch k

    pop[t,i,k]= sum(v[,t,i,k])
    N[t]=sum(pop[t, ,])
    tibnsp[t,i,k]= v[2,t,i,k]+v[3,t,i,k]+v[4,t,i,k]+v[5,t,i,k]
    tib[t]= sum(tibnsp[t, ,])
    sus[t,i,k]= v[1,t,i,k]+v[6,t,i,k]
```

```
    infts [t,i,k]=v[3,t,i,k]+v[5,t,i,k]+v[2,t,i,k]+ v[4,t,i,k]
    tot [t,i,k]=sus [t,i,k]+infts [t,i,k]
  } #end k
} #end i
} # end t
return (as.vector (list (N=N, v=v, pop=pop, flow=flow , plambda=plambda, nplambda=nplambda
, beta=beta, \
seasl=seasl, sus=sus, infts=infts, trtnsp=trtnsp, tibnsp=tibnsp, casensp=casensp, locmv=
locmv, inds=inds)))
} #end function
```


Appendix B

Ethical Clearance

MPUMALANGA PROVINCIAL GOVERNMENT

Building No.3
No. 7 Government Boulevard
Riverside Park Extension 2
Nelspruit
1200
Republic of South Africa



Private Bag X 11213
Nelspruit, 1200
Tel: 013 766 3429
int: +27 13 766 3429
Fax: 013 766 3491
int: +27 13 766 3491

Department of Health

Litiko Letemphilo

Umnnyango WezaMaphilo

Departement van Gesondheid

Enquiries: Molefe Machaba (013) 766 3009/3172

21 July 2011

Ms S.P. Silal
University of Cape Town
PD Hahn Building
Room 5.52
Cape Town



Dear Ms S.P. Silal

APPLICATION FOR RESEARCH & ETHICS APPROVAL: A SIMULATION APPROACH FOR MALARIA ELIMINATION IN MPUMALANGA IN THE FACE OF MIGRATION

The Provincial Research and Ethics Committee has approved your research proposal in the latest format that you sent. No issues of ethical consideration were identified.

Kindly ensure that you provide us with the report once your research has been completed.

Kind regards,

A handwritten signature in black ink, appearing to read 'Molefe Machaba'.

Molefe Machaba
Research and Epidemiology

21-07-2011
Date



FHS016: Annual Progress Report / Renewal

Principal Investigator

Use form [FHS010](#) if the study is completed within the approval period)

